

University of Southampton Research Repository

Copyright © and Moral Rights for this thesis and, where applicable, any accompanying data are retained by the author and/or other copyright owners. A copy can be downloaded for personal non-commercial research or study, without prior permission or charge. This thesis and the accompanying data cannot be reproduced or quoted extensively from without first obtaining permission in writing from the copyright holder/s. The content of the thesis and accompanying research data (where applicable) must not be changed in any way or sold commercially in any format or medium without the formal permission of the copyright holder/s.

When referring to this thesis and any accompanying data, full bibliographic details must be given, e.g.

Thesis: Jennifer Bramley (2020) "Investigating the mechanisms of soft tissue damage at the residual limb-socket interface", University of Southampton, Faculty of Engineering & Physical Sciences, PhD Thesis, pagination.

Data: Bramley (2020) Investigating the mechanisms of soft tissue damage at the residual limb-socket interface. URI [<https://doi.org/10.5258/SOTON/D1672>]

University of Southampton

Faculty of Engineering & Physical Sciences

School of Engineering

Investigating the Mechanisms of Soft Tissue Damage at the Residual Limb-Socket Interface

DOI [<https://doi.org/10.5258/SOTON/D1672>]

by

Jennifer Louise Bramley

ORCID ID 0000-0003-0414-3984

Thesis for the degree of Doctor of Philosophy

December 2020

Abstract

Investigating the Mechanisms of Soft Tissue Damage at the Residual Limb-Socket Interface

The residual limb tissues of an individual with below knee amputation form a critical loaded interface with the prosthetic limb. In the early stages of rehabilitation, residual limb tissues have not been conditioned to support loading and are vulnerable to damage. This impacts upon quality of life and can lead to rejection of the prosthesis. Bioengineers have established an array of measurements to understand the pathogenesis of soft tissue damage and assess multiple aspects of tissue tolerance during loading. However, to date, there is a scarcity of literature utilising these techniques to evaluate the residual limb-socket interface, resulting in a lack of evidence-based practice to prevent socket sores.

A protocol for applying representative mechanical loading on lower limb tissues was developed with a cohort of volunteers without amputation. This involved incremental pressure application through a pneumatic cuff and an array of measurements before, during and after this loaded period to characterise the response of the underlying skin and soft tissues. The protocol was then applied to a cohort of participants with unilateral transtibial amputation. In order to evaluate intrinsic factors (soft tissue composition), Magnetic Resonance Imaging was used to visualise tissue composition and gross soft tissue deformation and a MyotonPRO™ device was used to estimate tissue stiffness. Transcutaneous oxygen and carbon dioxide tensions were measured, and inflammatory biomarkers were collected at sites relevant to prosthetic load transfer, each of which reflected compromise to the skin tissues.

MRI revealed increased adipose infiltrating muscle tissue in residual limbs (median 2.5 %, range 0.2 - 8.9 %) compared to intact limbs (median ≤ 1.7 %, range 0.1 - 5.1 %), indicating muscle atrophy post-amputation. This effect was reduced significantly in the contralateral limbs of those individuals with greater socket use ($r = -0.88$, $p < 0.01$), indicative of adaptation post-activity. During prescribed loading, cuff pressure at the highest inflation of 60 mmHg resulted in mean interface pressures ranging from 66.2 - 83.6 mmHg. In the majority of cases, residual limbs displayed less compressive strain when loaded compared to intact limbs, the differences being statistically significant at a number of tested sites (median strains -6 to 2 % vs. 4 to 13 %, respectively). Cuff loading was observed to produce a transient compromise to tissue viability, reflected in a reduction in transcutaneous oxygen tension and an upregulation of inflammatory biomarkers, suggesting a degree of local ischaemia and inflammation, respectively. In most cases, reduced ischaemia and inflammatory biomarker upregulation was observed in residual limbs compared to intact limbs, suggesting enhanced tolerance to loading. Nonetheless there was considerable variation within the heterogeneous cohort of participants with amputation.

These studies represent a first-of-kind evaluation of residual limb tissue tolerance to representative prosthetic loads involving tissue characterisation and physiological monitoring. This experimental approach could be implemented to identify individual susceptibility to tissue damage which, in turn, could help inform appropriate rehabilitation programmes to maintain health of tissue during prosthetic rehabilitation. Furthermore, development of these techniques into real-time portable measurements would support both prosthetic users and prosthetists to assess in-socket tissue health, leading to more informed management of residual limb tissues.

Acknowledgements

To everyone who has played a part throughout my PhD journey, it really wouldn't have been possible without you. I am truly thankful and feel lucky to know such supportive and inspiring people.

To all my participants, thank you for giving up your time. I would have no results without your help and it was a pleasure to meet you all.

To my supervisory team, thank you for your unwavering patience in the face of my lengthy ramblings. To Prof. Dan Bader, for always following feedback with helpful guidance and for sharing your experiences of, and passion for travel in Japan. To Dr Peter Worsley, for always helping me to consider the clinical perspective and set realistic goals and thank you for providing Physio advice on the occasions when I got ahead of myself with running. Finally, to Dr Alex Dickinson, thank you for always providing support and inspiration, my PhD would have been much harder and a lot less fun without you.

Thanks to Dr Luciana Bostan for your support and help showing me all the measurement techniques, particularly the bioanalysis, in the lab. Thank you to the MRI team at Southampton General Hospital, particularly Chris Everitt and Dr Angela Darekar for their support setting up the protocols and fitting me in even during building works. Thank you to Dr Beth Keenan from the University of Cardiff for your support at conferences and help with MRI analysis. Thank you to Chantel Ostler for your help with learning more about rehabilitation at Portsmouth Enablement Center. Thank you to everyone who assisted with recruitment, particularly Dr Maggie Donavan-Hall and the Patient & Public Involvement (PPI) workshop team, Dr Alex Breen from AECC University College and Michael Hunt from the Travelwise office who provided free participant parking.

Thanks to everyone in the Bio office for all the snack breaks and friendly listening ears. Particular thanks to Charalambos Rossides for his help with MRI processing using his interpolation macro. Thanks to Dr Josh Steer for his support throughout, for lots of fun at conferences and for sharing his prosthetics dream. I hope Radii Devices goes far. Thank you to Shruti Turner for lots of PhD chats and her patient support during nervous conference presentation practice sessions.

Thank you to my friends, particularly Loren, Jenny, Claire, Sarah and Zoe, for always being there for fun, to listen with chocolate when needed and for your patience. Thank you to my mum, dad and brothers for all your love, support and patience. Finally thank you to my boyfriend Jon, my adventure buddy and chef, thank you for your love and always making me laugh. I don't think I'll ever stop learning, but I promise I have finished with higher education (for a while).

Funding for this PhD was provided by the University of Southampton's Institute for Life Sciences, and EPSRC Doctoral Training Program (ref EP/N509747/1).

Table of Contents

Abstract.....	i
Acknowledgements.....	iii
Table of Contents.....	v
Table of Tables.....	ix
Table of Figures.....	xi
Research Thesis: Declaration of Authorship	xvii
Abbreviations.....	xix
1 Introduction	1
1.1 Epidemiology and Demographics	1
1.2 Aetiology	3
1.3 Surgical Techniques and Tissue Healing.....	5
1.4 Early Rehabilitation & Residuum Tissue Changes.....	10
1.5 Residual Limb Tissue Health.....	13
1.6 Research Motivation & Overarching Aim	15
2 Literature Review	17
2.1 Residual Limb-Prosthesis Interface.....	17
2.1.1 Prosthetic Sockets and Suspension Mechanisms	17
2.1.2 Microclimate	21
2.1.3 Mechanical Conditions at the Interface.....	22
2.1.4 Internal Mechanics of the Residual Limb.....	29
2.2 Soft Tissue Damage and Tolerance to Loading.....	31
2.2.1 Mechanisms of Tissue Damage.....	32
2.2.2 Soft Tissue Response to Pressure and Shear	35
2.2.3 Measurement of Tissue Health and Damage Precursors	42
2.3 Motivation, Aim & Objectives.....	53
3 Protocol Development	55
3.1 Representative Prosthetic Loading	55
3.2 Measurement Areas.....	65
3.3 Characterisation of the Residuum Interface and Soft Tissue Parameters.....	66
3.3.1 Soft Tissue Constituents & Biomechanics.....	66
3.3.2 Ischaemia	68
3.3.3 Inflammatory Response	70
3.3.4 Lymphatic Activity.....	71
3.3.5 Measurement Techniques Decision Matrix	74

3.4	Developed Protocol	78
3.4.1	Ethical Consideration	78
3.4.2	Measurement Techniques	80
3.4.3	Participants without Amputation Testing Protocol	85
3.4.4	Participants with Transtibial Amputation Testing Protocol.....	88
3.5	Research Questions, Aims and Objectives	92
4	Soft Tissue Constituents and Biomechanics	95
4.1	Introduction	95
4.2	Materials and Methods	95
4.2.1	Study Design	95
4.2.2	Material and Methods	95
4.2.3	Data Analysis.....	96
4.3	Results.....	98
4.3.1	Interface Pressure.....	101
4.3.2	Soft Tissue Composition	103
4.3.3	Soft Tissue Properties	115
4.3.4	Deformation & Strain under Representative Prosthetic Loading.....	119
4.4	Discussion	124
4.4.1	Measurements and Analysis.....	124
4.4.2	Limitations	129
4.4.3	Summary.....	130
5	Physiological Response.....	131
5.1	Introduction	131
5.2	Materials and Methods	132
5.2.1	Study Design	132
5.2.2	Material and Methods	132
5.2.3	Data Analysis.....	133
5.3	Results.....	135
5.3.1	Interface Pressure.....	135
5.3.2	Tissue Ischaemia	137
5.3.3	Inflammatory Response.....	146
5.4	Discussion	155
5.4.1	Measurements and Analysis.....	155
5.4.2	Limitations	160
5.4.3	Summary.....	160
6	Overall Discussion.....	163
6.1	Achievement of Research Aim & Objectives	163

6.2	Advances in Scientific Understanding.....	165
6.3	Limitations of the Research	167
6.4	Clinical Implications	169
6.5	Future Work.....	172
6.5.1	Applications at Other Soft Tissue-Medical Device Interfaces.....	172
6.5.2	3D Strain Analysis.....	172
6.5.3	Temporal Inflammatory Response.....	173
6.5.4	Metabolite Response	173
6.5.5	Real Time Translation for Clinical and Daily Life Application.....	174
7	Appendices.....	175
	Appendix A-Preliminary temperature and humidity testing results	175
	Appendix B-Ethical Approvals (ERGO 29696 & ERGO 41864).....	176
	Appendix C-Step-by-Step Tissue Composition Image Analysis.....	212
	Appendix D-Detailed Testing Session Activity Checklist- Participants without Amputation	214
	Appendix E-Comprehensive List of Recruitment Avenues	219
	Appendix F-Detailed Testing Session Activity Checklist- Participants with Amputation	220
	Appendix G-Transcutaneous Gas Measurements for Cohort.....	225
8	References	235

Table of Tables

Table 1.1 Skin incision surgical techniques for below knee amputation.....	8
Table 1.2 Examples of Intrinsic and extrinsic factors that increase the risk of skin damage at the residuum-prosthesis interface.....	13
Table 2.1 Areas of the transtibial residual limb considered tolerant and intolerant to pressure [89]	19
Table 2.2 Transtibial prosthetic sockets and suspension mechanisms	20
Table 2.3 Residual limb measurement areas used during interface pressure and shear studies	23
Table 2.4 Measured interface pressure and shear at the residual limb-socket interface (NOTE: Participants were individuals with transtibial amputation unless otherwise stated, Measurement Site(s) refer to Table 3 and Figure 13, L = Lateral and M = Medial).....	24
Table 2.5 Summary of bioengineering techniques	51
Table 3.1 Design factors for representative loading application.....	56
Table 3.2 Comparison of pressure application methods	57
Table 3.3 Linear regression analysis showing relationship between measured Talley sensor pressure and applied cuff pressure, Note: RMSE is Root Mean Squared Error.....	64
Table 3.4 Transcutaneous Gas Tension (T_cPO_2 and T_cPCO_2) responses categorisation	68
Table 3.5 Scoring table for measurement techniques decision matrix	74
Table 3.6 Measurement techniques decision matrix	75
Table 3.7 Inclusion and exclusion criteria for testing protocols, Key: - = Participants without amputation only, * = participants with amputation only, ● Contraindications to MRI and « = Contraindications to use of Indocyanine Green contrast and therefore only relevant to participants without amputation.....	79
Table 3.8 Intraclass correlation of two raters taking MyotonPro™ measurements from two sites	83
Table 4.1 Statistical analysis to evaluate interface pressure, tissue composition, Myoton stiffness, deformation and strain between control, contralateral and residual limb groups and the relationship between some of these factors and BMI/time since amputation/socket use	97
Table 4.2 Participants without amputation characteristics, reported as median (range)	98
Table 4.3 Participants with unilateral transtibial amputation characteristics, reported as median (range).....	99
Table 4.4 Table detailing the mean (SD) interface pressure at three measurement sites, at baseline and a cuff pressure of 60 mmHg, applied to the right control limb of 10 participants without amputation and both residual and contralateral limbs of 10 participants with unilateral transtibial amputation	101
Table 4.5 Correlation analysis for percentage volume of A. infiltrating and B. superficial adipose from the tibial plateau to 60 mm distally in the ten control limbs and the contralateral and residual limbs of ten participants with transtibial amputation. Note: results displayed as r (p) and green represents a result indicating strong correlation ($r > 0.5$) and bold represents significance ($P < 0.05$).....	113
Table 4.6 Correlation analysis for Myoton stiffness in the right control limbs of 8 participants without amputation and the contralateral and residual limbs of 10 participants with unilateral transtibial amputation. Note: results displayed as r (p) and green represents a result indicating strong correlation ($r > 0.5$) and bold represents significance ($P < 0.05$)	116
Table 4.7 Correlation analysis between tissue compressive strain under 60 mmHg cuff inflation and tissue composition in control limbs and the contralateral and residual limbs of participants	

with transtibial amputation. Note: results displayed as r (p) and green represents a result indicating strong correlation ($r > 0.5$) and bold represents significance ($P < 0.05$)	123
Table 5.1 Statistical analysis to evaluate interface pressure, transcutaneous oxygen and carbon dioxide tension, IL-1 α /TP and IL-1RA/TP between control, contralateral and residual limb groups and the relationship between some of these factors and BMI/time since amputation/socket use	134
Table 5.2 Correlation analysis for A. baseline and B. percentage change at 60 mmHg cuff inflation in oxygen tension (T_{cPO_2}) at three measurement sites in the right control limbs of ten participants without amputation and the contralateral and residual limbs of ten participants with unilateral transtibial amputation. Note: results displayed as r (p) and green represents a result indicating strong correlation ($r > 0.5$) and bold represents significance ($P < 0.05$)	143
Table 5.3 Correlation analysis for A. baseline and B. percentage change at 60 mmHg cuff inflation in carbon dioxide tension (T_{cPCO_2}) at the patellar tendon measurement site in the right control limbs of ten participants without amputation and the contralateral and residual limbs of ten participants with unilateral transtibial amputation. Note: results displayed as r (p) and green represents a result indicating strong correlation ($r > 0.5$) and bold represents significance ($P < 0.05$)	143
Table 5.4 Correlation analysis for percentage change IL-1 α /Total protein at three measurement sites in the right control limbs of ten participants without amputation and the contralateral and residual limbs of ten participants with unilateral trans-tibial amputation. Note: results displayed as r (p) and green represents a result indicating strong correlation ($r > 0.5$) and bold represents significance ($P < 0.05$)	151
Table 5.5 Correlation analysis for percentage change IL-1RA/Total protein at three measurement sites in the right control limbs of ten participants without amputation and the contralateral and residual limbs of ten participants with unilateral transtibial amputation. Note: results displayed as r (p) and green represents a result indicating strong correlation ($r > 0.5$) and bold represents significance ($P < 0.05$)	151
Table 5.6 Effect size and variability for power analysis to determine approximate sample size required for transcutaneous gas and inflammatory response measurements	161
Table 6.1 Summary of current clinical applications of measurement techniques post-amputation and recommendations for use	170

Table of Figures

Figure 1.1 UK statistics on incidence of lower limb amputation by cause 2011 to 2012 [26].....	3
Figure 1.2 Flow chart depicting how diabetes can lead to ulceration and infection based on diagram from [31]	3
Figure 1.3 Schematics of A: Right leg residual limb, anterior view; B: Right leg residual limb with a transtibial prosthesis.....	5
Figure 1.4 A: Schematic transverse slice through the calf of the right lower limb, B: Magnified diagram of the soft tissue layers (thicknesses obtained from [33, 34])	6
Figure 1.5 Early inpatient post-amputation rehabilitation process.....	10
Figure 1.6 Left: Diagram of PPAM Aid [53], Right: Photo of Pneumatic Post-Amputation Mobility (PPAM) Aid main pneumatic bag (top) and distal end pneumatic bag (bottom)	11
Figure 2.1 Negative (left) and positive plaster casts (right), and rectification for prosthetic socket design	17
Figure 2.2 Pressure tolerant (A) and intolerant (B) areas of the transtibial residual limb (NOTE: Numbers refer to Table 2.1)	19
Figure 2.3 Residual limb areas used for measuring interface pressures and shear stresses	23
Figure 2.4 Summary of measured and predicted interface pressures in previous studies, during static weight bearing and walking, Note: 7.5 mmHg \approx 1 kPa	26
Figure 2.5 Summary of measured and predicted interface shear in previous studies, during static weight bearing and walking, Note: 7.5 mmHg \approx 1 kPa.....	27
Figure 2.6 International pressure ulcer classification [143]	32
Figure 2.7 Ischaemia and lymphatic impairment due to prolonged external loading.....	33
Figure 2.8 New PU conceptual framework [73].....	34
Figure 2.9 Relationship between load and magnitude for tissue damage based on a number of animal models, adapted and reprinted by permission from Springer Nature from [128] Copyright © 2005	35
Figure 2.10 Occurrence of ulceration in porcine due to pressure combined with friction (left) and pressure only (right) over five days, used with permission of W.B./Saunders CO. from [157] Copyright © 1974; permission conveyed through Copyright Clearance Center, Inc.	36
Figure 2.11 Reswick and Rogers (1976) pressure-time curve [82] with an updated version in the form of a sigmoid damage threshold in red, adapted and republished with permission of RCNi from, [158] Copyright © 2009 (Above pressure A all durations will lead to damage and for pressures lower than B no damage will occur).....	36
Figure 2.12 strain-time muscle cell graph from static indenter loading of bio-artificial muscle cells, adapted and reprinted from [163], Copyright © 2008, with permission from Elsevier	38
Figure 2.13 Transverse MRI slice at distal residual limb of an individual with an above knee amputation to investigate pain (a sciatic neuroma shown by arrow was observed) implementing A: T1 weighting, giving high contrast between adipose and muscle tissues, and B: T2 weighting, giving high signal in fluid-filled and inflamed [191].....	43
Figure 2.14 Transverse slice of lower limb using, A: ultrasound with limb motion compensation and B: MRI (NOTE these two slices are not directly comparable) [201] Copyright © 2015, IEEE	45
Figure 2.15 Tewameter TM300 (Courage + Khazaka Electronic GmbH., Cologne, Germany) measuring probe head (10 mm diameter, 20 mm height).....	45
Figure 2.16 Transcutaneous Gas Tension electrode (diameter 17 mm, thickness 15 mm)	46
Figure 3.1 Images of A: Inner and B: Outer surfaces of BOSO Sphygmomanometer selected to load calf tissues, C: BOSO Profitest Sphygmomanometer pump and gauge.....	59

Figure 3.2 Graph showing pressure loss over a 30 minute time period after inflation to 60mmHg (8 kPa)	60
Figure 3.3 Pressure cuff applied to residual limb plaster cast.....	60
Figure 3.4 Schematic indicating the application of external shear force to the calf tissue of a supine participant.....	61
Figure 3.5 Schematic showing geometry of polyacetal indenter used during preliminary testing- A: Front view, B: Plan view. Dimensions in mm.....	62
Figure 3.6 Diagrams depicting a transverse slice at mid-calf, A: under no loading condition, B: Pressure cuff applied at 60mmHg (8 kPa), C: Pressure cuff applied at 60mmHg (8 kPa) with indenter positioned at the tibialis anterior	62
Figure 3.7 A: Talley pressure sensors, B: Top view of wooden validation rig for Talley sensors, C: Front view of validation rig with Talley sensor being validated with pressurised cuff	63
Figure 3.8 Measured Talley sensor pressures at applied cuff pressures ranging from 20 to 200 mmHg (2.7 to 26.7 kPa)	64
Figure 3.9 Labelled 50 x 50 mm areas of measurement of the right lower limb (where measurements will be taken are in bold & highlighted blue)	65
Figure 3.10 Transverse MRI slices through calf at baseline, A: out of phase, in-slice resolution 1.3 x 1.3 mm, B & C: out of phase, in-slice resolution 0.6 x 0.6 mm, TE: 12.30 ms and 6.15 ms respectively (white arrows show oil tablets in-situ), D: fat saturated, in-slice resolution 0.6 x 0.6 mm.....	67
Figure 3.11 Shaved measurement areas of right lower leg prior to testing	69
Figure 3.12 Left: 3D printed replica of (TCM), Right: 3D printed TCM sensor in fixation ring	69
Figure 3.13 IL-1 α /Total protein at baseline and 0, 1, 3, 24 and 48 hours post- hair removal via shaving at a number of lower limb locations	70
Figure 3.14 A: Superficial lymphatic vessels in the foot and shank, B: Indocyanine Green contrast injected sub-dermally between toes.....	71
Figure 3.15 Lymphatic packet frequencies under incremental pressure cuff loading in the calf tissues of 10 participants.....	72
Figure 3.16 Foam support cushions to support participants during testing	80
Figure 3.17 Transverse MRI slices of a participant's calf at baseline displaying how measurements of gross tissue deformation under the indenter sites were made at the A) patellar tendon, B) lateral calf and C) posterior calf, Note: white represents construction lines and red represents measurement taken	81
Figure 3.18 Processing of transverse MRI fat saturated slice of lower limb at posterior calf measurement site showing A: Original, B: Post-thresholding, C: Superficial adipose mask, D: adipose infiltrating muscle mask.....	82
Figure 3.19 MyotonPRO™ device used to measure structural stiffness of the residuum soft tissue	82
Figure 3.20 Protocol testing set up for participants without amputation	85
Figure 3.21 Participants without amputation protocol liner, silicone gel and pressure cuff setup.....	85
Figure 3.22 Flow chart showing testing session 1 protocol for participants without amputation ..	86
Figure 3.23 Flow chart showing testing session 2 protocol for participants without amputation ..	87
Figure 3.24 Testing setup for participants with amputation.....	89
Figure 3.25 MRI testing set up.....	89
Figure 3.26 Flow chart showing testing session 1 protocol for participants with unilateral transtibial amputation.....	90
Figure 3.27 Flow chart showing testing session 2 protocol for participants with unilateral transtibial amputation.....	91

Figure 4.1 Residual limbs of participants with amputation, KEY: participant ID, sex, age, amputation cause, number of years post-amputation.....	100
Figure 4.2 Corresponding transverse MRI slices at the posterior calf measurement site for the right control limb of ten participants without amputation, with superficial adipose (yellow) and adipose infiltrating muscle (red) tissue overlays	104
Figure 4.3 Corresponding transverse MRI slices at the posterior calf measurement site for the residual (R) and contralateral (C) limbs of ten participants with unilateral transtibial amputation, with superficial adipose (yellow) and adipose infiltrating muscle (red) tissue overlays	105
Figure 4.4 Percentage of superficial adipose tissue throughout the right control limb of ten participants without amputation.....	106
Figure 4.5 Percentage of superficial adipose tissue throughout the contralateral (top) and residual (bottom) limbs of ten participants with unilateral transtibial amputation	108
Figure 4.6 Percentage of adipose infiltrating muscle throughout the right control limb of participants without amputation (left) and the contralateral (middle) and residual (right) limbs of ten participants with unilateral transtibial amputation	109
Figure 4.7 Percentage of muscle tissue throughout the right control limb of participants without amputation (left) and the contralateral (middle) and residual (right) limbs of ten participants with unilateral transtibial amputation.....	110
Figure 4.8 Median, interquartile range (IQR) and range of overall limb soft tissue percentage for all participant groups over an lower limb area from the tibial plateau to 60 mm distally. Note: * = $p \leq 0.05$ and ** = $p \leq 0.01$	111
Figure 4.9 residual limb overall infiltrating adipose percentage plotted against contralateral limb overall infiltrating adipose percentage in 10 participants with unilateral transtibial amputation. Note: number represents participant identification	112
Figure 4.10 Percentage volume of infiltrating adipose from the tibial plateau to 60 mm distally plotted against daily socket use (left) and time since amputation (right) for the contralateral limbs of ten participants with unilateral transtibial amputation. NOTE: number represents participant identification	114
Figure 4.11 Mean (\pm standard deviation) tissue stiffness under induced Myoton probe oscillations at three measurement sites in the right control limb of eight participants without amputation and both contralateral and residual limbs of ten participants with unilateral transtibial amputation. Note: * = $p \leq 0.05$	115
Figure 4.12 Myoton stiffness as a function of the superficial adipose percentage for the right control limbs of 8 participants without amputation	116
Figure 4.13 Myoton stiffness as a function of the superficial adipose percentage for the contralateral and residual limbs of 10 participants with unilateral transtibial amputation. NOTE: number represents participant identification and posterior calf site y axes only goes to 600 N/m	117
Figure 4.14 Myoton stiffness as a function of the socket use for the residual limb lateral calf site (top) and contralateral and residual limb posterior calf site (bottom) of 10 participants with unilateral transtibial amputation. NOTE: number represents participant identification and posterior calf site y axes only goes to 600 N/m.....	118
Figure 4.15 Transverse MRI slices at posterior calf measurement level at baseline outlining soft tissue at baseline (solid yellow line) and soft tissue under 60 mmHg cuff pressure (dashed yellow line), for participants without amputation	119
Figure 4.16 Transverse MRI slices at posterior calf measurement level at baseline outlining soft tissue at baseline (solid yellow line) and soft tissue under 60 mmHg cuff pressure (dashed yellow	

line), for participants with unilateral transtibial amputation (Note: #5A only pressurised to 40 mmHg)	120
Figure 4.17 Median, interquartile range (IQR) and range of lower limb soft tissue deformation under 60 mmHg pressure cuff loading for all participant groups. Note: ○ and + indicate outliers that are 1.5 and 3 times the Interquartile Range (IQR) respectively, *= $p \leq 0.05$ and **= $p \leq 0.01$...	121
Figure 4.18 Median, interquartile range (IQR) and range of lower limb soft tissue compressive strain under 60 mmHg pressure cuff loading for all participant groups. Note: ○ and + indicate outliers that are 1.5 and 3 times the Interquartile Range (IQR) respectively, *= $p \leq 0.05$ and **= $p \leq 0.01$	122
Figure 4.19 Tissue compressive strain under 60 mmHg cuff pressure at the posterior calf measurement site as a function of the infiltrating adipose percentage for the right control limbs of 10 participants without amputation (left) and the residual limbs of 10 participants with unilateral transtibial amputation (right). NOTE: number represents participant identification and left x axis is only to 4 %	123
Figure 4.20 Left: central sagittal, and Right: distal transverse MRI slice of the residual limb of a male participant with unilateral transtibial amputation collected for Eurostars ImpAmp project [121]. Note: red line shows the position of the distal transverse slice	125
Figure 5.1 The effects of incrementally applied cuff pressures on mean (\pm SD) interface pressures at three measurement sites in intact and residual lower limbs.....	136
Figure 5.2 Mean baseline oxygen (left) and carbon dioxide (right) tensions at three measurement sites in the right control limb of ten participants without amputation and both contralateral and residual limbs of ten participants with unilateral transtibial amputation. Note: error bars represent \pm SD and, ** = $p \leq 0.01$	137
Figure 5.3 Exemplar data showing percentage change from baseline T_cPO_2 and T_cPCO_2 measurements under incremental cuff pressures from 20 to 60 mmHg from the residual (left) and contralateral (right) limbs of participant #3A, revealing two main trends observed at the patellar tendon site within the research cohort: Trend 1 a Category 3 response (left) and Trend 2 a Category 2 response (right)	138
Figure 5.4 Ischaemic response at the patellar tendon to incremental cuff pressures using categorical analysis [215], to indicate tolerance in ten participants without amputation	139
Figure 5.5 Ischaemic response at the patellar tendon to incremental cuff pressures using categorical analysis [215], to indicate tolerance in ten participants with transtibial amputation	139
Figure 5.6 The effects of cuff pressures on mean (\pm SD) percentage decrease in T_cPO_2 at the three measurement sites in intact and residual lower limbs. Note: Dashed line at 25% decrease indicates Category 3 ischemia threshold	140
Figure 5.7 The effects of cuff pressure on mean (\pm SD) percentage increase in T_cPCO_2 at the three measurement sites in intact and residual lower limbs. Note: Dashed line at 25% increase indicates Category 3 Ischaemia threshold	141
Figure 5.8 Baseline T_cPO_2 (left) and percentage decrease in T_cPO_2 at 60 mmHg cuff inflation (right), against time since amputation for residual limb patellar tendon site of ten participants with unilateral transtibial amputation. NOTE: number represents participant identification	145
Figure 5.9 Percentage increase in T_cPCO_2 at 60 mmHg cuff inflation against time since amputation for the residual limb patellar tendon site of nine participants with unilateral transtibial. NOTE: number represents participant identification	145
Figure 5.10 Box and whisker plot showing IL-1 α /Total Protein (left) and IL-1RA/Total Protein (right) ratios, at three measurement sites on the control limbs of 10 participants without amputation (top) and the contralateral (middle) and residual (bottom) limbs of 10 participants with unilateral transtibial amputation, expressed as a percentage change from baseline resulting	

from cuff loading at 60 mmHg. Note: ○ and + indicate outliers that are 1.5 and 3 times the Interquartile Range (IQR) respectively.....	147
Figure 5.11 IL-1 α /Total Protein (top) and IL-1RA/Total Protein (bottom) ratios, at three measurement sites on the right limbs of 10 participants without amputation, at baseline and following cuff loading up to 60 mmHg.....	148
Figure 5.12 IL-1 α /Total Protein ratios, at three measurement sites on the contralateral (top) and residual (bottom) limbs of 10 participants with unilateral transtibial amputation, at baseline and following cuff loading up to 60 mmHg.....	150
Figure 5.13 IL-1RA/Total Protein ratios, at three measurement sites on the contralateral (top) and residual (bottom) limbs of 10 participants with unilateral transtibial amputation, at baseline and following cuff loading up to 60 mmHg.....	150
Figure 5.14 Percentage change in IL-1 α /Total Protein against time since amputation for the lateral (left) and posterior (right) calves of the residual limbs of ten participants with unilateral transtibial amputation	152
Figure 5.15 Percentage change in IL-1RA/Total Protein against approximate daily socket use for the residual limb posterior calf of ten participants with unilateral transtibial amputation.....	153
Figure 5.16 Percentage change in IL-1 α /Total Protein against superficial adipose for the contralateral limb lateral calf of ten participants with unilateral transtibial amputation	154
Figure 5.17 Percentage change in IL-1 α /Total Protein against carbon dioxide increase at 60 mmHg cuff inflation for the contralateral patellar tendon site of ten participants with unilateral transtibial amputation	154
Figure 6.1 Schematic summarising objectives and achievements of this research, Note: colour represents which research question is in-part being answered.....	164
Figure 6.2 Segmented participant #1A baseline MRI stack	172
Figure 7.1 Skin surface temperature (top) and humidity (bottom) under 60 mmHg applied pressure during preliminary testing.....	175
Figure 7.2 Data showing percentage change from baseline T _c PO ₂ and T _c PCO ₂ measurements under incremental cuff pressures from 20 to 60 mmHg from the right limb of participant #1	225
Figure 7.3 Data showing percentage change from baseline T _c PO ₂ and T _c PCO ₂ measurements under incremental cuff pressures from 20 to 60 mmHg from the right limb of participant #2	225
Figure 7.4 Data showing percentage change from baseline T _c PO ₂ and T _c PCO ₂ measurements under incremental cuff pressures from 20 to 60 mmHg from the residual (left) and contralateral (right) limbs of participant #3	226
Figure 7.5 Data showing percentage change from baseline T _c PO ₂ and T _c PCO ₂ measurements under incremental cuff pressures from 20 to 60 mmHg from the residual (left) and contralateral (right) limbs of participant #4	226
Figure 7.6 Data showing percentage change from baseline T _c PO ₂ and T _c PCO ₂ measurements under incremental cuff pressures from 20 to 60 mmHg from the residual (left) and contralateral (right) limbs of participant #5	226
Figure 7.7 Data showing percentage change from baseline T _c PO ₂ and T _c PCO ₂ measurements under incremental cuff pressures from 20 to 60 mmHg from the residual (left) and contralateral (right) limbs of participant #6	227
Figure 7.8 Data showing percentage change from baseline T _c PO ₂ and T _c PCO ₂ measurements under incremental cuff pressures from 20 to 60 mmHg from the residual (left) and contralateral (right) limbs of participant #7	227
Figure 7.9 Data showing percentage change from baseline T _c PO ₂ and T _c PCO ₂ measurements under incremental cuff pressures from 20 to 60 mmHg from the residual (left) and contralateral (right) limbs of participant #8	227

Figure 7.10 Data showing percentage change from baseline T_cPO_2 and T_cPCO_2 measurements under incremental cuff pressures from 20 to 60 mmHg from the residual (left) and contralateral (right) limbs of participant #9.....	228
Figure 7.11 Data showing percentage change from baseline T_cPO_2 and T_cPCO_2 measurements under incremental cuff pressures from 20 to 60 mmHg from the residual (left) and contralateral (right) limbs of participant #10.....	228
Figure 7.12 Data showing percentage change from baseline T_cPO_2 and T_cPCO_2 measurements under incremental cuff pressures from 20 to 60 mmHg from the residual (left) and contralateral (right) limbs of participant #1A	229
Figure 7.13 Data showing percentage change from baseline T_cPO_2 and T_cPCO_2 measurements under incremental cuff pressures from 20 to 60 mmHg from the residual (left) and contralateral (right) limbs of participant #2A	229
Figure 7.14 Data showing percentage change from baseline T_cPO_2 and T_cPCO_2 measurements under incremental cuff pressures from 20 to 60 mmHg from the residual (left) and contralateral (right) limbs of participant #3A	230
Figure 7.15 Data showing percentage change from baseline T_cPO_2 and T_cPCO_2 measurements under incremental cuff pressures from 20 to 60 mmHg from the residual (left) and contralateral (right) limbs of participant #4A	230
Figure 7.16 Data showing percentage change from baseline T_cPO_2 and T_cPCO_2 measurements under incremental cuff pressures from 20 to 60 mmHg from the residual (left) and contralateral (right) limbs of participant #5A	231
Figure 7.17 Data showing percentage change from baseline T_cPO_2 and T_cPCO_2 measurements under incremental cuff pressures from 20 to 60 mmHg from the residual (left) and contralateral (right) limbs of participant #6A	231
Figure 7.18 Data showing percentage change from baseline T_cPO_2 and T_cPCO_2 measurements under incremental cuff pressures from 20 to 60 mmHg from the residual (left) and contralateral (right) limbs of participant #7A	232
Figure 7.19 Data showing percentage change from baseline T_cPO_2 and T_cPCO_2 measurements under incremental cuff pressures from 20 to 60 mmHg from the residual (left) and contralateral (right) limbs of participant #8A	232
Figure 7.20 Data showing percentage change from baseline T_cPO_2 and T_cPCO_2 measurements under incremental cuff pressures from 20 to 60 mmHg from the residual (left) and contralateral (right) limbs of participant #9A	233
Figure 7.21 Data showing percentage change from baseline T_cPO_2 and T_cPCO_2 measurements under incremental cuff pressures from 20 to 60 mmHg from the residual (left) and contralateral (right) limbs of participant #10A	233

Research Thesis: Declaration of Authorship

Print name:	Jennifer Louise Bramley
-------------	-------------------------

Title of thesis:	Investigating the Mechanisms of Soft Tissue Damage at the Residual Limb-Socket Interface
------------------	--

I declare that this thesis and the work presented in it are my own and has been generated by me as the result of my own original research.

I confirm that:

This work was done wholly or mainly while in candidature for a research degree at this University;

Where any part of this thesis has previously been submitted for a degree or any other

qualification at this University or any other institution, this has been clearly stated;

Where I have consulted the published work of others, this is always clearly attributed;

Where I have quoted from the work of others, the source is always given. With the exception of

such quotations, this thesis is entirely my own work;

I have acknowledged all main sources of help;

Where the thesis is based on work done by myself jointly with others, I have made clear exactly

what was done by others and what I have contributed myself;

Parts of this work have been published as:

Bramley, J.L., et al., *Establishing a measurement array to assess tissue tolerance during loading representative of prosthetic use*. Med Eng Phys, 2020 [1]

Bramley, J.L., et al., *Investigating the Physiological Effects on Dermal Tissues Following Simulated Prosthetic Loading in Intact and Trans-Tibial Residual Limbs*. ISPO 17th World Congress Basics to Bionics Abstract Book, Kobe Convention Center, Kobe, Hyogo, Japan, 5-8th October 2019 [2]

Bramley, J.L., et al., *Investigating the Composition and Tissue Deformation During Simulated Prosthetic Loading of Intact and Trans-Tibial Residual Limbs*. ISPO 17th World Congress Basics to Bionics Abstract Book, Kobe Convention Center, Kobe, Hyogo, Japan, 5-8th October 2019 [3]

Signature:		Date:	December 2020
------------	--	-------	---------------

Abbreviations

ADL- Activities of Daily Living

AKA- Above Knee Amputation

AMA- Amputee Mobility Aid

AU- Arbitrary Units

BKA- Below Knee Amputation

BMI- Body Mass Index

CO₂- Carbon Dioxide

COF- Coefficient of Friction

CT- Computed Tomography

CRPS- Complex Regional Pain Syndrome

CTE- Congenital Talipes Equinovarus

DTI- Deep Tissue Injury

ELISA- Enzyme Linked Immunosorbent Assay

EM- Electromagnetic

FEA- Finite Element Analysis

ICC- Intraclass Correlation

ICG- Indocyanine Green

IL-8- Interleukin-8

IL-1 α - Interleukin-1 α

IL-1 β - Interleukin-1 β

IL-1RA- Interleukin-1 Receptor Antagonist

IQR- Interquartile Range

MDRPU- Medical Device Related Pressure
Ulcers

MRE- Magnetic Resonance Elastography

MRI- Magnetic Resonance Imaging

NIR- Near Infra-Red

O₂- Oxygen

OCT- Optical Coherence Tomography

P.I.R.P.A.G- Physiotherapy Inter Regional
Prosthetic Audit Group

PIV- Pressure-Induced Vasodilation

PORH- Post-Occlusive Reactive Hyperaemia

PPAM- Pneumatic Post-Amputation Mobility

PPI- Patient and Public Involvement

PTB- Patellar Tendon Bearing

PU- Pressure Ulcer

PVD- Peripheral Vascular Disease

ROS- Reactive Oxygen Species

SEM- Sub-epidermal Moisture

SPP- Skin Perfusion Pressure

TcPO₂- Transcutaneous Oxygen Tension

TcPCO₂- Transcutaneous Carbon Dioxide
Tension

TCM- Transcutaneous Measurement

TEWL- Transepidermal Water Loss

TE- Echo time

TNF- α - Tumour Necrosis Factor- α

TP- Total Protein

TR- Repetition time

TSB- Total Surface Bearing

VIBE- Volumetric Interpolated Breath-hold
Examination

WHO- World Health Organisation

1 Introduction

Amputation is the surgical or traumatic loss of all or part of a limb or extremity. Evidence of amputation dates back as far as the Neolithic period [4]. In the past, amputation may have been performed for ritualistic purposes or punishment as opposed to medical necessity. The first recording of amputation as a medical procedure was in Ancient Greece where Hippocrates (460 to 377 BC) amputated gangrenous tissue [4]. An amputated limb is often compensated for by the use of a prosthesis, which is designed to replace lost anatomy and restore function. The first recorded lower limb prosthesis for major amputation, i.e. above ankle, was found at Pompeii, dated 300 BC [4].

Progress within amputation procedure and subsequent rehabilitation has often been driven by conflict [5]. For example, the development of gunpowder created a new need for amputation due to irreparable and complex battle injuries. A 16th Century surgeon, Ambroise Paré, performed the first recorded Above Knee Amputation (AKA) and helped to integrate knee and ankle joints into prostheses [4]. In 1846, Robert Liston performed the first surgical procedure involving a transtibial (Below Knee) amputation (BKA), under anaesthetic [5]. In modern surgery the use of anaesthetics, sterile environments and antibiotics to fight infection have played a pivotal role in the development of successful procedures and outcomes for amputation.

As well as affecting quality of life (QoL), amputation has large cost implications on healthcare services resulting from surgical time and provision of post-surgical care and prosthetic componentry [6-11]. In the US, mean healthcare costs per person with a diabetes-related BKA were estimated at approximately \$70,000 per year in 2010 [8]. NHS England spends approximately £60 million per year on prosthetics centres which provide services for an estimated 60,000 people with limb loss [11]. It has been estimated that the annual cost of prosthetic provision alone is £2879 per person per year in the UK [10].

1.1 Epidemiology and Demographics

A worldwide retrospective systematic review of trends from 1989 to 2010 revealed a greater incidence of major lower limb amputation in the diabetic population, of median ≈ 212.5 per 100,000 compared to 8.8 per 100,000 in the total population [12]. Age trends and differences between sexes were similar across studies, with amputation incidence greater in males and increasing with age [12-14]. Sex differences could, in part, be attributed to an increased rate of peripheral neuropathy and Peripheral Vascular Disease (PVD) in males, caused by variations in peripheral nerve length and hormonal factors [15, 16].

It is difficult to compare global incidence of lower limb amputation due to differences in data collection, analysis and reporting methodologies [12]. Many retrospective studies also rely on the completion and accuracy of medical records or databases [13, 14, 17]. Some centres may demonstrate apparent bias owing to inaccessibility to certain groups. As an example, in developing countries there may be access problems to care and clinics due to distance and/or cost [18, 19]. In high income countries there are also differences in availability of health care provision, for example, access to vascular surgery services for limb salvage, and foot health clinics. Geographical variations have been observed both in the UK and in US states, with a higher amputation incidence in places with increased prevalence of diabetes and/or PVD [20-22].

A Global Report of Diabetes from the World Health Organization (WHO) stated a prevalence of diabetes of 8.5 % within the adult population in 2014, equating to over 400 million individuals, with an increase in associated risk factors particularly obesity [23]. In the UK, there are estimated to be 4.5 million people affected by diabetes with approximately 700 people diagnosed every day. Subsequently, there are over 160 lower limb amputations due to diabetes per week [24]. In addition, of those that have amputation due to vascular disease such as diabetes there is a poor prognosis with a contralateral limb amputation rate of approximately 55 % within 2 to 3 years of amputation and a morbidity rate of approximately 50 % within 5 years of amputation [25]. Despite the increasing prevalence of diabetes, analysis of data from English hospitals found that the incidence of major amputation had decreased by approximately 20 % from 2003 to 2013 [14]. These findings suggest improvements in diabetes care such as the introduction of diabetic foot clinics, and the success of prevention, education and awareness campaigns.

In 2011 to 2012, of the 5906 people with amputations referred to prosthetic centres in the UK, over 90% involved lower limb amputations and of these over 55 % were transtibial [26]. Where possible, BKA is the preferred surgical technique over AKA due to superior functional outcomes afforded by retention of the knee joint [27]. More than 65 % of people with BKA achieve ambulation with a prosthesis, compared to less than a third of people with AKA [27, 28]. Less successful rehabilitation and reduced activity after AKA is primarily due to the loss of the biological knee joint, which also leads to the requirement of a heavier and more complicated prosthesis for individuals often with complex co-morbidities. This thesis will focus on BKA, particularly transtibial, due to its higher prevalence. The higher activity of people with BKA compared to AKA may also mean enhanced risk of tissue damage during socket use.

1.2 Aetiology

Surgical amputation can be an elective or emergency intervention, and result from a number of reasons (Figure 1.1) [26].

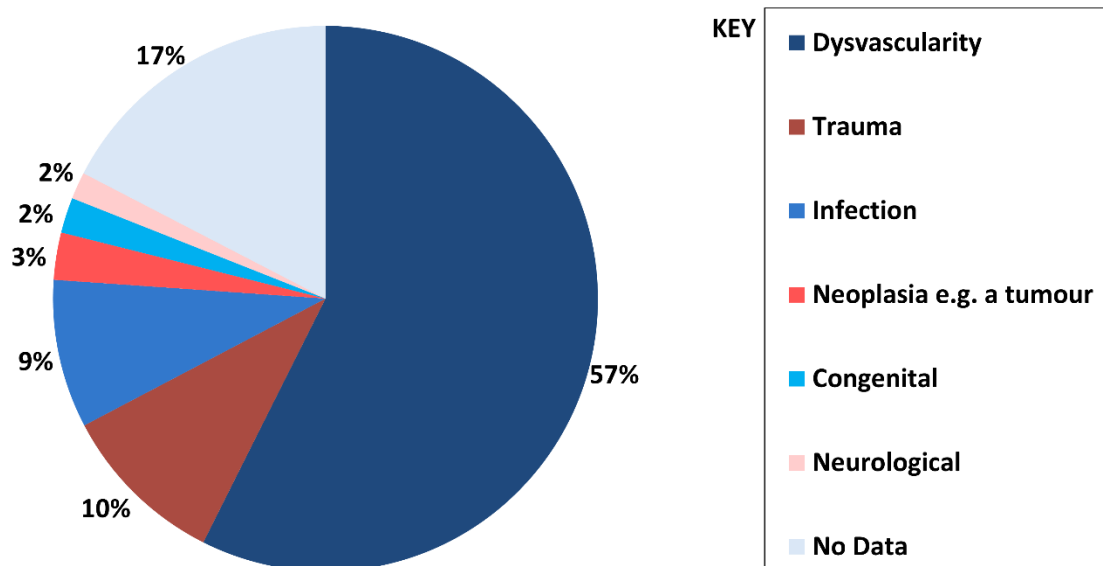


Figure 1.1 UK statistics on incidence of lower limb amputation by cause 2011 to 2012 [26]

Diabetes is a disease in which either the insulin-producing cells have been destroyed (Type 1) or where insulin production is insufficient (Type 2). The onset of Type 2 diabetes used to be observed primarily in adults over the age of 40. However, in recent years cases have become more common in children and young adults thought to be due to rising levels of obesity and high sugar diets [29]. Diabetes is a risk factor for amputation, due to its association with peripheral neuropathy and peripheral dysvascularity caused by systemic changes in the macro and microvascular structures. As a result, diabetic amputations are more likely to result in re-amputation (Figure 1.2) [30].

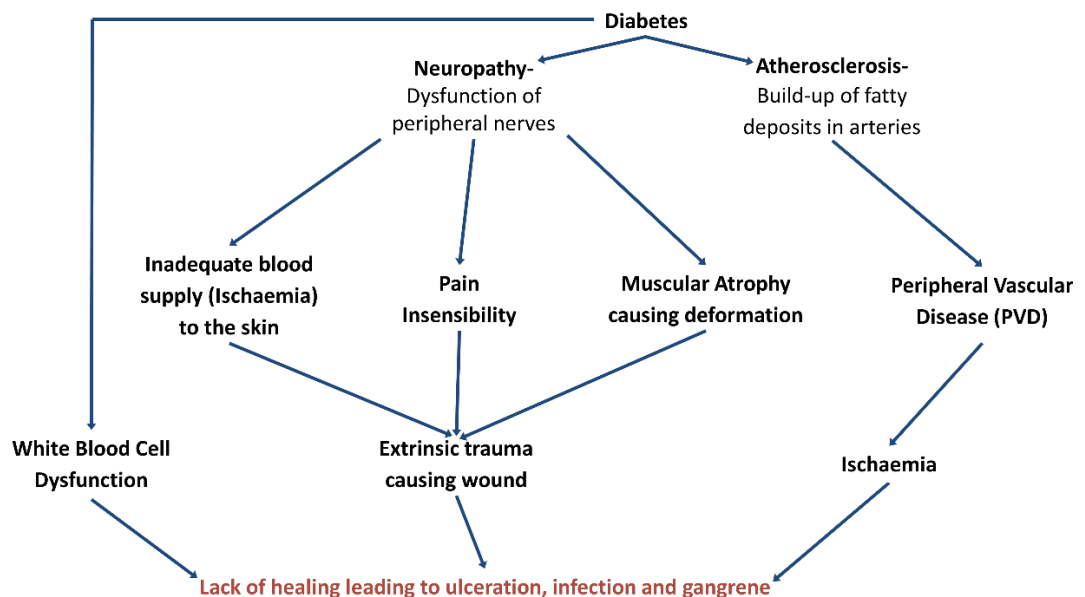


Figure 1.2 Flow chart depicting how diabetes can lead to ulceration and infection based on diagram from [31]

Neuropathy can increase the risk of tissue damage as an individual may have impaired sensation or pain insensibility where they will not be able to feel when something is wrong so could exacerbate the damage with continued loading (Figure 1.2). Dysvascularity refers to a vascular disease or malfunction, resulting in the loss of blood flow. Risk factors for dysvascularity include diabetes, ageing, obesity and smoking. In tissues with this vascular compromise wounds can develop, necessitating amputation when healing is limited and infection is observed (Figure 1.2). Amputation represents a last resort if vascular surgery or limb salvage are not possible. Often tissues are necrotic prior to amputation, with surgeons operating at the level of viable (vascularised) tissue.

In addition, a limb may need to be amputated as a direct result of trauma, including blast injuries, road traffic accidents and falls. Trauma with associated infection or unsuccessful limb salvage can also lead to delayed amputation.

Complex Regional Pain Syndrome (CRPS) is a chronic neurological disorder in which a person experiences excessive pain, inflammation, and colour and temperature change of a limb [32]. It is thought to be caused by impairment of the peripheral and central nervous systems and can be triggered by trauma. In some cases the pain can be debilitating and indicate elective amputation.

In the case of congenital musculoskeletal disorders such as severe or untreated Congenital Talipes Equinovarus (CTE), where one or both feet are plantarflexed and inverted, it may be necessary to perform BKA to improve load-bearing capacity through the foot and reduce pain during mobility.

1.3 Surgical Techniques and Tissue Healing

The residual limb forms a critical interface with the socket, which suspends the prosthetic limb. The transtibial residual limb typically consists of several tissues including the cut bones of the tibia and fibula, muscles including the gastrocnemius, subcutaneous fat, skin and scar tissues (Figure 1.3). These tissues can be further differentiated into individual muscle compartments and dermal (skin) layers (Figure 1.4).

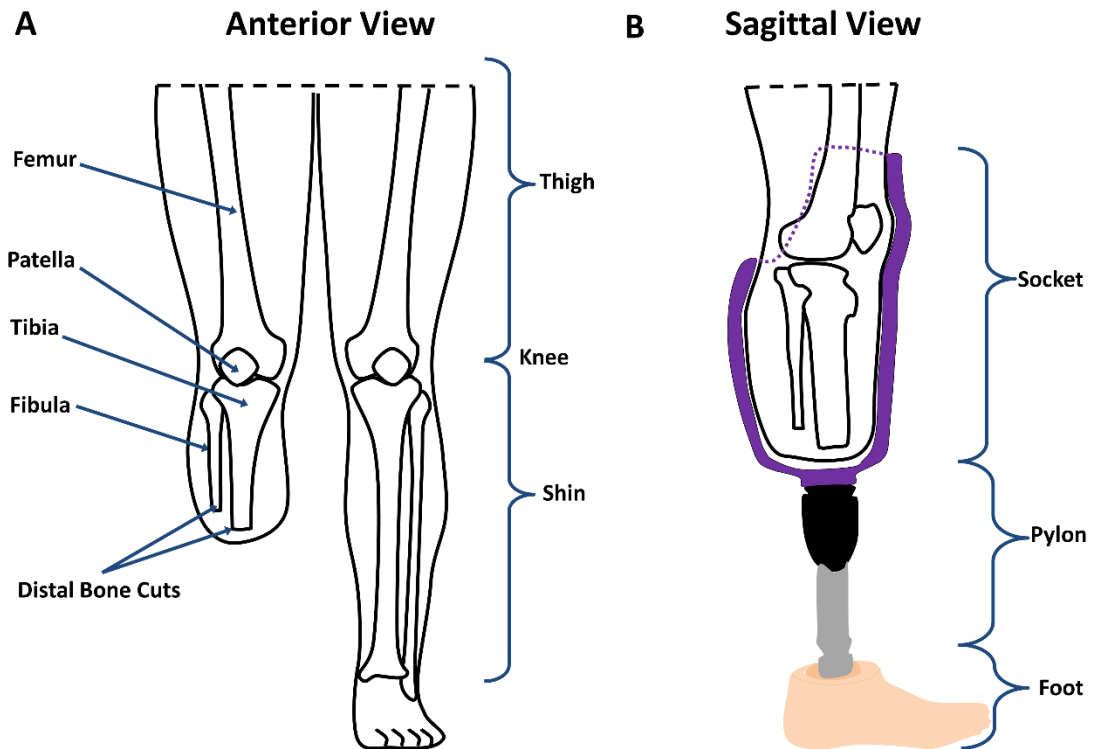


Figure 1.3 Schematics of A: Right leg residual limb, anterior view; B: Right leg residual limb with a transtibial prosthesis

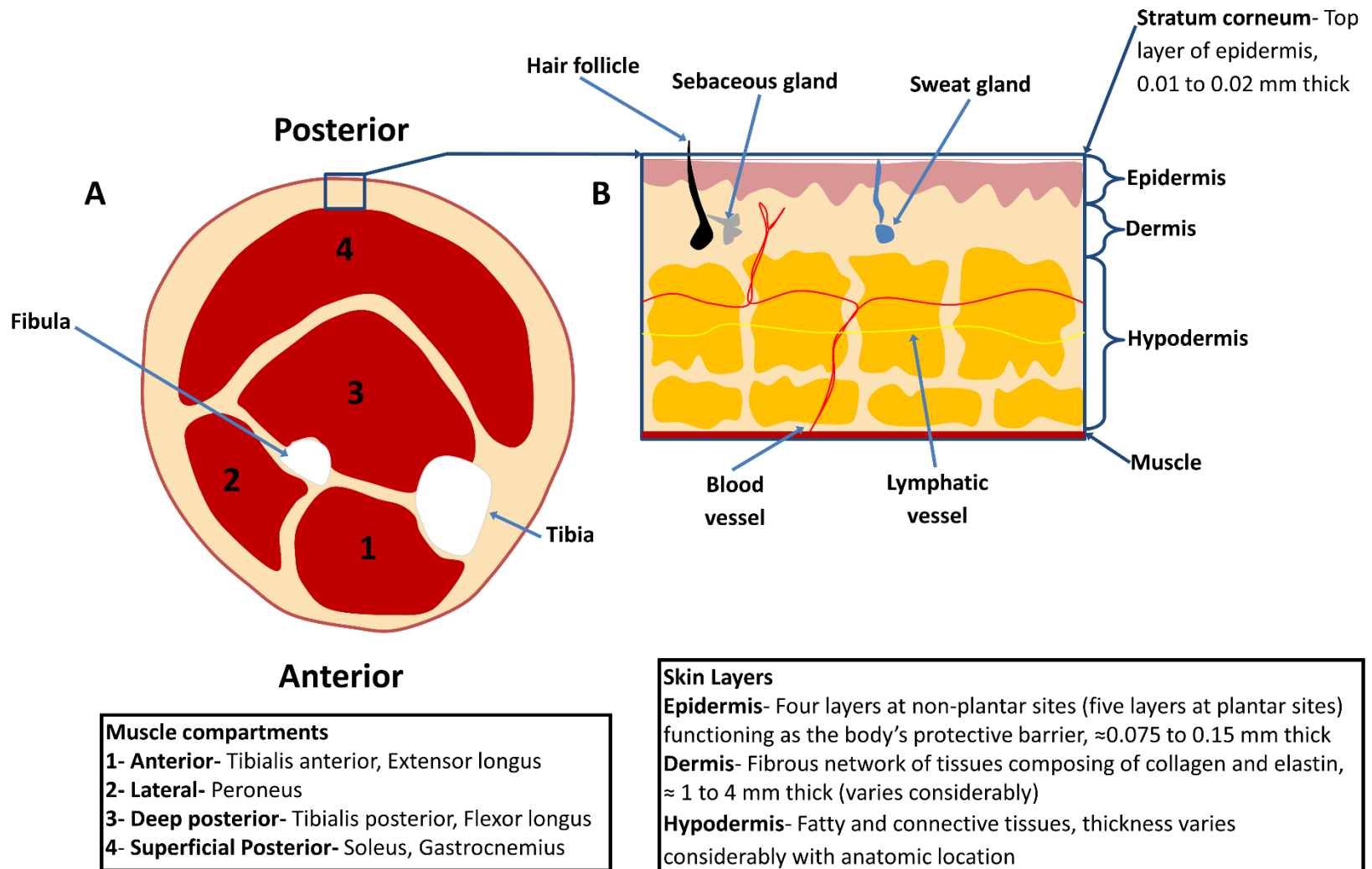
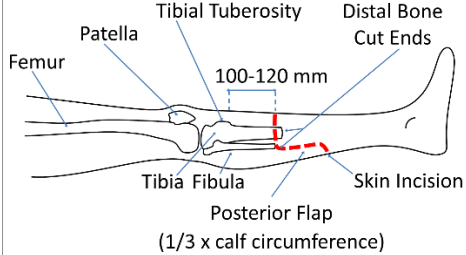
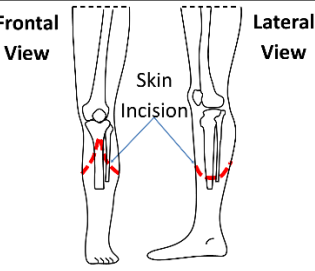
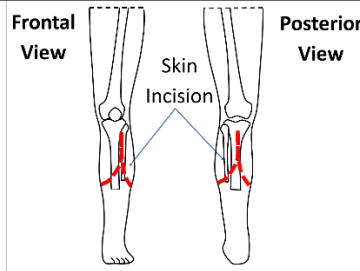
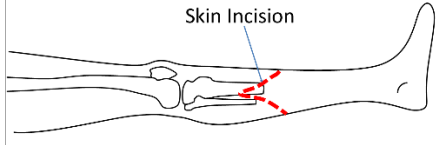


Figure 1.4 A: Schematic transverse slice through the calf of the right lower limb, B: Magnified diagram of the soft tissue layers (thicknesses obtained from [33, 34])

Amputation surgery will have a direct impact on the tolerance of a residual limb to prosthetic loading and there are many surgical considerations to create a functional and quick-healing residual limb. These include the removal of necrotic, infected or non-functional tissues. Furthermore, the operative technique aims to minimise the creation of scar tissue in locations where limb-socket loading will occur. A longer residual limb is advantageous as it can provide an enhanced weight-bearing area and an increased lever arm for transmitting socket-limb loads during movement, in particular during terminal stance [35]. However, residual limb length is limited by two primary factors; i) the condition of the lower limb soft tissues and ii) the length required to accommodate prosthetic componentry. Ideally a residual limb will have adequate soft tissue coverage to avoid bony prominences at the cut ends of the tibia and fibula, which could cause focal areas of pressure, potentially leading to pain and tissue breakdown. Traditionally in BKA, the fibula is cut slightly shorter (≈ 10 mm) than the tibia, to avoid creating a bony prominence. However, a fibula cut too short will result in a conical residuum that is more complex to fit with a prosthetic socket. The ends of the cut bone should be bevelled to avoid generating strain concentrations in the muscle [36]. Muscle compartments are transected and fixed to form a myodesis for optimal strength, shape, tension and circulation to promote wound closure [37]. Traction neurectomy is performed in the posterior flap to position nerves in areas more protected by muscle and soft tissue, where they are less likely to become symptomatic. Nerves can also be injected with a signal blocker to provide temporary pain relief.

The skin incision is designed to allow a flap to be created that will cover the distal end of the residual limb. The main considerations for the skin flap are maximising blood supply and healing, and optimising scar size and location given the intended prosthetic load bearing. To date there is limited consensus on the best approach, with a number of techniques cited in the literature [36] (Table 1.1). Reviews have been carried out to investigate which approach results in the best surgical and rehabilitation outcome [38-41]. In one systematic review involving 309 individuals undergoing amputation, there were no differences between the surgical approaches with respect to wound healing, post-operative infection rate, re-amputation and mobility scores [39].

Table 1.1 Skin incision surgical techniques for below knee amputation

Surgical Technique	Long Posterior (Burgess) Flap	Sagittal Flap	Skew Flap	Fish Mouth Flap
Description	<ul style="list-style-type: none"> - Most common - Skin incision starts 100 -120 mm below tibial tuberosity - Posterior flap preserves additional length of gastrocnemius - Flap wrapped over the residual bones and sutured to the anterior tibial endosteum [36] 	<ul style="list-style-type: none"> - Semi-circular medial and lateral flaps - Brought together over the ends of the tibia and fibula - Anterior-posterior scar 	<ul style="list-style-type: none"> - Anterolateral and posteromedial flaps - Anterior incision junction 20 mm lateral to the tibial crest - Posterior incision junction 180° from the anterior - Anterolateral-posteromedial scar 	<ul style="list-style-type: none"> - Early surgical technique - Semi-circular anterior and posterior skin flaps - Medial-lateral scar on the inferior surface of the residual limb
Approach				
Advantages	<ul style="list-style-type: none"> - Scar positioned anteriorly, on a non weight-bearing surface - Simpler technique [39] 	<ul style="list-style-type: none"> - Suitable if there's insufficient soft tissue to create a long posterior flap [36] - A larger width to length ratio of the sagittal flaps compared to a long posterior flap means less potential for ischaemia [37] 	<ul style="list-style-type: none"> - Well vascularised [37] - Anterior junction position avoids proximity to high pressure areas that may occur during prosthesis use [36] - Can create a more cylindrical residual limb, which is preferable to a bulbous shape when considering prosthetic fitting [36] 	<ul style="list-style-type: none"> - Simple technique but rarely used in modern surgery due to limitations listed below
Limitations	<ul style="list-style-type: none"> - Scar can still be vulnerable during prosthetic load bearing - Requires sufficient viable soft tissue to create the long posterior flap - Poor vascular function may cause problems with wound healing as folded flap can further compromise anterior vascularity [37] 	<ul style="list-style-type: none"> - Scar on distal tip of residuum vulnerable during prosthetic load bearing - More complicated than the long-posterior flap technique 	<ul style="list-style-type: none"> - Scar on distal tip of residuum vulnerable during prosthetic load bearing - More complicated than the long-posterior flap technique 	<ul style="list-style-type: none"> - Scar position across distal tip vulnerable during prosthetic load bearing - Anterior flap vulnerable to ischaemia as posterior calf has increased vascularity compared to the anterior

For any of the surgical methods, the soft tissue wounds will need to heal and in doing so will undergo inflammation, fibroplasia and maturation [42]. Immediately post-amputation, tissue inflammation will occur causing a cascade of responses, including the migration of macrophages to remove debris, perished tissues and harmful bacteria from the wound. After 2 to 3 days, fibroblasts infiltrate the wound region and secrete glycosaminoglycans and collagen, depositing fibrous tissue into the wound bed, thereby increasing its overall stiffness and strength. This fibroplasia phase lasts approximately 3 weeks until maturation begins, where collagen is remodelled and cross-linked further increasing the tissue stiffness and strength. This remodelling process can continue for up to two years post-amputation [42]. The strength and stiffness of the residual scar tissue is an important aspect when considering load-bearing areas for prosthesis design. Six weeks post-injury, scar tissue has been reported to reach approximately 60 % of its intact strength. Strength can increase with remodelling and functional adaptation, although scar tissue will only attain a maximum of approximately 80 % of the pre-injury strength [42]. This wound healing is not specific to amputation surgery and a number of factors will affect the healing process, including the severity of wound, co-morbidities, nutrition and age. Thus, vulnerable tissues of individuals with co-morbidities may inevitably result in a prolonged healing process with an associated increase in post-operative complications.

1.4 Early Rehabilitation & Residuum Tissue Changes

A number of changes can occur in the residual limb following amputation, including its volume, shape and tissue composition. The surgical trauma of amputation will cause a build-up and retention of intracellular and extracellular fluid (oedema) in the soft tissues [43]. Soft elastic compression or rigid plaster cast dressings are often applied to reduce acute oedema. The rigid cast dressings are thought to promote residuum maturation and reduce contractures by positioning the knee in extension. However, their application does occlude access and visualisation of the wound [44, 45].

An individual will generally spend around two weeks on the ward post-amputation to enable monitoring of their condition and then allow time to adjust, begin rehabilitation and ensure health and safety when discharged [46] (Figure 1.5).

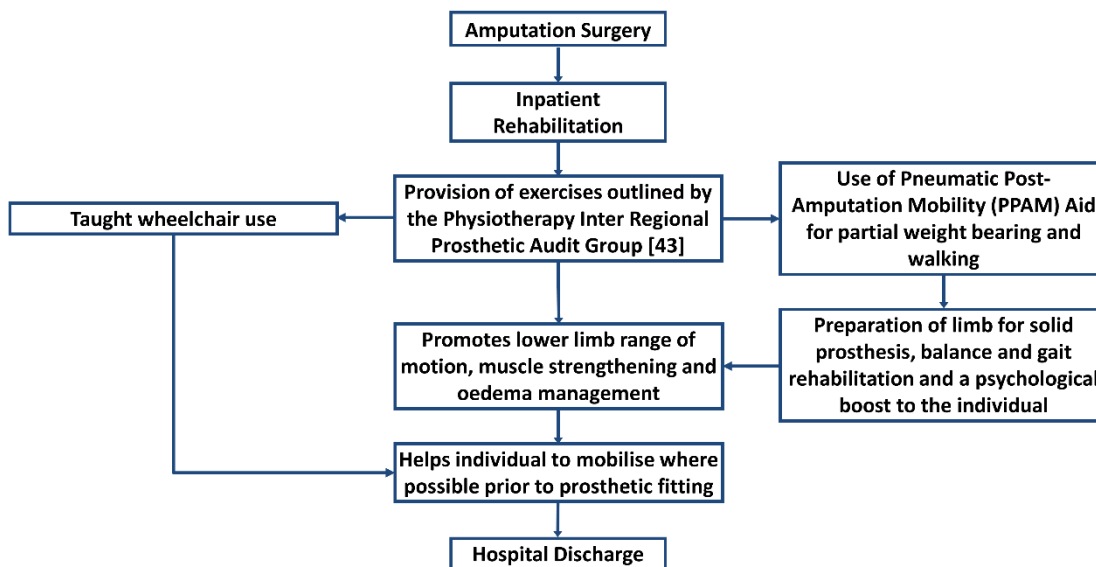


Figure 1.5 Early inpatient post-amputation rehabilitation process

Despite these interventions, the muscles of the amputated limb will inevitably atrophy, reducing in size and strength post-amputation due to denervation and disuse. The former occurs during amputation when nerve supplies are severed and the central nervous system cannot innervate the associated muscle fibres. Disused muscle will eventually be replaced by fat or fibrous tissue [47, 48]. Magnetic Resonance Imaging (MRI) has previously been used to observe the morphological changes of the transtibial residual limb of three participants 2, 6 and 28 weeks post-amputation [49]. The study reported an initial rapid and then slower decrease in both overall and medial muscular cross-sectional area. The lateral muscle group displayed the initial rapid decrease then increased, suggesting adaptation to support prosthetic suspension. The MRI images also depicted an increase in subcutaneous fat.

This observation of muscle atrophy was also observed by a Computed Tomography (CT) study [50]. Indeed, the CT study involving seven ambulatory individuals with a transtibial amputation revealed a mean \pm Standard Deviation (SD) reduction in muscle area in their residual limbs (compared to intact limbs) of 104 ± 33 %.

The Pneumatic Post-Amputation Mobility (PPAM) aid is used in the early stages of lower limb amputation rehabilitation from approximately seven days post-surgery, dependent on wound healing, as a partial weight bearing and walking aid [51-53]. It consists of two pneumatic bags, inflated to ≈ 5 kPa (40 mmHg) prior to weight bearing, enclosed by an adjustable frame with a distal rubber foot rocker [52, 53] (Figure 1.6). In a study involving 66 participants with unhealed dysvascular wounds, the use of a PPAM aid for mobilisation supported wound healing in the majority of the participants (74 %) within three weeks [54]. However, there are associated clinical guidelines for early mobilisation of unhealed dysvascular transtibial residual limbs, which recommends that if over a 2 week period there is a deterioration of >10 %, then use of the PPAM aid should be interrupted [55].

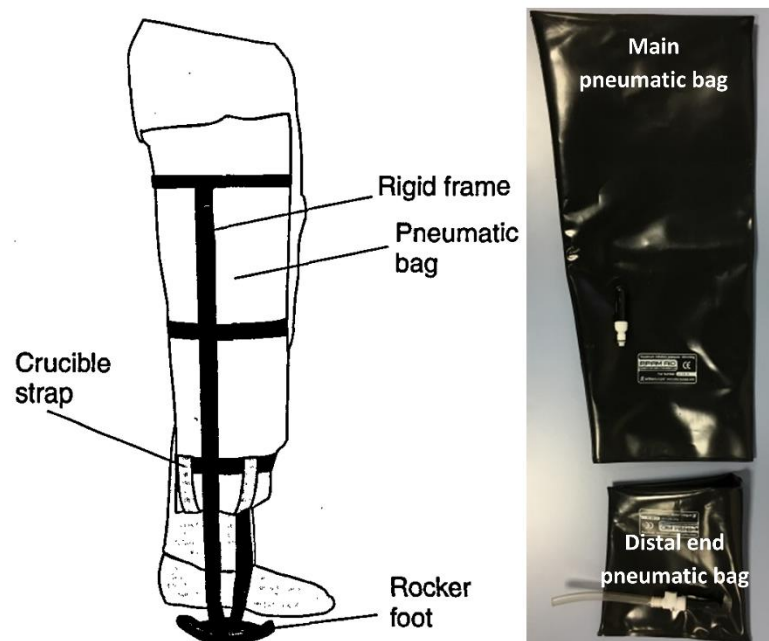


Figure 1.6 Left: Diagram of PPAM Aid [53], Right: Photo of Pneumatic Post-Amputation Mobility (PPAM) Aid main pneumatic bag (top) and distal end pneumatic bag (bottom)

Post-operative volume changes have been studied to determine appropriate prosthetic fitting timescales [43, 49]. Timing for definitive prosthetic fitting involves balancing the benefits of early rehabilitation with the stabilisation of the residual limb. Early fitting has potential advantages of quicker gait training and greater functional independence.

However, volume changes after early fitting can result in loss of fit and discomfort, requiring refitting of the prosthesis. Volume changes also occur throughout the day due to a number of factors, such as nutrition, fluid intake, activity levels and temperature [56-58]. A volumetric study [43] made the recommendation that an inexpensive temporary prosthesis should be fitted as early as possible prior to fitting a definitive prosthesis approximately 4 months post-amputation, and thereafter diurnal volume fluctuations must be accommodated by the socket design.

Transient volume changes can also occur due to muscle activity, blood flow and hydration. Indeed fluid volume changes have been observed ranging from -15.6 to +12 % per hour, with participants with PVD exhibiting major fluid loss [56, 58, 59]. Although interstitial fluid movement is expected to represent the major source of diurnal fluctuations, its measurement does not directly reflect the absolute residual limb volume, which has been observed to range from -4.4 to +10.9 % [60-62]. These volumetric variations can cause pain, discomfort and reduced mobility for prosthetic limb users [58, 63]. An increase in residuum volume can cause problems with obstruction of blood supply potentially leading to tissue damage. Conversely, volume reduction can lead to pain and tissue damage through increased pistoning (causing shearing) and elevated end-bearing. Research investigating the performance of transtibial sockets, produced using computer aided design and manufacture, concluded that volume changes as small as 1% can be clinically detectable [64].

Daily variations in the residual limb volume can sometimes be managed by the addition or removal of socks [56, 57, 61] or elevated vacuum devices [65]. The use of socks provides a simple solution but relies on patient perception, which will be affected in those with impaired sensation. Socks may also be less effective in cases where the volume variation is not uniform across the socket contact surface/area. Elevated vacuum suspension is thought to improve fluid retention in the lower limb during the day, by creating lower interstitial pressures inside the residual limb, as well as improving perfusion and preserving skin barrier function [65, 66].

Studies investigating the residual limb variation often select participants that are considered to have reached a stable volume and shape to exclude changes associated with post-operative oedema [56, 58, 59, 67]. Accordingly studies have included participants who are at least one year post-amputation [56, 59, 65, 68] to at least eighteen months post-amputation [63]. However, due to small cohorts and large heterogeneity in the patients recruited, definitive conclusions have not been possible.

1.5 Residual Limb Tissue Health

Newly reconstructed residual limb tissues have not been conditioned to tolerate load and thus are vulnerable to tissue damage during daily living activities using a prosthetic device. Previous studies have observed varying prevalence of skin problems in individuals with lower limb amputation, ranging from 36 to 66 % [69-71], with areas of scar tissue identified as being particularly vulnerable to damage [72]. The variability is representative of both the large heterogeneity in cohorts with amputation and the range of study methodologies. For example, one study reporting a 63 % prevalence employed a participant questionnaire but no clinical assessment, which may have resulted in an over-estimation of values [70]. Studies may have been subjected to selection bias as those visiting prosthetic centres or participating in the questionnaires might have been more likely to present skin problems. Observed prevalence is dependent on the time window for analysis, with point prevalence being cited as 36 % of participants, compared to a life time prevalence of 66 % [71]. A number of intrinsic and extrinsic factors are also thought to play a role in tissue viability and increase the risk of skin damage [73, 74] (Table 1.2). Indeed the prevalence of skin problems in individuals with transtibial amputation were reported to be four times higher than with transfemoral AKA [69], potentially due to the greater number of bony prominences in the transtibial compared to transfemoral residuum. Although, this increase in skin problems may also be attributed with the former groups' higher activity levels.

Table 1.2 Examples of Intrinsic and extrinsic factors that increase the risk of skin damage at the residuum-prosthesis interface

Intrinsic Factors	Extrinsic Factors
Reduction in skin elasticity, stiffness and structural integrity with age [75]	Seasonal increases in temperature and humidity
Decreased vascular perfusion and sensation	Geographical increases in temperature and humidity
Bony prominences resulting in higher pressures and shear forces	Higher activity levels
Changes in socket fit and prosthesis alignment, from residuum volume loss	

Transcutaneous oxygen tension (T_cPO_2) measurements have previously been used to assess dermal tissue health, in particular as a clinical indicator of amputation level to ensure adequate perfusion for healing [76-78]. Baseline values of healthy individuals are generally accepted to range from approximately 48 to 95 mmHg [79-81]. Thus tissue sites with levels below approximately 35 mmHg were considered to be at risk of poor healing post-amputation [76-78]. Rink et al collected T_cPO_2 measurements from participants with and without amputation to compare tissue status in residual and intact limbs at rest and with a prosthetic liner donned [82]. Laser doppler flowmetry and Transepidermal Water Loss (TEWL) were also measured to evaluate local perfusion and stratum corneum function, respectively. Lower baseline values of T_cPO_2 and TEWL were observed in residual limbs indicating an increased susceptibility of these tissues to damage [82].

1.6 Research Motivation & Overarching Aim

Currently there is little quantitative knowledge characterising residual limb soft tissue adaptation and tolerance to prosthetic loading. Indeed, it is critical to understand how loading affects these vulnerable tissues during rehabilitation and how they can adapt over time. This knowledge will help lead to more informed rehabilitation protocols and prosthetic use, assisting tissue adaptation to tolerate prosthetic loading and reducing the risk of tissue damage in clinical and community settings.

Various bioengineering tools are available to monitor the status and the effective tolerance to loading of dermal tissues [34, 83]. To date, they have been used in a few studies to assess tissues prior to amputation and residuum tissues at rest, and during periods of loading via prosthetic liners and a modified below knee socket for intact limbs [76-78, 82, 84]. However, there is a need to develop an array of measurement techniques to characterise adaptation and assess both the biomechanical and physiological response of soft tissues under representative prosthetic loading [85].

The global aim of the present research is:

“To evaluate soft tissue health and tolerance of residual and intact limbs under representative prosthetic loads”

The following chapter presents a critique of the scientific literature in this area. This knowledge of conditions at the residuum-socket interface, and soft tissue damage and tolerance was used to define the specific research questions, aims and objectives.

2 Literature Review

The literature review was designed to provide a comprehensive understanding of the conditions occurring at the residual limb-prosthetic socket interface. It focused on evidence involving the physiology of the residual limb and soft tissues, soft tissue viability and associated biophysical measures. This resulted in a critique of the identified prior research and a series of research objectives was established for the present thesis.

2.1 Residual Limb-Prosthesis Interface

This section provides a brief overview of the production of a transtibial prosthetic socket with consideration of the microclimate, mechanical loading conditions at the residuum-socket interface and internal mechanics.

2.1.1 Prosthetic Sockets and Suspension Mechanisms

A prosthetic socket provides the mechanical coupling between the person and prosthesis and its design and manufacture conventionally involves casting, rectification, fabrication, fitting and alignment in an iterative and labour-intensive process (Figure 2.1).

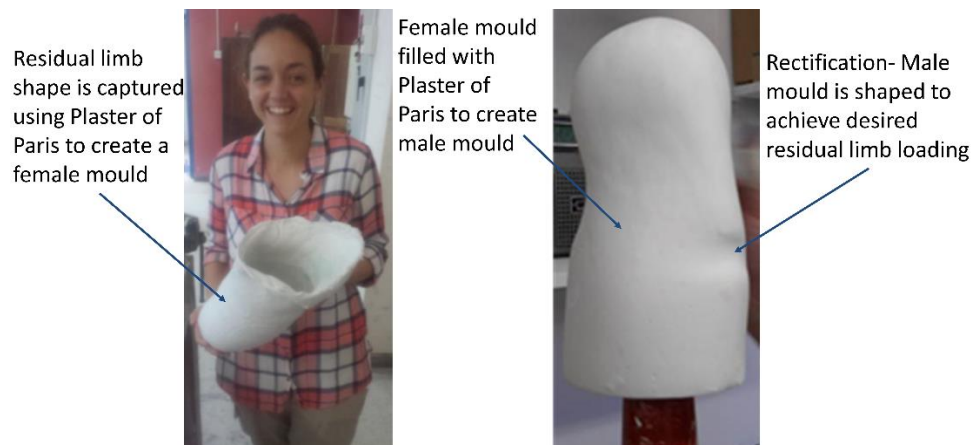


Figure 2.1 Negative (left) and positive plaster casts (right), and rectification for prosthetic socket design

When creating a transtibial prosthetic socket important landmarks, such as the tibial tuberosity, patellar tendon and sides of the tibia will be marked on the residuum, which are transferred to the female mould. During casting the prosthetist will begin moulding the cast to the required shape for loading, with due consideration to any muscle contractions [86]. A male mould will then be produced and locally modified with 'rectifications' to achieve the final shape. Trial sockets are usually produced using a transparent polymer to allow the prosthetist to inspect the limb-socket interface, compare rectifications to anatomical landmarks, and observe any blanching in order to identify potential areas of high pressure.

A series of trial fittings with local adjustments are used to achieve a definitive socket shape that can then be laminated or draped for the final socket. Typically, an iterative approach is used with several new or adjusted sockets as the residuum matures and stabilises to a more consistent shape. Two studies based in the US and Sweden, respectively, involved the interviewing of 960 individuals with amputations ($\approx 40\%$ below knee) and the surveying of 70 individuals with unilateral transfemoral amputation, reported an average of 9 separate visits to a prosthetist per year [87, 88].

Liners are generally worn inside the socket to provide a softer material interface with the residual limb, reducing pressure gradients and providing some tolerance to volume changes. These may take the form of a generically sized elastomer (silicone or polyurethane) sleeves, which are rolled over the residuum, or a personalised, removable foam liner (e.g. EVA or Pelite) pre-formed during socket fabrication.

An optimal socket will expedite biomechanical adaptation of the soft tissues to enable comfortable, stable and efficient load transfer. In addition to reduced comfort, an ill-fitting socket can result in extended rehabilitation periods, gait compensations at a greater metabolic cost and secondary musculoskeletal conditions, such as lower back pain and contralateral limb osteoarthritis. A socket will be designed to preferentially load areas of the residual limb considered to be pressure tolerant as opposed to the more intolerant areas [89, 90] (Table 2.1) (Figure 2.2).

Table 2.1 Areas of the transtibial residual limb considered tolerant and intolerant to pressure [89]

Common Pressure Tolerant Areas	Common Pressure Intolerant Areas
1. Supracondylar	7. Femoral Condyles
2. Suprapatellar	8. Patella
3. Popliteal Fossa	9. Fibula head
4. Patellar Tendon	10. Crest of Tibia
5. Either side of tibia	11. Cut end of Tibia and Fibula
6. Lateral shaft of Fibula	12. Hamstrings
	-. Scar tissue or neuroma

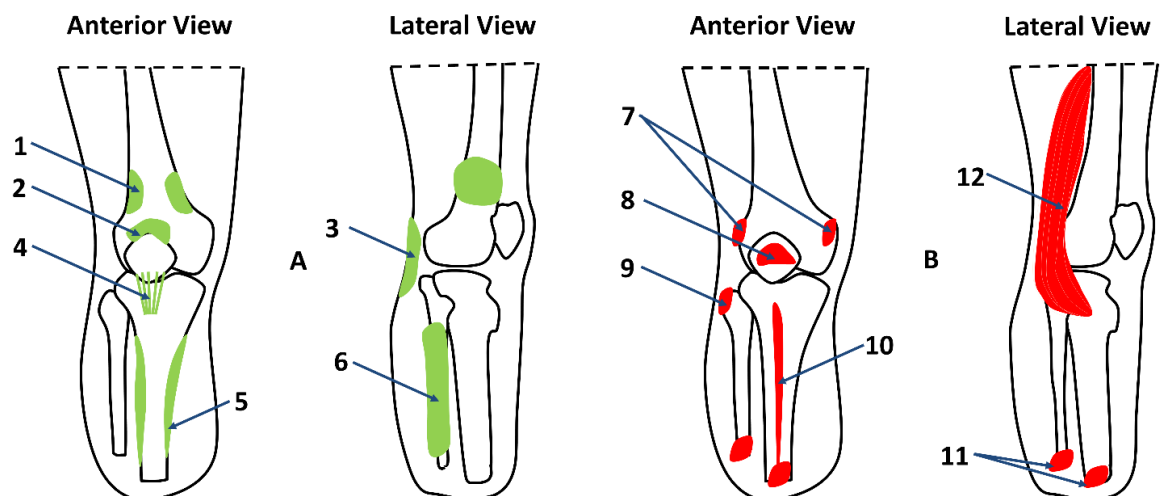


Figure 2.2 Pressure tolerant (A) and intolerant (B) areas of the transtibial residual limb (NOTE: Numbers refer to Table 2.1)

A number of different socket designs exist dependent on how they apply load to the residual limb for weight bearing (Table 2.2). Each design incorporates a suspension mechanism, which forms a critical coupling between the socket and prosthesis. It is important to eliminate pistoning and improve rotational stability between the socket and residual limb, as far as possible, to facilitate effective gait and protect tissue integrity.

Table 2.2 Transtibial prosthetic sockets and suspension mechanisms

Socket	Loading Area(s)	Suspension Mechanism(s)	Advantages	Limitations
Patellar Tendon Bearing (PTB)	- Primarily the anterior proximal region (patellar tendon)	1. Belt- Tightened around distal part of thigh 2. Supracondylar- Medial and lateral compression above the femoral condyles [91] 3. Supracondylar/Suprapatellar - Generated at the medial and lateral femoral condyles and patellar [91]	- Easier to don/doff particularly if a person has visual or sensory disturbances [92, 93] - Increased knee stability with supracondylar /suprapatellar suspension [93] - Easier fabrication [94] - Less expensive socket manufacture [95]	- Heavier than TSB sockets [94] - Can cause pistoning [94] - Suspension mechanisms can be restrictive in knee flexion [93]
Total Surface Bearing (TSB)	Entire residual limb is used to evenly distribute load bearing	1. Pin/Lock- Pin at distal part of silicone liner locks into mechanisms of prosthetic components 2. Suction- Adhesion/friction between tight silicone liner and residual limb	- Reduced pistoning [94, 96] - Total contact with residual limb reducing pressures and can assist proprioception [94] - Greater activity levels and satisfaction in active users, users with traumatic cause of amputation and younger users [92] - Lighter [94] - Can be effective in cases where there is excessive soft tissue, particularly at the distal residual limb [97]	- Less suitable early post-amputation or for individuals on dialysis due to volume changes [93] - Can be difficult to don/doff [92, 93] - Silicone liner may cause increased perspiration [92]

2.1.2 Microclimate

The environment at the interface is important to maintain tissue integrity, comfort and function for an individual with amputation. Microclimate in this context refers to the temperature and humidity at the residual limb-prosthesis interface [98].

Research has revealed elevated temperature and humidity at the residual limb-socket interface [99]. Contacting surfaces such as socks, liners and prosthetic sockets can increase the skin temperature and moisture particularly if they are non-permeable in nature. It is also important to consider that people with amputation have less body surface area for temperature management [100]. Microclimate can also be influenced by several physiological and pathological factors associated with individuals with amputation, such as stress, pain and co-morbidities.

A raised temperature is thought to increase the susceptibility to tissue damage by reducing the stiffness and strength of the outer layer of epidermis, the stratum corneum, with, for example, a four-fold reduction in mechanical strength at 35°C compared to 30°C [98]. Increasing temperature will also increase metabolic demands, thereby reducing the perfusion threshold for ischaemia [98, 101]. By contrast, decreased peripheral temperatures indicate poor peripheral perfusion [101]. When the ambient humidity is high, the rate of evaporative heat loss will be reduced causing an accumulation on the skin. Moisture can reduce the skin's resilience to pressure and shear by weakening the collagen crosslinks in the dermis, reducing the stiffness of the stratum corneum and increasing the Coefficient of Friction (COF) at the interface [98, 102]. Elevated microclimate conditions will also decrease the comfort of prosthetic users. Indeed, in a cross-sectional survey of 121 individuals with lower limb amputation, 66 % reported that sweating interfered with their activities of daily living [103].

2.1.3 Mechanical Conditions at the Interface

During weight bearing loads will be transmitted from the socket to the residual limb in the form of pressure (normal stress) and external shear stress generating compressive and shear strain.

Pressure will occur due to forces applied from the socket perpendicular to the surface of the residuum. External shear stress will be generated when donning the socket and under axial and torsional loading applied during the stance phase of the gait cycle. Additional cyclic longitudinal interface shear stress is likely to be generated by sagittal plane moments at the heel-strike and toe-off instants of gait [104]. Friction is the force that resists the relative motion between two contacting objects and is involved in the development of external shear at the surface [105]. It contributes to the production of shear stresses when external forces generate a relative displacement between the residual bone and prosthesis. Friction (tangential force) is a product of perpendicular force and the COF between the contacting surfaces, the latter of which will vary for different material combinations and lubrication conditions. As an example, the use of a rough socket or liner material, or the presence of elevated moisture at the interface will increase the COF [98, 102]. Indeed, one study investigating variations in both the hydration states of the forearm of participants and the contacting fabric reported a strong positive linear correlation between skin moisture and COF [102]. However, it is important to note that elevating moisture beyond a certain level may produce a lubricating film. Few studies have examined the static and dynamic COF between the skin and prosthetic components. Of these, Sanders et al performed static COF measurements between skin, socks and socket and liner materials, while Zhang and Mak later examined similar dynamic COF tests [106, 107]. By contrast, the effect of microclimate at the interface on COF has not been reported [102]. Increased quantitative knowledge of prosthetic liner characteristics and COF at the interface under differing conditions may assist in clinical selection of prosthetic componentry.

A stiff coupling between the residual limb and socket is desired to avoid in-socket motion and instability. As an example, decoupling of the socket from the residual limb can result in movement at the interface, physical rubbing and skin damage. Conversely, coupling that is too stiff could result in high pressure transmitted to tissues potentially causing discomfort and damage.

A number of factors will affect this coupling including:

- The composition and geometry of the reconstructed covering of soft tissues over the amputated bone (as discussed in Section 1.3) [36].
- Rectifications made to the socket to accommodate the pressure tolerant and intolerant areas of the residual limb [89, 90] (Table 2.1) (Figure 2.2).
- Variation in residual limb volume, associated both with short-term diurnal fluctuations and long-term losses (previously discussed in Section 1.4), can create a considerable challenge for the prosthetist to maintain a comfortable and functional socket fit.

Studies have measured or predicted interface pressures and, in a few cases, shear stresses at a various residuum sites during both static weight bearing and gait to clarify the loading conditions at the residuum-socket interface [53, 60, 97, 108-112] (Figure 2.3 to Figure 2.5 and Table 2.3 to Table 2.4). Knowledge of interface pressures and shear stresses in combination with biophysical measurements will help investigate soft tissue tolerance under prosthetic loading.

Table 2.3 Residual limb measurement areas used during interface pressure and shear studies

Measurement Areas	
1. Lateral and Medial Condyles	10. Lateral Mid-Limb
2. Patellar Tendon	11. Lateral Distal
3. Tibial Tubercles	12. Lateral and Medial Gastrocnemius
4. Antero Proximal	13. Posterior Proximal
5. Antero Mid-Limb	14. Posterior Mid-Limb
6. Antero Distal	15. Posterior Distal
7. Distal End	16. Medial Proximal
8. Popliteal Area	17. Medial Mid-Limb
9. Lateral Proximal	18. Medial Distal

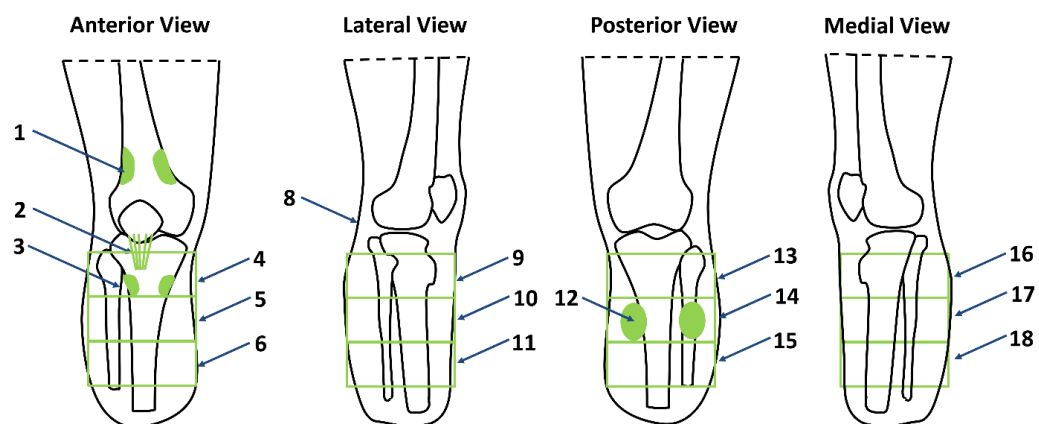


Figure 2.3 Residual limb areas used for measuring interface pressures and shear stresses

Table 2.4 Measured interface pressure and shear at the residual limb-socket interface (NOTE: Participants were individuals with transtibial amputation unless otherwise stated, Measurement Site(s) refer to Table 3 and Figure 13, L = Lateral and M = Medial)

Study	Aim	Participants	Measurement Site(s)	Measurement Characteristics
[108]	Investigation of pressure and shear stress at multiple points of the residual limb during standing and self-selected speed walking (15 m walkway)	N=5, Aged 43-75 Sockets- 4 PTB, 1 TSB	- 1, 2 - L and M 6 - 8, 12	Triaxial force transducers: - Shear components measured using magnetoresistors - Normal force component measured using strain gauge diaphragm - Diameter 16 mm x 4.9 mm thickness, weight <5 g - Total RMS error is 1.75% or 41.25 mmHg (5.5 kPa) for pressure and 6% or 18.75 mmHg (2.5 kPa) for shear (whichever is greater)
[113]	Comparison of measured and predicted interface pressure and stress during gait as in [108]	N=1 Established BKA Socket- PTB	- 1, 2 - L and M 6 - 7, 8, 12	Same Triaxial force transducers as used in study [108]
[53]	Comparison of PPAM and Amputee Mobility Aid (AMA) early mobility aids during standing and supported walking using parallel bars (four lengths)	N=10 males, N=2 females Aged 45-84 Aetiology- 7 PVD, 4 PVD plus diabetes, 1 trauma 7 to 45 days post-amputation	- 7	Fluid-filled sensor at interface and piezoelectric transducer: - Linearity: $r=0.99$ - Calibration factor varied <2.5% over 10 months
[109]	Comparison of within socket interface pressures and shear stresses during weight bearing and walking	N=2 males Aetiology- Trauma ≥ 2 years post-amputation Sockets- PTB	- L and M 4-6 - 8, 9-11, 14-15	Instrumented PTB socket: - Custom made for study - Strain-gauge transducers
[60]	Comparison of daily and long-term (6 months) differences in pressure and shear during self-selected speed walking (20.8 m walkway)	N=7 males, N=1 female Aged 28-61 Aetiology- Trauma 2 to 54 years post-amputation Sockets- PTB	- 1, 3 - L and M 4 & 6 - 8, 14, 15	Instrumented PTB socket: - Custom made for study - Strain-gauge transducers - Sock ply not changed throughout 6-month study

Study	Aim	Participants	Measurement Site(s)	Method of Measurement
[110]	Characterise mechanical conditions after donning socket and during loadbearing	N=1 female	- 4-6 - 13-15	Flexible pressure mats based on piezoresistivity: - Thickness = 0.3 mm, Sensor area: 1.024 cm ² - Accuracy $\pm 10\%$ - Hysteresis $\pm 5\%$ - Non-linearity $\pm 1.5\%$
[111]	Pilot self-selected walking test for pressure and shear sensor system	N=1 male Aged 28 Knee disarticulation amputation Since \approx birth	- 4, 7, 13	Flexible TRIPS sensor system, developed at the Southampton University: - Capacitive measurement - Wireless transmission - Linearity error $< 3.8\%$ - 6.75 mmHg (0.9 kPa) pressure and 1.5 mmHg (0.2 kPa) shear resolution - Hysteresis error 15% pressure and 8% shear
[97]	Comparison of interface pressure when using a PTB and TSB prosthesis during self-selected speed walking on level ground, a ramp and stairs (5 trials per condition)	N=1 female Aged 25 Bulbous stump with excessive soft tissue distally 2 years post-amputation Socket- previously had PTB, used TSB socket for 1 month prior to study	- 4-6 - 9-11 - 13-15 - 16-18	- Four F-socket Tekscan sensors - Calibrated prior to use using a pneumatic bladder
[112]	Investigate design of 3D printed socket inserts for monitoring limb-socket interactions of prosthesis users	N=1 male Aged 74 Aetiology- Trauma 38 years post-amputation Socket- New uniformly enlarged TSB to accommodate insert	- 4 - L 6 - 13 - 15	- Four Force Sensing Resistors (model FSR 402, Interlink Electronics, California) - 18.28 mm diameter, 0.48 mm thickness

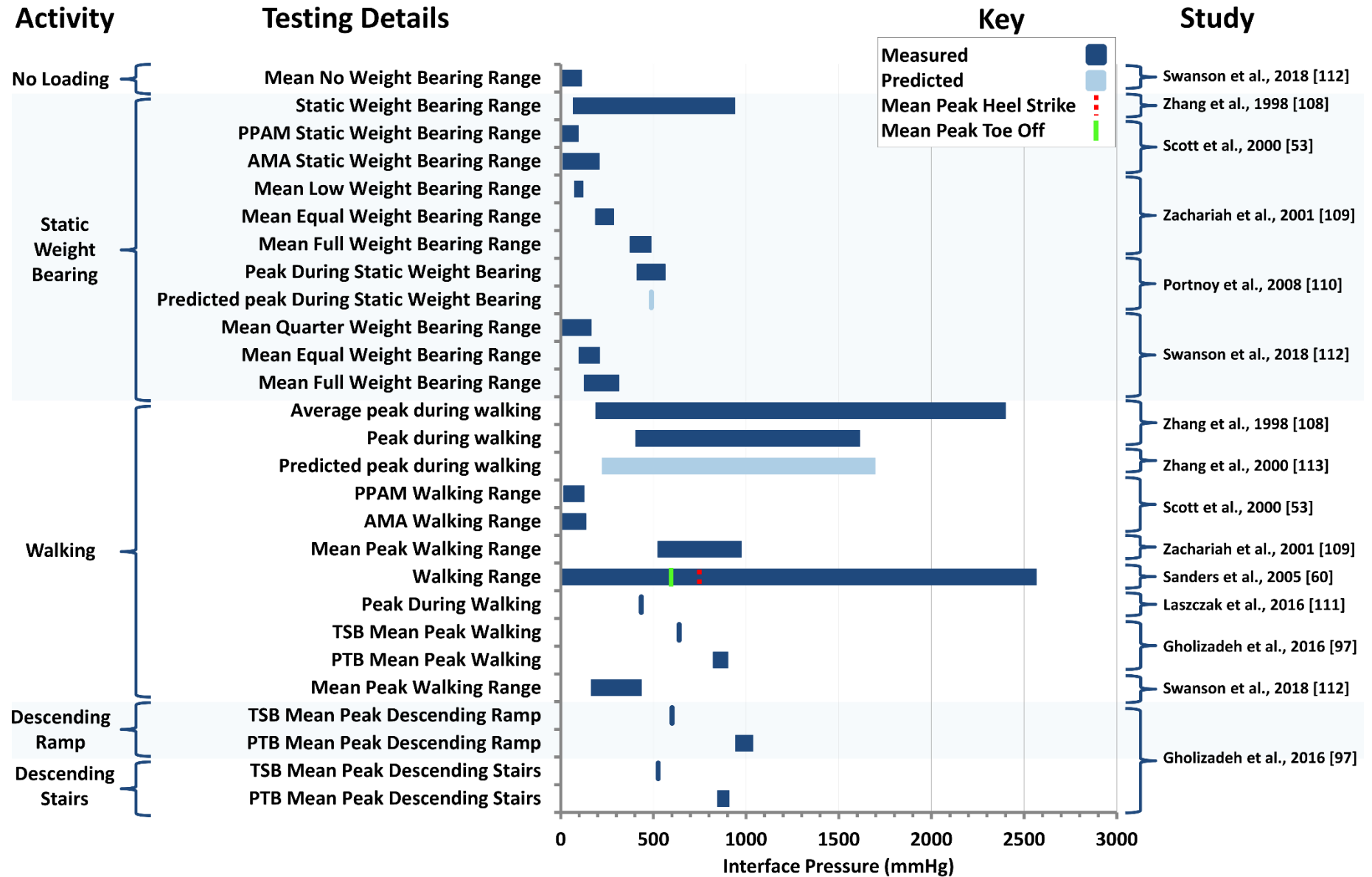


Figure 2.4 Summary of measured and predicted interface pressures in previous studies, during static weight bearing and walking, Note: 7.5 mmHg≈ 1 kPa

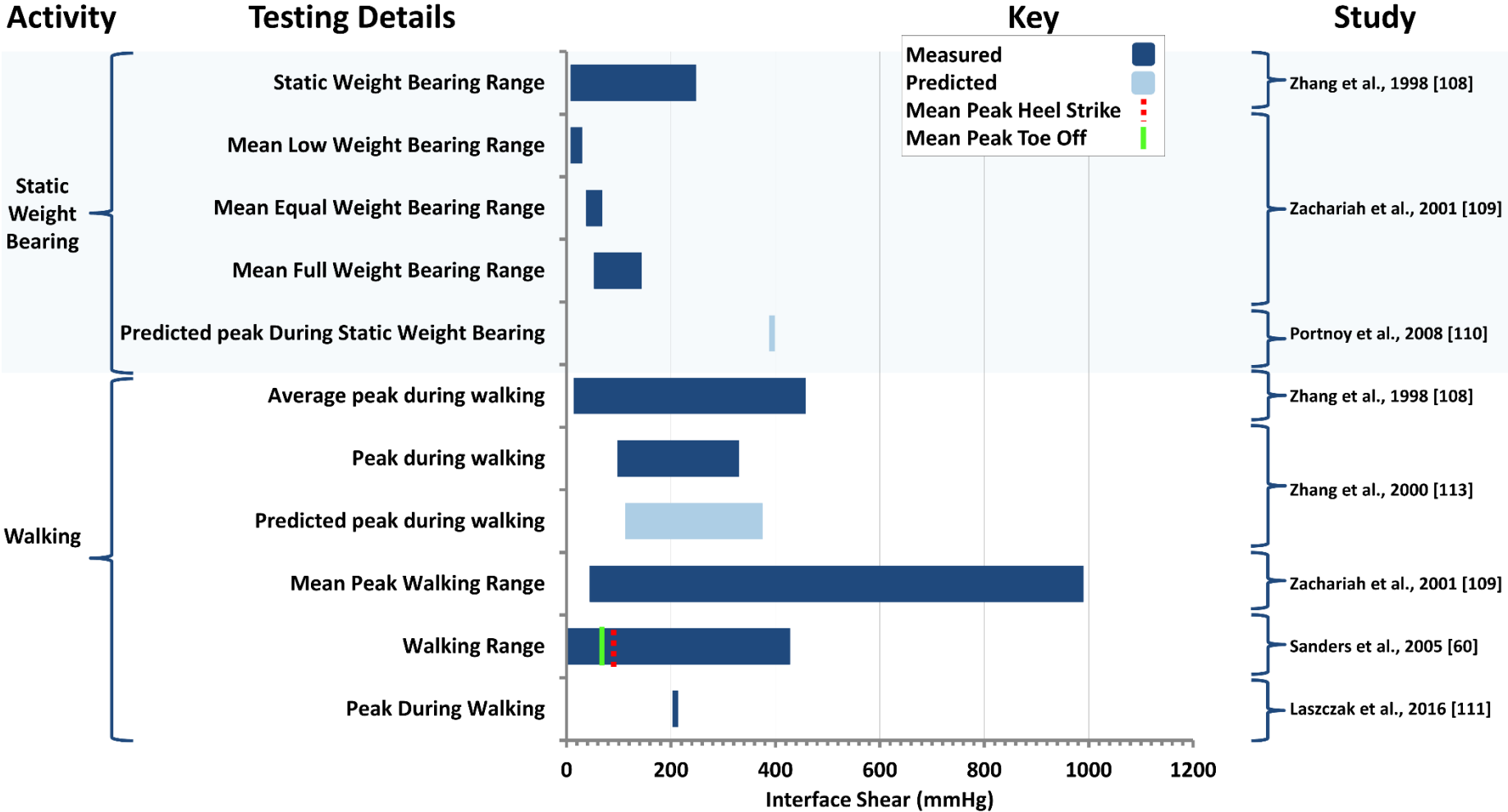


Figure 2.5 Summary of measured and predicted interface shear in previous studies, during static weight bearing and walking, Note: 7.5 mmHg≈ 1 kPa

Both Figures 2.4 and 2.5 reveal the considerable variation in measured pressures and shear stresses, which can be attributed to a host of variables including participant weight, gait, surgical technique, residual limb size, muscle atrophy, socket design and position of sensors. In addition, specific measurement sensors and approaches will be prone to different errors and while in-situ measurement devices could cause local stress concentrations thereby altering interface loading. The number of years post-amputation would certainly have influenced the measured results [60, 108]. As an example, more experienced prosthesis users with more adapted and tolerant tissues at the interface may have greater confidence when weight bearing and walk faster or more symmetrically, resulting in higher measured pressures and shear stresses. By contrast, the reduced pressures observed when using the PPAM aid and AMA, could be attributed to the use of parallel bars and reduced confidence during early rehabilitation, resulting in partial weight bearing. Walking in a laboratory environment and the use of an unfamiliar socket could affect a participant's confidence and alter gait. The highest recorded pressure values of ≈ 2500 mmHg (≈ 333 kPa) were observed during a 6 month study comparing daily and long-term pressure and shear values [60]. It was noted that unlike in other studies, a large number of sites were measured and the use and thickness of interface socks was not adjusted throughout the study and increased pressures correlated with a reduction in residual limb volume [60]. Higher pressures could also have been associated with stumbling events during gait, which might have been detected with the incorporation of force plates into the test protocols.

Zhang and Roberts compared interface pressures and shear stresses predicted by Finite Element Analysis (FEA) and measured experimentally using triaxial force sensors at 8 sites [113] (Table 2.4, Figure 2.4, Figure 2.5). A PTB socket was modelled donned upon a residual limb, with soft tissue and bone geometry captured using a digitiser and x-rays, respectively. Material properties were assumed to be isotropic and linearly elastic. Predicted results were found to be on average 11 % lower than experimental measurements. This could be due to the series of assumptions in the model implemented to simplify the complex residual limb-socket interface. These include a single combined soft tissue 'bulk' model which would not reflect the multiple, inhomogeneous, anisotropic material structures and a Coulomb 'stick slip' COF at the interface as opposed to multiple contact asperities between structures.

In summary, the interface conditions between the residuum and the socket have been characterised using a variety of sensor arrays, based on various physical principles [108-110, 112]. For simplicity this research has been focused on static prosthetic loading with results varying considerably from ≈ 4 to 938 mmHg (0.5 to 125 kPa) and ≈ 8 to 389 mmHg (1 to 52 kPa) for pressure and shear stress, respectively. This range spans three orders of magnitude and is largely dependent on a number of factors including individual socket design, sensor characteristics and measurement location as well as a participant's weight bearing tolerance and confidence. Furthermore, it must be recognised that interface measurements will not necessarily represent the internal conditions within the residuum soft tissues

2.1.4 Internal Mechanics of the Residual Limb

Prosthetic loading will cause compression of the residual limb tissues, which are made up of different structures with a range of mechanical stiffnesses. At a constant residuum volume the resulting deformation of the tissue layers will produce internal shear strains, which can be characterised by deviatoric strains.

Residual limb-socket interactions have been studied predictively using FEA to enable improved understanding of the mechanical state of the underlying tissues. This approach offers the opportunity for analysis and optimisation of medical devices, specifically lower-limb prostheses, that interact with the soft tissues. For more representative predictions a model should replicate the biological system. However, such models are highly complex requiring knowledge of anatomy and tissue characteristics accounting for the different behaviour and interactions between soft tissue layers, resulting in the inevitable high computing costs. Technologies such as MRI have enabled experimental-numerical approaches to obtain information of the detailed geometry of the residuum tissues distinguishing between muscles, tendons, ligaments and adipose tissue [110, 114-117]. However, many of the models are simplified and assign a uniform set of mechanical parameters to a single body representing all tissue structures. The development of models over the last two decades, for prosthetic applications, has been captured in a recent systematic review highlighting approaches to this highly complex mathematical problem [118]. Models have advanced from linear elastic simplifications to incorporating hyperelastic and viscoelastic material properties [119], although still assuming isotropy and within-tissue homogeneity [120]. A degree of model simplification is inevitable and careful consideration is required to match a model complexity to the questions it is designed to answer [121, 122]. Comparative analysis, for example, comparing load distributions for different socket designs, does not require a highly biofidelic model [122]. Simpler models offer considerable time and computational savings enabling further parametric studies to be performed.

In contrast, when considering soft tissue damage risk a more biofidelic model including representative soft tissue material properties is required [122]. A recent example includes a study using diffusion tensor MRI to enable segmentation of individual muscles and their fibre direction to create a detailed subject-specific residuum model [117]. It used nonlinear, hyperelastic material properties to predict internal muscle Von Mises stress as an indicator for Deep Tissue Injury (DTI).

Gefen's group in Israel has carried out extensive mechanical analysis of the residuum soft tissues [110, 114, 123]. For example, Portnoy et al predicted the strain in the muscle flap of a transtibial residual limb during donning the prosthesis and weight-bearing [110]. Stresses at the internal soft tissues were calculated to be ≈ 4 times greater than those at the interface and results were validated by measurement of interface pressures (Table 2.4). A subsequent study examined the effects of surgical and morphological factors, such as tibia length and bone bevelling, scarring and muscle properties. The model predicted that stiff muscle flaps, sharper bone edges and the presence of osteophytes could all increase the risk of tissue damage [114]. Studies defining tissue characteristics have often been limited by the use of *in vitro* animal tissues [124-126] or small cohorts tested *in vivo* [115, 127]. The use of the former approach assumes similarities in properties across species, which is limited particularly when intended for translation to humans [126, 128]. Tissue characteristics have also been examined using soft tissue indentation to determine constitutive coefficients of material models [115, 129]. One US study collected radial indentation forces at eighteen indentation sites around a residual limb, and used inverse FEA based on four locations to achieve predictions on the other sites to within $7 \pm 3\%$ [115]. It is also recognised that although most studies were limited to estimating direct pressures due to static or fixed loading rates, in the clinical situation dynamic properties are important in predicting the response to cyclic loading.

A commercial device (MyotonPRO™, Myoton AS, Estonia) has been used to investigate the structural characteristics of soft tissues to further understand the effects of a range of circumstances including ageing, stroke, sports participation and massage post-exercise [130-133]. The Myoton probe applies a 0.4 N mechanical impulse of 15 ms duration to induce damped oscillations of the soft tissues. The response is measured using a triaxial accelerometer to calculate parameters described as the tone, stiffness and elasticity of the soft tissues. Although these parameters are not directly equivalent to mechanical properties, i.e. Young's Modulus, they offer insight into tissue behaviour and enable simple comparisons.

2.2 Soft Tissue Damage and Tolerance to Loading

The residual limb represents a vulnerable site in which chronic wounds can occur due to the repetitive pressures and shear forces encountered during daily living activities. Activities such as walking result in large deformations of the soft tissues that have generally not been conditioned to support the encountered loads (Table 2.4, Figure 2.4, Figure 2.5). This section will explore:

- how soft tissues respond to the mechanical loading conditions described in Section 2.1.3;
- the damage mechanisms that can occur under different magnitudes and durations of loading; and,
- early indicators of soft tissue damage.

2.2.1 Mechanisms of Tissue Damage

When soft tissues are exposed to prolonged periods of pressure, or pressure in combination with shear, damage may occur in the form of pressure ulcers (PUs) [134]. Damage associated with skin layers represent the most common form, although underlying muscle damage, termed DTI, represents a particularly problematic condition due to difficulties in early identification [135, 136]. Superficial PUs generally occur over a bony prominence and are labelled as Category I-IV according to the depth of soft tissue damage (Figure 2.6). A DTI initially develops in the subcutaneous tissues, often adjacent to a bony prominence, and progresses up towards the skin surface. In 2003, Bouten and colleagues highlighted the importance of loading mode, with superficial PUs caused mainly by pressure and shear stresses in the skin layers and DTI caused by high levels of compressive stress [137]. Indeed PUs can also occur at a number of sites and are often associated with support surfaces and medical devices such as ventilation masks [138], cervical collars [139] and spinal boards [140]. The term “Medical device related pressure ulcers” (MDRPUs), is now internationally recognised [83, 141, 142]. MDRPUs can be superficial or DTI and would include that developed at the residuum-socket interface.

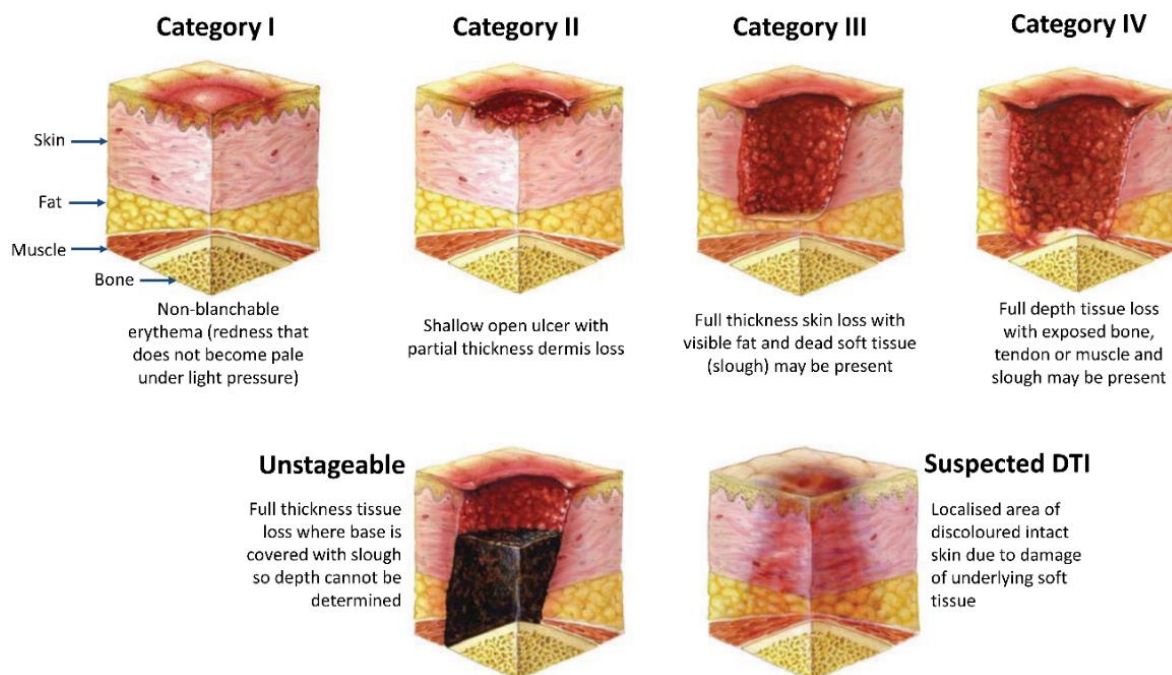


Figure 2.6 International pressure ulcer classification [143]

There are four main physiological mechanisms associated with soft tissue damage, namely, [137]:

- **Direct cell deformation damage** - external loading generates excessive strains within the soft tissues leading to a loss of cell integrity via disruption of its membrane and internal structures [144] (Figure 2.7);
- **Ischaemia** - compression of the soft tissues compromises the transport of oxygen-carrying blood leading to hypoxia and eventual cell death [137] (Figure 2.7);
- **Reperfusion Injury** - restoration of blood flow following load removal to previously ischaemic tissues causes damage, via the production of cytotoxic reactive oxygen species (ROS), inflammation and the recruitment of white blood cells [145, 146]; and
- **Lymphatic impairment** - compression of the soft tissues prevents transport via the lymph circulation, resulting in a local build-up of toxic waste products [147-149] (Figure 2.7).

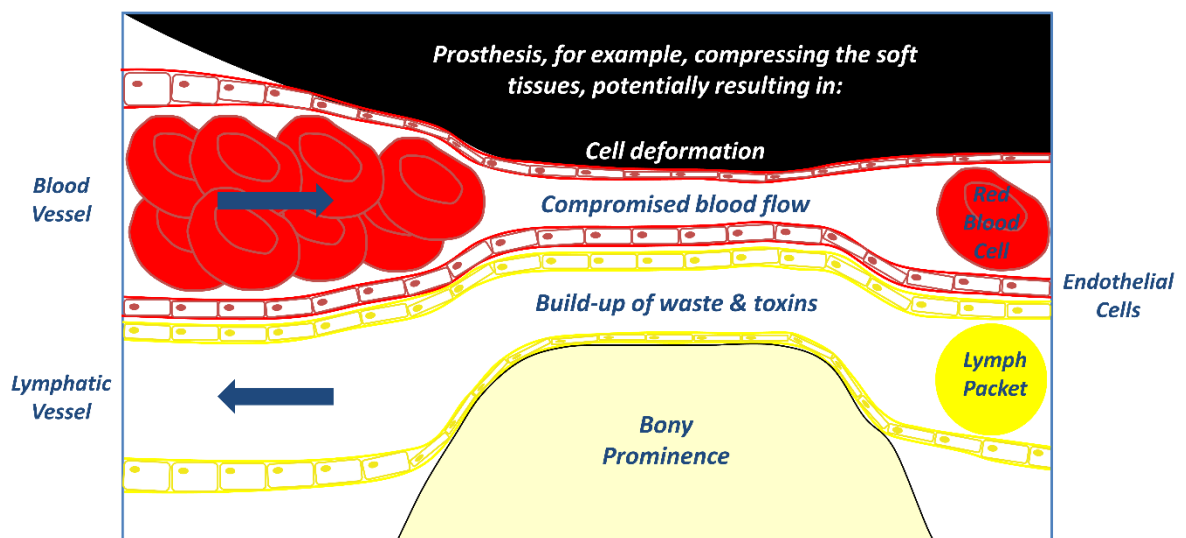


Figure 2.7 Ischaemia and lymphatic impairment due to prolonged external loading

The risk of damage can be enhanced by impaired sensory perception and elevated microclimate conditions, as previously discussed. A number of other factors are also thought to play a role in compromising tissue integrity and the development of PUs, both extrinsic (e.g. friction) and intrinsic (e.g. nutrition, circulation, age) [73, 74, 144, 150, 151]. An evidence-based PU conceptual risk assessment framework was developed by a consensus panel of international experts. It demonstrates a causal pathway for PU development identifying direct and indirect factors [73, 74]. Factors were based on the influence of the mechanical conditions at the interface and/or the susceptibility of the individual (Figure 2.8). These circumstances are particularly relevant when considering the residuum-socket interface.

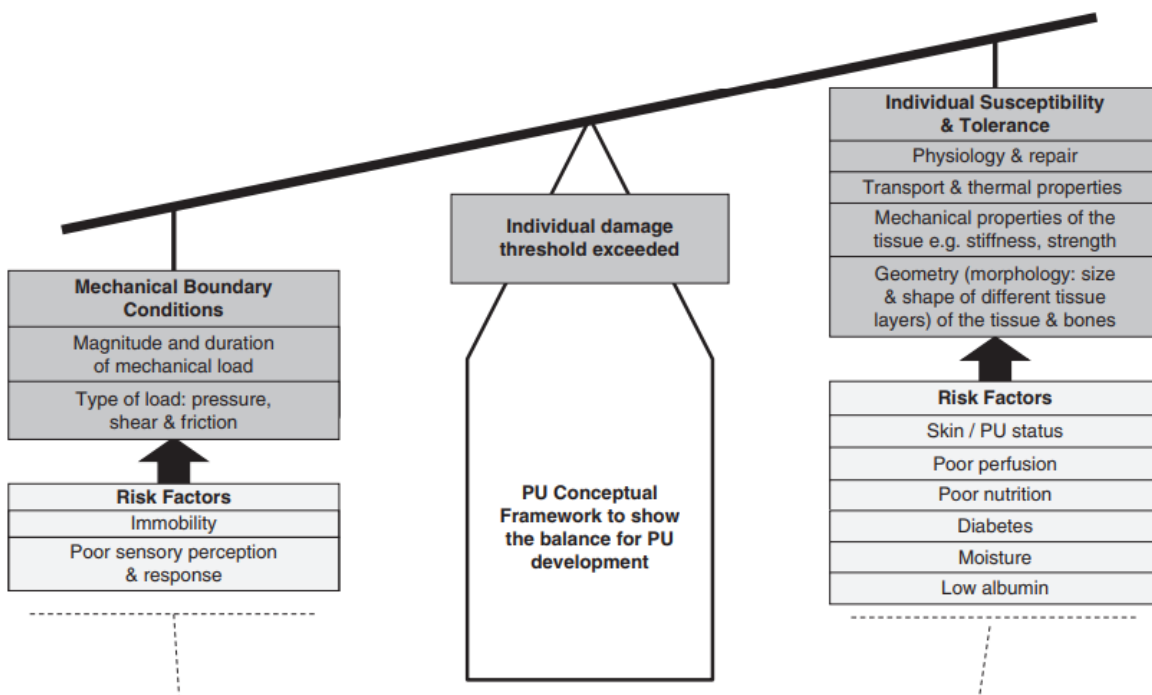


Figure 2.8 New PU conceptual framework [73]

2.2.2 Soft Tissue Response to Pressure and Shear

Early research used animal models to explore the pressure magnitude and durations which can lead to tissue damage [152-155]. In the 1940s, Groth implemented a weighted balance beam to apply a range of forces over varying periods to the gluteus maximus of rabbits, and identified via histological examination a loading threshold above which irreversible and permanent damage was evident [154]. Subsequently, Husain applied a pressure cuff to the legs of rats and guinea pigs, implementing a range of pressures (up to 300 mmHg, 40 kPa) and durations (up to 3 hours) [155]. Microscopic evidence of damage in the form of oedema, cellular infiltration and muscle degeneration was first observed at pressures of between 100 and 200 mmHg (13.3 and 26.7 kPa) applied for 2 hours. Kosiak used a hydraulic piston to apply indentation at varying loads equivalent to pressures of ≈ 500 mmHg (67 kPa) and durations (1 to 12 hours) to the femoral trochanter and ischial tuberosity of greyhounds [152]. Histological analysis revealed oedema and cellular infiltration above certain loads and durations (Figure 2.9). Kosiak also applied indentation to the hamstring muscles of rats investigating both constant and intermittent loading [156]. Histological analysis revealed that the tissues were more susceptible to damage under constant loading. In a seminal study, an indenter incorporating a force transducer was used to apply pressures ranging from 30 to 1000 mmHg (4.0 to 133.3 kPa) for 2 to 18 hours to the femoral trochanter of pigs and examined the effects with tissue histology [153]. These studies generally revealed hyperbolic relationships with both small magnitudes applied for long durations and large magnitudes applied for short durations revealing tissue damage [152, 153, 156] (Figure 2.9).

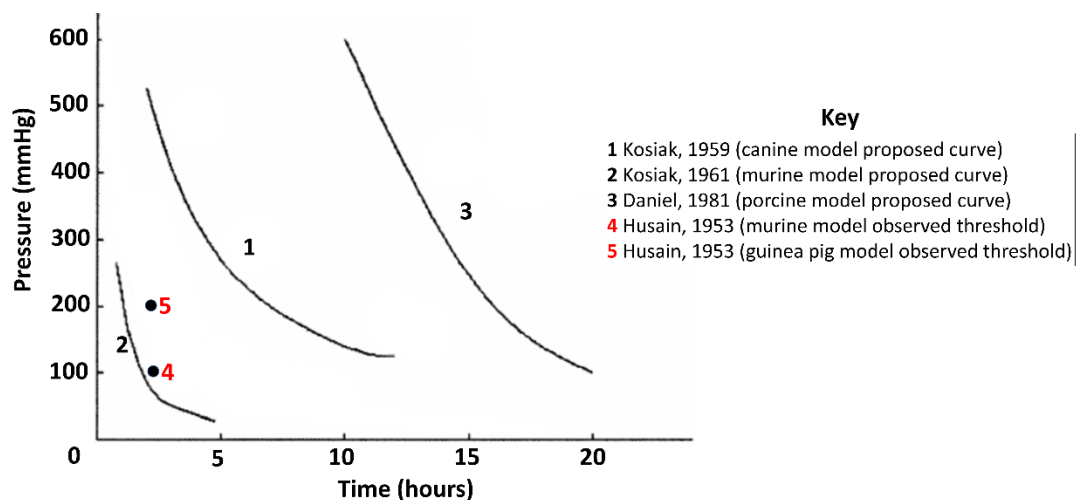


Figure 2.9 Relationship between load and magnitude for tissue damage based on a number of animal models, adapted and reprinted by permission from Springer Nature from [128] Copyright © 2005

Large differences between studies were observed, attributed to differences between test conditions and the employed animal models. Porcine and murine models are the most commonly used for tissue damage research [128]. Porcine skin is the most comparable to human, being relatively fixed and presenting with a similar cardiovascular system. However, porcine experiments are relatively expensive and difficult to scale due to the large size of the animal.

By contrast, rats are easier to obtain and handle, but their loose skin is less comparable to that of humans. The use of animal models offers an insight into tissue response to loading and risk of tissue damage, but they generally involve labour intensive histological examination of excised tissue, which prevents further analysis of the temporal aspects of damage.

In 1974, Dinsdale used a porcine model to investigate the effect of friction combined with pressure [157]. Intermittent loading was applied to the posterior iliac spines of eight pigs, with pressure alone on one side and pressure combined with friction on the other side, over a five-day period. A higher occurrence of ulceration was observed when both pressure and friction were applied and ulceration occurred with pressures as low as 45 mmHg compared to ulceration observed at pressures ≥ 290 mmHg when only pressure was applied (Figure 2.10) [157].

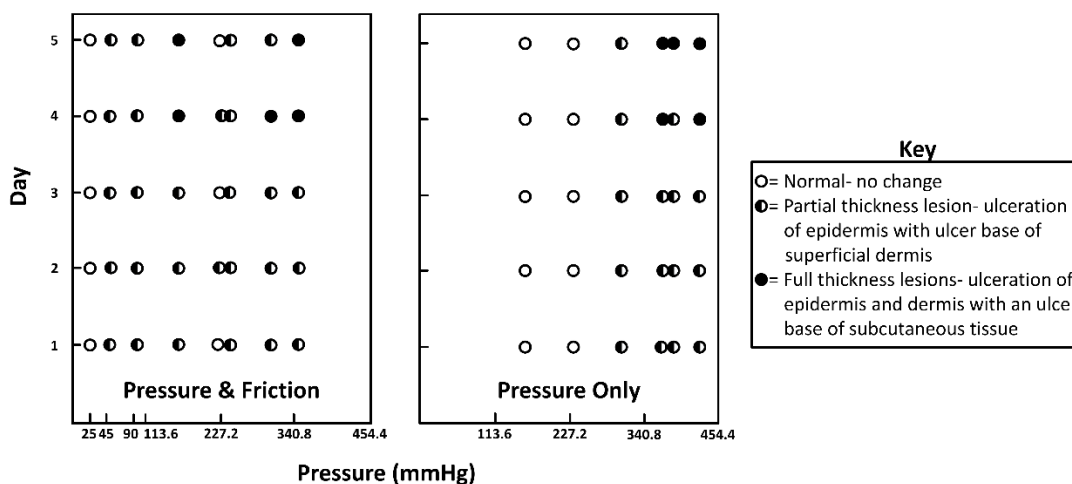


Figure 2.10 Occurrence of ulceration in porcine due to pressure combined with friction (left) and pressure only (right) over five days, used with permission of W.B./Saunders CO. from [157] Copyright © 1974; permission conveyed through Copyright Clearance Center, Inc.

In the 1970's pressure magnitude and duration thresholds for damage were first applied in a human study, based on 980 patient and volunteer observations at Rancho Los Amigos Hospital in the US. Results indicated a hyperbolic relationship between pressure and time (Figure 2.11).

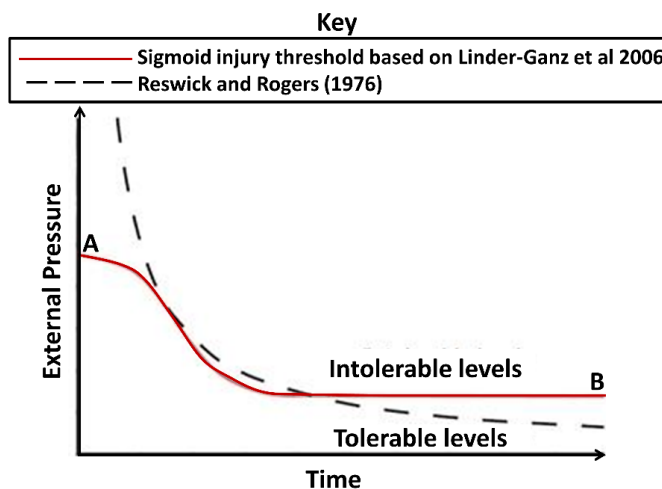


Figure 2.11 Reswick and Rogers (1976) pressure-time curve [82] with an updated version in the form of a sigmoid damage threshold in red, adapted and republished with permission of RCNi from, [158] Copyright © 2009 (Above pressure A all durations will lead to damage and for pressures lower than B no damage will occur)

Data for the proposed pressure-time curve was accumulated from patient experiences by clinicians commenting on tissue damage occurrences, and pressure measurement between support surfaces and bony prominences of patients whose skin showed clinical signs of tissue breakdown under normal conditions, and under applied pressure in testing [159]. This study led to guidelines to keep the pressure under 300 mmHg (40.0 kPa) divided by the duration in hours to avoid pressure ulcers. However, the curve was developed using relatively subjective comments of tissue damage occurrences and uncontrolled measurements of interface pressure, for which magnitude and duration were not reported. Furthermore the Reswick and Roger's threshold curve is not suitable for clinical use as it is inaccurate at the extremes of the scale, under-estimating long-term pressure tolerance and, representing a greater risk, over-estimating short-term pressure tolerance (Figure 2.11) [160]. It is evident that a more rapid tissue damage process will occur in response to larger applied pressures [144, 161]. The Reswick and Roger's curve also only measures interface pressure without consideration of internal tissue loads or individual tolerance [159, 160].

Subsequent research using animal models questioned the validity of the hyperbolic curve at short time periods [158, 162-164]. The updated sigmoid pressure-time curve (Figure 2.11) highlighted the failure of soft tissues at short durations provided the mechanical input, in the form of pressure and resulting deformation, was significantly high. The focus of this approach was directed towards the tolerance of muscle tissue and the development of DTI. Tissue histology revealed that for short exposures of 15 to 30 minutes applied loads equivalent to pressures of 263 mmHg (35.1 kPa) and 525 mmHg (70.0 kPa) caused muscle cell damage. Although as previously mentioned these animal studies provide an insight into the nature of tissue response to mechanical loading but are not directly translatable to human tissues, or useable in a clinical setting as internal loading cannot be measured directly and non-invasively.

Researchers have also worked to provide a similar approach to examine the mechanical-induced damage of bio-artificial muscle (BAM) cells [163]. A sigmoid curve similar in shape to the pressure-time curve was fitted to experimental data (Figure 2.12). It revealed a 95 % likelihood of muscle cells being able to tolerate strains <65 % for a 1 hour period and strains <40 % for 5 hour periods. However, this purely compressive strain does not account for sub-surface shear strains and the BAM model could be criticised for its lack of hierarchical organisation and vasculature when compared to real muscle cells [162].

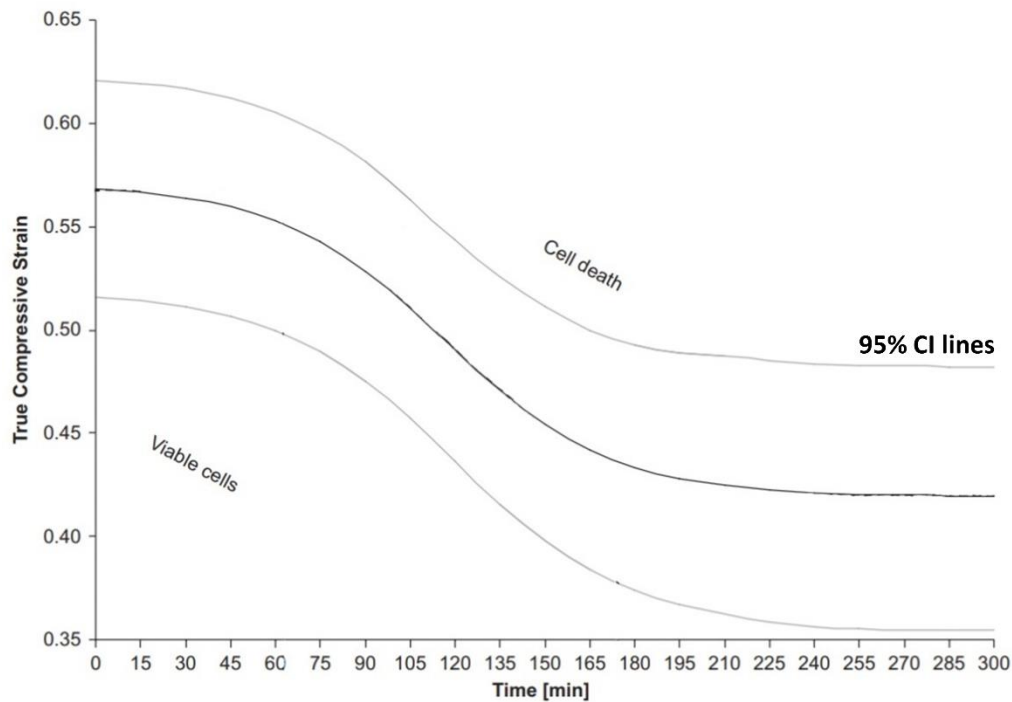


Figure 2.12 strain-time muscle cell graph from static indenter loading of bio-artificial muscle cells, adapted and reprinted from [163], Copyright © 2008, with permission from Elsevier

Research has also focused on investigating the relative importance of the tissue damage mechanisms using both in-vitro BAM specimens and an in-vivo murine model. Indentation (resulting in surface pressures of ≈ 1125 mmHg, 150 kPa for 2 hours) over muscle tissue indicated that large deformations had a detrimental effect within 10s of minutes, whereas ischaemic damage was evident over prolonged loading periods i.e. >48 hours.

In the in-vivo studies indentation damage was visualised using MRI observations of increased T2 signals corresponding to necrotic regions [165]. In contrast, ischaemic loading applied using an inflatable tourniquet (1050 mmHg, 140 KPa for 2 hours) resulted in reversible tissue changes of decreased perfusion during loading and reactive hyperaemia once released, observed via contrast-enhanced MRI. During in-vitro experiments, with hypoxic engineered muscles, cell viability was maintained up to 48 hours [164, 166]. The external validity of experimental studies is limited unless methods such as FEA can provide insight to enable generalisation of results. FEA was used to provide additional insight into the strain magnitudes and distributions generated by the indenter, enabling the relationship between internal strains and damage to be further explored at a local level particularly in the experiments where damage had occurred [167, 168]. Numerical strains were generally observed to underestimate true strain potentially due to not considering shear strain. However, there was a linear relationship between numerical and experimental strains and this work revealed that once a strain threshold had been surpassed there was a monotonic increase in damage with increasing strain. Interestingly damage was also not confined to areas with strains exceeding the threshold. This could be due to tissue inhomogeneity which had not been accounted for in the model and has been observed to have a large effect on internal deformations [167, 169]. Damage could also be due to loaded tissue becoming stiffer and causing higher strains in surrounding tissues, which has previously been observed by Gefen et al in rat limbs [170]. A developed FEA model, with a higher order of non-linearity and inclusion of friction between the rat limb and indenter, demonstrated that two minute load-relief periods within the 2 hour protocol were insufficient to reduce deformation-induced damage above a critical threshold, although relief might reduce ischaemia-induced damage [168]. Loerakker et al has also explored the effects of reperfusion extending continuous loading to six hours [171, 172]. Results were variable depending on specific region of the muscle, although they did indicate some benefits, after which reperfusion will exacerbate damage. Recently the 2 hour indenter protocol has been investigated using 3D FE modelling, observing that damage propagates away from the loaded region and instead of a distinct strain threshold for tissue damage a transition region of higher risk of damage was observed [173, 174]. This may provide insights into the mechanisms behind subject-specific tolerance to damage, and indicates that tissue damage is not dictated by the loading alone [174].

The collective work from a bioengineering community, encompassing both experimental and numerical models indicates that over short periods of loading application deformation is the most important factor in the causal pathway for damage of muscle tissue [144, 164-168, 171, 172, 175]. Research in the area of pressure ulcer aetiology has so far provided valuable insight into the deformation, ischaemia and reperfusion damage mechanisms for muscle tissue. However, it is important to remember that skin and adipose are also involved in superficial PU development. Individual variability in tissue damage susceptibility is also large, and as discussed previously is influenced by many intrinsic and extrinsic factors (Section 2.2.1).

As well as using FEA to understand conditions experienced in deep tissues under surface loads, PU aetiology research may assist in the interpretation of tissue tolerance under more complex loading conditions, such as prosthetic limb use. FEA studies [118] in conjunction with measurements of pressure at the residual limb-socket interface (Table 2.4) can be used to predict tissue damage, considering appropriate injury threshold data. It should be noted however that the above-cited sigmoid relationships were collected in animal (mostly murine) or BAM cell models and may therefore not be valid for the residual limb. In particular, it is acknowledged that the associated soft tissues adapt functionally such that their tolerance to prosthetic interface loading is enhanced [176]. This was demonstrated in a young porcine skin model where skin was subjected to repetitive compressive and shear stress [177]. Cyclic loading, applied for 1 hour/day, 5 days/week for four weeks, was found to significantly change collagen fibril architecture, with an increase in diameter and a decrease in density, thus suggesting an adaptive response to improve load tolerance. It should be recognised that these findings may not reflect adaptive changes that occur in more mature animal skin or indeed human skin. However, further research in this area could assist in the development of techniques to optimise skin adaptation and load tolerance, leading to enhanced gait rehabilitation and a reduced risk of tissue damage [178].

Compression of the soft tissues will cause internal shear stress due to the relative deformation between the differing stiffness tissue layers. The forces exerted on the residual limb from the socket will also include a tangential element, generating cyclic external shear forces during gait [104, 105, 179]. One study investigated the effects of shear on the superficial and subcutaneous layers of porcine skin with an underlying bony prominence, after the application of various wound dressings [180]. The dressings were reported to reduce the stresses observed within the subcutaneous layer by 31 to 45 % [180]. These tangential forces result in deformation of the soft tissues, equivalent to a shear strain. Shear stress will also be caused by localised and uneven pressure gradients, for example, at the patellar tendon when using a PTB socket, causing compression in these tissues and deforming adjacent tissues.

These pressure gradients are important considerations when trying to reduce tissue damage. The relative deformation between the tissues depends on their stiffness and the interface conditions between the layers. Enhanced shear stresses will occur between layers with large differences in stiffness, for example, between the muscle and bone of the residual limb. This highlights the importance of considering internal tissue mechanics, as opposed to external surface pressure and shear alone and explains why muscle tissue can be more susceptible to damage.

Currently limited experimental research has explored damage mechanisms within the soft tissues of the residuum [76], however as discussed in Sections 2.1.3 and 2.1.4 experimental-numerical methods have been implemented to investigate the effect of loading [110, 114-116]. The sigmoid strain-time curve (Figure 2.12) was used to predict muscle tissue damage risk and a time-based stiffening of damaged tissue, to characterise conditions of the muscle flap, while in a sitting posture with knees at both 30° and 90° flexion [123]. The curve was also recently used by Mbithi et al to help define a control system for developing an active prosthetic socket system involving in-situ load measurement and estimation of tissue damage risk [181]. Although still subject to the limitations discussed previously, particularly as derived from animal and artificial cell models, they offer insight into residuum tissue tolerance and how damage risk can be mitigated.

Lee and Zhang took a different approach by focusing on pain perception and opportunities for patient feedback in socket design and fitting [182]. Socket fit was analysed by evaluating a FEA socket model using indenter pressures at perceived onset of pain, enabling quantitative analysis prior to definitive socket fabrication and fitting. Very high peak indenter pressures (≈ 6075 mmHg, 810 kPa) were identified indicating that this methodology could be risky in clinical application as damage could occur prior to the perceived onset of pain, particularly in individuals with limited sensation. Portnoy developed a portable monitor to calculate subject-specific internal stresses in the residual limb in real-time [183], which was proposed for evaluation of DTI risk by comparison with muscle cell death threshold levels [162]. This physiology-based approach provides a safer alternative to pain thresholds for prosthesis users with neuropathy but could be enhanced by implementing specific human and dynamic DTI thresholds.

Researchers have attempted to use individual geometry, material properties and pressure tolerances to inform socket design, although none of these data-based methods is currently in clinical use. Such approaches may be strengthened by knowledge of soft tissue physiological response under load, furthering understanding of tissue viability and damage risk. As an important part of the clinical translation of this research, the efficacy of these methods should be validated against established methods of socket design.

2.2.3 Measurement of Tissue Health and Damage Precursors

This sub-section will explore measurements of tissue health and precursors to the damage mechanisms discussed in Section 2.2.1.

Pressure mapping uses an array of elements sensitive to normal (compressive) force to provide real time measurement of interface pressure, and provides a tool to complement clinical decision-making in the selection and use of support surfaces for PU prevention [184]. Various sensors are available using different principles, such as capacitance and piezo resistivity, to convert a mechanical deformation into an electrical signal. Studies have evaluated the potential of this measurement as an effective predictor of PU development [185, 186], although standards for calibration and test methods have not been established [187]. However, as described in Section 2.1.3, interface measurements do not necessarily reflect either the internal conditions of soft tissues or their physiological response. To address this, various bioengineering tools have been used to monitor the status of dermal tissues when exposed to mechanical loading [34]. A critical analysis of these tools to assess tissue adaptation and tolerance to loading will be discussed in this section.

Visualisation of Tissue Composition and Deformation

Volumetric imaging techniques can be used to observe tissue composition and deformation of all the soft tissues throughout a limb, providing some quantification on tissue adaptation and internal strains.

As an example, **MRI** is a non-invasive volume imaging technique primarily used for diagnosis of soft tissue disorders. An MRI scanner uses a superconducting magnet to expose the body to a magnetic field and electromagnetic (EM) waves for short periods of time (1 to 5 ms bursts) and measure the effects on the hydrogen atoms within the tissues. Hydrogen nuclei consist of single protons, which have a spin property that effectively acts as a small magnetic field. These spin properties are reflected at spin frequencies, with hydrogen atoms spinning at 42.57 MHz/T [188]. In MRI the magnetic field causes the nuclei to align their spin axis, either with or against the magnetic field. EM waves are then sent through the body, also exciting the hydrogen atoms and effecting their spin frequency and axis alignment. Once the EM excitation stops, the nuclei will relax back to their original state i.e. random spin frequency and axis alignment. This relaxation alters the magnetic field creating an EM signal that can be detected. The strength and timing of the signals that the hydrogen atoms create during the spin-relaxation phase are dependent on the nature of the tissue in which they are located. Different MRI parameters can be altered to focus on different spin characteristics, depending on the focus of the investigation.

The main two MR imaging parameters are represented by the repetition time (TR), the time interval between excitation pulses of EM waves and the echo time (TE), the time between excitation and recording data.

T1 weighting focuses on the longitudinal relaxation of the protons i.e. the time for the unaligned to align and provides images that distinguish anatomical characteristics such that adipose tissue appears bright and water appears dark. For T1 images, a short TE (typically <15 ms) and short TR (typically <600 ms) should be used given that full T1 relaxation is of the order of seconds [189]. In a relevant study, T1 weighting was implemented to investigate the biomechanical response of the human leg when wearing an elastic compression garment for maximal contrast between adipose and muscle tissues for segmentation [190].

By contrast, T2 weighting focuses on the transverse relaxation of the protons i.e. the time for the de-phasing of spins and can be used to investigate fluid-filled regions with the water appearing brighter than adipose tissues. For T2 weighted images, long values of TE (typically ≈80 to 100 ms) and a long TR (typically >3000 ms) are used [189]. Spatial information is generated in 2D slices by exciting only the nuclei in the slice of interest, using a magnetic field gradient. This is illustrated with a relevant case study in Figure 2.13 [191].

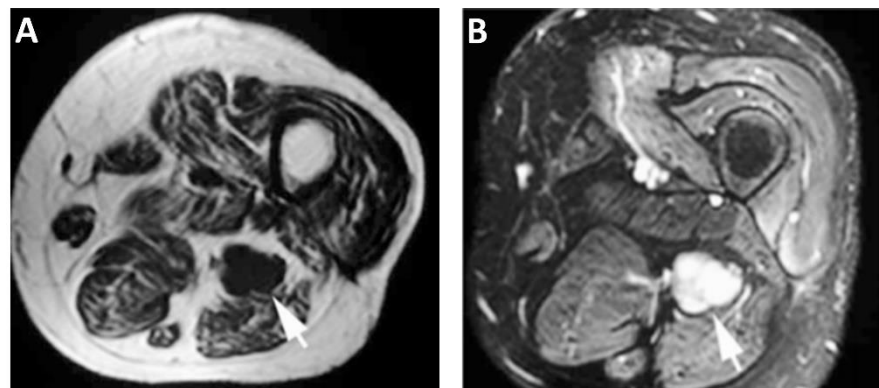


Figure 2.13 Transverse MRI slice at distal residual limb of an individual with an above knee amputation to investigate pain (a sciatic neuroma shown by arrow was observed) implementing A: T1 weighting, giving high contrast between adipose and muscle tissues, and B: T2 weighting, giving high signal in fluid-filled and inflamed [191]

MRI has previously been used to observe the morphological changes of the transtibial residual limb and can help to differentiate between changes due to oedema and muscular atrophy, depicting the adaptation of different muscles [49]. It has also been extensively used to estimate the degree of fatty infiltration in a number of diseases, such as those involving the liver, demonstrating its potential for use in further exploring soft tissue composition and adaptation [192, 193]. It represents a very versatile technique, although it is expensive with limited access, and can cause claustrophobia and is not appropriate for participants with metallic implants or who cannot remain still during the imaging process.

Computed Tomography (CT) is another volume imaging technique widely used within healthcare.

It works using an x-ray source and detector, which rotates around the patient. The resulting x-rays are detected after passing through the body and their attenuation will depend on the tissue structures. Multiple planar radiographs are reconstructed using algorithms to calculate the spatial distribution of attenuation coefficients to create a 3D image.

CT offers a cheaper alternative to MRI and can produce high contrast images of bony anatomy. However, it is limited in the differentiation of the soft tissues with typically much lower contrast between soft tissue structures compared to MRI. CT is also less used in research due to exposure of its ionizing radiation. Nonetheless, it has been used to compare differences in muscle and adipose tissues in amputated and contralateral limbs, observing atrophied muscle and increased adipose tissue in the residual limb [50]. It has also been used to calculate adipose infiltration in gluteal muscle and lower extremity tissues of participants with spinal cord injury to analyse tissue adaption and status leading to insight into tissue tolerance and damage risk [194, 195]. It has been validated against 3T MRI as a suitable alternative technique to estimating adipose, except intramuscular adipose tissue which it was found to significantly underestimate [196, 197]. This underestimation was also observed to increase with increasing participant BMI and thigh circumference [196].

Ultrasound is a medical imaging technique using the transmission and detection of high frequency sounds waves (1 to 35 MHz). Sound waves are transmitted into the body where they are reflected at tissue boundaries. The distance to the boundary and intensity of the echo can be calculated and the signal is often displayed as a 2D image.

Ultrasound imaging has been used in past studies to investigate the development of PUs [198] and the physiological effect of foot plantar tissue compression in the laboratory [199] and during gait, incorporating the transducer within a 3D printed orthosis [200]. These studies suggest that this relatively low-cost non-invasive imaging modality has potential for detecting soft tissue damage prior to visible signs. When used with motion compensation, ultrasound has also been trialled for full volume limb imaging [201] (Figure 2.14). When compared to MRI of the same limb many of the same anatomical structures were observed within the ultrasound image, although direct comparison is problematic due to registration of the individual slices. However, direct image correlation could be achieved in future extended cohort studies involving the use of surface markers.

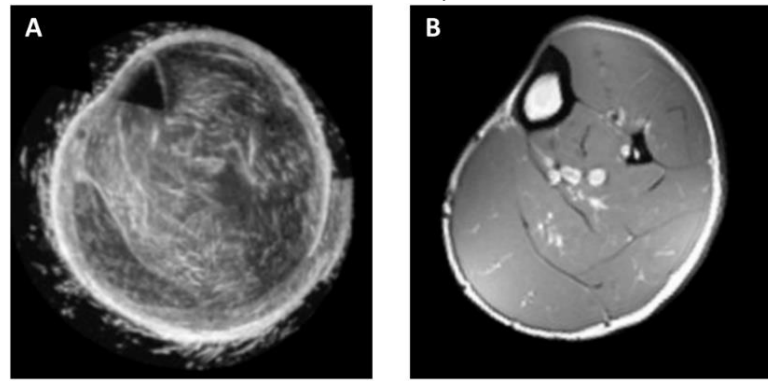


Figure 2.14 Transverse slice of lower limb using, A: ultrasound with limb motion compensation and B: MRI (NOTE these two slices are not directly comparable) [201] Copyright © 2015, IEEE

Measurements of Soft Tissue Vulnerability to Superficial Damage

Skin surface measurements can be acquired to investigate the vulnerability of the dermal soft tissue to damage, including temperature, humidity and moisture and water loss measurements [98].

Corneometry indicates skin moisture based on its capability as a dielectric medium. The system is composed of two electrodes with different electrical charges, which create an electromagnetic field that penetrates the stratum corneum to a depth of 10 to 20 μm , and its output in arbitrary units (AUs) is dependent on the water content of skin [191]. It has been used to investigate the effect of moisture on COF, revealing a high positive correlation [102].

Transepidermal Water Loss (TEWL) is a measure of water loss through the epidermis using an open or closed chamber that creates a homogeneous diffusion zone, typically measured in g/h.m^2 [202] (Figure 2.15). It provides an indication of the structural integrity of the stratum corneum, as water evaporates from the skin as part of normal homeostasis. Higher TEWL values indicate greater water loss and past studies have found this to correlate with structural damage [203-206]. In a relevant study comparing soft tissue health between amputated and intact limbs, results indicated significantly higher TEWL values in amputated limbs indicative of skin barrier disfunction [82].

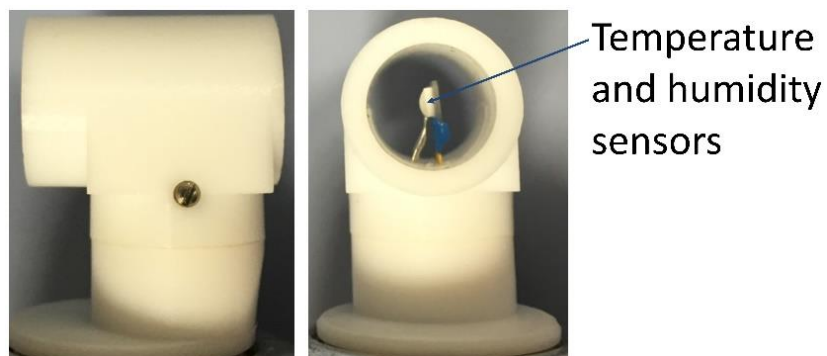


Figure 2.15 Tewameter TM300 (Courage + Khazaka Electronic GmbH., Cologne, Germany) measuring probe head (10 mm diameter, 20 mm height)

A **Sub-epidermal moisture (SEM)** meter (Bruins Biometrics, US) assesses the epidermal barrier function of the skin using a dermal phase meter that measures the surface electrical capacitance. Higher values in AUs have been observed to reflect localised oedema and inflammation. SEM values have been reported to increase in localised skin areas indicating PU damage prior to visible erythema [207].

A disadvantage of corneometry and SEM is that skin moisture measurements are estimated in AUs, which is limited in terms of its relevance to physical parameters offered by other measurement systems [208]. AU's can be calibrated using known conditions to increase the meaning of measurements. For example, in open air SEM is 0.3 and submerged in water SEM is 3.9 [207]. It is also worthy of note that both moisture and water loss measurements are subject to variability in intra- and inter-rater reliability, and baseline values vary with anatomical site [34, 207, 209].

Superficial Ischaemia and Reperfusion Damage

Transcutaneous Oxygen and Carbon Dioxide Tensions (T_cPO_2/T_cPCO_2) have been employed as a measure of local dermal tissue ischaemia in response to different loading applications with reference to indenters [210], the residuum-socket/liner interface [54, 82] and various support surface designs [211-214]. Such studies have revealed distinct categorical responses in terms of T_cPO_2 and T_cPCO_2 values relative to the loading regimens [215]. Electrochemical electrodes are placed on the skin and heated to 43.5°C to ensure maximum vasodilation [216] (Figure 2.16). This causes localised hyperaemia and facilitates gas diffusion by lowering the solubility of blood gases in the tissue and increasing metabolic activity. Oxygen (O_2) and carbon dioxide (CO_2) diffuse through the stratum corneum and the semi-permeable membrane of the electrode. The gas mixes with an electrolyte solution, altering its pH level. This varying pH is sensed by the difference in the polarisation voltage between a platinum cathode (for O_2) or a glass cathode (for CO_2) and a silver reference electrode. This electrical signal is converted to a corresponding measurement of T_cPO_2 and/or T_cPCO_2 in the underlying skin in units of mmHg. The measurements thus provide a relative change in perfusion with time.



Figure 2.16 Transcutaneous Gas Tension electrode (diameter 17 mm, thickness 15 mm)

Research on the measurement of T_cPO_2 as a predictor for lower limb amputation healing

complications as reviewed in 2012, concluded that T_cPO_2 could provide an important parameter reflecting the extent of compromised dermal tissue, and thus assist in clinical decisions of appropriate amputation level to optimise the resulting wound healing [76]. A more recent review associated with the prediction of wound healing in the diabetic foot supported the view that T_cPO_2 was predictive for wound healing and risk of amputation [217]. In both these clinical studies tissue sites which demonstrated T_cPO_2 levels below 35 mmHg were considered to be at risk of poor healing post-amputation [76, 217]. In a more recent study significantly lower baseline T_cPO_2 in residual limbs were reported when compared to intact limbs highlighting the vulnerability to tissue damage [82].

It has been suggested that sustained elevated levels of carbon dioxide may be a strong indicator of cell damage, through the accumulation of anaerobic metabolites and local changes in pH [218]. Indeed, CO_2 plays a vital role in maintaining the homeostasis of the human body and is important for O_2 transportation, reducing the affinity of O_2 to haemoglobin (Bohr Effect), and regulation of blood pH [218]. This review also indicated that threshold levels of CO_2 might be indicative of ischaemia while tissue damage is still reversible [218].

Laser Doppler flowmetry (LDF) provides a direct measure of microcirculatory blood perfusion and has been shown to be an effective measure of the skin response to pressure and shear, with decreased perfusion during loading and hyperemia post-loading [161, 219]. Two monochromatic, coherent, collimated laser beams are crossed to create straight fringes perpendicular to the blood flow. As the blood particles traverse the fringes, light is reflected and the resulting Doppler shift between the incident and scattered light is proportional to the particle velocity. Measurements of microcirculatory perfusion have been observed to consistently differ between diabetic participants with and without neuropathy, potentially providing a useful tool for diagnosis of microcirculatory dysfunction within the diabetic population [220]. In a separate study, Rink et al. reported no significant differences in LDF measurements when comparing amputated and intact limbs [82]. Previous studies have reported large variability in the data with measurements affected by the ambient temperature, measurement site, movement artefacts, emotional status of the participant, the environment and inter-operator variability [82, 220, 221]. Furthermore, the output of LDF is in AUs making comparisons and contextualisation difficult.

Inflammatory Biomarkers have been shown to provide a non-invasive measurement technique to analyse the effect of applied loads on dermal soft tissues [138-140, 161, 206, 211, 222-224].

Cytokines are proteins released by cells and affect cellular interactions. As an example, Interleukin-1 α (IL-1 α) and its competitive inhibitor, Interleukin-1 Receptor Antagonist (IL-1RA), are inflammatory cytokines released in response to cell deformation or damage and represent precursors to cell death [222, 225]. These cytokines are released in sebum from the sebaceous glands located at the base of hair follicles in the dermis (Figure 1.4) or from epidermal cells known as keratinocytes [225]. IL-1 α is also released from keratinocytes in response to hypoxia [226]. IL-1RA is released to compete with IL-1 α and the ratio of these biomarkers is thought to reflect homeostatic regulation against inflammation [227, 228]. Sebum is often collected for analysis via a hydrophobic, lipid-absorbent tape (e.g. SebuTape) at the skin surface.

De Wert et al compared a ratio of IL-1 α /Total Protein (TP), used to account for inter-participant variations, after the application of pressure and pressure in combination with shear on the skin surface [161]. A significant increase in this ratio was evident after 30 minutes of combined pressure and shear loading when compared to all the other test conditions. A separate study compared the inflammatory response of the skin to spinal immobilisation on rigid and soft boards [140]. IL-1 α and lactate release at the sacrum, although not significantly different between boards, both increased with prolonged exposure and decreased during unloading. Temporal skin response has also been investigated by Soetens et al implementing 2 hours of intermittent and continuous mechanical sacral loading with IL-1 α /TP analysed from sebum collected every 20 minutes [224, 229]. The highest ratio increase from baseline was 3.7 fold after 1 hour continuous loading and results were observed to stabilise in the final third of loading for both regimens. Participant variability was observed in this and other studies investigating the effects of cervical collar design and sacral indenter loading with distinct sub-populations of healthy cohorts [139, 206, 224]. Indeed, they generally demonstrate both high and low inflammatory responses suggesting susceptibility of inflammation which is worthy of further investigation.

Ratios of other inflammatory cytokines, such as interleukin-8 (IL-8), interleukin-1 β (IL-1 β) and Tumour Necrosis Factor- α (TNF- α) have also been analysed pre- and post-loading, but revealed less consistent trends [138], although there were reported increases after the onset of structural tissue damage [223].

Inflammatory biomarkers offer a simple, quick non-invasive sampling technique providing insight into the status of skin integrity and its tolerance to loading prior to irreversible tissue damage. Current sampling methods are limited by the low sample volumes and concentrations and the sensitivity of biomarkers to other known stimuli e.g. tape stripping and chemical agents. Additionally, the extraction and quantification processes for these cytokines are time consuming and costly.

Metabolites of Anaerobic Respiration- Lactate and urea are two of the metabolites up-regulated during anaerobic respiration and also represent waste products that can be excreted in sweat, and thus may provide useful predictive indicators of ischaemic dermal tissue damage. Indeed Knight et al reported up to a 2.35-fold increase compared to baseline in concentrations of lactate and urea under applied sacral indenter loading of 120 mmHg (16 kPa) [211]. There was also a significant inverse relationship between lactate and urea concentration and measured T_cPO_2 values [211]. The anaerobic metabolites, lactate and pyruvate, were also recently analysed during the continuous and intermittent sacral loading of an able-bodied cohort [224, 229]. An up-regulation of both metabolites were measured during the loading phase although they returned to baseline following load removal, indicating sensitivity to mechanical loading and their potential as indicators of tissue status. Sweat purines have also been shown to represent the release of Oxygen Free Radicals and could therefore help to indicate enhanced tissue damage during the reperfusion phase [34]. These sweat biomarkers offer a simple sampling technique, although the requirement of a controlled environment to ensure the collection of sufficient sample volume can add complexity to testing protocols and prove an uncomfortable experience for some participants. The analysis is also limited, like inflammatory biomarkers, by the costly extraction and quantification processes.

Optical Coherence Tomography (OCT)-based Microangiography provides a non-invasive technique to measure post-occlusive reactive hyperaemia (PORH) of skin, which can indicate the effectiveness of blood reperfusion post-loading [230]. OCT uses light to produce volumetric images. It has been used in past research to investigate the vascular perfusion response of the skin to loading [231]. It has also been used in preliminary research to investigate blood flow response and vessel density post-walking with both a stiff foot brace with two participants without amputation and a prosthesis with participants with transtibial amputation [230]. Participants with limb loss were reported to exhibit smaller denser vessels and displayed a faster PORH return to baseline values, suggesting tissue adaptation to continual socket loading. Swanson et al recently implemented OCT to assess skin vascular function and structure in the lower limbs of 8 participants without amputation after two weeks of modified prosthetic socket use [84]. No statistically significant differences were found between baseline measurements and those taken at time points throughout the socket use. OCT-based microangiography allows fast acquisition, but is limited by a small field of view (2.5 x 2.5 mm) and a depth resolution of 1 mm and sensitivity to motion artefacts, as well as high cost and availability compared to measurement of transcutaneous gas tensions for example [230].

Lymphography represents a semi-invasive technique, which involves detecting fluorescence after contrast injection, using Near Infra-Red (NIR) imaging. It provides a non-ionising alternative to lymphoscintigraphy, a radioisotope-based technique [232]. The latter was used in seminal papers in the 1980's, where pressures of between 60 and 75 mmHg (8 and 10 kPa) were reported to impair lymphatic clearance in a canine limb [233, 234]. By contrast, lymphography has been used in recent studies to characterise the activity of the lymphatic vessels, in the skin, in human models when exposed to both applied pressures and compression garment therapies [148, 235, 236]. One study investigated the cuff pressure at which lymph containing contrast agent passed the upper border of the cuff applied to the lower limbs [235]. Results indicated mean \pm SD cuff pressures of 29.3 ± 16 mmHg for healthy participants and 13.2 ± 14.9 for lymphoedema participants. Changes in lymphatic activity under loading and therapies have been observed. Lymphography does however require administration of a contrast agent by injection and the imaging requires expensive detection equipment and a darkened environment for visualisation. Lymphography is sensitive to a resolution depth within the dermis of ≈ 1 to 4 mm, thus limiting the visualisation of deeper lymph vessels. It does not provide knowledge of the lymphatic architecture, which would enhance the understanding of lymph packet volume. Variable baseline values and thresholds for pressure and shear also require further investigation.

An alternative technique, termed Magnetic resonance lymphography, involves the injection of a Gadolinium contrast agent to image lymphatic vessels. It has been used in a number of studies to investigate lymphatic activity and disorders [237-240]. However, the additional logistics and discomfort to participants outweigh the benefit of implementing this technique, with its inherent ability to image deeper lymph vessels. Indeed, the primary changes in the proposed loading can be predicted in the superficial lymphatics, which are adequately imaged using NIR lymphography.

In summary, there are a collection of bioengineering tools to monitor the status of loaded tissues ranging from large, expensive imaging modalities, such as MRI that enable visualisation of all soft tissues, to small hand-held devices that provide real-time analysis of superficial dermal tissues, such as TEWL, and easy to sample dermal inflammatory biomarkers that then require costly and time consuming analysis [34] (Table 2.5). Indeed, many techniques are currently limited in their clinical application due to expense or analysis time. Transcutaneous gas monitoring represents the most established technique to assess tissue health within the field of amputation, and has been used to assist in clinical decisions of amputation level and evaluate wound healing [76, 217]. It has also been implemented in conjunction with TEWL, LDF and a number of other perfusion measurements to compare soft tissue health in amputated and intact limbs [82]. MRI and CT have also been used to visualise soft tissue adaptation post-amputation [49, 50]. However, there is currently a need for the development of a suitable measurement array that can bring knowledge of both tissue adaptation and tolerance to loading that will aid the decision making of clinicians in minimising the risk of soft tissue damage.

Table 2.5 Summary of bioengineering techniques

Technique	Soft Tissue Analysed	Advantages	Disadvantages
Pressure mapping	Dermal surface	<ul style="list-style-type: none"> - Real time - Simple use - Non-invasive - Used to assist selection of support surfaces for PU prevention 	<ul style="list-style-type: none"> - Does not inform internal conditions or physiological response of tissues
MRI	All	<ul style="list-style-type: none"> - Non-invasive - Non-ionising - High contrast between tissues - Previous use investigating tissue composition and adaptation post-amputation 	<ul style="list-style-type: none"> - Expensive - Limited access - Can cause claustrophobia - Not suitable for individuals with metallic implants
CT	All	<ul style="list-style-type: none"> - Non-invasive - Cheaper than MRI - Previous use investigating tissue composition and adaptation post-amputation 	<ul style="list-style-type: none"> - Ionising - Less contrast between soft tissues than MRI
Ultrasound	All	<ul style="list-style-type: none"> - Non-invasive - Non-ionising - Low cost easier to access imaging modality - Can observe same anatomical structures as MRI - Studies suggest potential for detecting tissue damage prior to visible signs 	<ul style="list-style-type: none"> - Less contrast between tissues than MRI - Requires motion compensation

Technique	Soft Tissue Analysed	Advantages	Disadvantages
Corneometry	Epidermal	<ul style="list-style-type: none"> - Non-invasive - Simple surface measurements 	<ul style="list-style-type: none"> - Measurements in AUs - Variability in intra- and inter-rater reliability
TEWL	Epidermal	<ul style="list-style-type: none"> - Non-invasive - Simple surface measurements - Past studies found high values correlated with structural damage 	<ul style="list-style-type: none"> - Variability in intra- and inter-rater reliability
SEM	Epidermal	<ul style="list-style-type: none"> - Non-invasive - Simple surface measurements - Past studies found high values reflect localised oedema and inflammation 	<ul style="list-style-type: none"> - Measurements in AUs - Variability in intra- and inter-rater reliability
TcPO ₂ /TcPCO ₂	Dermal	<ul style="list-style-type: none"> - Non-invasive - Continuous real time measurements - Used to support clinical decision making for amputation height and healing potential - Previously established protocols to characterise tissue ischaemia at loaded tissue interface 	<ul style="list-style-type: none"> - Indirect information on perfusion - Requires constant skin attachment at raised temperature (43.5°C)
Laser Doppler Flowmetry	Dermal	<ul style="list-style-type: none"> - Non-invasive - Direct measure of blood perfusion - Shown to be effective measure of skin response to pressure and shear 	<ul style="list-style-type: none"> - Measurements in AUs - Large variability in measurements
Inflammatory Biomarkers (IL-1 α and IL-1RA)	Dermal	<ul style="list-style-type: none"> - Non-invasive - Simple sampling - Shown to be sensitive to pressure and shear loading - Response prior to damage 	<ul style="list-style-type: none"> - Low sample volumes and concentration - Time consuming and expensive extraction and analysis - Response not specific to mechanical loading
Metabolites of Anaerobic Respiration	Dermal	<ul style="list-style-type: none"> - Non-invasive - Simple sampling of sweat - Shown potential as predictive indicators of ischaemic damage 	<ul style="list-style-type: none"> - Controlled environment required for collection of sufficient sample - Time consuming and expensive extraction and analysis
OCT Based Microangiography	Dermal	<ul style="list-style-type: none"> - Non-invasive - Used to investigate perfusion and vessel density post-loading - Fast acquisition 	<ul style="list-style-type: none"> - Small field of view - Sensitivity to motion artefacts - High cost and limited availability compared to TcPO₂/TcPCO₂ measurement
Lymphography	Dermal	<ul style="list-style-type: none"> - Non-ionising - Changes in lymphatic activity under loading and therapies have been observed 	<ul style="list-style-type: none"> - Invasive - Imaging required expensive equipment and darkened room - Limited visualisation of deeper vessels

2.3 Motivation, Aim & Objectives

There is limited quantitative knowledge of soft tissue response to prosthetic loading in clinical and community settings. To date, some of the bioengineering techniques discussed in Section 2.2.3 have been used to assess tissues subjected to prosthetic loading. However, there is a need to develop a suitable array of measurements to assess both the biomechanical and physiological response of tissues under loading experienced at the residuum-socket interface. It is critical to further understand the vulnerability of soft tissues at the residual limb that have not been adapted to load bearing. Knowledge of soft tissue damage mechanisms, adaptation and load tolerance at this interface can be used to select suitable measurement tools to help maintain tissue health during prosthetic rehabilitation and subsequent long-term usage. This provided motivation leading to the following aims and objectives.

Overarching Aim- To evaluate soft tissue health and tolerance of residual and intact limbs under representative prosthetic loads

This was accomplished by a series of objectives:

1. Develop a testing protocol to mimic loading representative of that experienced during early rehabilitation post-amputation

In order to assess the suitability of selected measurement techniques a protocol with representative loading was required. Applied loading would be representative of that typically encountered during early rehabilitation when using devices such as the PPAM aid i.e. 0.5 to 13 kPa (≈ 4 to 95 mmHg) [53] (Section 2.1.3), as this represents the period in which the residuum tissues are most vulnerable. Success of this objective was determined by measuring the interface pressure while applying the representative loading and comparing measurements with those encountered when using the PPAM aid.

2. Select appropriate measurement techniques to assess status or tolerance and adaptation of residual limb soft tissues, and measure the physiological response to representative applied loads in a cohort of healthy participants without amputation

The physiological response was measured in terms of precursors to the damage mechanisms discussed in Section 2.2.1 to provide a more comprehensive assessment of tissue tolerance:

- **Direct deformation** measured using a suitable imaging technique, which could also enable visualisation of tissue composition, and thus provide insight into tissue adaptation;
- **Ischaemia** characterised by compromised oxygenated blood flow; and
- **Lymphatic impairment** characterised by activity under loading.

Inflammatory response was also measured as a more general measure of tissue tolerance.

Determination of the appropriateness of the test equipment and protocol was needed prior to translation to testing of individuals with amputation. Appropriate techniques were selected by thoroughly researching current literature (Section 2.2.3), carrying out preliminary testing (detailed in Section 3.3) and then scoring techniques within a decision matrix table according to their ability to detect changes in local tissue physiology (relevance), scientific novelty and practicality (Table 3.5 and Table 3.6).

Testing was first implemented on a cohort of healthy participants without amputation to obtain baseline data. Calf tissues of participants without amputation have not been conditioned to support loading, and so provided a reasonable simulation of pre-conditioned tissues in the newly reconstructed residual limb.

3. Investigate soft tissue adaptation and measure the physiological response to these applied loads in participants with transtibial amputation

Further to objective 2, the adaptation in physiological response was described as change in onset of precursors to ischaemia and inflammation, providing assessment of tissue tolerance. Tissue adaptation itself was described as relative difference in tissue composition between residual and contralateral limbs.

The refined protocol was applied to a cohort of participants with transtibial amputation. Practical issues defined recruitment and therefore participants presented a range of causes of amputation and time post-amputation. This enabled insight into changes in tissue tolerance at the interface following amputation and provided information regarding the mechanical conditioning of soft tissues.

4. Investigate associations between adaptation and tissue tolerance to loading and cause of amputation/time post-amputation

This objective was designed to collate all strands of the experimental data to investigate trends and determine suitability of the implemented techniques at assessing tissue tolerance and early detection of tissue damage during prosthetic use. This led to recommendations for future research to provide clinically useable measurement tools to help assess tissue tolerance, and therefore assist in creating patient-specific rehabilitation protocols to minimise the risk of tissue damage. In the future, real-time in-socket measurements could enable monitoring of both the mechanical boundary conditions between the residual limb and socket, as well as the status of tissues providing a prosthesis user with increased independence and confidence managing their residual limb health in both hospital and community settings.

3 Protocol Development

A novel protocol combining an array of biophysical measurements was developed to evaluate changes in soft tissue health at the residual limb-socket interface. This chapter explores the development from determination of a representative loading methodology to preliminary testing and final selection of suitable measurement techniques.

3.1 Representative Prosthetic Loading

This section covers the first objective:

1. Develop a testing protocol to mimic loading representative of that experienced during early rehabilitation post-amputation

As discussed in Section 2.1.3, a considerable range of interface pressures and shear stresses during static prosthetic weight bearing have been reported [108-110, 112]. In the present work, it was critical to reproduce the interface pressures at the residual limb-socket interface, while avoiding damage. A loading protocol was sought to simulate the pressures experienced when using the PPAM Aid, which have been reported to range from ≈ 4 to 95 mmHg (0.5 to 13 kPa) under an applied inflation pressure of 40 mmHg (5.3 kPa) [53]. A method of measuring the interface pressure is required, particularly at vulnerable sites where tissue tolerance may be compromised. A repeatable methodology was necessary as testing was carried out on multiple participants/limbs. A volumetric imaging technique using MRI, CT or ultrasound modalities was required to visualise deformation under the applied loading. In the former, metallic objects associated with the prosthesis would be prohibited. Another practical consideration with ultrasound imaging is that the probe needs to be in direct contact with the soft tissues.

The developed testing protocol would inevitably include a number of distinct measurement techniques to provide a comprehensive view on the tissue health and tolerance. Thus, it was critical to employ a loading methodology that would be relatively simple to implement alongside measurement techniques. Loading could initially be achieved with the application of pressure alone, although as discussed in Section 2.1.3 shear represents an important factor in prosthetic loading so would be a useful addition to the devised loading methodology.

The design factors considered when developing the representative loading application have been summarised with the level of requirement of the individual features (Table 3.1).

Table 3.1 Design factors for representative loading application

Specification Feature	Essential or Preferable
1. Enables pressure application representative of the values experienced when using the PPAM Aid during early rehabilitation i.e. 0.5 to 13 kPa (\approx 4 to 95 mmHg) [53]	Essential
2. Ability to measure applied load or pressure	Essential
3. Repeatable application	Essential
4. Able to use in-situ with selected volumetric imaging technique; MRI, CT or Ultrasound	Essential
5. Easy to use	Preferable
6. Ability to add an external shear component within range of previously reported interface shear, 1 to 52 kPa (\approx 8 to 389 mmHg) [108-110]	Preferable
7. Ability to add an internal shear component representative of socket rectification	Preferable

A number of different potential pressure application methods were considered (Table 3.2) [53, 115, 190, 199, 210, 235, 236, 241].

Table 3.2 Comparison of pressure application methods

Method of Load Application	Examples of use in previous studies	Advantages	Limitations
Indentation	<p>[115]</p> <ul style="list-style-type: none"> - Investigate the viscoelastic response of the residual limb tissues - Indentation depth was determined by indenting until maximum comfort level was attained - Indenter size-20x20 mm² - Maximum experimental forces, ranged from 7.5 to 16.7 N (equivalent to pressures of 140 to 313 mmHg, 18.7 to 41.7 kPa) <p>[210]</p> <ul style="list-style-type: none"> - Instron 1122 Universal testing Machine applied directly to TcPO₂ electrode (≈19 mm diameter) applied normal to the tibial aspects of the skin - Estimated interface pressures 0 to 125 mmHg (≈17 kPa) 	<ul style="list-style-type: none"> - Replicates socket design of loading pressure at appropriate sites of the residuum - Will cause internal shear stresses due to relative movement of soft tissue layers under indenter - Could incorporate an ultrasound probe within the indenter 	<ul style="list-style-type: none"> - The indenter would need to be constructed of non-metallic materials to be suitable for some volumetric imaging techniques - Shape of indenter would need to be considered to predict underlying stress profiles - Might prove complicated to implement simultaneous indentation at multiple sites
Air Pressure	<p>[235]</p> <ul style="list-style-type: none"> - Transparent pressure cuff applied to the calf and inflated to 60 mmHg (8 kPa), then deflated by 10 mmHg (1.3 kPa) every 5 minutes. Investigated the lymphatic pressure needed to overcome the cuff pressure 	<ul style="list-style-type: none"> - Simple application - Loading applied to entire calf, replicating static loading from PPAM aid during early rehabilitation [53] 	<ul style="list-style-type: none"> - Loading across whole residual limb will not be consistent - Pressure reduction with time can occur - Would have to ensure no metallic parts for MRI or CT suitability and may be difficult to image measurement sites using ultrasound

Method of Load Application	Examples of use in previous studies	Advantages	Limitations
Elastic Compression Material	<p>[190]</p> <ul style="list-style-type: none"> - Elastic compression garment applied to calf tissues - Maximum interface pressure estimated, via a FEA model, of 40.3 mmHg (5.3 kPa) at posterior calf 	<ul style="list-style-type: none"> - Simple application - Loading applied to whole calf replicating loading when donning a prosthesis - Non-uniformity of garment tension due to leg geometry is representative of state in prosthetic socket 	<ul style="list-style-type: none"> - Dependence of garment tension to achieve defined pressures across participants - Lymphoedema therapy currently implements this technique to encourage lymphatic activity [236]
Adjustable straps	<p>[199]</p> <ul style="list-style-type: none"> - Wooden foot support and tension adjustable straps - Used to investigate tolerance of heel plantar tissues 	<ul style="list-style-type: none"> - Replacing the wooden support with a residual limb cast or test socket could provide a simple method of pressure application on the residuum, replicating donning of socket - Could be adapted to apply shear - Non-metallic components 	<ul style="list-style-type: none"> - Unsuitable for applying pressure to the calf tissue of control participants without amputation
Water Pressure	<p>[241]</p> <ul style="list-style-type: none"> - Comparison of hydrostatic pressure casting (PCAST) and hand cast PTB socket manufacture PCAST Technique: <ul style="list-style-type: none"> - Residual limb wrapped in plaster and immersed in water in PCAST tank - Hydrostatic pressure increased until equal weight bearing achieved - Water depressurised once plaster has hardened 	<ul style="list-style-type: none"> - Representative of TSB socket - Safer loading due to application over a large area 	<ul style="list-style-type: none"> - Would require adaptation for use with participants without amputation - Might prove complicated to incorporate biophysical measurement sensors and use in-situ with volumetric imaging techniques

After consideration of the above factors a thigh blood pressure cuff was determined the most appropriate method to match the project aims. Accordingly, a commercial device was selected (Aneroid Sphygmomanometer, Model Ref 0124, SN 4874466, Bosch + Sohn GmbH, Germany), as illustrated in Figure 3.1.



Figure 3.1 Images of A: Inner and B: Outer surfaces of BOSO Sphygmomanometer selected to load calf tissues, C: BOSO Profitest Sphygmomanometer pump and gauge

A large adult size (600 x 180 mm) cuff was selected, which contains no metallic parts so could be appropriate for use in-situ during MRI or CT imaging. The pump and pressure gauge do contain metallic components, but the incorporation of a three-way valve and 10 m length of PVC tubing enabled them to be used at a safe distance from imaging systems, therefore meeting this design requirement.

A maximum applied cuff pressure of 60 mmHg (8 kPa) for up to 30 minutes was determined to represent a safe pressure similar to a value subjected to an individual with lower limb amputation during the early rehabilitation phase and static weight bearing using the PPAM Aid [52, 53]. Comparable studies have applied similar pressures over the planned time period with no adverse effects and have demonstrated effects on both vascular and lymphatic supplies to local tissues [147, 211, 235].

Preliminary testing with one participant (female, aged 28) was implemented to determine whether the pressure cuff was able to hold a pressure of 60 mmHg over a 30 minute period (Figure 3.2). The cuff was donned then inflated to 60 mmHg and applied to the right and left calves for three repeat tests. Pressure was measured using the pump's integral gauge, which enabled a measurement precision of 2 mmHg, at 5 minute intervals. The accuracy of the gauge measurement is reported as ± 3 mmHg by the manufacturers [242].

The cuff was attached to the three-way valve and 10 m length of PVC tubing to simulate the testing situation in which the most pressure losses would be expected to occur, due to the most connections. Six further repeat tests were carried out using a gypsum powder 3D printed residual limb model representing a male plaster cast, to investigate the proportion of pressure loss which occurs due to the mechanical system or intracellular fluid movement in response to pressure application (Figure 3.3).

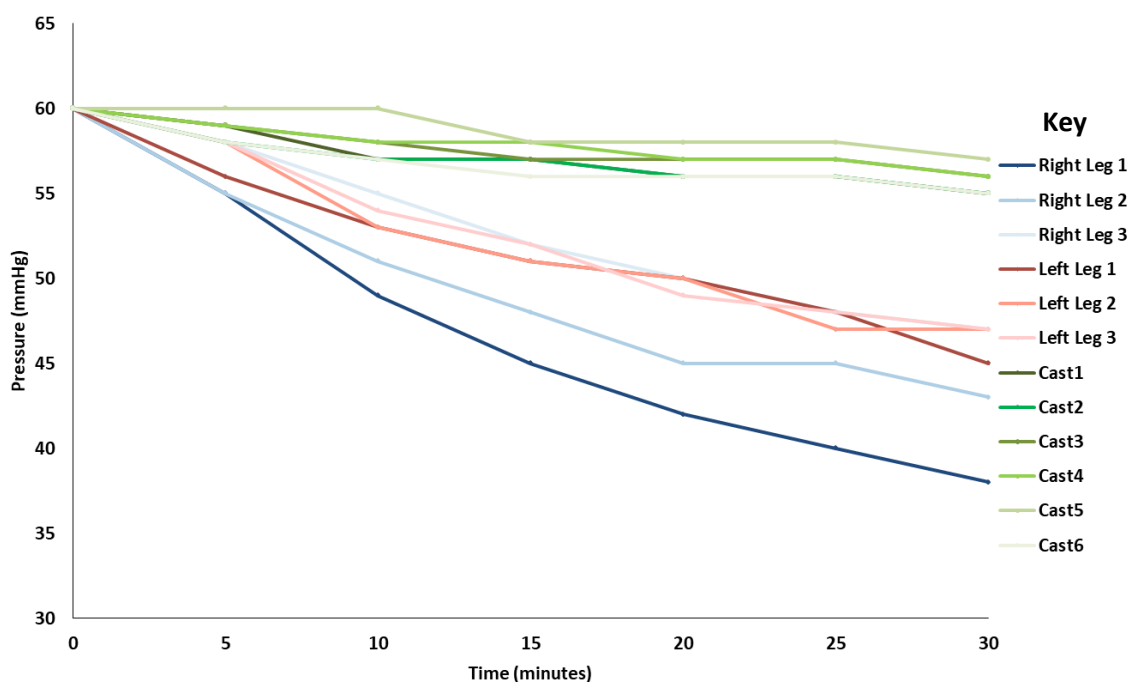


Figure 3.2 Graph showing pressure loss over a 30 minute time period after inflation to 60mmHg (8 kPa)



Figure 3.3 Pressure cuff applied to residual limb plaster cast

Pressure was observed to decrease over the test period when the pressure cuff was applied to the calf (3 to 5 mmHg, mean 4.3 mmHg), and even more so when it was applied to the right or left calf (13 to 22 mmHg, mean 15.5 mmHg) (Figure 3.2). This difference suggests that approximately 70 % of the pressure decrease was due to the physiological effects of pressure application. In addition, increased variability was evident when pressure was applied on the limbs, most likely due to various levels of participant activity. The increased pressure loss observed during the first right leg test could have been due to the fact that the participant had just been running. This preliminary work helped define the testing procedure such that participants relaxed before the pressure cuff was applied. The mechanical losses are thought to occur at either the connection points or in the pump, gauge or pressure release valve assembly. The reliability of the pressure was considered suitable for testing, particularly as loading periods of 10 minutes were decided upon to shorten the protocol, reducing demand on participants.

In order to examine the physiological response at lower cuff pressures, a protocol was established in which cuff pressures were prescribed at 10 mmHg (1.3 kPa) increments every 10 minutes between 20 and 60 mmHg (2.7 and 8.0 kPa). In addition, to reduce the time and cost during the imaging sessions only three time points were captured, namely, at baseline and at cuff pressures of 20 mmHg and 60 mmHg (2.7 and 8.0 kPa).

It was predicted that the application of a proximally directed shear force in the vertical axis most closely replicated the socket environment, as this axis will have the largest force component during weight bearing [104, 179]. During preliminary testing, external shear was generated by applying a ≈ 65 N force along the tibial axis, with a mass on a pulley system, as shown schematically in Figure 3.4.

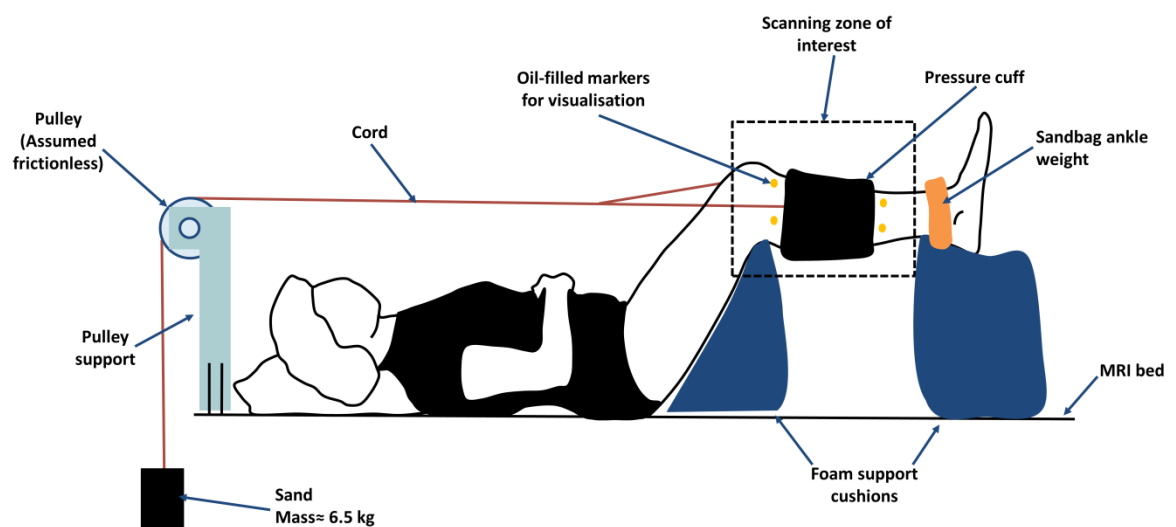


Figure 3.4 Schematic indicating the application of external shear force to the calf tissue of a supine participant

The design of an indenter was critical if it was to replicate the load applied by focal rectifications at the residuum-socket interface. Its presence would inevitably produce a gradient of shear strains in the underlying soft tissues. During preliminary testing an indenter of diameter 40 mm and thickness of 14 mm was applied at the tibialis anterior muscle, underneath the pressure cuff, to investigate its use as an additional loading condition (Figure 3.5 and Figure 3.6).

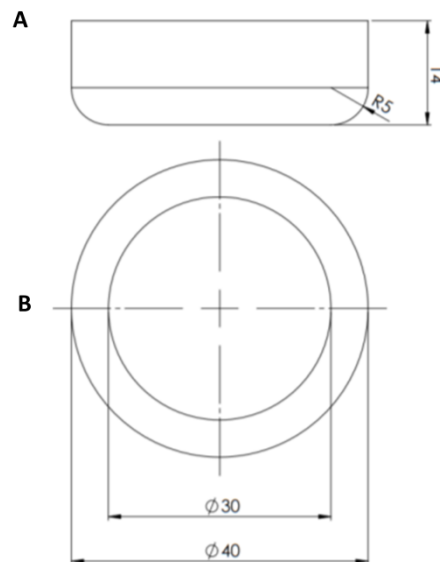


Figure 3.5 Schematic showing geometry of polyacetal indenter used during preliminary testing- A: Front view, B: Plan view. Dimensions in mm

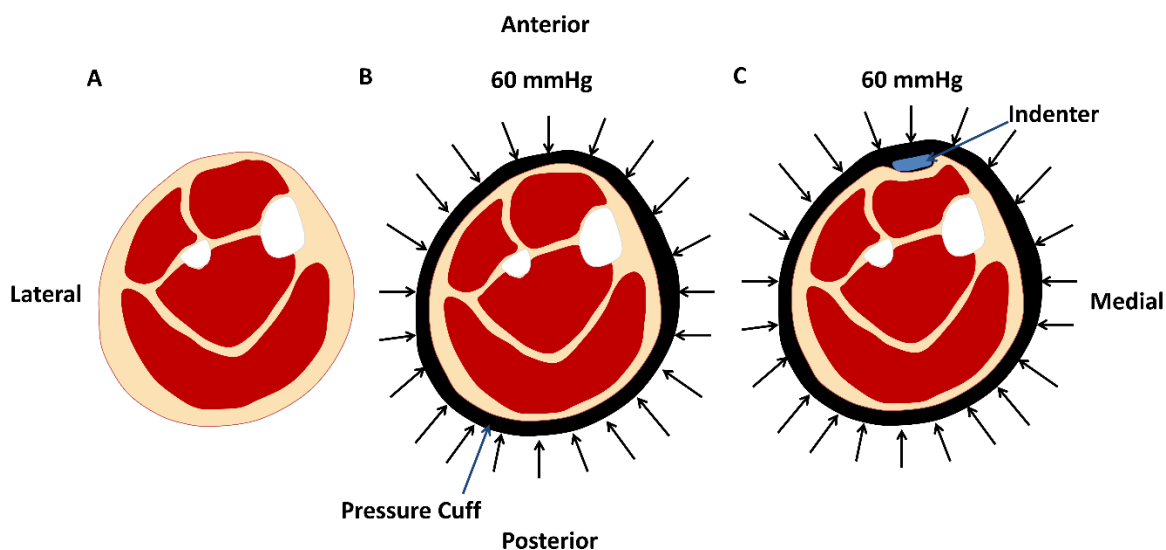


Figure 3.6 Diagrams depicting a transverse slice at mid-calf, A: under no loading condition, B: Pressure cuff applied at 60mmHg (8 kPa), C: Pressure cuff applied at 60mmHg (8 kPa) with indenter positioned at the tibialis anterior

Preliminary testing demonstrated the complexity of proximal shear application via the pulley system with the cuff slipping and moving tangentially during testing, as well as relieving pressure at the proximal anterior cuff edge. It also proved difficult to support the pulley during the test. As previously discussed, during prosthesis usage external shear is caused by tangential forces and friction occurring when donning a socket and carrying out daily activities, such as walking. The tangential load applied during preliminary testing was not considered to be representative of the real-life situation.

It was decided that an indenter would be positioned at measurement areas, underneath the pressure cuff during testing to create internal shear forces resulting in deviatoric strain and some representation of socket rectification. Dependent on the selected measurement techniques, the indentation would be provided by either the measurement electrode or 3D printed indenters.

A Prosthetic liner (ContexGel Liner, RSL Steeper, UK) was positioned underneath the cuff to replicate the environment, particularly the microclimate, experienced by the residual limb and increase comfort during testing. Holes were cut to accommodate the indenters and the addition of silicone gel rings, on top of the liner around the indenters, reduced pressure gradients resulting from the indenter.

Interface pressures were measured using an air-filled bladder pressure monitoring system (Mk III, Talley Medical, Romsey, UK) using 28 mm diameter cells (Figure 3.7), which have a reported mean error of 12 ± 1 % and a repeatability of ± 0.53 mmHg (0.07 kPa) [243].

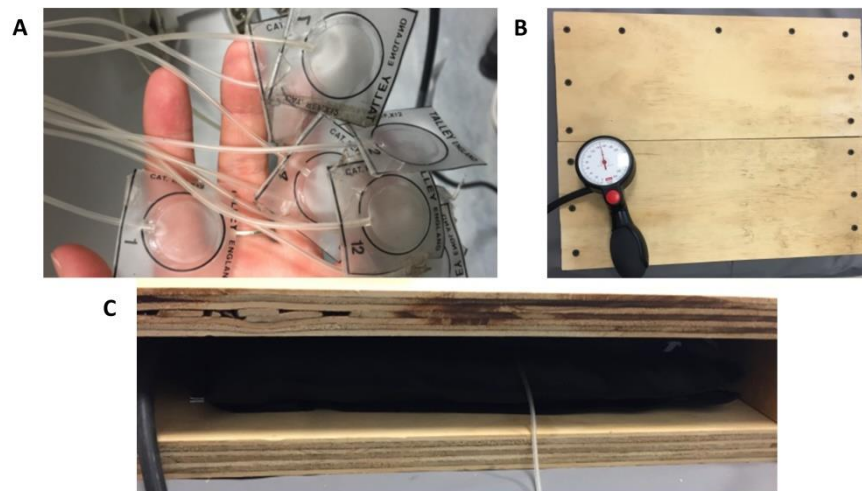


Figure 3.7 A: Talley pressure sensors, B: Top view of wooden validation rig for Talley sensors, C: Front view of validation rig with Talley sensor being validated with pressurised cuff

In order to validate the Talley sensors, for use measuring the interface pressure during pressure cuff application, they were positioned in the pressure cuff in a hollow wooden validation rig (Figure 3.7). The pressure cuff was then inflated incrementally from 20 to 200 mmHg (2.7 to 26.7 kPa) in 10 mmHg (1.3 kPa) steps. Talley sensor measurements were recorded, after a ≈ 10 second equilibration period as judged when the fluctuation in values was < 3 mmHg (0.4 kPa), at each pressure. Linear trends were evident over the anticipated pressure range, with strong correlation for each of the four sensors tested, validating their use for measuring interface pressure during the test protocol (Figure 3.8 and Table 3.3). Root Mean Squared Errors (RMSEs) indicated a measurement precision of ≈ 1.4 mmHg.

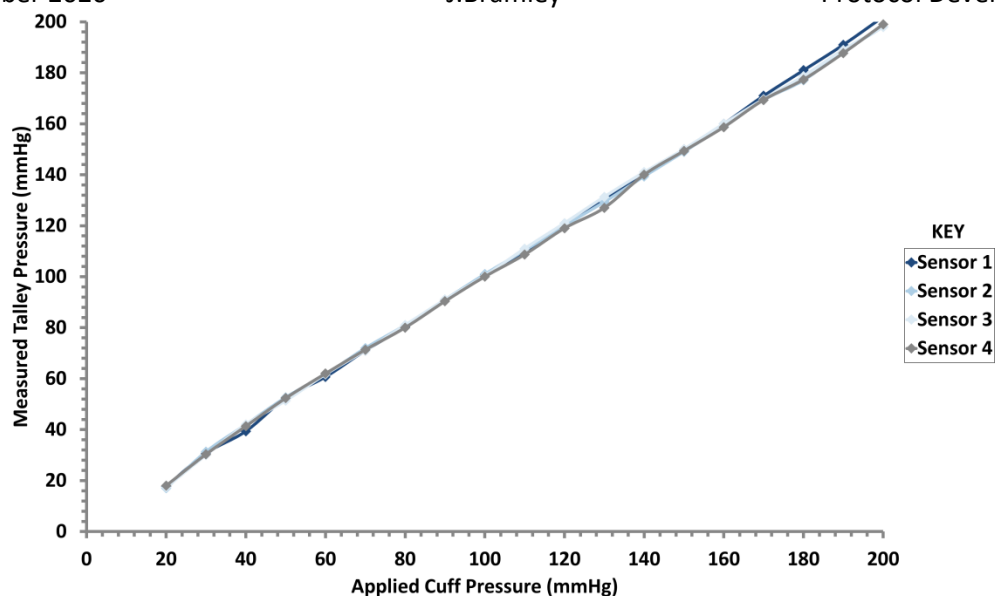


Figure 3.8 Measured Talley sensor pressures at applied cuff pressures ranging from 20 to 200 mmHg (2.7 to 26.7 kPa)

Table 3.3 Linear regression analysis showing relationship between measured Talley sensor pressure and applied cuff pressure, Note: RMSE is Root Mean Squared Error

Sensor	Linear regression slope	R ²	RMSE (mmHg)
1	1.01	0.99	1.07
2	0.98	0.99	1.64
3	0.99	0.99	1.27
4	0.98	0.99	1.54

Accordingly, the indenter-skin interface pressures were measured under the applied cuff pressures at each measurement location using the individual pressure sensors. Measurements were taken after a ≈ 10 second stabilisation period once fluctuations were < 3 mmHg (0.4 kPa).

3.2 Measurement Areas

Three regions of interest for measurement were selected as they represent distinct anatomical structures that are commonly pressure tolerant areas used in prosthetic design for load transfer when creating sockets (Figure 3.9). Three 50 x 50 mm sites were selected for measurement on each limb: the patellar tendon (above and located centrally with the tibial tuberosity), the lateral calf (just below and forward of the fibula head) and positioned at the same height centrally on the posterior calf.

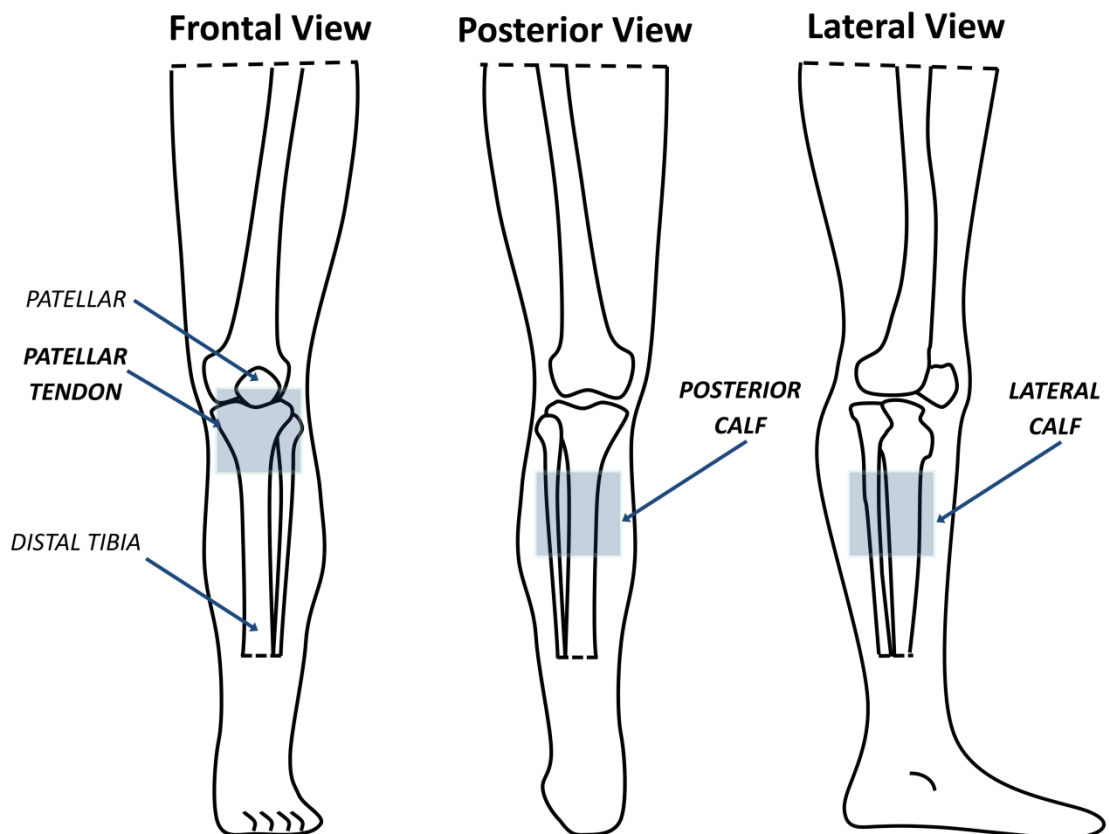


Figure 3.9 Labelled 50 x 50 mm areas of measurement of the right lower limb (where measurements will be taken are in bold & highlighted blue)

3.3 Characterisation of the Residuum Interface and Soft Tissue

Parameters

This section covers aspects of the second objective:

2. Select measurement techniques that may be suitable to assess status or tolerance and adaptation of residual limb soft tissues and measure the physiological response to representative applied loads in a cohort of healthy participants without amputation

The bioengineering tools introduced in Section 2.2.3 provide an array of measurement techniques with potential for assessing tissue status under representative loading. This section discusses the selection of suitable techniques to investigate adaptation and the biomechanical and physiological response of soft tissues under representative prosthetic loading.

3.3.1 Soft Tissue Constituents & Biomechanics

It will be informative to visualise tissue composition and deformations under loading, providing an insight into adaptation of the residuum tissues and response to loading. MRI is established for characterising the geometry of residual limbs and the subsequent creation of computational models, with benefits over CT of enhanced intra-tissue contrast and lower risk [50, 115, 118]. With higher resolution images, MRI is also a more suitable technique to provide detailed characterisation of soft tissue constituents and deformation than ultrasound.

A 3T MRI scanner (MAGNETOM Skyra, Siemens, Germany) at the Faculty of Medicine, University Hospital Southampton site, was used during this research. Preliminary testing enabled selection of T1 DIXON Volumetric Interpolated Breath-hold Examination (VIBE) sequencing that involves two signal echoes from the same excitation. This enables in-phase, out-of-phase, fat saturated and water saturated images providing different contrasts between soft tissues to assist with segmentation and tissue composition analysis. The out-of-phase images were determined to be appropriate for segmentation and deformation analysis due to a fat-water boundary highlighting the different tissues. Preliminary testing helped to determine appropriate resolution and echo and repetition times (Figure 3.10).

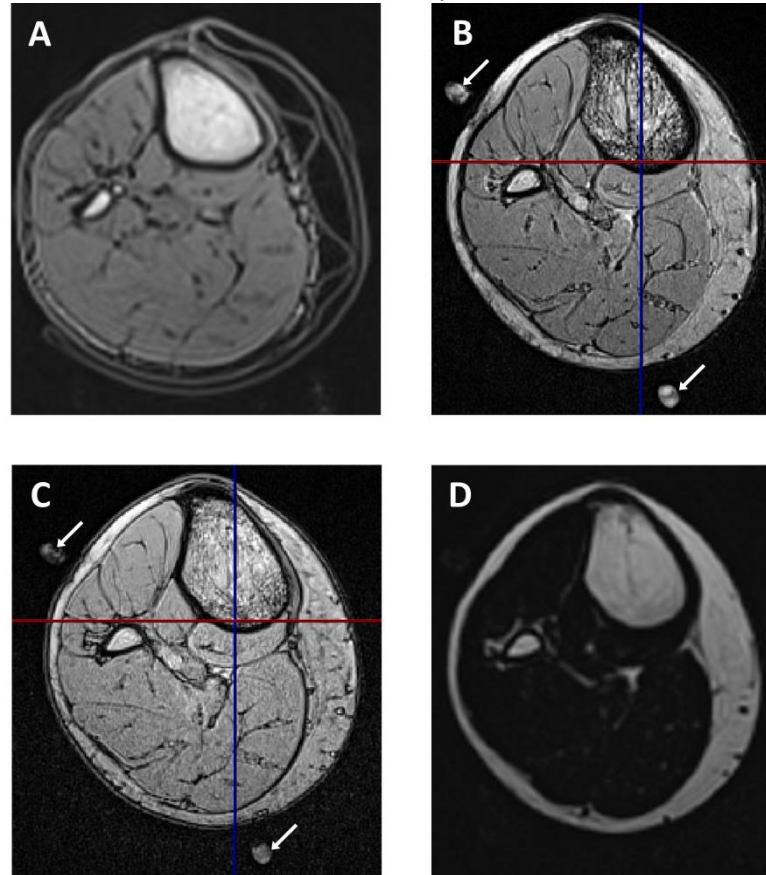


Figure 3.10 Transverse MRI slices through calf at baseline, A: out of phase, in-slice resolution 1.3 x 1.3 mm, B & C: out of phase, in-slice resolution 0.6 x 0.6 mm, TE: 12.30 ms and 6.15 ms respectively (white arrows show oil tablets in-situ), D: fat saturated, in-slice resolution 0.6 x 0.6 mm

A higher in-slice resolution improved distinction between tissues, aiding segmentation. A shorter echo time of 6.15 ms was selected enabling visualisation of skin and a thinner fat-water boundary (Figure 3.10C). Sunflower oil tablets were placed centrally within the indenters positioned within the measurement areas (Figure 3.10B & C). These provided visual points to enable selection of the transverse MRI slice at the centre of the indenter during image processing to investigate deformation.

Fat saturated images (Figure 3.10D) were used for tissue composition analysis to calculate the proportion of superficial and infiltrating adipose tissue.

3.3.2 Ischaemia

Laser doppler flowmetry provides a direct measure of blood perfusion. However, previous studies have reported large variability, and the Arbitrary Unit measurements have limited relevance to physical parameters [82, 220, 221]. T_cPO_2 and T_cPCO_2 measurements enable indirect information on the perfusion and characterisation of skin ischaemia [34, 211, 213, 215]. Measurements are continuous and electrodes could be easily incorporated into the current protocol, positioned underneath the pressure cuff where they would act as indenters. Indeed protocols have been previously established to measure T_cPO_2 and T_cPCO_2 in order to characterise tissue ischaemia in the loaded body interface and assess the performance of a range of support surfaces [211, 213, 215]. These studies have yielded three distinct categorical responses as detailed in Table 3.4.

Table 3.4 Transcutaneous Gas Tension (T_cPO_2 and T_cPCO_2) responses categorisation

Category	T_cPO_2 Response	T_cPCO_2 Response
1	Minimal changes in steady state (basal level $\approx 45-90$ mmHg)	Minimal changes in steady state (basal level $\approx 36-50$ mmHg)
2	>25% decrease	minimal change (reaches steady state value $\approx 50-60$ mmHg)
3	>25% decrease	>25% increase (reaches steady state values ≈ 80 mmHg)

Category 1 is considered to be a low risk response in which the tissue viability is minimally compromised. By contrast, Categories 2 and 3 are thought to be indicative of localised tissue ischaemia if the applied pressures are sustained for prolonged periods [211, 213]. In particular, a Category 3 response is considered to represent the most damaging to local tissues as the anaerobic metabolism results in an accumulation of CO_2 which is toxic to the localised cell niche [218]. These criteria have been used to assess a variety of other device-skin scenarios [212-214].

For use of the Transcutaneous Measurement (TCM) electrodes hair was removed from the three 50 x 50 mm measurement sites, as illustrated in Figure 3.11.

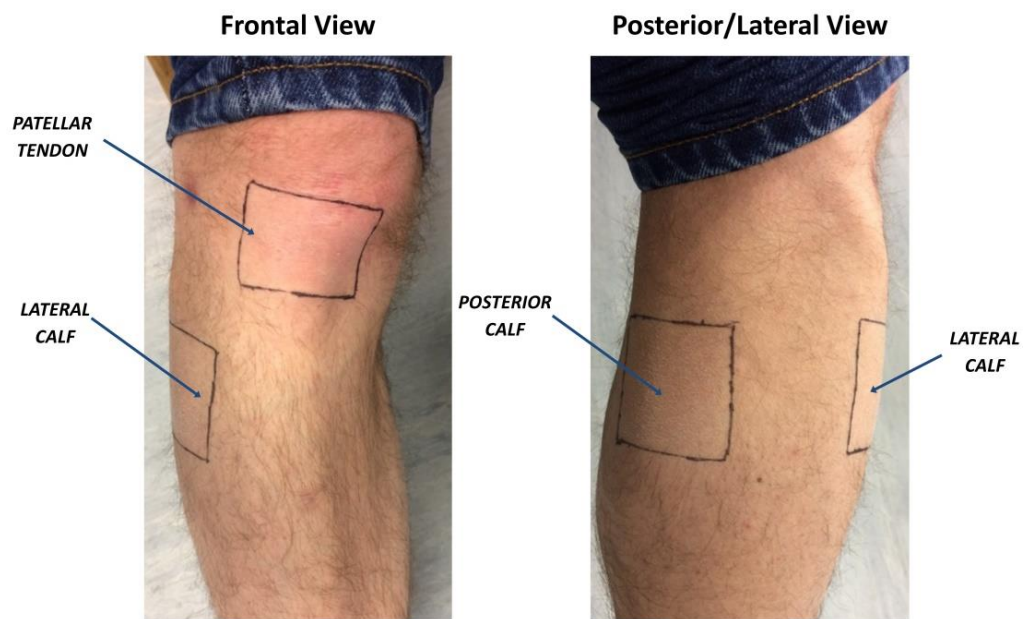


Figure 3.11 Shaved measurement areas of right lower leg prior to testing

The TCM electrodes, which are approximately 17 mm in diameter and 15 mm thick, were used as indenters, already located at relevant measurement sites. During the MRI studies, however, substitute polymer sensors which were 3D printed were used to recreate loading conditions in-situ (Figure 3.12).

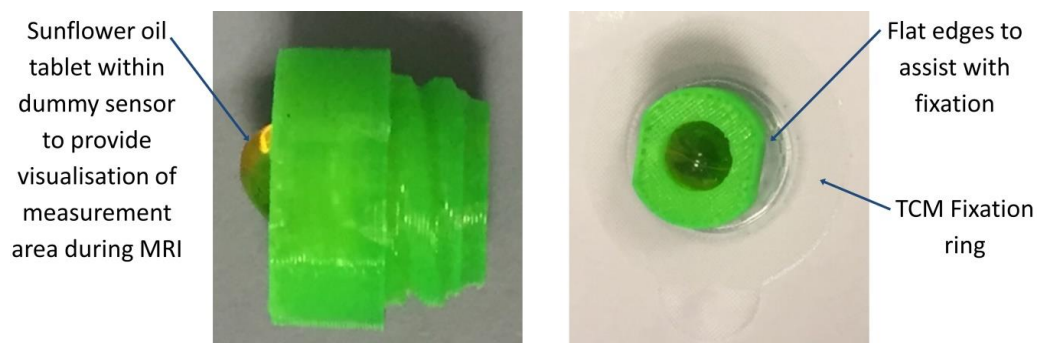


Figure 3.12 Left: 3D printed replica of (TCM), Right: 3D printed TCM sensor in fixation ring

3.3.3 Inflammatory Response

In the case of an inflammatory response to loading a range of cytokines are up-regulated, including IL-1 α and IL-1RA as precursors to non-reversible tissue damage [138-140, 161, 206, 211, 222-224, 244]. IL-1 α and IL-1RA have revealed the most consistent trends and have been successfully implemented in studies evaluating the effects of indenter loading and medical device use [138-140, 161, 206, 211, 222-224]. Results are often analysed as a ratio over total protein (TP) to account for inter-participant variation.

Inflammatory biomarkers are not specific to mechanical loading and can be upregulated due to other known stimuli such as hair removal [245]. As discussed previously hair was removed from measurement sites for use of the TCM electrodes (Figure 3.11). Preliminary testing was implemented to determine how far in advance of sessions hair should be removed to reduce the risk of biomarker upregulation due to the mechanical irritation of hair removal affecting results. The right leg of one participant (female, aged 28) was shaved in three 50 x 50 mm locations, each of which is load-bearing at the residuum-socket interface; the patellar tendon, medial calf and posterior calf. Preliminary tests involved collection of sebum with Sebutape prior to and at 1, 3, 24 and 48 hours post-hair removal. Measurements were also taken at a hairless 50 x 50 mm site on the lateral aspect of the foot, which acted as a negative control. Results as illustrated in Figure 3.13 indicate an upregulation of IL-1 α , normalised to TP, which was evident at the three test sites compared with the control site. The ratio values had decreased to lower than basal levels at 24 and 48 hours following hair removal (Figure 3.13).

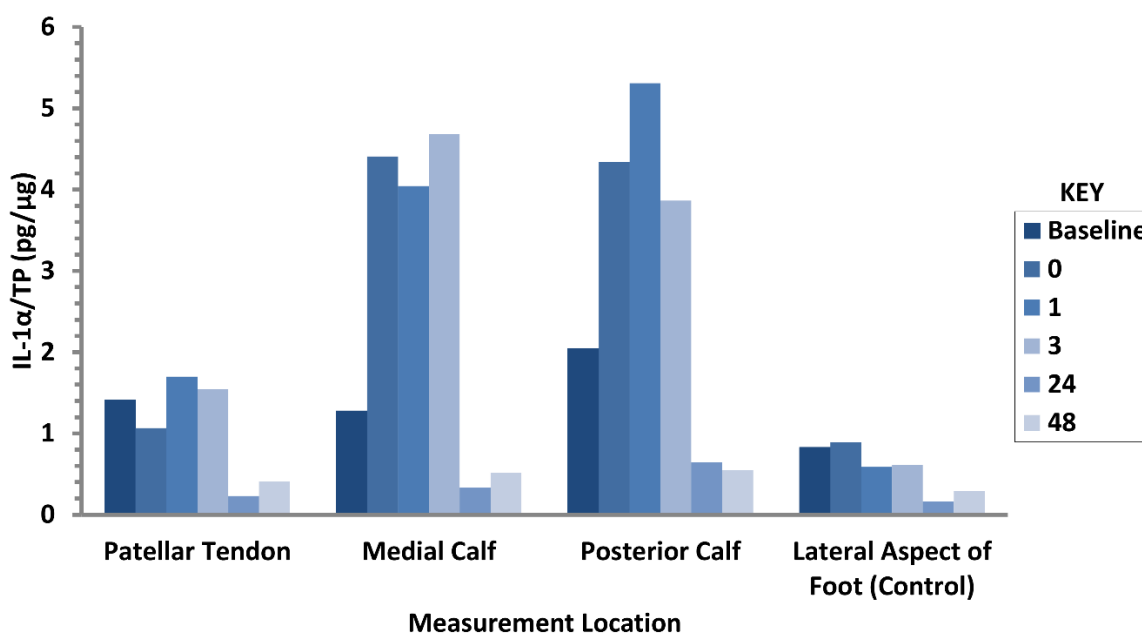


Figure 3.13 IL-1 α /Total protein at baseline and 0, 1, 3, 24 and 48 hours post- hair removal via shaving at a number of lower limb locations

3.3.4 Lymphatic Activity

During the preliminary testing phase, lymphatic function of 10 healthy participants without amputation was characterised using a NIR lymphatic imaging methodology [147]. Lymphatic activity was analysed during incremental pressure cuff loading from 20 mmHg to 60 mmHg (2.7 to 8.0 kPa) in 10 mmHg (1.3 kPa) steps every 10 minutes. During these tests the refractory period was also investigated. The findings revealed that after 35 minutes the lymphatic activity had returned to baseline levels, so this refractory period was subsequently adopted into the final test protocol. To review briefly, a micro-dose of Indocyanine Green (ICG, 50 μ L, 0.05% w/v) was injected sub-dermally, with half between the hallux and the second toe and half between the second and third toes of each participant (Figure 3.14). Following the injection, fluid pressure differentials caused the micro-dose to enter lymphatic vessels with the surrounding interstitial fluid. Lymphatic vessels are thin-walled and contain valves to ensure one-way flow, which is primarily controlled by external pressure from surrounding tissues. Under this pressure the microdose was transported within the lymphatic vessels towards the cervical lymphovenous portal, where filtered lymph re-enters the venous bloodstream [246].

The micro-dose was tracked, in the superficial lymphatic vessels that follow veins (Figure 3.14), by the NIR camera system (Fluobeam® 800, Fluoptics, Grenoble, France). The camera system consists of a 780 nm-centred laser light source that activates the ICG which emits light at a wavelength of 760 nm, and a charge-coupled device sensor. Following identification of active dermal lymphatic vessels, images were collected at baseline (5 minutes), within loading periods (the final 5 minutes) and within refractory periods (the first 5 minutes post-loading and the final 5 minutes) to investigate recovery.

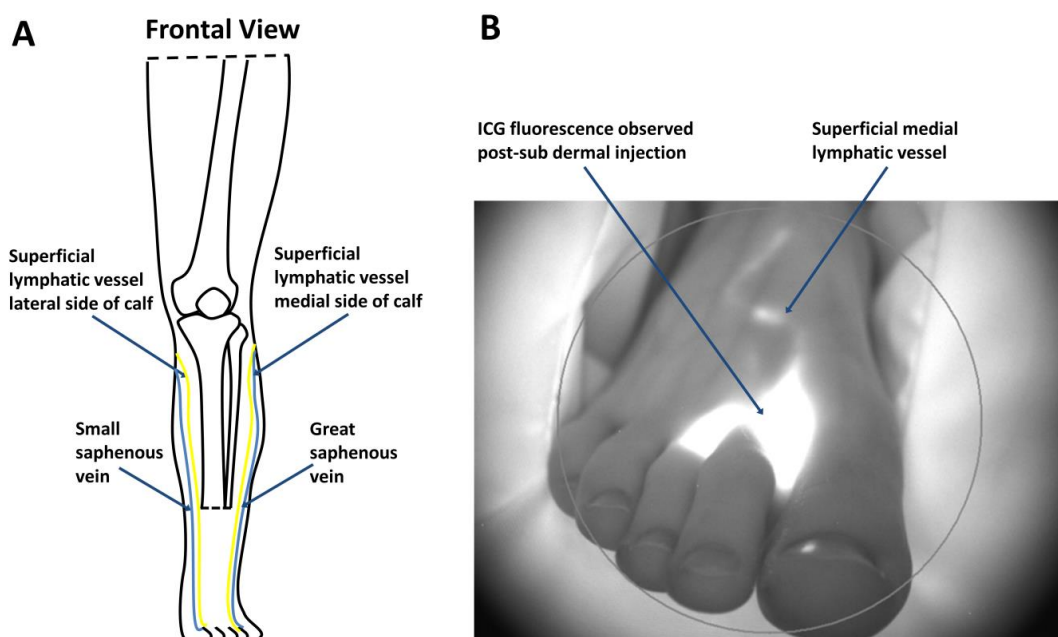


Figure 3.14 A: Superficial lymphatic vessels in the foot and shank, B: Indocyanine Green contrast injected sub-dermally between toes

For each participant, a distinct visibly active lymphatic vessel was selected and the camera was positioned perpendicular to its long axis at a height of ≈ 300 mm above the limb. The length of the visualised vessel within the field of view was measured using a tape measure.

Parameters of lymphatic activity were identified from the recorded images using a numerical computing environment (MATLAB, The MathWorks, USA) and a droplet morphometry and velocimetry tracking approach [247]. To review briefly, imaging videos were imported into MATLAB and the length of the visualised area was inputted in order to scale pixels to actual distances in mm. The lymphatic vessel was selected as the region of interest to discriminate it from the rest of the image, cropping out the background via averaging over 5 frames. An intensity threshold of ≈ 20 was applied to remove noise, while enabling detection of intensity peaks that correspond to lymphatic packets.

The frequency of transient lymph packets travelling past the cuff or image border were calculated, with the lymphatic response divided into three categories, namely,

Category 1: Normal function- Number of transient packages during each phase was similar to baseline

Category 2: Increased activity post-loading- Increased number of transient packages compared to baseline, returning to baseline following recovery phase

Category 3: Decreased activity post-loading- Decreased number of transient packages immediately post-loading with function possibly returning during recovery phase.

The estimated lymphatic packet frequency following the application of the incremental loading and recovery phases for each of the 10 participants are illustrated in Figure 3.15.

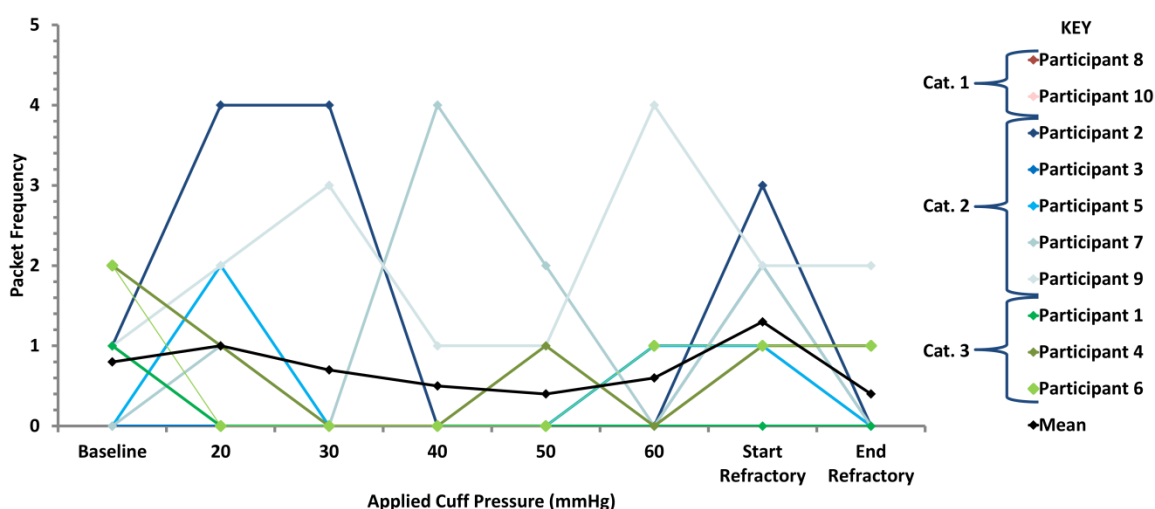


Figure 3.15 Lymphatic packet frequencies under incremental pressure cuff loading in the calf tissues of 10 participants

Compared with baseline, mean lymphatic packet frequency increased by 50% after pressure release, returning to baseline by the end of the refractory period (Figure 3.15). Individual variation was evident with a Category 1, 2 and 3 response observed in two (#8 and #10), five (#2, #3, #5, #7 and #9) and three (#1, #4 and #6) participants respectively (Figure 3.15). At 50 to 60 mmHg, pooling at the cuff and backflow events were observed, but in three participants (#5, #6 and #9) there was sufficient accumulation to overcome occlusion. However, we cannot determine whether these packets also passed the upper cuff border as imaging took place below the pressure cuff. A previous study reported that the flow of lymphatic packets was only evident when the cuff pressure was reduced from 60 mmHg (8 kPa) to 29.3 ± 16 mmHg (3.9 ± 2.1 kPa), in healthy participants [235]. It is interesting to note that in the present study packet activity actually increased at lower pressures in a number of individuals e.g. #2. This behaviour is similar to that observed in compression garment therapy to assist with manual lymphatic drainage [236].

Results in a previous study from the host lab involving mechanical loading of the arm reported 1 to 8 lymphatic packets at baseline [148]. This suggests biological variation in lymphatic activity between sites. Indeed in the present preliminary study, lymphatic activity was difficult to observe close to the pressure cuff, in a number of participants, as vessels which initiated superficially in the foot were presumed to drain deeper out of the viewing range. The supine position of participants with their leg raised by foam supports could have affected activity, although it did facilitate increased participant comfort and support of the measured limb and access to sensors.

3.3.5 Measurement Techniques Decision Matrix

A large number of measurement techniques are available to investigate the physiology of soft tissues and mechanisms of soft tissue damage. A decision matrix was implemented to further focus this research and ensure that selected techniques were suited to successfully complete the overarching research aim; evaluate changes in soft tissue health and tolerance at the residual limb-socket interface. This involved tabulating the techniques used in the preliminary tests and scoring them against relevance to the research question, scientific novelty and practicality (Table 3.5 and Table 3.6).

Table 3.5 Scoring table for measurement techniques decision matrix

Score	Relevance	Scientific Novelty	Practicality
1	Not at all- Does not help complete overarching research aim, not enabling evaluation of soft tissue health and tolerance to loading	Absolute uncertainty- Saturated area of research, not novel use	Not at all- Very complicated logistically to carry out measurement technique, not really possible to use in-situ with MRI
2	Very Remote	Very Remote	Very Impractical
3	Remote	Remote	Impractical
4	Very Low	Very Low	Very Low
5	Low	Low	Low
6	Moderate- Helps to complete overarching research aim partly- Indirectly helps evaluation of soft tissue health and tolerance to loading	Moderate- Some research using this technique including some amputation research	Moderate- More complex to implement with participants with amputation or in-situ with MRI
7	Moderately High	Moderately High	Moderately High
8	High	High	High
9	Very High	Very High	Very High
10	Almost Certain- Helps to complete overarching research aim by enabling evaluation of soft tissue health and tolerance to loading	Almost certain - Little research using this recognised technique, no amputation research using this technique	Almost Perfect- Easy to implement with both participants with and without limb loss

Table 3.6 Measurement techniques decision matrix

Criteria and Scoring								
Measurement Technique (soft tissue analysed)	Tissue Damage Mechanism Characterisation	Question to Answer	Relevance Score/10	Novelty	Publishability Score/10	Ease of Use	Practicality Score/10	Total Score/30
Temperature & Humidity (Dermal Surface)	- Vulnerability of skin to superficial damage by indication of skin tissue tolerance to loading	- Does skin temperature and humidity increase under loading? - Is testing representative of microclimate observed at interface in real life?	6	- We already know the temperature and humidity will increase at the residuum-socket interface [99]	5	- Simple sensors - Sensors may have to be open to the air to function - Sensors could influence pressure distribution themselves - Real time	9	20
Transcutaneous Gas Tension (Dermal)	- Ischaemia	- How do TcPO ₂ and TcPCO ₂ alter under loading? - Magnitude of pressure/shear that can be applied prior to ischemia? - Is there a difference in TcPO ₂ and TcPCO ₂ measurements between amputated and intact limbs?	10	- Used in previous studies establishing tissue perfusion in response to mechanical loads and repositioning, as a predictive indicator for ischaemia and pressure ulcers [210, 211, 213-215] - Amputation research with regards to level and healing [217]	7	- Requires heating of sensors and constant attachment to participant throughout testing session [216] - Sensors will influence pressure distribution - Real time	8	25

Collection of Inflammatory Biomarkers (Dermal)	- Inflammatory Response	- Does level of IL-1α or IL-1RA increase under representative prosthetic loading? - Is there a difference in upregulation between amputated and intact limbs?	9	- Used in a number of studies to evaluate the effect of applied pressure and pressure in combination with shear [138-140, 161, 211, 222, 223] - No amputation research known	9	- Easy technique though labour intensive analysis - Low sample volumes and concentrations - Biomarkers are sensitive but not specific - Not real time measurement	7	25
	- Lymphatic Impairment	- How is lymphatic activity affected by loading conditions representative of prosthesis loading?	10	- Little research-Canine models [233, 234] and more recent studies using lymphoedema participants [148, 235, 236] - No amputation research known	10	- Involves injection of contrast to observe lymphatics - Unknown and variable lymphatic structures after amputation present a risk to participants	4	24
	- Direct deformation	- How does applied loading deform tissues? - How does the muscle and adipose tissue composition differ between amputated and intact limbs	10	- Visualisation of musculoskeletal damage under loaded conditions in rat models [165, 172, 173] - MRI based subject specific FE models of transtibial residuum have been created [110, 114-116]	7	- Expensive and limited availability - Not suitable for claustrophobic participants - Compromise between scan time and image resolution	7	24

From the results in Table 3.6, the lowest scoring technique, namely temperature and humidity measurements, were discarded from the final test protocol. As discussed in Section 2.1.2 the interface between the limb and the socket typically exhibits an elevated temperature and humidity, each of which will reduce the tissue tolerance to loading and increase friction at the interface [103, 248]. As expected during preliminary testing temperature and humidity were observed to increase under pressure application as the cuff is non-permeable and provides a barrier to heat loss and sweat removal. These results can be observed in Appendix A.

Microclimate is an important consideration when investigating skin tolerance to loading and can negatively impact a prosthetic user's quality of life [103]. However, this protocol was focussed on visualising adaptation of the tissues and measuring the physiological response of the soft tissue to representative loading in terms of the damage mechanisms discussed in Section 2.2.1. Therefore, temperature and humidity measurements were not included in the final testing protocol.

All other potential measurement methods were considered appropriate for inclusion in the test protocol for participants without amputation and were reviewed after implementation within this cohort prior to final protocol development for participants with amputation. Due to the practical aspects of NIR lymphography and the need for ethics approval to include injection of contrast agent into the residual limb and consideration of the measurement techniques matrix, it was decided to exclude this measurement from the protocol associated with the cohort with amputation. NIR lymphography results for the cohort without amputation are presented in Section 3.3.4.

3.4 Developed Protocol

This section in-part covers objective 2:

2. Select measurement techniques that may be suitable to assess status or tolerance and adaptation of residual limb soft tissues and measure the physiological response to representative applied loads in a cohort of healthy participants without amputation

Skin surface measurements of T_{cPO_2} , T_{cPCO_2} and inflammatory biomarkers released into sebum and collected on the skin surface were taken specifically from the patellar tendon, lateral calf and posterior calf of the right control limb of ten participants without amputation, and the residual limb and contralateral limb of 10 participants with unilateral transtibial amputation. In each case, loading was applied using an incrementally imposed pressure representative of static weight bearing using the PPAM aid. MRI was implemented to observe the tissue composition and volumetric soft tissue deformations which resulted from the loading.

3.4.1 Ethical Consideration

Ethical approval for protocols with participants without amputation and participants with transtibial amputation were provided after review by the Faculty of Engineering and the Environment (FEE) ethical review board, respectively (Study Refs. ERGO29696 and ERGO41864, Appendix B).

If a participant matched any of the exclusion criteria or did not adhere to the inclusion criteria they were excluded from the study (Table 3.7).

Table 3.7 Inclusion and exclusion criteria for testing protocols, Key: - = Participants without amputation only, * = participants with amputation only, ● Contraindications to MRI and « = Contraindications to use of Indocyanine Green contrast and therefore only relevant to participants without amputation

Inclusion Criteria	Exclusion Criteria
Aged over 18 years old (* with unilateral transtibial amputation)	● Pacemaker, metallic or active implants
Able to give informed consent	● Presence of metal fragments in eyes
No contraindications to use of MRI	● High risk of deep vein thrombosis; genetic clotting disorders, use of recreational drugs, malignant tumour or cancer, recent surgery, obesity, smoking, congestive heart failure, irritable bowel disease
Healthy	●« Pregnancy or « nursing
- No active or history of vascular, skin or lymphatic conditions such as diabetes No active skin conditions in measurement areas	« Sensitivity or allergy to iodide, Micropore or Sebutape
Individuals able to remain still for ≈20 minute periods during MRI	« Kidney, liver or thyroid conditions
Individuals able to hold their bladder for ≈1.5-2 hours	● Claustrophobia

3.4.2 Measurement Techniques

Characterisation of Soft Tissue Constituents and Deformation

A 3T MRI scanner (MAGNETOM Skyra, Siemens, Germany) based at the Faculty of Medicine, University Hospital Southampton site, was used to implement volumetric T1 DIXON sequencing with an TE of 6.15 ms and TR of 17.10 ms as determined during preliminary testing (Figure 3.10).

A 30 minute acclimatisation and set up period was implemented. Participants lay supine within the MRI scanner, with their test leg elevated and resting on foam supports (Figure 3.16). A radio frequency anterior abdominal body coil (Body 60/Body30, Siemens, Germany) was positioned over the limb to be imaged to transmit the MRI excitation pulse and receive the corresponding signals.

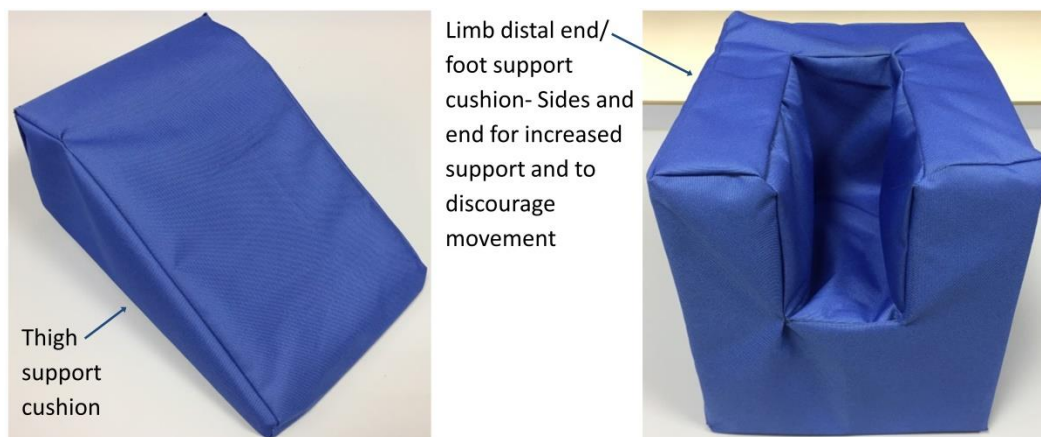


Figure 3.16 Foam support cushions to support participants during testing

At the start of the testing session sunflower oil tablets were positioned within dummy 3D printed TCM electrodes. Images were taken at baseline and during cuff inflation pressures of 20 mmHg (2.7 kPa) and 60 mmHg (8.0 kPa) with a 13.4 cm Field of View. Images had an in-slice resolution of 0.6 x 0.6 mm and a slice thickness of 1.2 mm.

Image slices were saved as DICOMs and imported into image segmentation and processing software (Simpleware ScanIP 2018.03 (Synopsys, California, US) and Image J 1.52p (Rasband, W. National Institutes of Health, US)). Watershed tools and thresholding were used for segmentation of the sunflower oil tablets at the measurement sites. Segmentation masks were automatically interpolated across slices to create 3D mask volumes. ScanIP mask calculations were implemented to determine the centroid of the sunflower oil tablets. By subtraction of the Image patient position, within the DICOM information, the slice corresponding to the centre of the oil tablets could be determined.

These selected slices were then imported into ImageJ to use the line measurement tools for calculation of gross strain under the indenter at each of the three measurement sites (Figure 3.17).

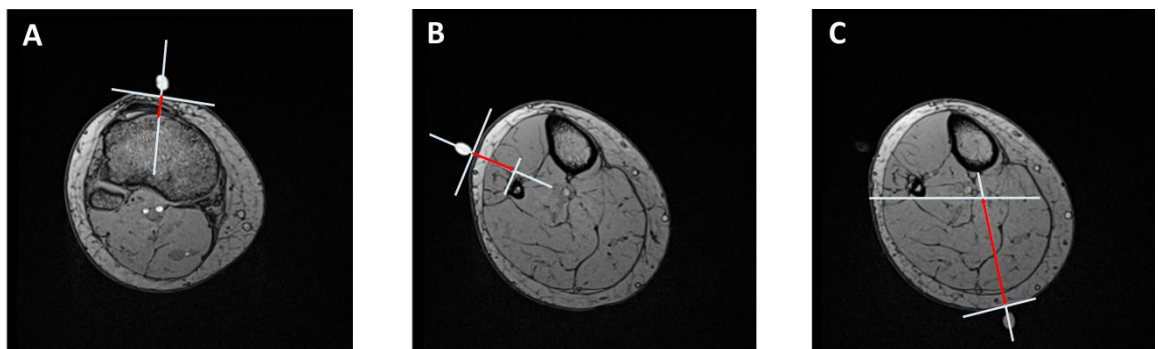


Figure 3.17 Transverse MRI slices of a participant's calf at baseline displaying how measurements of gross tissue deformation under the indenter sites were made at the A) patellar tendon, B) lateral calf and C) posterior calf, Note: white represents construction lines and red represents measurement taken

Measurements were taken normal to the soft tissue from the outer edge of the skin to in line with a bony feature (Figure 3.17). Measurements were repeated three times at each site and a mean value was calculated.

Tissue composition was analysed by quantifying superficial adipose and adipose infiltrating muscle, using the fat saturated images. DICOM stacks were imported into ImageJ 1.52p (Rasband, W. National Institute of Health, US). Background noise was removed by subtracting a pixel intensity of 10 and the in-built Auto Threshold Stack tool was used to convert the images to binary, as illustrated in Figure 3.18A & B. An interpolation macro, developed by a colleague Charalambos Rossides, was used to create masks of the whole soft tissue area, tibia, fibula and muscle for slices spanning the measurement areas on the limb [249]. These masks were then subtracted from the binary stack to create masks just including the superficial adipose and adipose infiltrating muscle tissue (Figure 3.18C & D). The in-built ImageJ function 'Analyse Particles' was then used to calculate the area of overall soft tissue, superficial adipose and adipose infiltrating muscle. A more detailed step by step description of this process is provided in Appendix C.

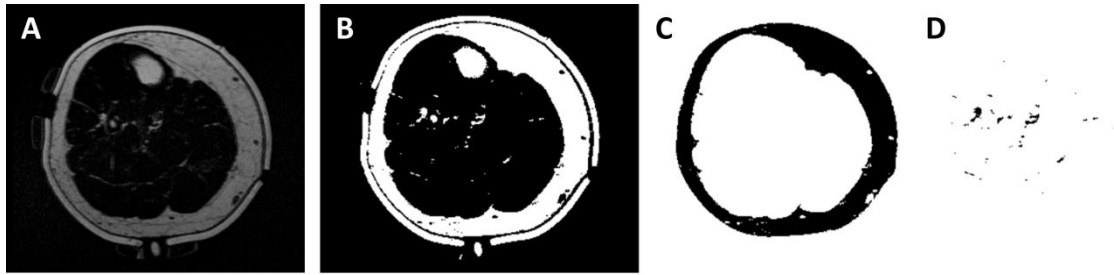


Figure 3.18 Processing of transverse MRI fat saturated slice of lower limb at posterior calf measurement site showing A: Original, B: Post-thresholding, C: Superficial adipose mask, D: adipose infiltrating muscle mask

The MyotonPro™ (Myoton AS, Estonia) was also available for use to measure the structural stiffness of soft tissues to assess the potential adaptation post-amputation of soft tissues. The Myoton probe includes a triaxial accelerometer and a system which allows multidirectional measurements in relation to the gravity vector. The probe, 3 mm in diameter, was held perpendicular to the skin surface to ensure that the energy from a mechanical impulse is transferred to the muscle maximally in a constant manner (Figure 3.19).



Figure 3.19 MyotonPRO™ device used to measure structural stiffness of the residuum soft tissue

The probe applies a mechanical impulse (15 ms, 0.4 N) to induce damped natural oscillations of the soft tissues. The device was used in multi-scan mode consisting of 10 single measurements, at one second intervals, and the mean value for the stiffness parameter was calculated [130, 131]. The device has been shown to produce high levels of inter- and intra-rater reliability across several muscles in a previous studies [130-133, 250]. To investigate inter-rater reliability, MyotonPro™ measurements were performed at the patellar tendon and tibialis anterior from 16 participants by two raters as part of a larger research study investigating the Inter- and Intra-rater reliability in ultrasound scanning and Myoton technique of various skeletal muscles (Study Ref. ERGO40307). Intraclass Correlations (ICCs) for stiffness extracted from the damped natural oscillations were calculated. The findings in Table 3.8 reveal a high ICC (0.97) at the tibialis anterior site. By contrast the ICC value was 0.62 at the patellar tendon site, probably due to its more complex and stiff anatomy.

Table 3.8 Intraclass correlation of two raters taking MyotonPro™ measurements from two sites

Measurement Site	Stiffness Intraclass Correlation (ICC)
Patellar Tendon	0.619
Tibialis Anterior	0.974

Characterisation of Tissue Ischaemia

Physiological measures of T_cPO_2 and T_cPCO_2 were monitored, at the patellar tendon using combined electrodes (E5280 and TCM5 O_2 & CO_2 combined, Radiometer, Denmark), while T_cPO_2 alone was monitored at the lateral and posterior calf using single channel electrodes (E5250, Radiometer, Denmark) attached to separate monitors (TCM4, TCM400 Radiometer, Denmark, respectively).

The patellar tendon was selected for the combined measurement as it is considered to represent a load tolerant structure that is typically loaded by a prosthetist and could be susceptible to biomechanical adaptation in response to regular prosthetic loading. The transcutaneous gas tensions were recorded continuously during load application at a frequency of 1 Hz (TCM5 combined sensor), 0.5 Hz (E5280 combined sensor) and 0.033 Hz (T_cPO_2 sensors). As part of a preconditioning period, each electrode was heated to 43.5°C to ensure maximum vasodilation in the soft tissues [216].

A percentage change from baseline of T_cPO_2 and T_cPCO_2 was used to accommodate individual variation, i.e. participants acted as their own control. As in previous research, values of T_cPO_2 and T_cPCO_2 at the patellar tendon were categorised according to that described in Table 3.4 [211, 213, 215].

Characterisation of Inflammatory Biomarkers

A sebum sample was collected, at each of the measurement sites, by applying Sebutape (CuDerm, Dallas, TX, USA) to the skin for two minute periods at baseline and immediately after loading. Although Perkins et al utilised a 1 minute sampling period [244], in recent research 2 minute sampling periods have been used [138-140, 161, 206, 224] to provide sufficient time to sample the biofluid, namely sebum. The Sebutape was positioned carefully on the skin using blunt tweezers, a roller, and gloved hands, to avoid cross contamination of skin proteins. All Sebutapes were labelled and stored in tubes in the freezer at -80 °C prior to biochemical analysis.

Quantities of proteins were determined using immunoassays in an Enzyme Linked Immunosorbent Assay (ELISA) technique, based on a previous protocol [138, 244]. To review briefly, the frozen tapes were thawed to room temperature and 1.7 ml of phosphate buffered saline (PBS; Sigma-Aldrich Co, St. Louis, Missouri, USA) + 0.05% Tween (Sigma-Aldrich Co, St. Louis, Missouri, USA) solution was added to each tube to facilitate recovery of proteins from the tapes. After immersion for one hour, the tapes were sonicated for 10 minutes in a room temperature water bath. Tubes were then vortexed vigorously for 2 minutes.

Capture antibody, specific to the protein, was pre-coated onto a cytokine assay plate (Meso Scale Diagnostics, USA), and formed the bottom of the immunoassay sandwich. After refreezing overnight at -80 °C, the tape extracts were thawed. Proteins from the tapes were processed and analysed by adding the samples and detection antibody, specific to the protein, to the wells using Immunoassay kits (Meso Scale Diagnostics, USA). The TP on each tape was also estimated using a protein assay kit (Thermo Fisher Scientific, UK). Briefly, serial dilution of bovine serum was completed to produce standards from 0 to 500 µl/ml. 150µl of Coomassie Blue (Sigma-Aldrich Co, USA) was then added to 150µl of each standard and sample plated in triplicate. The optical densities of samples were then compared to prepared standards to estimate concentrations of TP, IL-1α and IL-1RA.

Percentage change in ratios of IL-1α/TP and IL-1RA/TP, from baseline, were reported and analysed to account for participant variations (e.g. uptake and concentrations) in sebum, in a similar protocol to that reported previously [161, 244].

3.4.3 Participants without Amputation Testing Protocol

A pre-testing questionnaire was used to obtain each participant's demographics (sex, age). Weight, height and maximum calf circumference were measured using the lab scales, a 'drop down' tape measure and a soft tape measure, respectively.

Biophysical measurements and MRI were implemented in two separate testing sessions as follows:

Pre-test session Shaving of test areas implemented 48 hours in advance of testing sessions.

Testing Session 1- TCM, biomarker collection and lymphatic imaging while right limb was unloaded, loaded incrementally with representative pressures and during the following unloading period. The test set up is shown in Figure 3.20 and Figure 3.21.

Testing Session 2- MRI while the calf was unloaded, and during the application of two cuff pressures. There was a minimum time of 90 minutes between testing sessions to enable the participant to have a break and leave time for setting up.

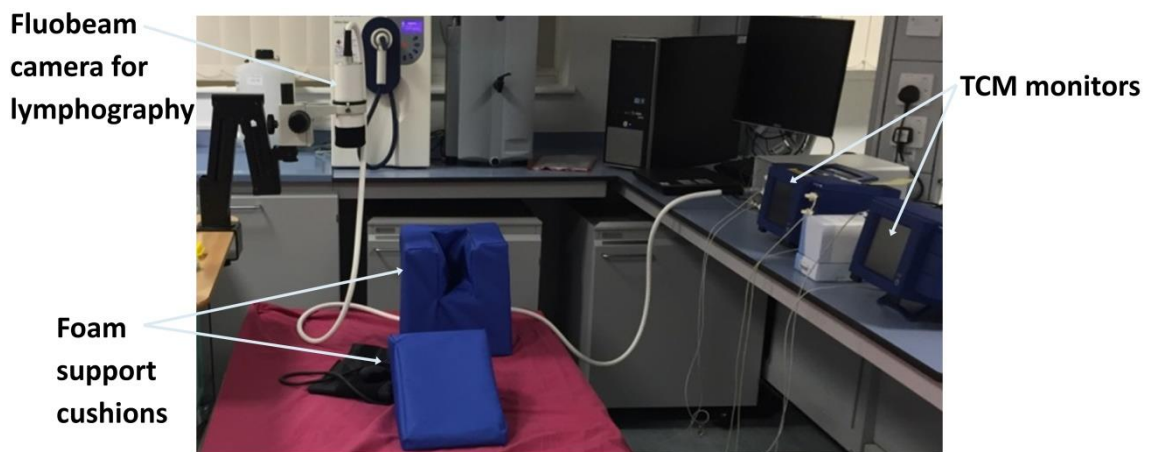


Figure 3.20 Protocol testing set up for participants without amputation

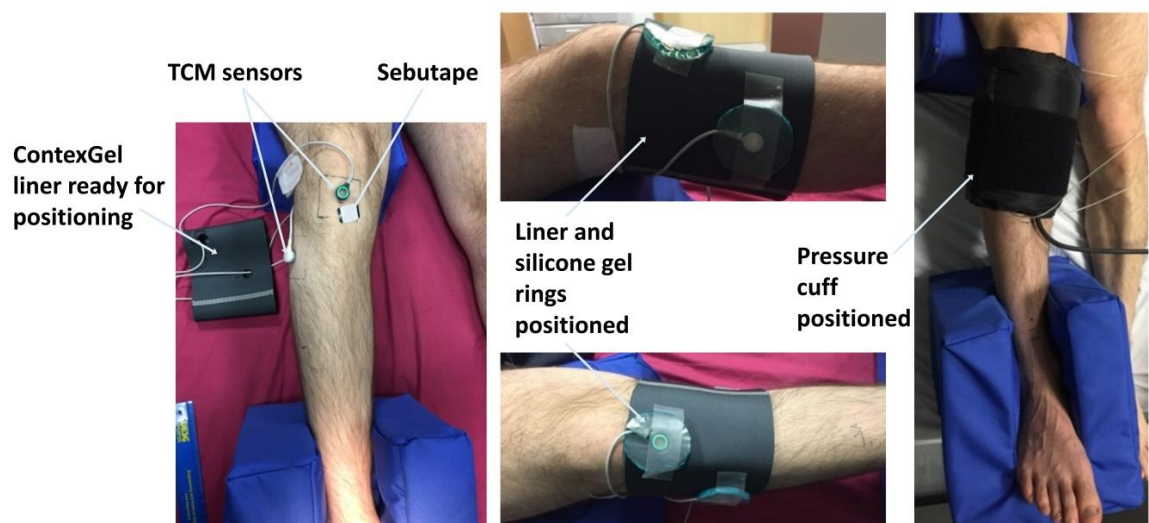


Figure 3.21 Participants without amputation protocol liner, silicone gel and pressure cuff setup

The protocol for the two test sessions is described on the two following pages (Figure 3.22 and Figure 3.23). For a detailed activity checklist for each test session see Appendix D.

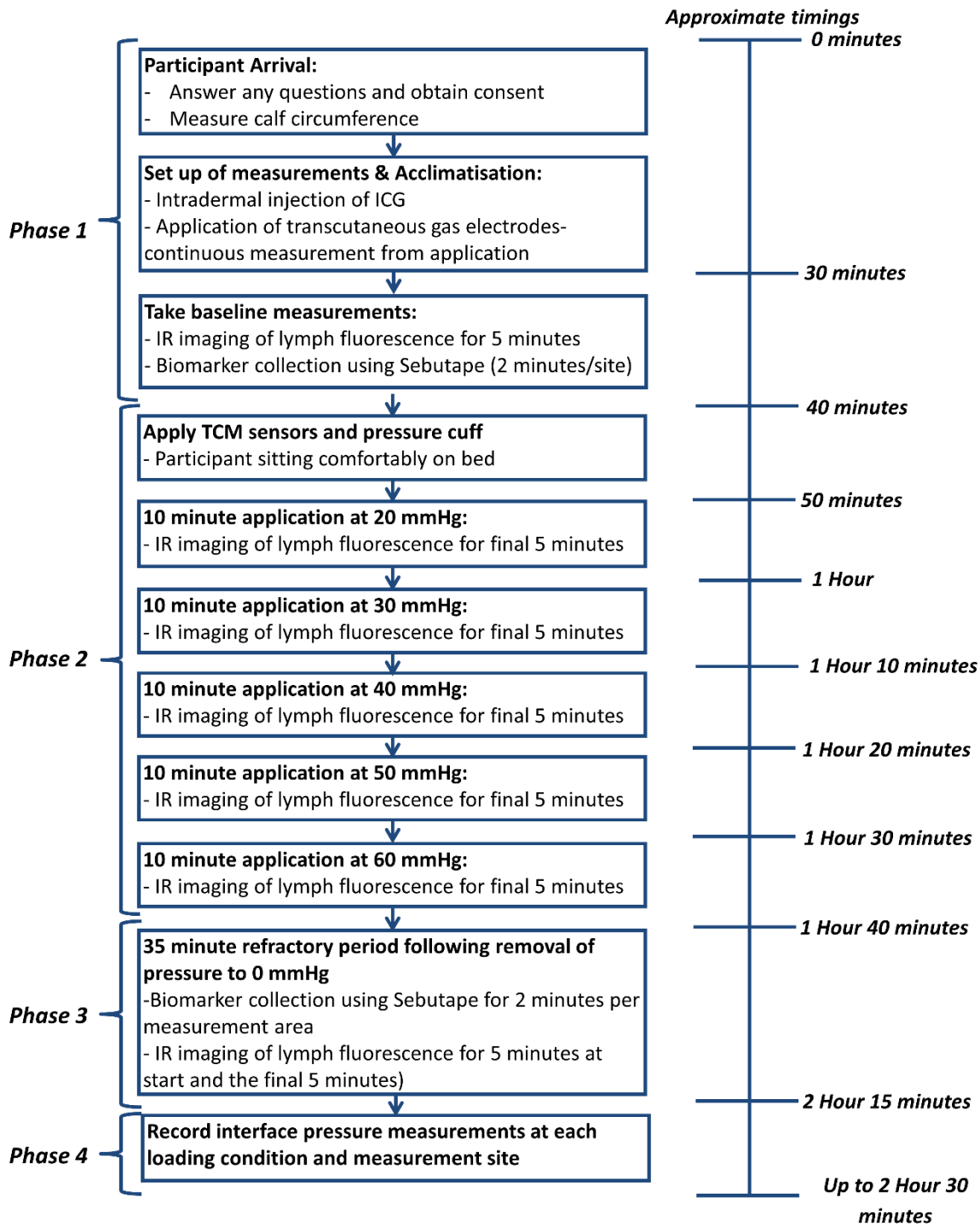
Testing Session 1 Protocol:

Figure 3.22 Flow chart showing testing session 1 protocol for participants without amputation

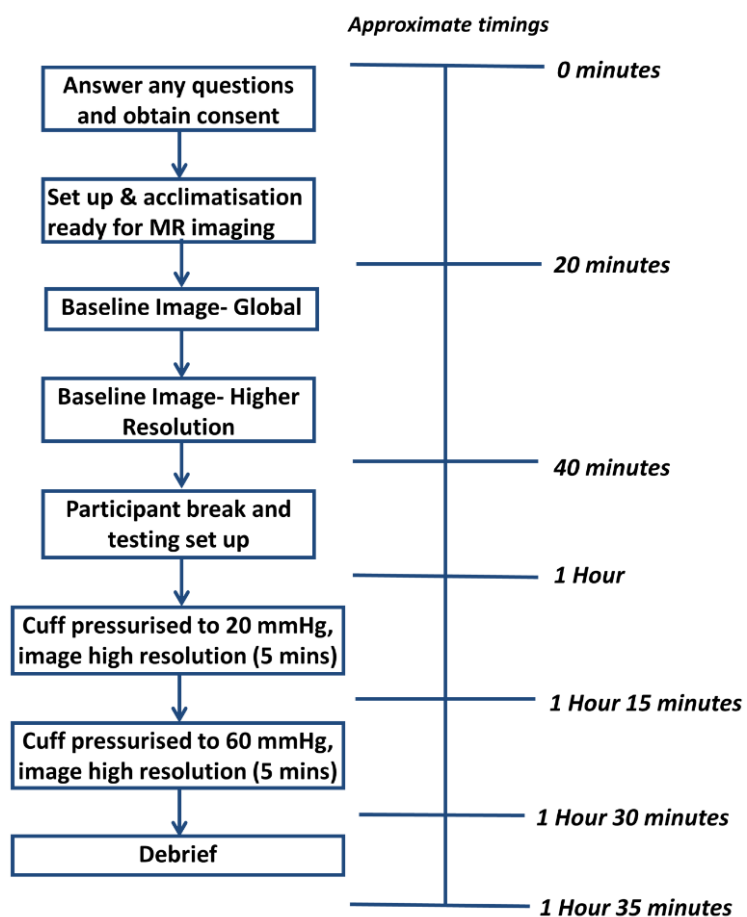


Figure 3.23 Flow chart showing testing session 2 protocol for participants without amputation

3.4.4 Participants with Transtibial Amputation Testing Protocol

Participants with transtibial amputation were recruited from the community via poster advertisement through organisations, such as Finding Your Feet and LimbCare, a Patient & Public Involvement (PPI) workshop with prosthetic limb users local to Winchester and word of mouth. A comprehensive list of recruitment avenues explored for this study is provided in Appendix E.

The main adaptations from the protocol adopted with individuals without amputation were:

1. Removal of the lymphatic imaging as discussed in Section 3.3.5.
2. Use of the MyotonPro™ to measure structural stiffness of the tissues.
3. The MRI testing session (2) was not part of a diagnostic session. However, due to the presence of pathologies in the population with amputation, T2 sagittal screening scans were taken to identify any pathology as reviewed by a Radiology Consultant. If any obvious abnormality was observed the GP of the participant was contacted by letter to decide if further investigation was required.
4. A 20 minute comfort break was introduced to the MRI testing session due to the longer duration on account of imaging both lower limbs and implementing screening scans. Only the right limb of participants without amputation was imaged so testing would have stopped prior to the comfort break.

A pre-testing questionnaire (Appendix B) was used to obtain each participant's demographics (sex, age) as well as cause of amputation, approximate amputation date and approximate daily socket use in hours. Weight and height were measured using the combined lab scales and 'drop down' tape measure and maximum calf circumferences and residual limb length were measured using a soft tape measure.

Biophysical measurements and MRI were implemented in two separate testing sessions as follows:

- Shaving of measurement areas implemented at least 48 hours in advance of testing sessions where possible.

Testing Session 1- TCM, biomarker collection while both residual and contralateral limbs were unloaded, loaded incrementally with representative pressure and following unloading. The testing set up is shown in Figure 3.24. MyotonPro™ measurements were taken at the end of the refractory period during this session.

Testing Session 2- MRI while residual and contralateral limbs were unloaded, and during the application of two cuff pressures, as illustrated in Figure 3.25. There was a minimum time of 90 minutes between testing sessions to enable the participant to have a break and leave time for setting up.

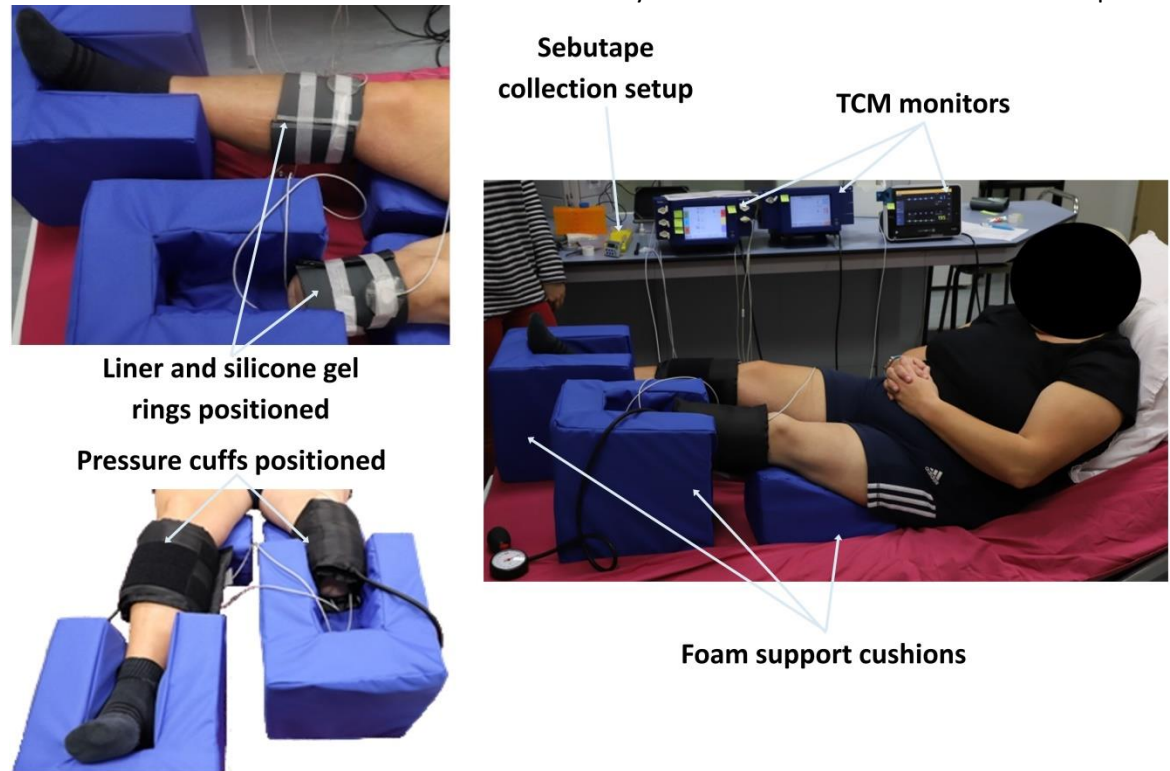


Figure 3.24 Testing setup for participants with amputation

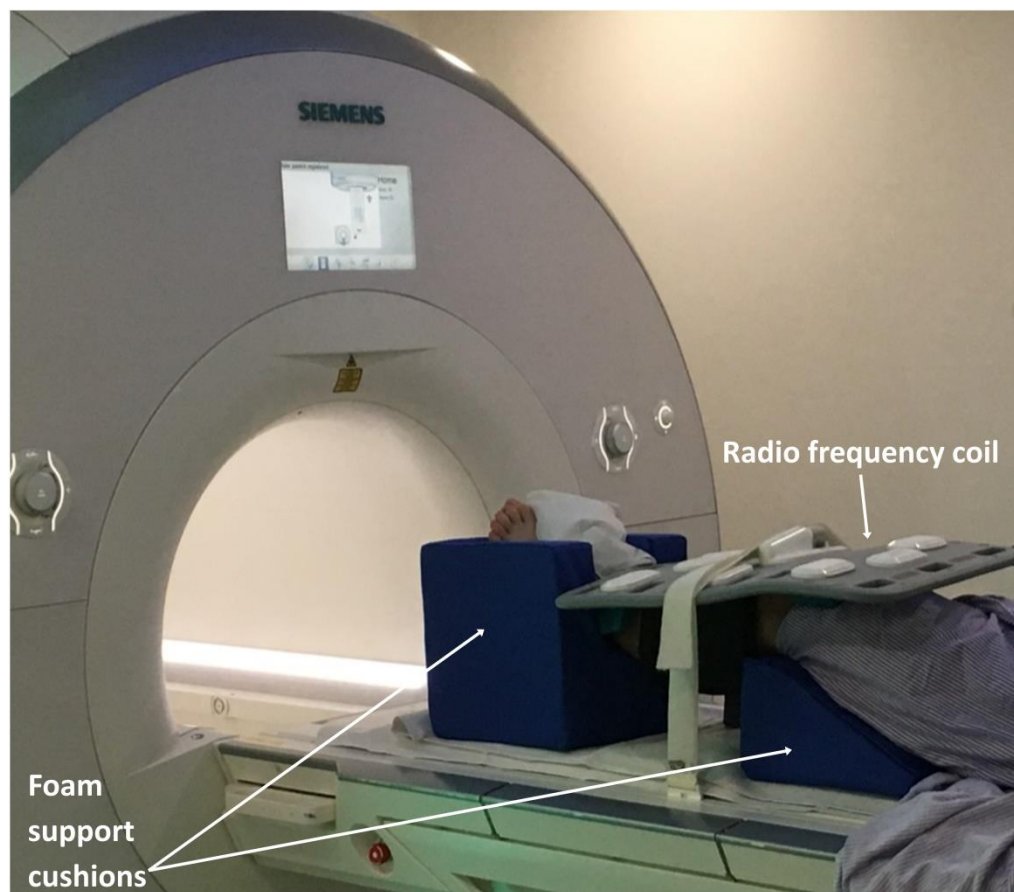


Figure 3.25 MRI testing set up

The protocol for the two testing sessions is described on the following two pages (Figure 3.26 and Figure 3.27). A detailed activity checklist for the test sessions is provided in Appendix F.

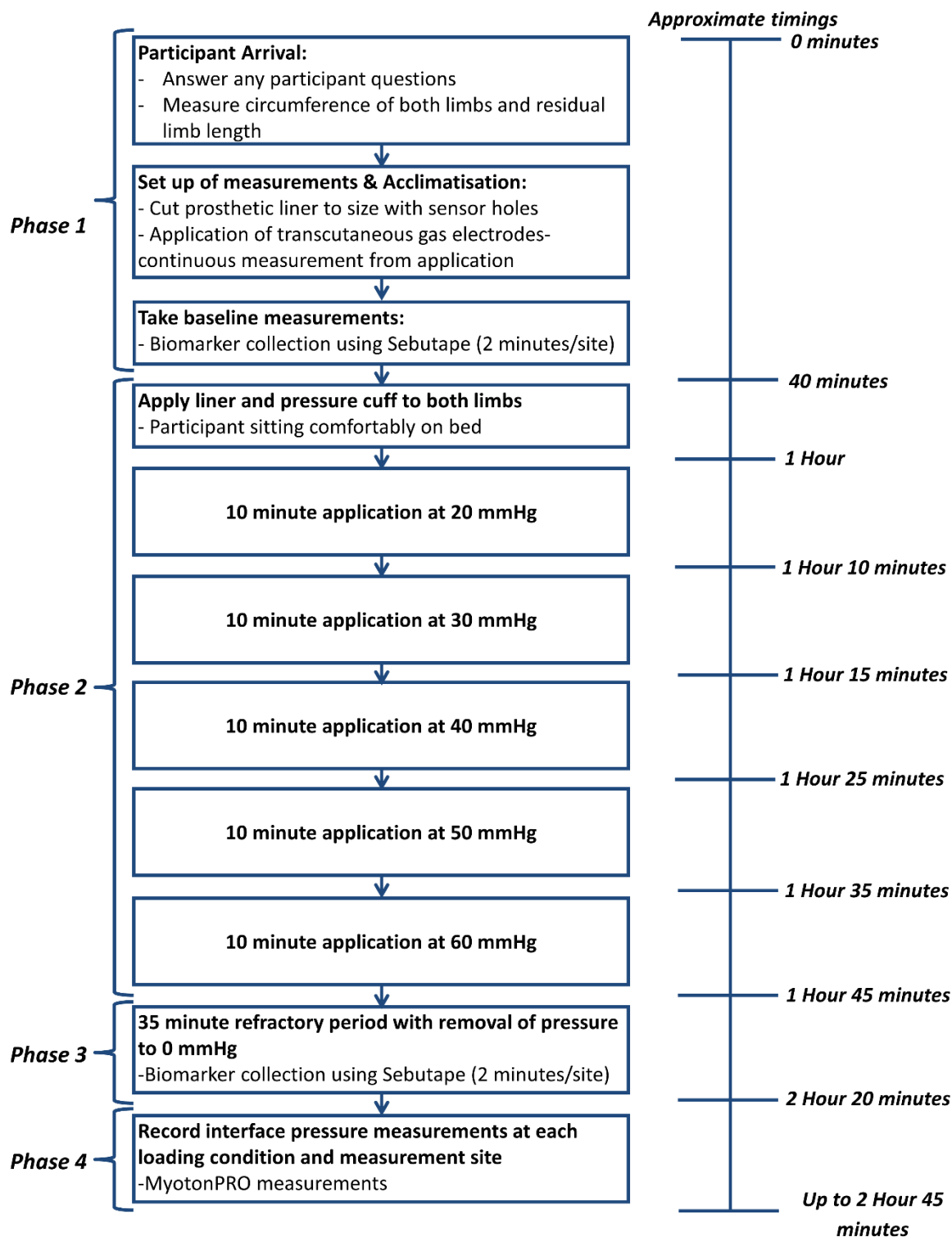
Testing Session 1 Protocol:

Figure 3.26 Flow chart showing testing session 1 protocol for participants with unilateral transtibial amputation

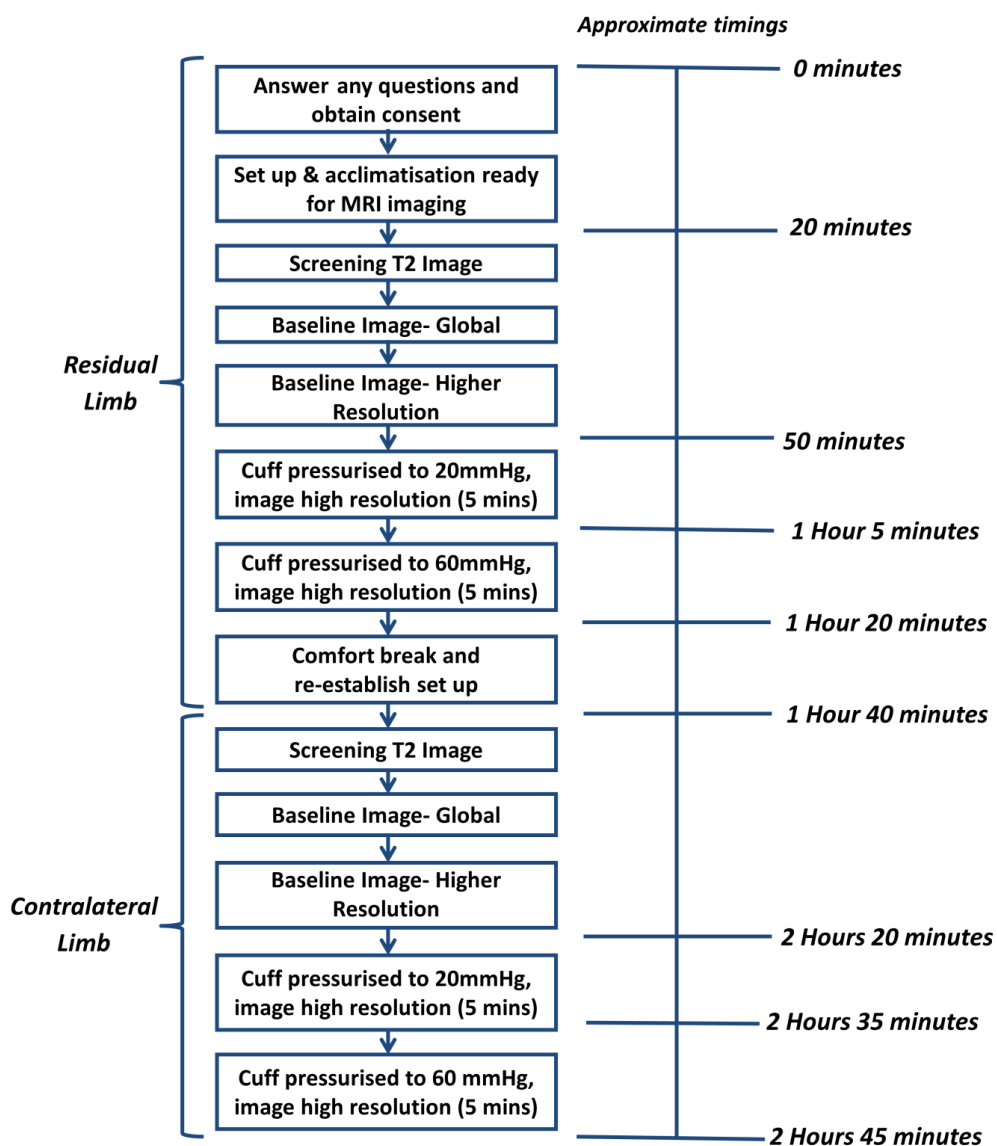


Figure 3.27 Flow chart showing testing session 2 protocol for participants with unilateral transtibial amputation

3.5 Research Questions, Aims and Objectives

This section covers parts of objectives 2, 3 and 4:

- 2. Select measurement techniques that may be suitable to assess status or tolerance and adaptation of residual limb soft tissues and measure the physiological response to representative applied loads in a cohort of healthy participants without amputation**
- 3. Investigate soft tissue adaptation and measure the physiological response to applied loads in participants with transtibial amputation**
- 4. Investigate associations between adaptation and tissue tolerance to loading and cause of amputation/time post-amputation**

To help focus the data analysis the overarching research aim was revisited and split into three research questions to be answered.

Overarching Research Aim: To evaluate soft tissue health and tolerance of residual and intact limbs under representative prosthetic loads

Research Questions:

- 1. Are there changes in tissue composition in the residual limb following amputation?**

Research Question 1 Aims

- a) To evaluate and compare tissue composition between residual and contralateral limbs in participants with unilateral transtibial amputation
- b) To compare tissue composition in participants with unilateral transtibial amputation to a control cohort of aged matched participants without amputation
- c) To assess correlations between BMI and tissue composition
- d) To assess the effects of time, cause of amputation and socket use on tissue composition in residual and contralateral limbs

Research Question 1 Objectives

- Take MRI scans of individuals with and without amputation, using a 3T MRI scanner (MAGNETOM Skyra, Siemens, Germany), with a focussed fat saturation protocol involving T1 DIXON Volumetric Interpolated Breath-hold Examination (VIBE) sequencing
- Analyse MRI images using ImageJ to differentiate muscle, bone, superficial adipose and fat infiltrating adipose tissue.
- Present soft tissue (superficial adipose, infiltrating adipose and muscle) percentages through the limb for each participant

- Calculate percentage volume of superficial and, infiltrating and overall adipose tissue for each of the limbs, presenting results on a box and whisker plot and evaluating statistical differences between groups (control, contralateral and residual limbs)
- Compare the associations between control, residual and contralateral adipose and BMI
- Compare the associations between residual and contralateral adipose and time since amputation, amputation cause and socket use, using scatter plots and correlation analysis

2. How do residual and intact limbs respond biomechanically and physiologically to representative prosthetic loading?

Research Question 2 Aims

- a) To evaluate and compare how tissues deform under representative prosthetic loading in residual and intact limbs through MRI image analysis
- b) To evaluate and compare the physiological response of tissues in residual and intact limbs through biophysical and biomarker analysis.
- c) To assess the effects of time since amputation, cause of amputation and socket use on physiological response in residual and contralateral limbs

Research Question 2 Objectives

- Use MRI images obtained for research question 1 to estimate deformation and strain under 60 mmHg applied cuff pressure, evaluating statistical differences between groups (control, contralateral and residual)
- Categorise the ischaemic response for each participant using standardised criteria by assessing change in T_cPO_2 and T_cPCO_2 [215] at the applied cuff pressures, and evaluate statistical differences between groups
- Evaluate the change in pro-inflammatory (IL-1 α /TP) and anti-inflammatory biomarkers (IL-1RA/TP) following incremental pressure cuff loading up to 60mmHg and evaluate statistical differences between groups
- Compare the associations between residual and contralateral T_cPO_2 and T_cPCO_2 change and time since amputation, amputation cause and socket use, using scatter plots and correlation analysis
- Compare the associations between residual, contralateral inflammatory response and time since amputation, amputation cause and socket use, using scatter plots and correlation analysis
- Compare the associations between residual, contralateral and control T_cPO_2 and T_cPCO_2 change and inflammatory response, using scatter plots and correlation analysis

3. How does soft tissue composition affect response to loading/tissue tolerance?

Research Question 3 Aims

- a) To assess the relative effects of tissue composition including adipose percentage on tissue response to representative prosthetic loading
- b) Evaluate the relative effects of tissue composition on tissue structural properties estimated with the MyotonPro™

Research Question 3 Objectives

- Evaluate the trends between tissue strain and adipose percentage using scatter plots and correlation analysis
- Collect Myoton stiffness data on the limbs of each group at relevant socket loading sites and evaluate trends between stiffness and adipose percentage using scatter plots and correlation analysis
- Assess the associations between T_cPO_2 and T_cPCO_2 change and adipose percentage using scatter plots and correlation analysis
- Compare the change in inflammatory response against adipose percentage using scatter plots and correlation analysis

4 Soft Tissue Constituents and Biomechanics

This section answers in part research questions 1, 2 and 3, namely:

Research Question 1. Are there changes in tissue composition in the residual limb following amputation?

Research Question 2. How do residual and intact limbs respond biomechanically and physiologically to representative prosthetic loading?

Research Question 3. How does soft tissue composition affect response to loading/tissue tolerance?

4.1 Introduction

As described in the above review of the scientific literature, to date there is limited quantitative characterisation of residual limb soft tissues following amputation. In addition, there is a critical need to understand how tissues adapt to prosthetic loading and what factors affect their vulnerability during early prosthetic rehabilitation. This study aims to compare the morphology and biomechanical response of residual and intact limb tissues during representative prosthetic loading in people with and without transtibial amputation.

4.2 Materials and Methods

4.2.1 Study Design

An observational study was conducted in a cohort of consenting participants, 10 without amputation and 10 with unilateral transtibial amputation. A list of inclusion and exclusion criteria can be viewed in Table 3.7. Ethics Committee approval for this protocol was granted by the University of Southampton (ERGO IDs: 29696 and 41864).

4.2.2 Material and Methods

The final protocol is described in detail in Section 3.4. Briefly, a pressure cuff (Ref 0124 Aneroid Sphygmomanometer, Bosch + Sohn GmbH, Germany) was applied to the right calf of participants without amputation (control limbs) and both the residual and contralateral limbs of participants with amputation. At the start of the testing session, measurements of maximum calf circumference and residual limb length were taken using a soft tape measure. Throughout testing participants were positioned in supine within the MRI scanner with their test-limb elevated and resting on foam supports (Figure 3.25). A prosthetic liner (ContexGel Liner, RSL Steeper, UK) was positioned underneath the cuff to provide a representative material to interface with the skin.

Three sites were selected for deformation and Myoton stiffness measurement on each limb: the patellar tendon, lateral calf and posterior calf (Section 3.2). 3D printed indenters were positioned underneath the cuff at these sites. Sunflower oil capsules were located centrally within the indenters to enable visualisation in the MR images (Figure 3.10 and Figure 3.12). Volumetric images were acquired on a 3T MRI scanner (MAGNETOM Skyra, Siemens, Germany) based at the Faculty of Medicine, University Hospital Southampton site. Images were taken at i) baseline (no load) and ii) a cuff inflation of 60 mmHg (8 kPa) to characterise tissue deformation at the aforementioned sites and visualise morphological changes [49] (Figure 3.23 and Figure 3.27). Tissue composition for the whole cross-sectional area was visualised over a limb length of 13.4 cm that included the three measurement sites. Composition was analysed using ImageJ 1.52p (Rasband, W. National Institute of Health, US) by processing the fat saturated images, as detailed in Section 3.4.2 and shown in Figure 3.18, to quantify superficial adipose and adipose infiltrating muscle.

Single slices at the centre of the measurement sites, located via the centroid of the sunflower oil tablets, were imported into ImageJ, and linear measurement tools were used for calculation of gross strain under each indenter (Figure 3.17).

Within the same testing session interface pressure and Myoton measurements were collected while participants were in a seated position on an Enterprise Hospital Bed (Arjo Huntleigh, Malmö, Sweden) with adjustable backrest, with their test-limb elevated and resting on foam supports. Interface pressures were measured using a Talley pneumatic pressure monitoring system as described in Section 3.1. One 28 mm diameter cell (see Figure 3.7) was placed at each measurement site positioned between the skin and indenter.

Finally, with the cuff and all indenters removed, the MyotonPro™ (Myoton AS, Estonia) was used to apply a mechanical impulse at each of the three measurement sites in eight participants without amputation and all ten participants with transtibial amputation. Briefly, this device induces oscillations which are measured using a triaxial accelerometer, from which the structural stiffness of the soft tissues was calculated (Section 3.4.2, Figure 3.19).

4.2.3 Data Analysis

Raw data from each measurement technique were processed using MATLAB (Mathworks, USA) and analysed using SPSS Statistics (IBM, USA). All data were first examined for normal distribution prior to analysis using the histograms and the Shapiro-Wilk test, in order to determine appropriate descriptive and inferential statistics (Table 4.1). Interface pressure and Myoton data are presented using parametric descriptors, namely means and standard deviation, and MRI data are presented using non-parametric descriptors, namely medians, quartiles and range.

Appropriate statistical testing methods were applied to answer the three research questions

detailed in Section 3.5 (Table 4.1).

Table 4.1 Statistical analysis to evaluate interface pressure, tissue composition, Myoton stiffness, deformation and strain between control, contralateral and residual limb groups and the relationship between some of these factors and BMI/time since amputation/socket use

Research Question to be Answered	Measurement	Hypothesis: There is a significant...	Normal Distribution	Statistical Test Used
2	Interface Pressure	... difference in the measurement between limb groups and measurement sites	Yes	T-Test
1	Percentage of Adipose Tissue	... difference in the measurement between limb groups	No	Mann-Whitney U
1		... relationship between the measurement in residual limbs and contralateral limbs	No	Spearman's Correlation
1		... relationship between the measurement and BMI (Sections 3.4.3-3.4.4 and 4.3) for control/contralateral/residual limbs	No	Spearman's Correlation
1		... relationship between the measurement and time since amputation/socket use (Sections 3.4.3-3.4.4 and 4.3) for contralateral/residual limbs	No	Spearman's Correlation
2	Myoton Stiffness	... difference in the measurement between control, contralateral and residual limb groups	Yes	T-Test
2		... relationship between the measurement and time since amputation/socket use (Sections 3.4.3-3.4.4 and 4.3) for contralateral/residual limbs	Yes	Pearson's Correlation
3		... relationship between the measurement and percentage of adipose tissue (Sections 3.4.2 and 4.3.2) for control/contralateral/residual limbs	Yes	Pearson's Correlation
2	Deformation and Strain	... difference in the measurements between limb groups	No	Mann-Whitney U
3		... relationship between strain and percentage of adipose tissue (Sections 3.4.2 and 4.3.2 for control/contralateral/residual limbs	No	Spearman's Correlation

Differences and associations were considered to be statistically significant at the 5 % level

($p < 0.05$) as this is a well-used benchmark of significance. Strength of association can be examined using the correlation coefficient (r) and guidelines specify that an $r > 0.5$ indicates strong correlation [251]. However, r doesn't take into account the number of participants and with an n of 10 in each limb group correlations are somewhat arbitrary and therefore, although r will be reported, the significance (p) of the correlation provides a more appropriate measure of the relationships.

Given the sample size and heterogeneity of participants, it was deemed appropriate to also analyse data on a case-by-case basis and focus on the clinical relevance as opposed to r and p values. The full correlation analysis for each measurement has been presented in tabulated form and significant or clinically interesting results have been graphically presented to provide context.

4.3 Results

The recruited cohort of ten participants without amputation had a median age of 28 years (range 23 to 36 years), including 6 males and 4 females (Table 4.2). The median (range) height and weight were 1.78 m (1.60 to 1.92 m) and 66 kg (56 to 90 kg), respectively. The corresponding BMI was 22.1 kg/m² (18.3 to 29.4 kg/m²). Testing was successfully completed in all recruited participants without any adverse events.

Table 4.2 Participants without amputation characteristics, reported as median (range)

Participant Characteristic	Overall (n=10)	Males (n=6)	Females (n=4)
Age (years)	28 (23 - 36)	26 (23 - 34)	28 (27 - 36)
Height (m)	1.78 (1.60 - 1.92)	1.82 (1.75 - 1.92)	1.66 (1.60 - 1.76)
Mass (kg)	66 (56 - 90)	78 (66 - 90)	58 (56 - 64)
BMI (kg/m²)	22.1 (18.3 - 29.4)	23.6 (18.3 - 29.4)	21.5 (18.4 - 23.5)
Max. Calf Circumference (mm)	360 (320 - 410)	390 (350 - 410)	360 (320 - 360)

The recruited cohort of ten participants with unilateral transtibial amputation had a median age of 41 years (range 25 to 62 years), including 8 males and 2 females (Table 4.3). The median (range) height and weight were 1.76 m (1.63 to 1.88 m) and 79 kg (51 to 127 kg), respectively. The corresponding BMI was 27.3 kg/m² (19.2 to 37.5 kg/m²). Testing was successfully completed in all recruited participants without any adverse events.

Table 4.3 Participants with unilateral transtibial amputation characteristics, reported as median (range)

Participant Characteristic	Overall (n=10)	Male (n=8)	Female (n=2)
Age (years)	41 (25 - 62)	45 (25 - 62)	38 (30 - 46)
Height (m)	1.76 (1.63 - 1.88)	1.79 (1.65 - 1.88)	1.65 (1.63 - 1.68)
Mass (kg)	79 (51 - 127)	79 (73 - 127)	76 (51 - 100)
BMI (kg/m ²)	27.3 (19.2 - 37.5)	27.3 (20.7 - 37.5)	27.4 (19.2 - 35.6)
Amputated Side	4 left, 6 right	2 left, 6 right	2 left
Max. Residual Calf Circumference (mm)	290 (250 - 450)	300 (260 - 450)	270 (250 - 290)
Max. Contralateral Calf Circumference (mm)	390 (340 - 530)	390 (350 - 530)	390 (340 - 440)
Residual Limb Length (mm)	150 (100 - 300)	150 (100 - 300)	210 (140 - 270)
≈Time Since Amputation (years)	7.5 (1 - 35)	5.0 (1 - 35)	18.5 (8 - 29)
Amputation Cause	Chronic Regional Pain Syndrome- 2, Congenital abnormality- 2, Trauma- 5, Type 1 Diabetes- 1	Chronic Regional Pain Syndrome- 1, Congenital abnormality- 1, Trauma- 5, Type 1 Diabetes- 1	Chronic Regional Pain Syndrome- 1, Congenital abnormality- 1
≈Daily Socket Use (hours)	12.5 (6 - 16)	11.5 (6 - 16)	14.5 (14 - 15)

There was a mixture of reasons for amputation including Chronic Regional Pain Syndrome, congenital abnormality, trauma and diabetes (Figure 4.1). There was also a wide range of time since amputation, from 1 to 35 years.



Figure 4.1 Residual limbs of participants with amputation, KEY: participant ID, sex, age, amputation cause, number of years post-amputation

4.3.1 Interface Pressure

At baseline (i.e. before the cuff was inflated, 0 mmHg), finite interface pressures were observed although we can't be sure of the absolute values as the lower sensitivity threshold of the Talley is ≈ 20 mmHg [243]. These finite values indicated preloading due to the mass of the pressure cuff (anterior sensors), the self-mass of the limb (posterior sensors), and the cuff's uninflated tension (Table 4.4). At a cuff pressure of 60 mmHg (8 kPa), the mean interface pressures ranged from 66.2 to 73.7 mmHg (8.8 to 9.8 kPa), 69.9 to 75.1 mmHg (9.3 to 10.0 kPa) and 72.0 to 83.6 mmHg (9.6 to 11.1 kPa) in control, residual and contralateral limbs, respectively (Table 4.4). No significant differences between participant groups were observed at any of the three measurement sites. The highest values generally occurred at the patellar tendon, the measurement area with lowest soft tissue coverage over the underlying tendon anatomy. Interface pressures were significantly different between the patellar tendon and lateral calf ($p = 0.02$) and the lateral calf and posterior calf ($p = 0.02$) sites of control limbs. However, no significant differences between sites were observed in contralateral or residual groups potentially due to higher variance in these limb groups (Table 4.4).

Table 4.4 Table detailing the mean (SD) interface pressure at three measurement sites, at baseline and a cuff pressure of 60 mmHg, applied to the right control limb of 10 participants without amputation and both residual and contralateral limbs of 10 participants with unilateral transtibial amputation

		Mean (Standard Deviation)	
		Interface Pressure at Applied Cuff	
		Inflation Pressure (mmHg)	
	Measurement Site	0 (Baseline)	60
Control Limbs of Participants Without Amputation	Patellar Tendon	13.1 (7.4)	73.7 (8.2)
	Lateral Calf	4.7 (2.9)	72.6 (5.5)
	Posterior Calf	0.5 (1.3)	66.2 (5.0)
Contralateral Limbs of Participants with Amputation	Patellar Tendon	17.7 (15.2)	83.6 (34.3)
	Lateral Calf	7.7 (11.1)	75.1 (6.7)
	Posterior Calf	2.8 (6.3)	72.0 (11.7)
Residual Limbs of Participants with Amputation	Patellar Tendon	13.6 (13.4)	73.1 (21.6)
	Lateral Calf	13.9 (12.4)	75.1 (11.4)
	Posterior Calf	11.9 (13.4)	69.9 (12.7)

4.3.2 Soft Tissue Composition

The percentages of superficial adipose and adipose infiltrating muscle were calculated for each participant to analyse tissue composition (Figure 4.2 and Figure 4.3). Non-amputated limbs were observed to have a greater cross-sectional area and generally a more uniform shape. However, the residual limbs often showed a shape artefact within the Field of View, arising from the supine support required during imaging and testing.

Key

Participant, Sex, Age		Superficial adipose
		Adipose infiltrating muscle



Figure 4.2 Corresponding transverse MRI slices at the posterior calf measurement site for the right control limb of ten participants without amputation, with superficial adipose (yellow) and adipose infiltrating muscle (red) tissue overlays

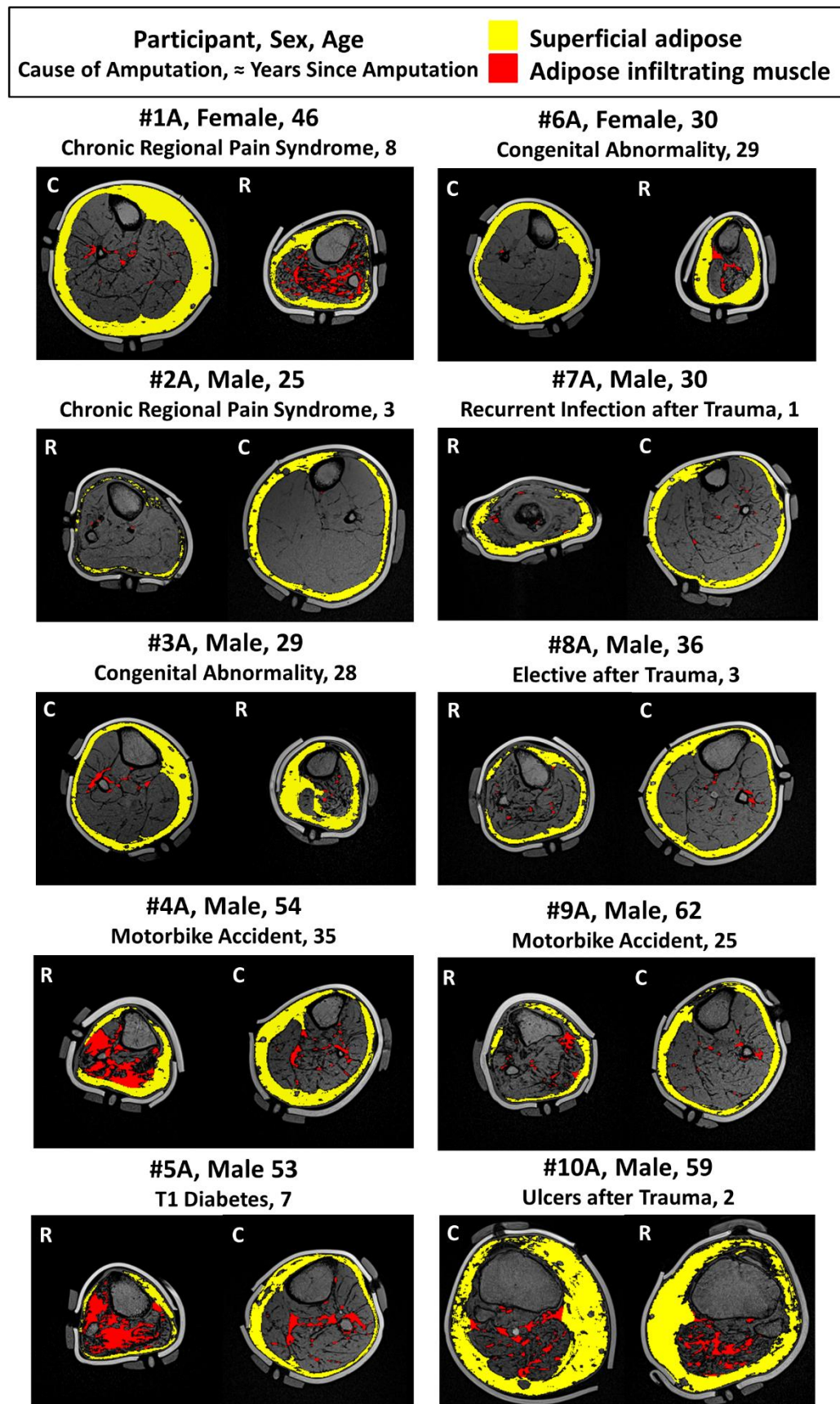


Figure 4.3 Corresponding transverse MRI slices at the posterior calf measurement site for the residual (R) and contralateral (C) limbs of ten participants with unilateral transtibial amputation, with superficial adipose (yellow) and adipose infiltrating muscle (red) tissue overlays

The residual limbs appeared to have greater adipose tissue infiltrating muscle than intact limbs, from the MR images. This was particularly apparent in the more established residual limbs, for example #4A, #6A and #9A who were 35, 29 and 25 years post-amputation respectively (Figure 4.2 and Figure 4.3). However, a similar difference in limb tissue composition was also observed in individuals at an earlier stage post-amputation, notably #1A and #5A who were 8 and 7 years post-amputation. This could be associated with their causes of amputation. #1A used a wheelchair for mobility for a number of years prior to amputation, when additional muscle atrophy may have occurred. #5A has Type 1 diabetes and research has shown that insulin resistance and diabetes has been linked to a higher level of adipose infiltrating muscle [252]. The following figures show the percentage of superficial adipose, adipose infiltrating muscle and muscle tissue, relative from the proximal to distal portion of the limbs for all participants (Figure 4.4 to Figure 4.7). In the control group the percentage of superficial adipose tissue ranged from 4.6 to 38.3 %, generally peaking at around 30 to 40 mm below the tibial plateau (Figure 4.4). Higher percentages of superficial adipose were generally observed in female compared to male control limbs, as shown in Figure 4.4 by #4, #6 and #9 having the highest percentages across the whole measured limb length [253].

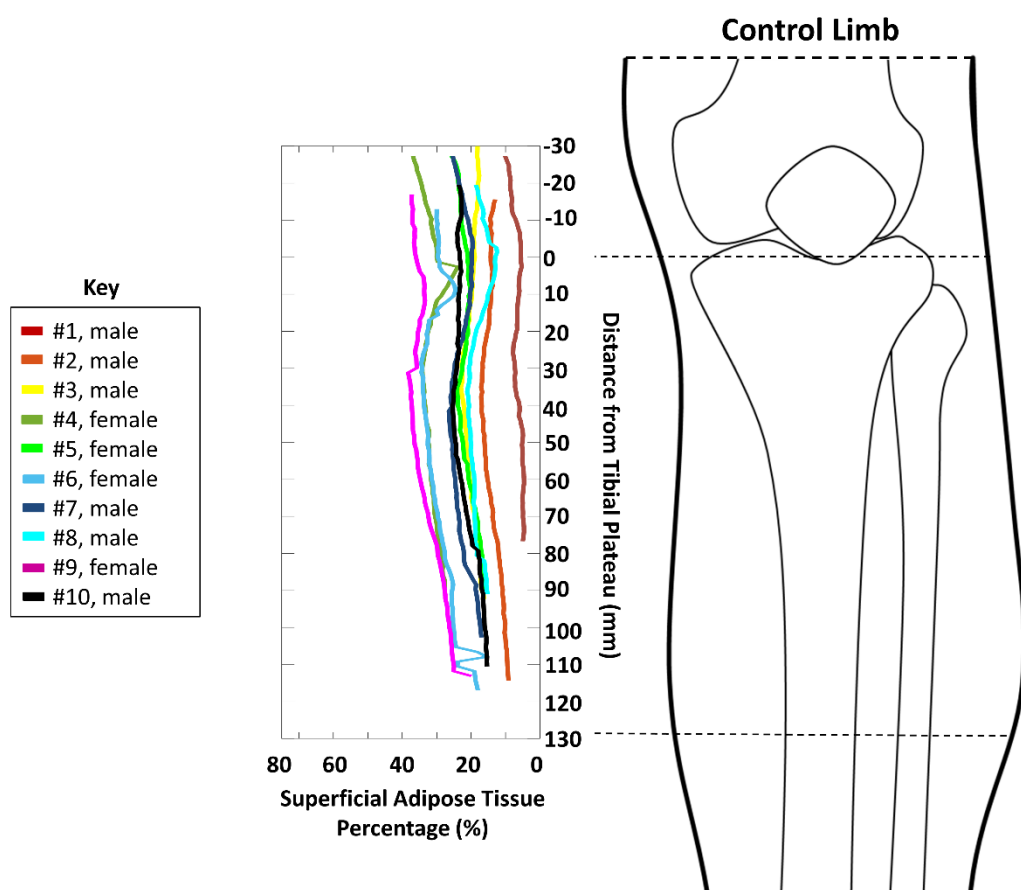


Figure 4.4 Percentage of superficial adipose tissue throughout the right control limb of ten participants without amputation

Similar trends were observed in the contralateral limbs of participants with amputation, with the percentage of superficial adipose tissue ranging from 11.0 to 44.2 %, generally peaking at around 20 to 40 mm below the tibial plateau (Figure 4.5). Higher percentages of superficial adipose were also generally observed in female compared to male contralateral limbs, as shown in Figure 4.5 by #1A having the highest percentage across the visualised limb length and only #1A and #6A consistently having superficial adipose percentages above 20 % [253].

A greater variability in the proportion of superficial adipose tissue was observed in residual limbs compared to intact limbs with values ranging from 2.3 to 47.3 % (Figure 4.5). There was a general trend of increasing residual limb superficial adipose with increasing distance from the tibial plateau distally with superficial adipose peaking around 60 to 100 mm (Figure 4.5). This trend was particularly apparent in participants #1A, #3A, #4A and #6A. At equivalent distances from the tibial plateau after around 50 mm, superficial adipose percentages were often higher in residual limbs compared to contralateral limbs. Despite this tendency, lower superficial adipose was observed in #2A's residual limb (2.3 to 5.5 %) compared to their contralateral limb (11.4 to 20.1 %) across the whole Field of View. Differences between male and female participant groups were not observed in the residual limb group. Interestingly, the highest superficial adipose cases from 30 mm distal of the tibial plateau were #3A and #6A, who both had amputations due to congenital abnormality 28 and 29 years ago, respectively (Figure 4.5).

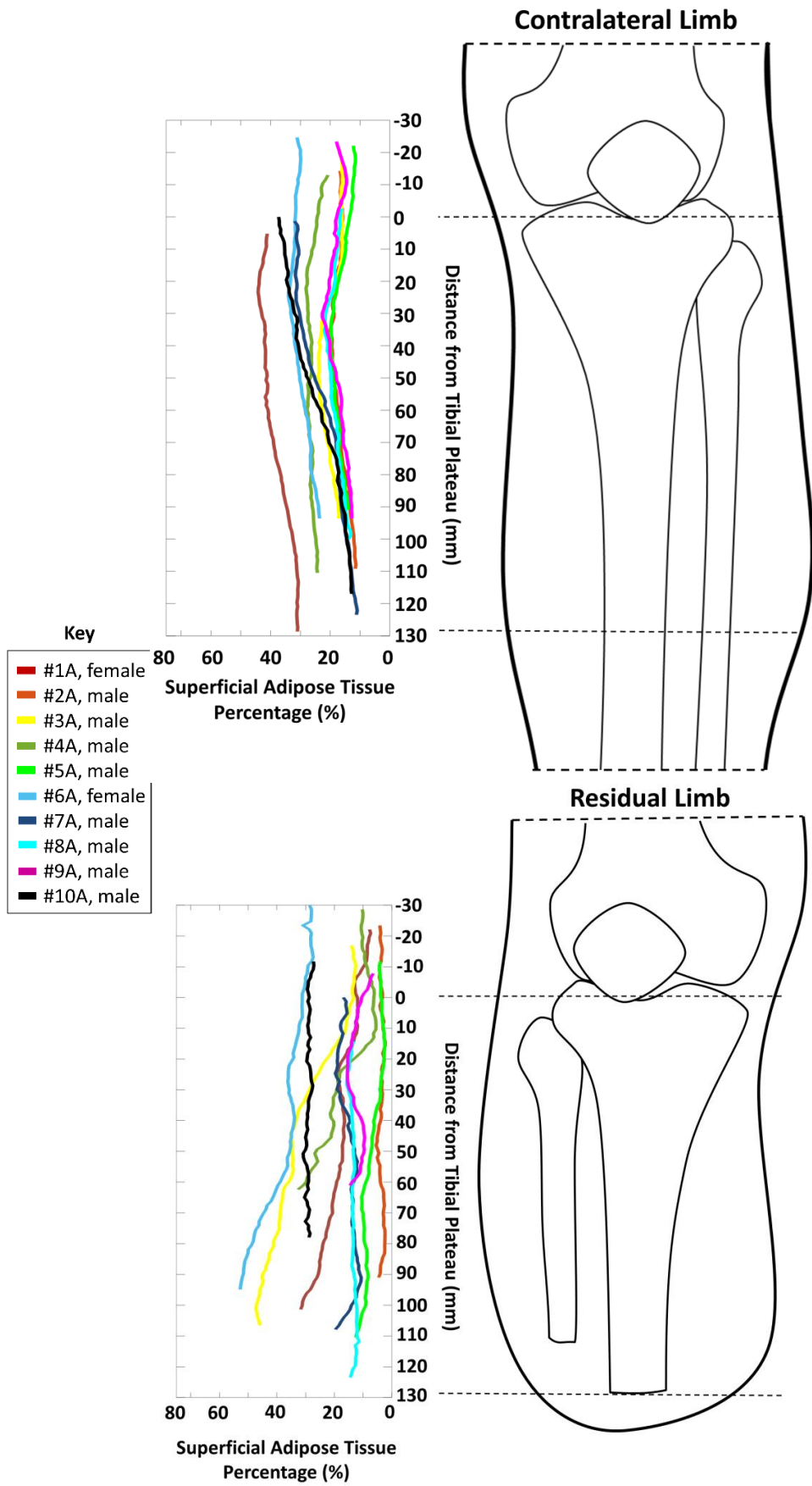


Figure 4.5 Percentage of superficial adipose tissue throughout the contralateral (top) and residual (bottom) limbs of ten participants with unilateral transtibial amputation

Adipose infiltrating muscle was observed to be lowest (0.0 to 3.8 %) in the control limbs of the cohort without amputation. A higher degree of variability was evident in the contralateral (0.0 to 10.4 %) and residual (0.0 to 21.2 %) limbs of participants with amputation (Figure 4.6). In the latter case, infiltrating adipose was particularly apparent at the distal end, most likely due to muscle atrophy in the residual limb. The highest case of infiltrating adipose was #5A, potentially an effect of their Type 1 diabetes. The highest infiltrating adipose case in the contralateral limb group was in #10A, who had $\approx 10\%$ infiltrating fat in the distal third of their shank. This individual had the highest BMI of all participants (37.5 kg/m^2) and was largely dependent on a wheelchair for mobility which could explain greater atrophy and therefore higher infiltrating adipose.

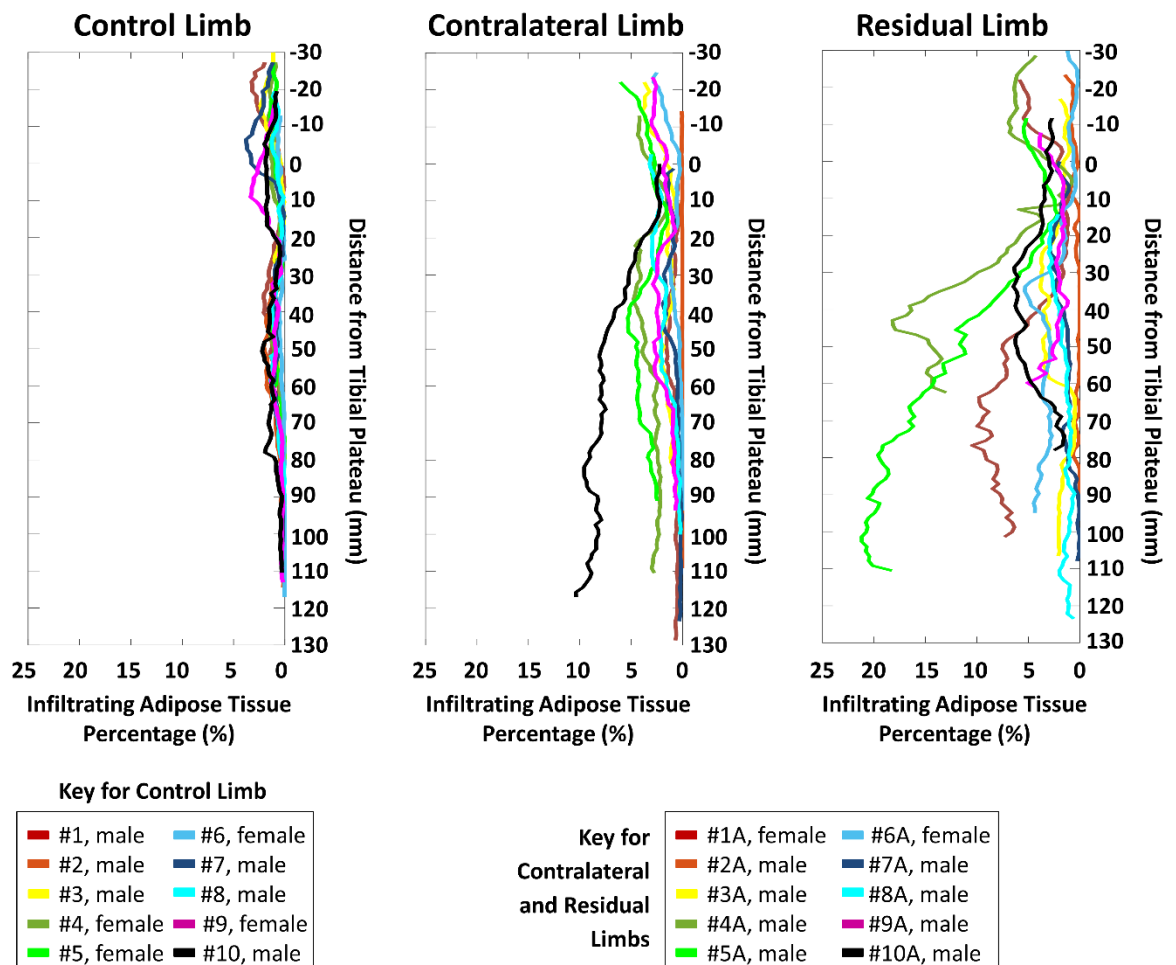


Figure 4.6 Percentage of adipose infiltrating muscle throughout the right control limb of participants without amputation (left) and the contralateral (middle) and residual (right) limbs of ten participants with unilateral transtibial amputation

Muscle percentage was again most variable in the residual limb data, particularly at the distal end where muscle composition ranged from approximately 35 to 85 % in the residual limb group compared to 60 to 85 % in intact limbs (Figure 4.7). All three limb groups presented increasing muscle composition from the primarily bony structures at the knee into the calf muscle.

Participants #3A and #6A had the lowest muscle percentages (25.7 to 50.3 %) corresponding with the high superficial adipose tissue percentages observed in their residual limbs (Figure 4.5). In one case (#2A), comparable muscle percentages were observed in their contralateral (43.7 to 84.6 %) and residual (49.9 to 89.0 %) limbs. This may be explained by this participant's occupation as a professional athlete and very active lifestyle involving running and lower limb activity. In the control group, this may also explain the highest muscle percentages (51.3 to 85.5 %) and lowest superficial adipose percentages (4.6 to 10.1 %) observed in #1 who is a keen cyclist (Figure 4.4 and Figure 4.7).

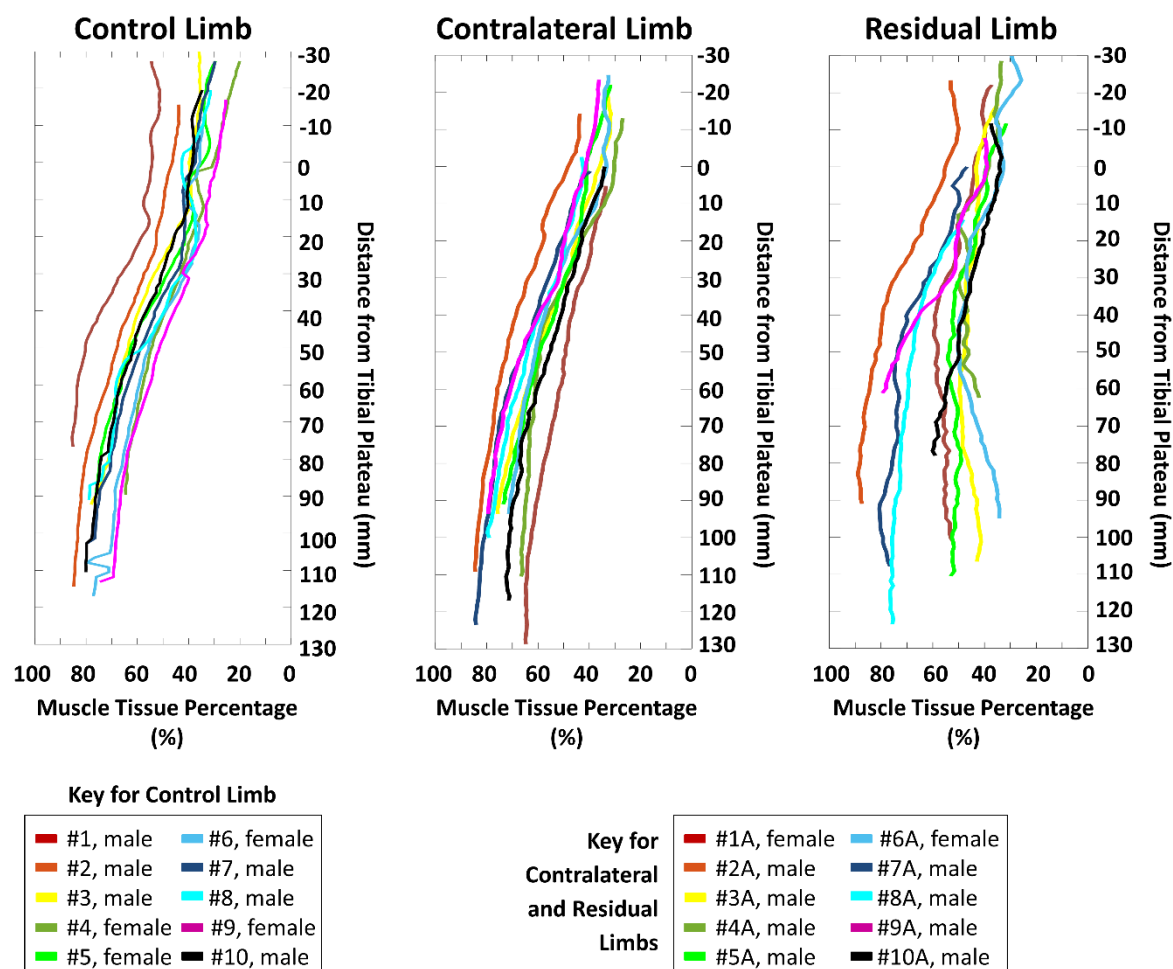


Figure 4.7 Percentage of muscle tissue throughout the right control limb of participants without amputation (left) and the contralateral (middle) and residual (right) limbs of ten participants with unilateral transtibial amputation

Soft tissue percentages were estimated between the tibial plateau and 60 mm distally from this point, corresponding to images captured for all 30 limb cases. It is interesting to note that a larger superficial and overall adipose percentage was observed in intact limbs compared to the residual limbs (Figure 4.8). This is potentially due to the 60 mm measurement window used to calculate overall soft tissue percentages. Indeed, Figure 4.4 and Figure 4.5 show the differing trends in superficial adipose down the length of the limb for intact compared to residual limbs. Intact limbs demonstrated a concave relationship with peak superficial adipose generally approximately 30 mm distal of the tibial plateau. By contrast, a convex curve of superficial adipose tissue percentage was evident in residual limbs, peaking upwards of 60 mm distal of the tibial plateau. This more distal superficial adipose peak could be due to the surgical flap procedure used or muscle atrophy.

Conversely, there was approximately 3 and 1.5 times higher percentage of infiltrating adipose in residual limbs (median 2.5 %, range 0.2 to 8.9 %) compared to control limbs (median 0.9 %, range 0.4 to 1.3 %) and contralateral limbs (median 1.7 %, range 0.1 to 5.1 %), respectively. The difference was found to be statistically significant for infiltrating adipose between control and residual limb groups ($p < 0.01$) and was at the significance threshold between control and contralateral limb groups ($p = 0.05$). Superficial adipose differences between residual (median 17.2 %, range 3.7 to 34.4 %) and contralateral (median 20.5 %, range 17.6 to 42.2 %) limbs was also statistically significant ($p = 0.03$).

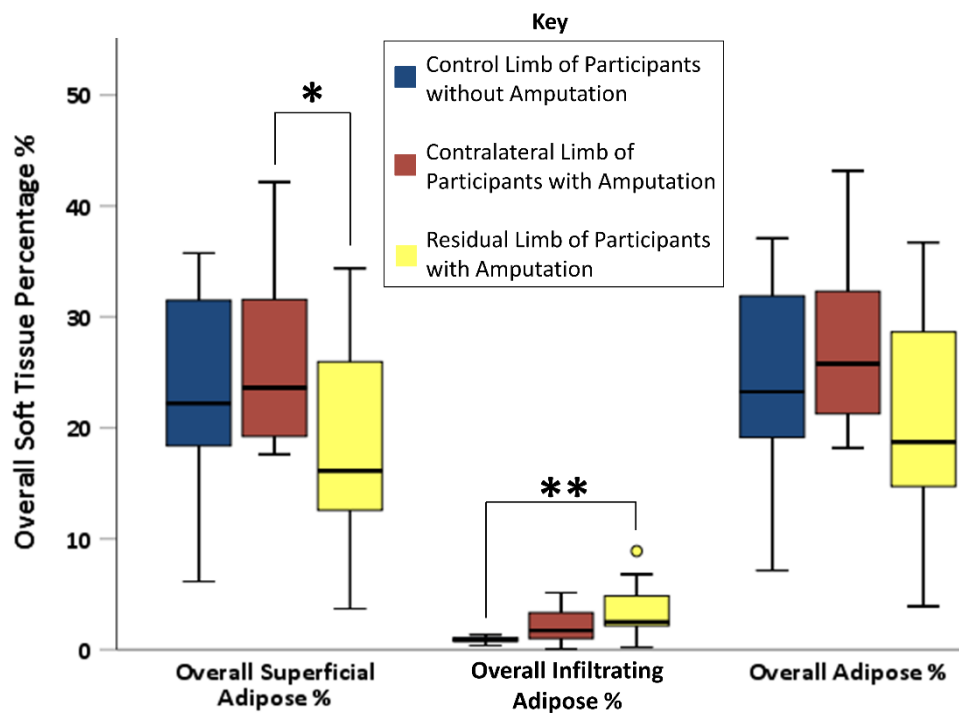


Figure 4.8 Median, interquartile range (IQR) and range of overall limb soft tissue percentage for all participant groups over an lower limb area from the tibial plateau to 60 mm distally. Note: * = $p < 0.05$ and ** = $p < 0.01$

To further explore adipose tissue percentage in participants with amputation, residual and contralateral limb measurements were plotted against each other (Figure 4.9). Similar tissue compositions were observed between residual and contralateral limbs, evidenced by a significant positive correlation for both superficial and infiltrating adipose groups (Figure 4.9). However, high superficial adipose did not necessarily correspond to high infiltrating adipose in either contralateral ($r = -0.20$, $p = 0.58$) or residual ($r = 0.24$, $p = 0.50$) limbs. Distinct differences in tissue composition were observed within cases. For example, participant #10A had the highest BMI (37.5 kg/m^2) and highest infiltrating adipose percentage in their contralateral limb. However, this case corresponded to the third highest infiltrating adipose in their residual limb, potentially due to being only 2 years post-amputation (Figure 4.9 to Figure 4.10). Case #7A had an above average BMI (29.4 kg/m^2), but both limbs were among the lowest for infiltrating adipose percentage within the cohort with amputation. This could be explained by this participant having above average activity (13hrs daily socket use), causing increased muscle mass and therefore BMI, or the fact that they were only one year post-amputation (Figure 4.9 to Figure 4.10). Indeed, all the participants with above-medial BMIs were known to have lived or currently be living very active lifestyles within the military or as professional athletes, with the exception of #5A who had Type 1 diabetes.

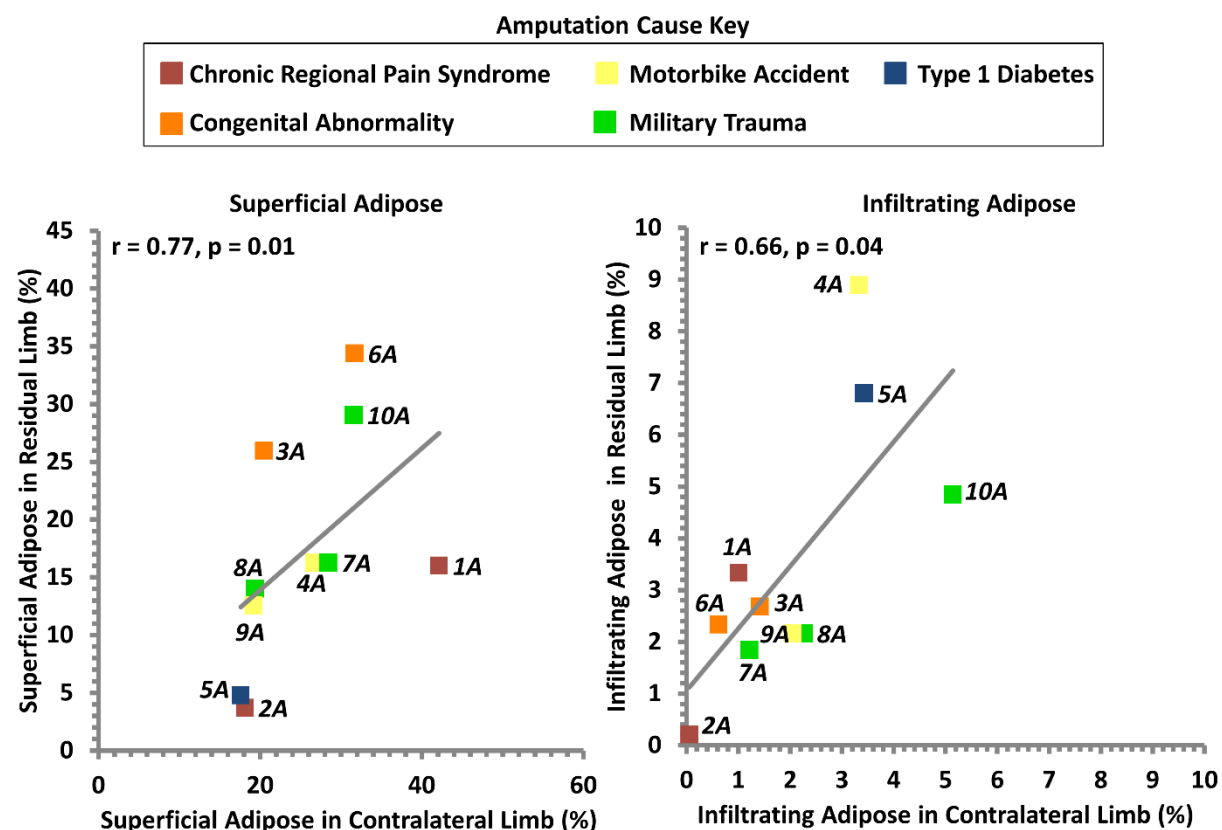


Figure 4.9 residual limb overall infiltrating adipose percentage plotted against contralateral limb overall infiltrating adipose percentage in 10 participants with unilateral transtibial amputation. Note: number represents participant identification

Trends between adipose tissue percentages and demographic factors (BMI, time since amputation and daily socket use) were evaluated in the same way (Figure 4.10 and Table 4.5). The only significant association was a negative trend between infiltrating adipose in the contralateral limb and socket use. Correlation analysis suggests that infiltrating adipose percentage increases with BMI for both intact limb groups (Table 4.5). This trend was stronger in control limbs although not significant in either. Control limbs also presented a small range of low adipose infiltrating muscle percentages (0.4 to 1.3 %) as presented in Figure 4.8, limiting the correlation analysis.

Table 4.5 Correlation analysis for percentage volume of A. infiltrating and B. superficial adipose from the tibial plateau to 60 mm distally in the ten control limbs and the contralateral and residual limbs of ten participants with transtibial amputation. Note: results displayed as r (p) and green represents a result indicating strong correlation ($r > 0.5$) and bold represents significance ($P < 0.05$)

A

Correlation between Percentage Volume of Infiltrating Adipose and:	Limb	Correlation, r (significance, P)
BMI	Control	0.55 (0.10)
	Contralateral	0.35 (0.33)
	Residual	0.12 (0.75)
Time Since Amputation	Contralateral	-0.06 (0.88)
	Residual	0.45 (0.19)
Socket Use	Contralateral	-0.88 (<0.01)
	Residual	-0.38 (0.28)

B

Correlation between Percentage Volume of Superficial Adipose and:	Limb	Correlation, r (significance, P)
BMI	Control	0.18 (0.63)
	Contralateral	0.08 (0.83)
	Residual	-0.19 (0.60)
Time Since Amputation	Contralateral	0.12 (0.75)
	Residual	0.20 (0.59)
Socket Use	Contralateral	0.07 (0.85)
	Residual	-0.06 (0.88)

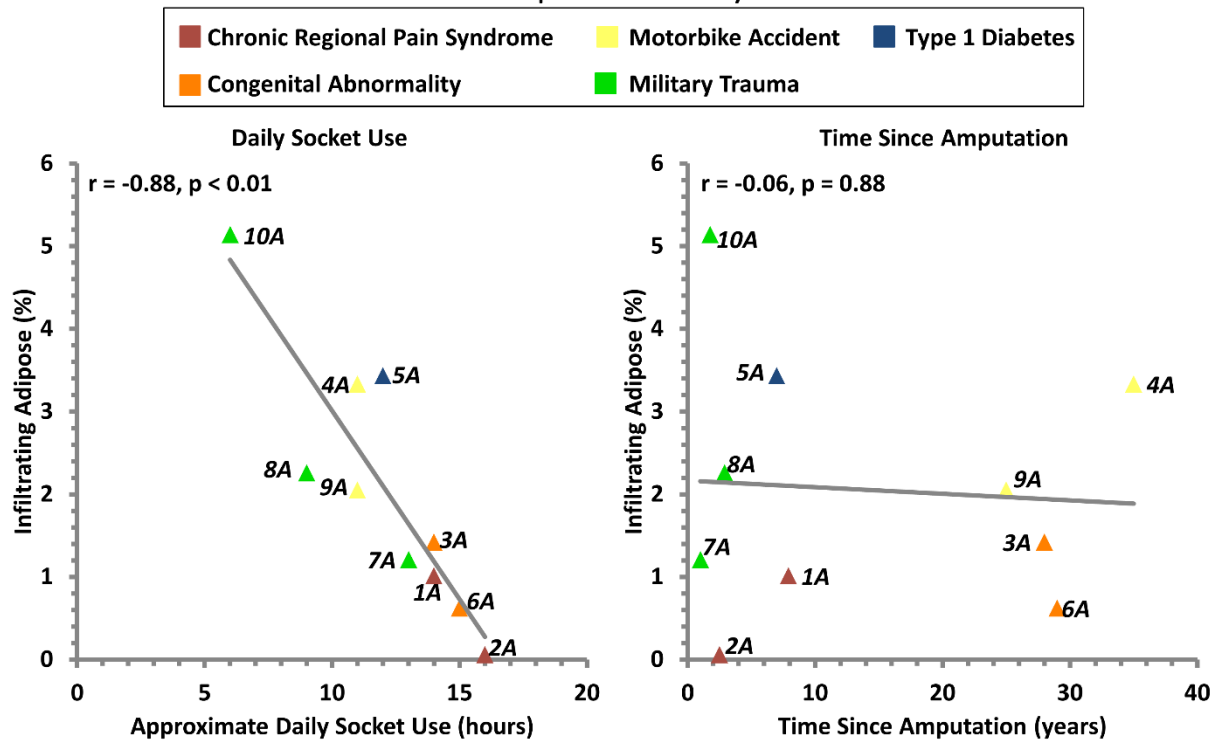


Figure 4.10 Percentage volume of infiltrating adipose from the tibial plateau to 60 mm distally plotted against daily socket use (left) and time since amputation (right) for the contralateral limbs of ten participants with unilateral transtibial amputation. NOTE: number represents participant identification

With greater socket use there was a trend of lower infiltrating adipose tissue in both limbs, more so and significantly in the contralateral limbs (Table 4.5 and Figure 4.10). This may be indicative of greater activity levels and therefore muscle mass required. Neither superficial nor infiltrating adipose were observed to simply correspond with time since amputation with greater variation observed in participants with a shorter time since amputation (Table 4.5 and Figure 4.10). Participants who had their amputation due to Chronic Regional Pain Syndrome (#1A and #2A) or congenital abnormality (#3A and #6A) typically had the lowest infiltrating adipose and highest socket use (Figure 4.10). Interestingly, as well as similar infiltrating adipose percentages, times since amputation and socket use #3A and #6A, one female and one male were age-matched and both had their amputations at approximately 12 months old. They had Symes amputation where the heel pad is attached to the distal residual limb to enable load bearing, which they both reported doing regularly and could explain lower infiltrating adipose percentage due to increased muscular use.

4.3.3 Soft Tissue Properties

Stiffness measurements taken using the Myoton probe are presented in Figure 4.11. Stiffness represents the resistance of the tissue to changing shape and was observed to be highest at the patellar tendon site. This corresponds to the thinner soft tissue coverage adjacent to a bony prominence. The highest stiffness values (mean 739 N/m \pm SD 187 N/m) were observed in the residual limb group which could be due to adaptation under patellar tendon socket load bearing. The residual limbs displayed a higher stiffness response (mean ranging from 284 N/m to 739 N/m) compared to control limbs (mean ranging from 275 N/m to 520 N/m), reaching significance at the patellar tendon measurement site ($p=0.04$). No significant difference between groups was observed in stiffness at the calf sites.

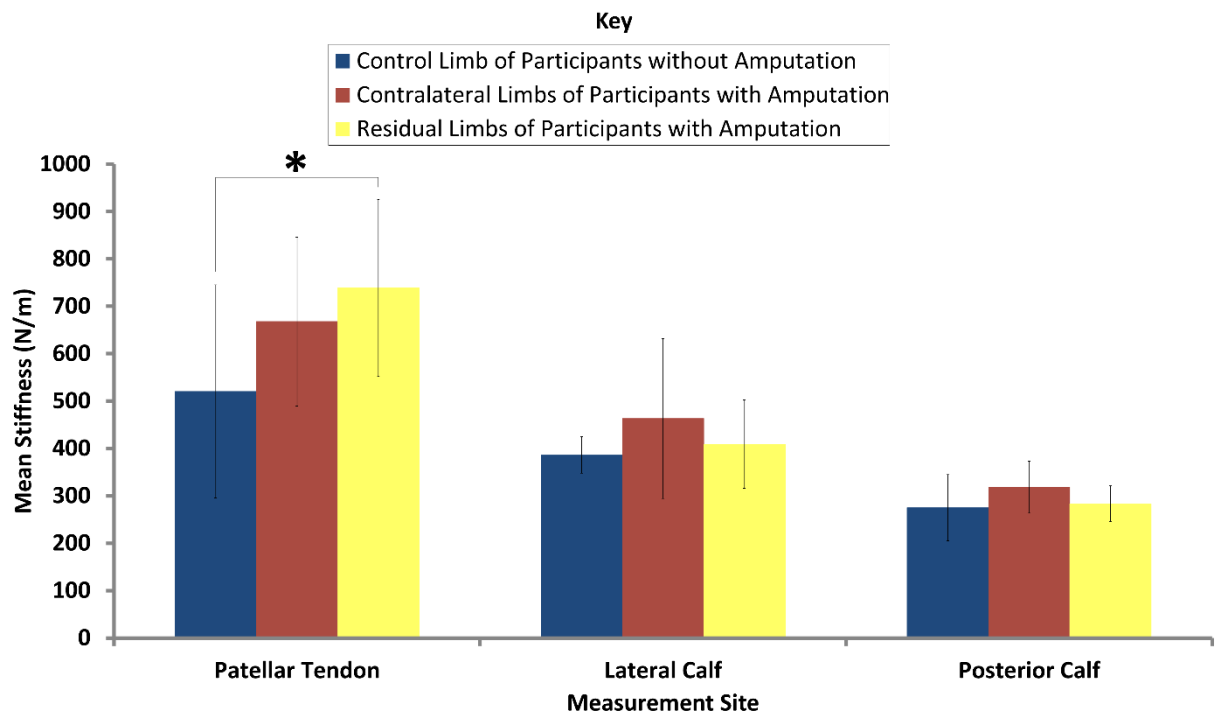


Figure 4.11 Mean (\pm standard deviation) tissue stiffness under induced Myoton probe oscillations at three measurement sites in the right control limb of eight participants without amputation and both contralateral and residual limbs of ten participants with unilateral transtibial amputation. Note: * = $p \leq 0.05$

Trends between Myoton stiffness and superficial adipose, time since amputation and socket use

were evaluated using scatter plots and correlation analysis (Table 4.6, Figure 4.12 and Figure

4.14). Myoton stiffness correlated weakly with superficial adipose and time since amputation at

most sites for all limb groups. A stronger trend was observed between Myoton stiffness and

socket use, but this was only statistically significant at the posterior calf ($p=0.04$).

Table 4.6 Correlation analysis for Myoton stiffness in the right control limbs of 8 participants without amputation and the contralateral and residual limbs of 10 participants with unilateral transtibial amputation. Note: results displayed as r (p) and green represents a result indicating strong correlation ($r > 0.5$) and bold represents significance ($P < 0.05$)

Correlation between Myoton Stiffness and:	Limb	Measurement Site		
		Patellar Tendon	Lateral Calf	Posterior Calf
Superficial Adipose %	Control	0.29 (0.49)	-0.38 (0.36)	-0.43 (0.28)
	Contralateral	0.49 (0.15)	-0.14 (0.70)	0.11 (0.76)
	Residual	0.02 (0.96)	-0.17 (0.65)	-0.39 (0.27)
Time Since Amputation	Contralateral	-0.04 (0.92)	-0.23 (0.53)	-0.28 (0.43)
	Residual	0.28 (0.43)	-0.23 (0.52)	-0.08 (0.83)
Socket Use	Contralateral	-0.14 (0.70)	0.02 (0.96)	-0.65 (0.04)
	Residual	-0.13 (0.73)	-0.53 (0.12)	-0.51 (0.13)

It is interesting to note that in general calf sites of female participants without amputation tended

to have lower Myoton stiffness, in correspondence with their previously-described higher

superficial adipose (Figure 4.5 and Figure 4.12).

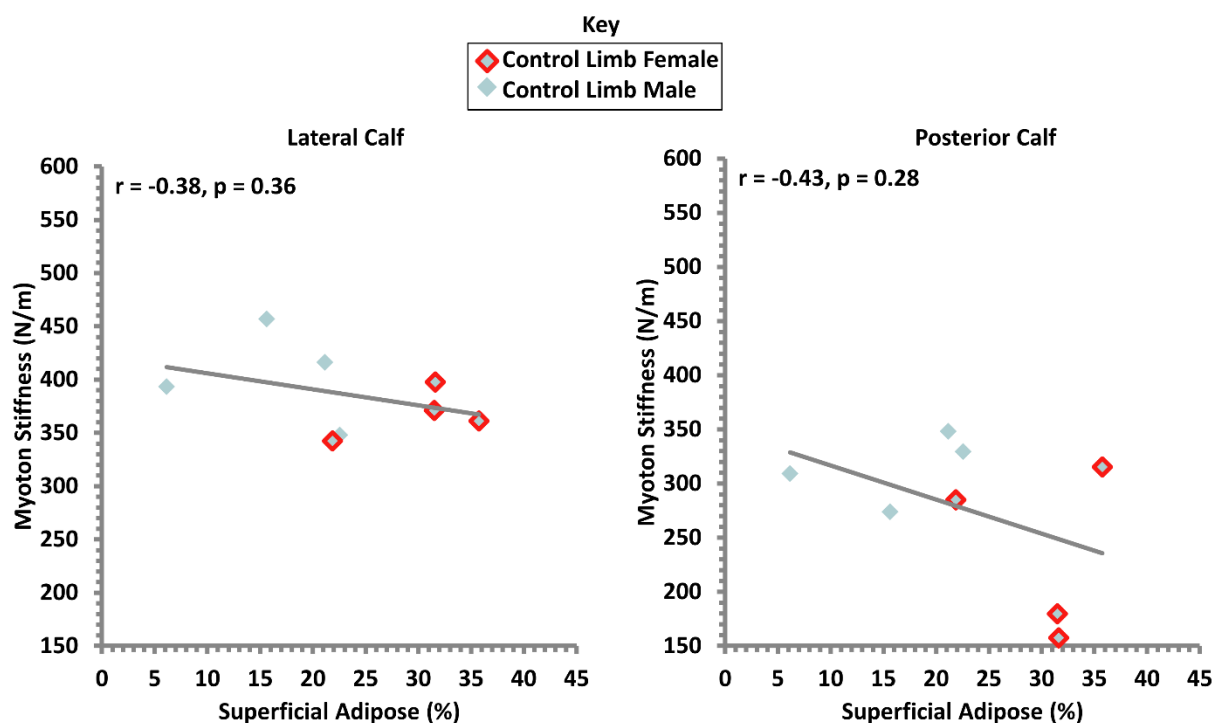


Figure 4.12 Myoton stiffness as a function of the superficial adipose percentage for the right control limbs of 8 participants without amputation

Only two of the ten participants with amputation were female (#1A and #6A) so sex trends could not be analysed for the cohort with amputation. However, when comparing #6A to the age, cause and time since amputation -matched male participant #3A, lower Myoton stiffness and higher superficial adipose were observed at all sites for #6A (Figure 4.13).

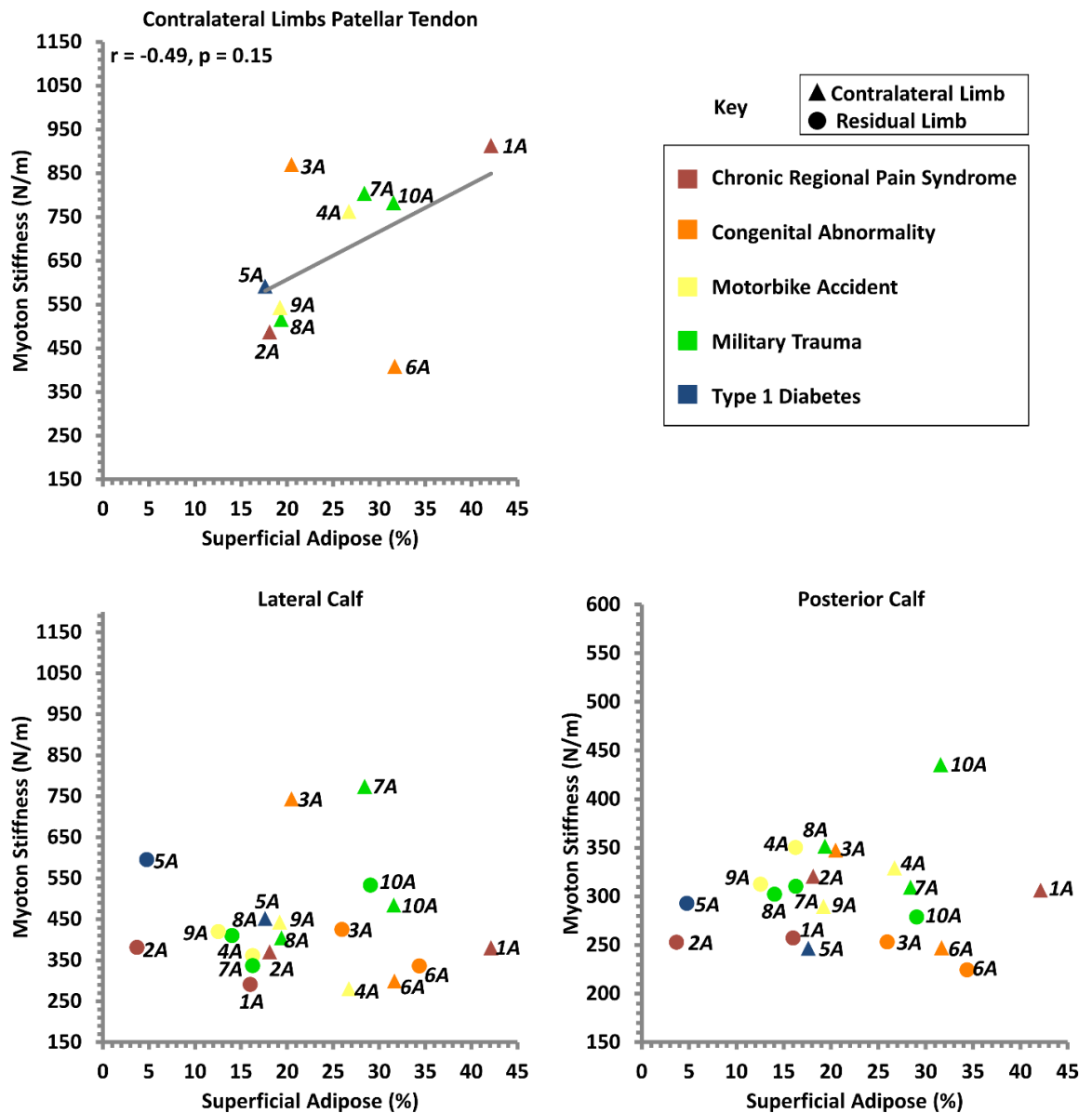


Figure 4.13 Myoton stiffness as a function of the superficial adipose percentage for the contralateral and residual limbs of 10 participants with unilateral transtibial amputation. NOTE: number represents participant identification and posterior calf site y axes only goes to 600 N/m

Correlation analysis suggested a trend of lower Myoton stiffness with increased socket use at both calf sites of residual limbs and the posterior calf of contralateral limbs (Table 4.6, Figure 4.14). However, this trend is counter intuitive as it would be expected that increased socket use would result in higher stiffness in the calf muscles, and correlation was only significant at the contralateral limb posterior calf. In general stiffness was higher at lateral compared to posterior calf sites of residual limbs, particularly in cases #5A and #10A. Participants who had their amputation due to Chronic Regional Pain Syndrome (#1A and #2A) or congenital abnormality (#3A and #6A) typically had the lowest residual limb stiffness and highest socket use (Figure 4.14).

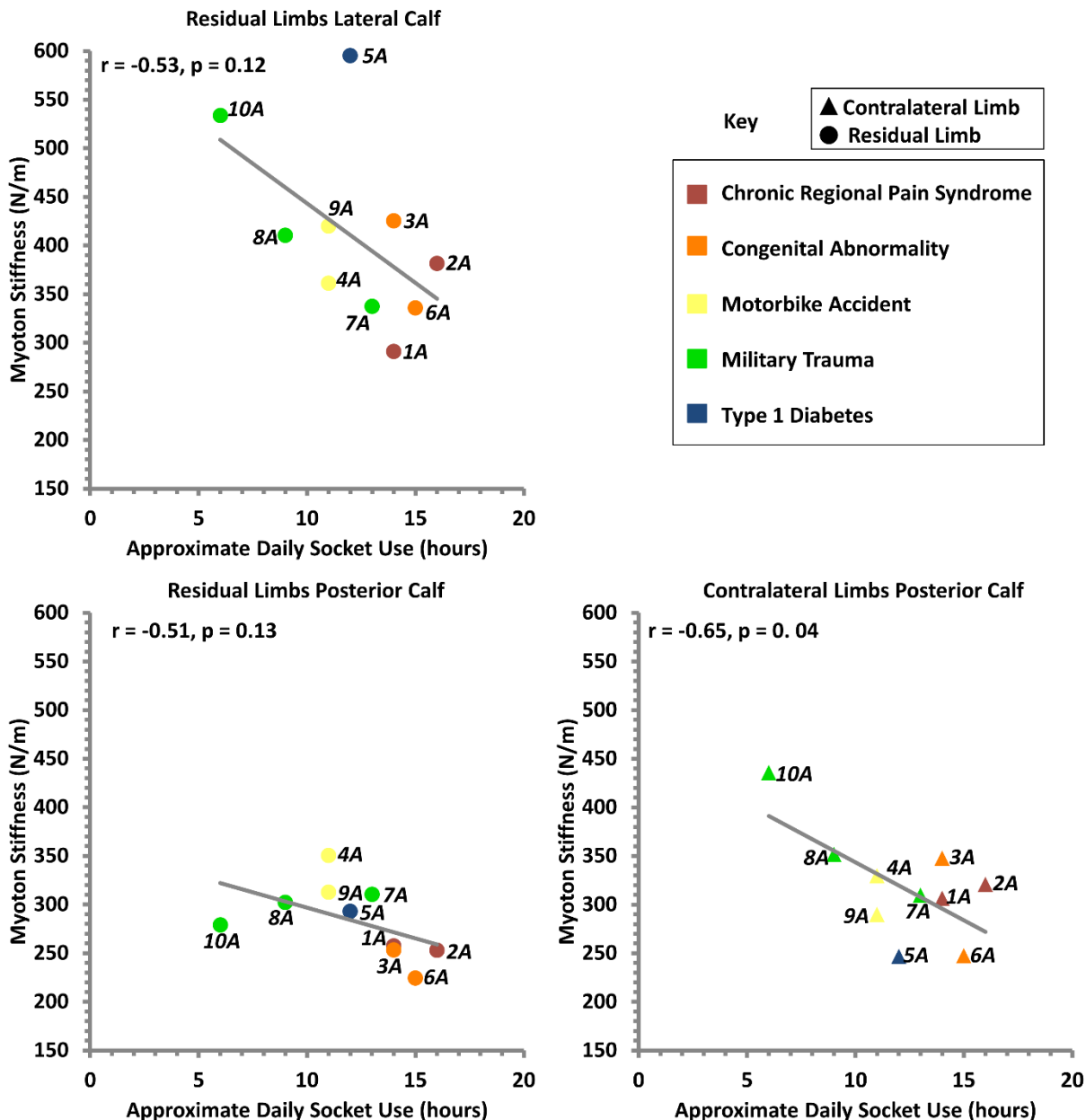


Figure 4.14 Myoton stiffness as a function of the socket use for the residual limb lateral calf site (top) and contralateral and residual limb posterior calf site (bottom) of 10 participants with unilateral transtibial amputation. NOTE: number represents participant identification and posterior calf site y axes only goes to 600 N/m

4.3.4 Deformation & Strain under Representative Prosthetic Loading

The soft tissue shape change at the posterior calf measurement site under a cuff pressure of 60 mmHg (8 kPa) for each limb tested are shown in Figure 4.15 and Figure 4.16.

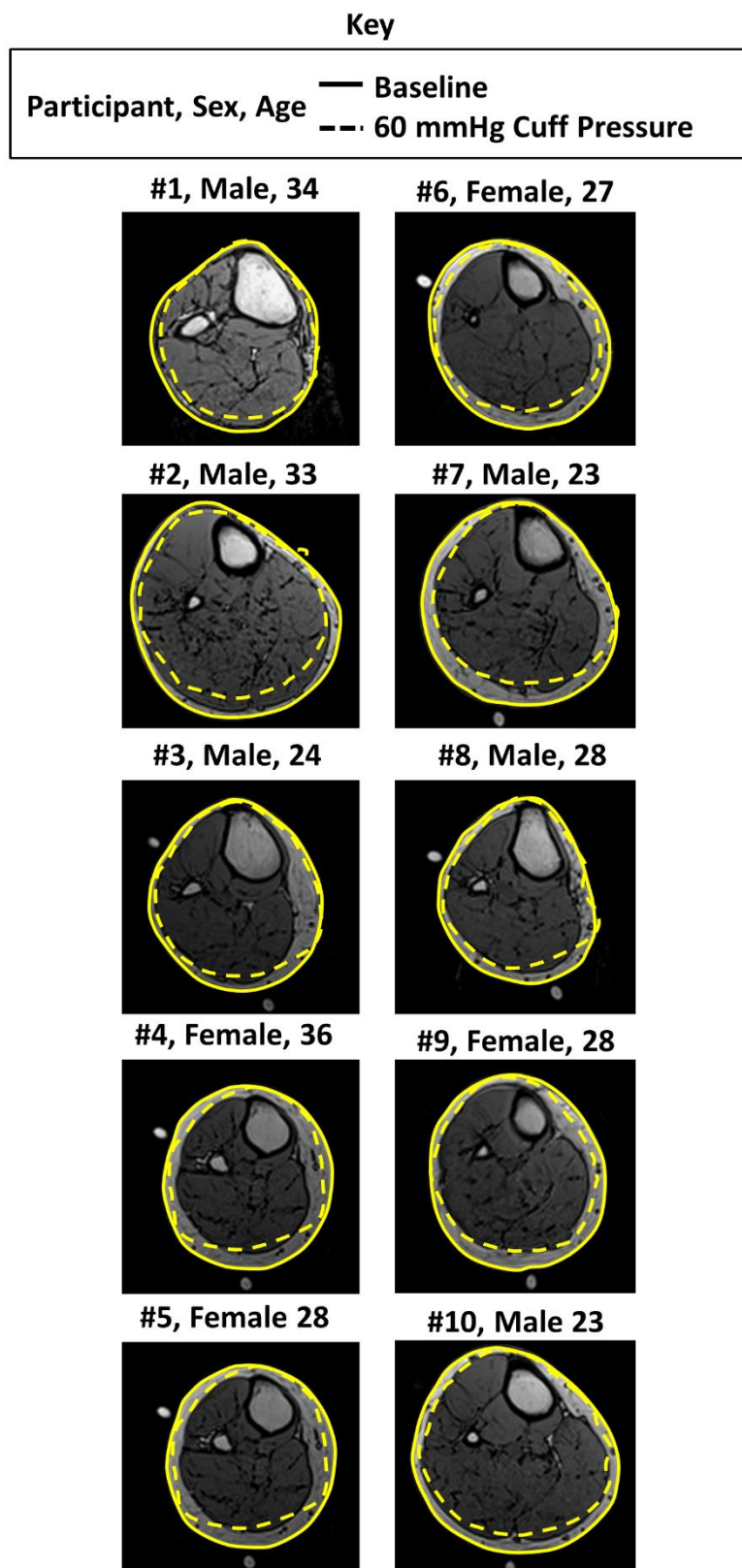


Figure 4.15 Transverse MRI slices at posterior calf measurement level at baseline outlining soft tissue at baseline (solid yellow line) and soft tissue under 60 mmHg cuff pressure (dashed yellow line), for participants without amputation

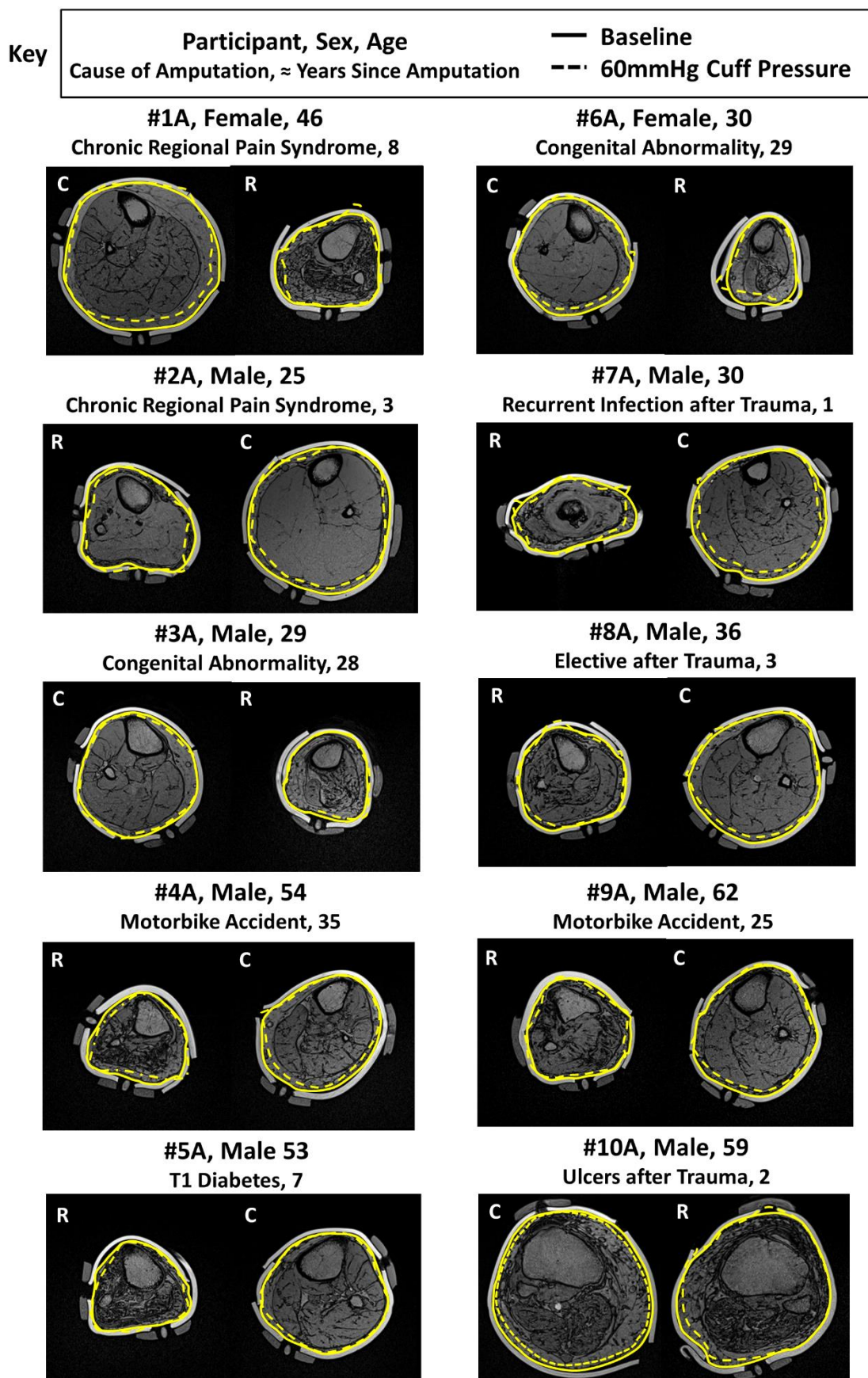


Figure 4.16 Transverse MRI slices at posterior calf measurement level at baseline outlining soft tissue at baseline (solid yellow line) and soft tissue under 60 mmHg cuff pressure (dashed yellow line), for participants with unilateral transtibial amputation (Note: #5A only pressurised to 40 mmHg)

Gross tissue deformation and strain under a pressure cuff inflation of 60 mmHg was calculated for each participant (Figure 4.17 and Figure 4.18). Strain was observed to be significantly higher ($p<0.01$) in control limbs (median ranged from 12 to 18 %) than residual limbs (median ranged from -6 to 2 %) at the patellar tendon and lateral calf sites. Strain values were also generally higher in control limbs (median ranged 12 to 18 %) compared to contralateral limbs (median ranged from 4 to 13 %), although this was only significant at the patellar tendon ($p<0.01$). Strain measurements were significantly different between residual and contralateral limbs at the lateral calf site ($p<0.01$). In control limbs although the largest deformations occurred at the posterior calf, the largest strains were observed at the patellar tendon site, due to its thinner soft tissue coverage.

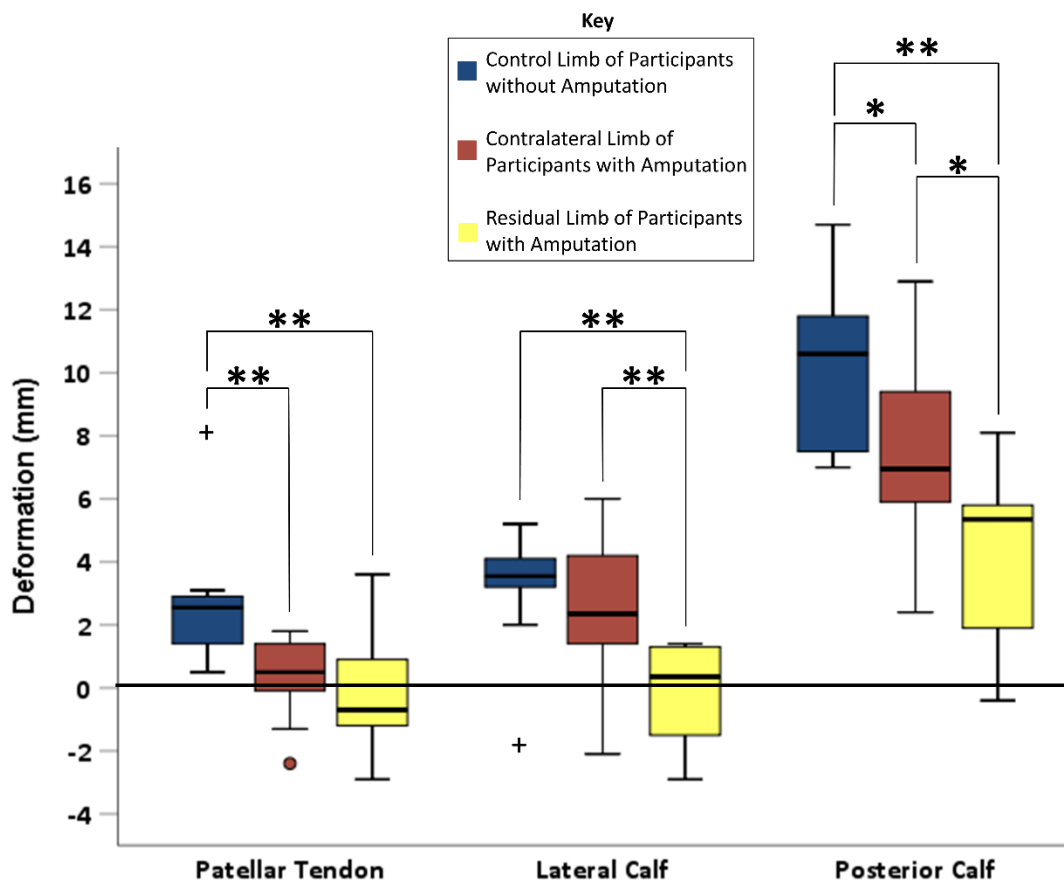


Figure 4.17 Median, interquartile range (IQR) and range of lower limb soft tissue deformation under 60 mmHg pressure cuff loading for all participant groups. Note: ○ and + indicate outliers that are 1.5 and 3 times the Interquartile Range (IQR) respectively, *= $p\leq0.05$ and **= $p\leq0.01$

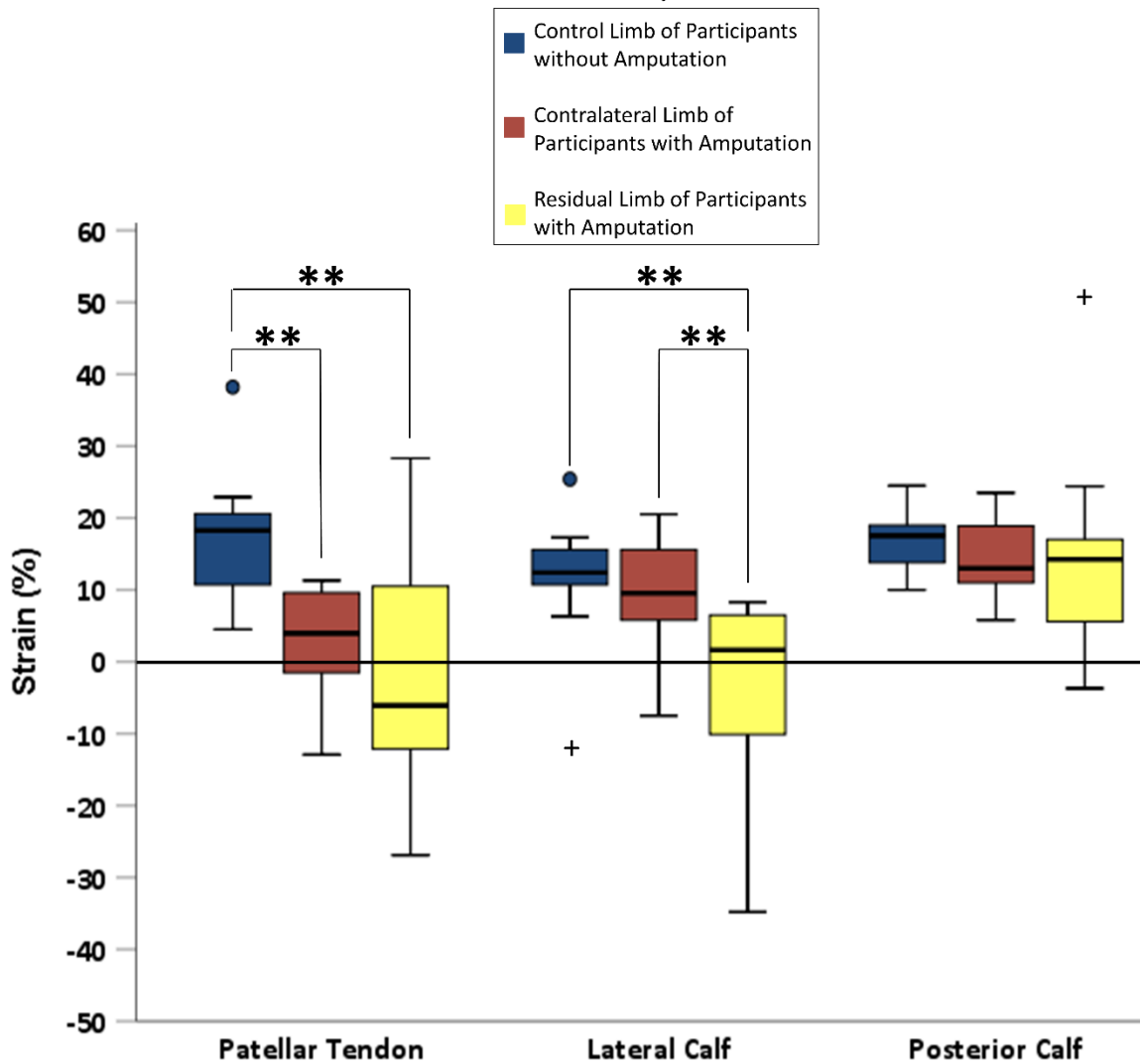


Figure 4.18 Median, interquartile range (IQR) and range of lower limb soft tissue compressive strain under 60 mmHg pressure cuff loading for all participant groups. Note: o and + indicate outliers that are 1.5 and 3 times the Interquartile Range (IQR) respectively, *= $p \leq 0.05$ and **= $p \leq 0.01$

Strain is more representative of tissue response than deformation because it is normalised to the tissue thickness, which explains its preferred use in tissue damage thresholds. Trends between tissue strain under 60 mmHg cuff pressure and tissue composition were evaluated (Table 4.7). Weak and insignificant correlation was observed between strain and superficial adipose percentage in all limb groups at all measurement sites. A stronger and significant trend of increasing strain with increasing infiltrating adipose was observed in the posterior calf of control limbs (Table 4.7 and Figure 4.19). It does not appear that the high strain observed in #5A ($\approx 51\%$) was linked to infiltrating adipose percentage though could be linked to this patient's co-morbidity of Type 1 Diabetes (Figure 4.19).

Table 4.7 Correlation analysis between tissue compressive strain under 60 mmHg cuff inflation and tissue composition in control limbs and the contralateral and residual limbs of participants with transtibial amputation.
 Note: results displayed as r (p) and green represents a result indicating strong correlation ($r > 0.5$) and bold represents significance ($P < 0.05$)

Correlation between Strain and:	Limb	Measurement Site		
		Patellar Tendon	Lateral Calf	Posterior Calf
Superficial Adipose %	Control	0.30 (0.40)	-0.20 (0.58)	-0.36 (0.31)
	Contralateral	-0.22 (0.53)	0.12 (0.75)	0.07 (0.86)
	Residual	-0.09 (0.80)	-0.01 (0.99)	-0.19 (0.60)
Infiltrating Adipose %	Control	0.32 (0.37)	-0.36 (0.31)	0.67 (0.03)
	Contralateral	-0.09 (0.80)	0.08 (0.83)	0.29 (0.43)
	Residual	0.44 (0.20)	-0.32 (0.37)	0.36 (0.31)

Key

- ◆ Control Limb
- Residual Limb

Amputation Cause Key

- Chronic Regional Pain Syndrome
- Motorbike Accident
- Type 1 Diabetes
- Congenital Abnormality
- Military Trauma

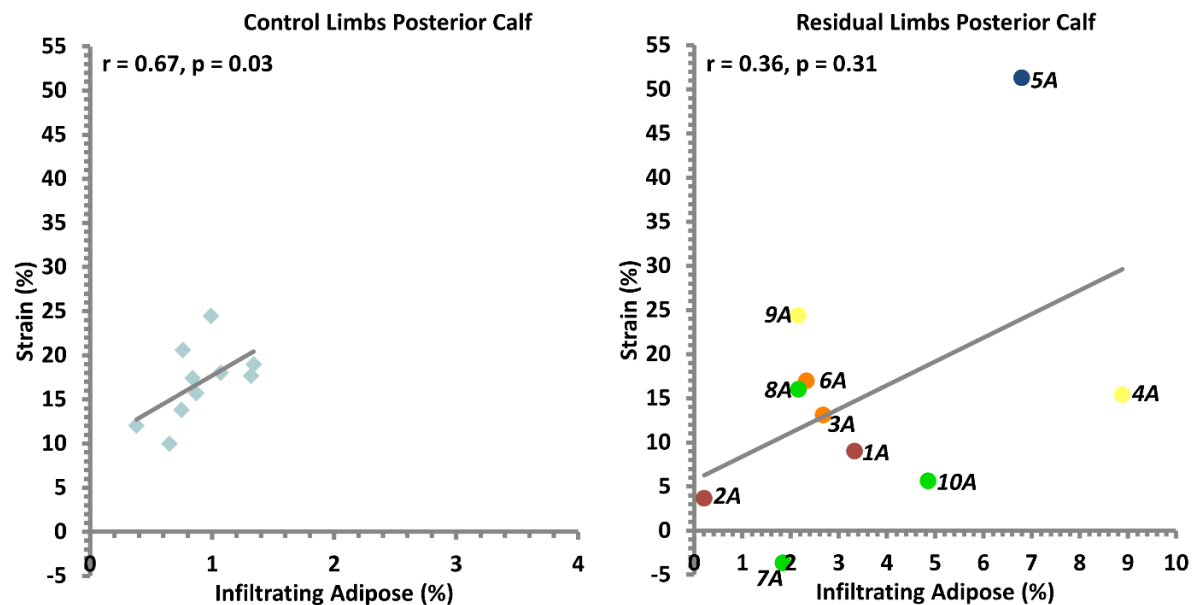


Figure 4.19 Tissue compressive strain under 60 mmHg cuff pressure at the posterior calf measurement site as a function of the infiltrating adipose percentage for the right control limbs of 10 participants without amputation (left) and the residual limbs of 10 participants with unilateral transtibial amputation (right). NOTE: number represents participant identification and left x axis is only to 4 %

4.4 Discussion

This study was designed to investigate residual limb soft tissue composition and how loading affects vulnerable residuum tissues. For the first time MRI has been used in conjunction with Myoton stiffness measurements to compare adipose tissue composition and visualise the biomechanical response to low representative loads applied via a pressure cuff to the lower limbs of participants with and without unilateral transtibial amputation, alongside a suite of other measurement techniques which will be described in Section 5.

4.4.1 Measurements and Analysis

An applied cuff pressure of 60 mmHg (8 kPa) equating to interface pressures ranging from 66.2 to 83.6 mmHg (8.8 to 11.4 kPa) was used to apply load to limb tissues (Table 4.4). The pressures applied were representative of PPAM aid use during rehabilitation, which has been estimated to apply interface pressures at the distal residuum ranging from 4 to 95 mmHg, median 26 mmHg (0.5 to 12.7 kPa, median 3.5 kPa) during static weight bearing [53]. Interface pressure was typically highest at the patellar tendon, potentially due to the thin soft tissue coverage at this measurement site. At 60 mmHg (8 kPa), calf sites had a larger change in interface pressure from baseline than the patellar tendon site. This was potentially due to muscle contractions increasing muscle volume at the calf measurement sites; however the differences between sites was small compared to the reported error of the Talley pressure sensors ($12 \pm 1\%$) [243].

MRI data enabled clear visualisation of the soft tissues and suitable contrast to distinguish between bone, muscle and adipose (Figure 4.2 and Figure 4.3). Volume percentage of infiltrating adipose tissue in residual limbs was approximately three times higher when compared the control limbs of participants without amputation. Increased infiltrating adipose tissue would be expected post-amputation due to muscle atrophy caused by denervation and disuse [47, 48]. This finding is in agreement with a previous MRI study that observed increased total adipose between muscles in four transtibial residual limbs post-amputation [49]. However, adipose infiltrating muscle was not quantified, and the present study is the first to discriminate between superficial and infiltrating adipose in residual limbs. This discrimination is important as adipose infiltrating muscle has been linked to disease progression, so more detailed knowledge of adipose composition will lead to better understanding of tissue health [192, 193, 254]. Previous research on muscle atrophy after spinal cord injury has observed infiltrating adipose to be a risk factor for DTI, further highlighting the importance of discriminating between adipose type when investigating tissue tolerance [194, 255, 256].

Another study used CT and observed a mean \pm SD relative fat mass difference of 39 ± 42 % in residual over contralateral limbs for 7 participants with transtibial amputation [50]. This larger adipose increase could be because measurements were only taken at the distal end of the residual limb where muscle atrophy, and therefore the greatest adipose differences, would be most likely to occur. Indeed, in this current study the greatest differences were observed distally (Figure 4.5 and Figure 4.6). If the residuum has a relatively uniform or continuous layer of subcutaneous adipose, there are likely to be transverse slices distal to the residual bone tip which will have a high adipose proportion, dependent on the surgical flap procedure used and degree of atrophy. This distal increase of adipose can be observed on the MR image below, of a participant 10 years post unilateral transtibial amputation due to PVD [121] (Figure 4.20). In the present study transverse slices inferior of the tibia cut end were not used in the comparative analysis.

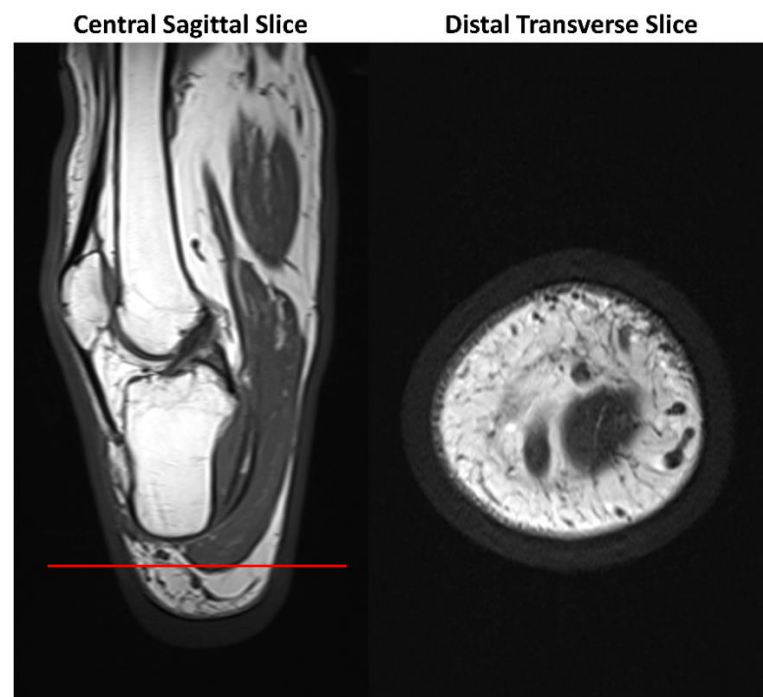


Figure 4.20 Left: central sagittal, and Right: distal transverse MRI slice of the residual limb of a male participant with unilateral transtibial amputation collected for Eurostars ImpAmp project [121]. Note: red line shows the position of the distal transverse slice

Subcutaneous adipose tissue plays an important role in energy homeostasis, metabolic and endocrine function within the human body [254]. In the context of residuum tissue health, adipose could be acting as a cushioning factor for soft tissue protection. Indeed, one of the functions of adipose tissue is to provide a protective surround for organs [257]. Adipose tissue consists mainly of adipocytes with most of their volume taken up by lipid droplets. Mechanical loads will alter the cytoskeletal tension of adipocytes which will change signalling pathways affecting the formation of further adipose cells (adipogenesis) [257]. Adipose cells of different maturity and type have been observed to behave differently to mechanical loading, although generally static tensile loading has been observed to promote adipogenesis and increase the size and number of lipid droplets [257-259].

An increase in lipid droplet size and number will increase the stiffness in adipocytes, changing the response of adipose tissue to loading as well as changing the cytoplasm tension of adjacent adipocytes leading to adipose hypertrophy [260]. This could in part explain higher adipose in the residuum distal end due to factors such as flap suturing and socket donning leading to adipose tissue under tension. Generally dynamic cyclic loading has been observed to inhibit adipogenesis which is intuitive as physical activity, such as walking, will cyclically load tissues and is associated with a decrease in adipose tissue mass.

However, there are negative clinical implications associated with adipose tissue that infiltrates muscle [254]. Previous research suggests strong correlation between higher levels of infiltrating adipose tissue and impaired glucose tolerance which could explain why higher levels of adipose infiltrating muscle were observed in this study's diabetic participant (Figure 4.6) [196, 254]. Indeed, infiltrating adipose has been linked to insulin resistance and diabetes [252]. This is thought to be due to insulin's involvement in the breakdown of fats with insufficient management of insulin provision causing elevated circulating free fatty acids [261].

Evidence also suggests elevated markers of inflammation with increased adipose infiltrating muscle [196, 254] which will be explored in Section 5. High variability in infiltrating adipose percentage was observed in the residual limbs of participants with amputation, particularly at the distal end (Figure 4.6), which agrees with Sherk et al's findings, described previously [50]. These variations will be due in part to the surgical approach used to create the distal residual limb among other variables such as co-morbidities, cause of amputation, time since amputation and socket use.

Correlation analysis gave an insight into the relationship between contralateral and residual limbs and how different variables may affect tissue composition post-amputation. High residual adipose was observed to correlate strongly with contralateral adipose for both superficial and infiltrating types (Figure 4.9). However, high superficial adipose did not necessarily correspond to high infiltrating adipose indicating different factors affect each of the adipose tissue types. It was important to consider the relationship between BMI and infiltrating adipose, where it could be hypothesised that those with a high BMI would have high levels of adipose. However, the present study revealed limited associations between BMI and adipose tissue types (Table 4.5). In particular a more varied percentage of infiltrating adipose with BMI was observed in the residual limb group, indicating that factors due to amputation affected tissue composition more.

The present study also revealed limited associations with time since amputation and daily socket use (Table 4.5). It would be expected that with increased socket use both contralateral and residual limbs would be more active and therefore require lean muscle mass to function. This trend was observed in contralateral limbs but not residual limbs, indicating that other factors of amputation are affecting tissue composition (Figure 4.10).

To explore how tissue composition may affect the soft tissue properties, structural stiffness was analysed using the MyotonPro™ device. Stiffness measurements were highest at the patellar tendon (Figure 4.11), indicating that this tissue has the highest resistance to shape change. Between the test groups, the highest stiffness measurements were observed in the residual limbs, which could indicate adaptation under patellar tendon socket load bearing. At calf measurement sites, the highest stiffness measurements were observed in the contralateral limbs which could be due to increased use during early rehabilitation or due to compensatory gait prior to amputation in some circumstances.

Further analysis to explore how superficial adipose composition affects structural stiffness revealed limited associations. In the calves of participants without amputation, particularly the posterior site, male participants generally tended toward the high stiffness/low superficial adipose percentage quadrant, while female participants generally tended more towards low stiffness and high superficial adipose percentage (Figure 4.12). This trend was also observed when comparing a male participant (#3A) with an age, cause and time since amputation -matched female participant (#6A) within the cohort with amputation (Figure 4.13). Evidence of sex-related differences has also been observed in a previous Myoton study with male participants having greater stiffness than females at a rectus femoris muscle site, indicating that the measurement does consider both the muscle and superficial adipose, which is generally higher in females [131, 253]. These results are consistent with known sex-related differences between muscle characteristics, with larger proportions of type 2 fibres in males causing increased strength and larger proportions of type 1 fibres in females leading to increased endurance [262]. Age related differences were not observed in this study but have been identified previously, with increased stiffness in older (65 to 90 years old) participants compared to a younger group of participants aged 18 to 35 years [131]. However, this study was analysing the biceps brachii and rectus femoris muscles, and different muscle anatomies may produce different results.

Correlation analysis exploring tissue properties and participant demographics suggested that with increased daily socket use the tissue stiffness was lower in both calf sites of residual limbs and the posterior calf of contralateral limbs (Figure 4.14). This trend is unintuitive as increased socket use would be expected to increase stiffness. The socket use variable in this study provides insight into the approximate daily time over which the socket is donned but does not capture the person's activity types and levels (sitting, walking, running etc.) or the accumulation of loading post-amputation. This accumulation will be dependent on several factors including an individual's general health and fitness, rehabilitation interventions and when a socket was fitted. The Myoton probe was also designed for measuring superficial skeletal muscles so measurements may have lower validity in participants with higher superficial adipose tissue such as case #10A [132]. Adipose tissue is very complex and can change its size and function in response to a number of factors such as loading, exercise, temperature and nutrition [257, 263]. As discussed above, under static tension adipose tissue hypertrophy has been observed with larger and higher numbers of lipid droplets increasing the stiffness of the tissue [257]. This could explain why cases such as #10A had high stiffness as their socket use is likely to be mostly statically loading their tissues as they mobilise using a wheelchair (Figure 4.14).

The composition and properties of tissues will affect how they respond to and tolerate loading. MRI also enabled analysis of gross tissue deformation and strain of the calf tissues under 60 mmHg cuff inflation (Figure 4.15 to Figure 4.18). The lowest deformation was observed at the residual limb patellar tendon site, which is consistent with this location's higher tissue stiffness measurements. A larger range of strain was observed at residual limbs compared to intact limbs potentially due to more variable tissue composition and circumference, and therefore greater differences in shape change between participants. This is reflected in the tensile strain results and shown in the outlined residual images (Figure 4.16 and Figure 4.18). Residual limbs were also generally smaller than contralateral limbs so the same deformations would represent higher strains at residual limb sites.

Over short periods of loading application, strain is thought to be the most important factor in the causal pathway for damage of muscle tissue [144, 164-168, 171, 172, 175]. The largest strains observed in this study were generally approximately 20 to 30 % and were applied for short periods of less than 15 minutes, much lower and for shorter durations than studies investigating magnitude and temporal aspects of tissue damage [163]. The relationship between strain and superficial and infiltrating adipose was explored in this research revealing limited associations. A general pattern of increased strain with increased infiltrating adipose was observed in the posterior calf of control limbs (Figure 4.19 and Table 4.7).

4.4.2 Limitations

The small sample size of this current study ($n = 10$ for each group) limited generalisations and due to the heterogeneity of the cohort with amputation a case by case approach was deemed more appropriate in the data analysis. We are not aware of the tissue composition or tolerance to loading prior to amputation so can only hypothesise on what has happened since and a heterogeneous cohort enabled further insight into factors that may affect tissue adaptation and tolerance post-amputation.

During the testing sessions it was often difficult to support limbs in a consistent manor due to differing shapes, lengths and sensitivities. For example, one participant required a degree of knee flexion to avoid muscle spasms in his residual limb. Others, with shorter residua were supported from below for participant comfort. Differing participant anatomies particularly in the residual limb resulted in varying measurement position from the centre of measurement sites. These factors meant that the length of imaged limb consistent across all 30 limbs was reduced from the potential ≈ 100 mm (the height of two measurement areas) to ≈ 60 mm.

Segmentation of MR images can be a subjective and time-consuming process. Within the MRI testing session, the surface coil used introduced a gradient in the images with some regions having a poorer signal-to-noise ratio than others. To reduce manual processing effects ImageJ macros were used and the same person carried out all processing.

Regarding Myoton measurements, it is important to note that the stiffness parameter obtained does not directly equate to mechanical properties, such as Young's Modulus, but offers an insight into the behaviour of a particular structure of layered tissues. Although as far as possible limbs were kept in a consistent supported position during Myoton measurement, relaxation of the muscles was not measured objectively (i.e. by electromyography) so it is not possible to be certain that muscles were relaxed. A previous study of skeletal muscle properties observed that contracted muscles are generally more tense, stiff and elastic [130].

Deformation results were variable and it is important to note that the in-slice resolution was 0.6 mm which limits the strain resolution to approximately $\pm 3\%$, although deformations were generally >0.6 mm. Two-dimensional simplified analysis was used in this study. However, 3D deviatoric strains would capture more realistically what happens to the limbs under applied pressure as the limbs are changing shape, not volume, under cuff loading due to the incompressibility of the soft tissues.

4.4.3 Summary

For the first time to the authors' knowledge, MRI has been used in combination with MyotonPro™ measurements to observe soft tissue composition and structural properties, and biomechanical response under representative prosthetic loading in intact and amputated limbs. An increased percentage of adipose infiltrating muscle was observed in residual limbs when compared to intact limbs, indicating muscle atrophy post-amputation. Residual limbs were also observed to be stiffer at the patellar tendon site and generally underwent less strain than intact limbs. Large variation in results was possibly due to the differences between participants such as amputation cause, time since amputation and co-morbidities. This study provides a first insight into how residual limb soft tissues can change post-amputation within a range of amputation causes. Longitudinal studies with increased participants that control for or record prosthetic loading and duration could help to determine more predictive variables that affect tissue composition and response to loading post-amputation. Investigation of morphology and response to loading will help to further understanding of how the soft tissues adapt to tolerate prosthetic loading, contributing knowledge to help minimise the risk of tissue damage during prosthetic use.

5 Physiological Response Under Representative Loads

This section answers in part research questions 2 and 3, namely:

Research Question 2. How do residual and intact limbs respond biomechanically and physiologically to representative prosthetic loading?

Research Question 3. How does soft tissue composition affect response to loading/tissue tolerance?

5.1 Introduction

As discussed in Section 2.2.3, various strategies have been used to monitor the status of loaded dermal tissues [34, 83]. To date, some of these techniques have been used to monitor tissues subjected to prosthetic liner loading [82]. However, there is a need to develop an array of measurement tools with associated robust parameters to assess both the biomechanical and physiological response of soft tissues under loading experienced at the residuum-socket interface [85].

The present protocol was designed to assess the appropriateness of selected parameters to identify tissue tolerance during periods of mechanical loading. This was achieved by establishing a series of measurements, including interface pressures, transcutaneous oxygen and carbon dioxide tensions and inflammatory biomarkers, at relevant tissue sites before, during and after loading representative of prosthetic socket use.

5.2 Materials and Methods

5.2.1 Study Design

This chapter reports on data collected during a laboratory testing session as part of the same observational study reported in Section 4.

5.2.2 Material and Methods

Full details of the materials and methods are included in Section 3.4. Briefly, a pressure cuff (Ref 0124 Aneroid Sphygmomanometer, Bosch + Sohn GmbH, Germany) was applied over the right calf of participants without amputation (control limbs) and both the residual and contralateral limbs of participants with amputation.

Hair was removed at each site by shaving at least 48 hours prior to testing to ensure that any up-regulation of pro-inflammatory cytokine due to shaving irritation [245] was minimised. At the start of the testing session participant weight and height were measured using the combined lab scales and 'drop down' tape measure (Table 4.2 to Table 4.3). Throughout testing participants were in a seated position on a Hospital Bed (Enterprise, Arjo Huntleigh, Malmö, Sweden) with adjustable backrest (Figure 3.24). A Prosthetic liner (ContexGel Liner, RSL Steeper, UK) was positioned underneath the cuff to provide a representative material to interface with the skin. Three sites were selected for measurement on each limb as described in Section 3.2.

To review briefly, T_{cPO_2} and T_{cPCO_2} were monitored for a 20 minute unloaded period, in order to both reach a temperature equilibrium and estimate baseline values prior to cuff application. These values were subsequently monitored at 0.033 Hz throughout cuff application and during a refractory period. Rings of silicone gel were used to minimise pressure gradients at the electrode-skin interface (Figure 3.21). After application of the cuff and a 10 minute settling period it was inflated by 10 mmHg increments every 10 minutes from pressures of 20 to 60 mmHg. The pressures were subsequently released incrementally over 60 seconds until the cuff was deflated, and data collection continued for a 35 minute refractory period (Figure 3.22 and Figure 3.26). A sebum sample was collected from each measurement site by applying adhesive tape (Sebutape™ CuDerm, Dallas, TX, USA) for a 2 minute period at baseline (prior to cuff application) and post-loading (immediately after cuff removal). The concentrations of the pro-inflammatory cytokine, IL-1 α , and the anti-inflammatory cytokine, IL-1RA, and the total protein (TP) on each tape were estimated using an ELISA protocol (see Section 3.4.2).

After the refractory period, a single 28mm diameter pneumatic cell was positioned at the skin surface of each measurement site and connected to the Talley pressure monitoring system as described in Section 3.1 (Figure 3.7). Interface pressures were recorded when the cuff was first applied and subsequently after each incremental inflation pressure (20 to 60 mmHg).

5.2.3 Data Analysis

Raw data from each measurement technique were processed using MATLAB (Mathworks, USA) and analysed using SPSS Statistics (IBM, USA). The percentage changes in T_cPO_2 from baseline during each loading condition were calculated as a measure of tissue ischaemia. At the patellar tendon test site, where combined T_cPO_2 and T_cPCO_2 parameters were estimated the data was categorised according to established criteria [215]:

- Category 1 (minimal changes in T_cPO_2 and T_cPCO_2),
- Category 2 (>25% decrease in T_cPO_2 with minimal change in T_cPCO_2) and
- Category 3 (>25% decrease in T_cPO_2 and >25% increase in T_cPCO_2).

Ratios of IL-1 α /TP and IL-1RA/TP were calculated at each measurement site to account for intra-participant variation of proteins [161], and presented as the percentage change from baseline.

All data were first examined for normal distribution prior to analysis using histograms and the Shapiro-Wilk test, in order to determine appropriate descriptive and inferential statistics. As a result, interface pressure and transcutaneous gas tension data were presented using parametric descriptors, namely mean and standard deviation, and inflammatory response data presented using non-parametric descriptors, namely median, quartiles and range. Appropriate statistical testing methods were applied to answer the three research questions detailed in Section 3.5 (Table 5.1).

Table 5.1 Statistical analysis to evaluate interface pressure, transcutaneous oxygen and carbon dioxide tension, IL-1 α /TP and IL-1RA/TP between control, contralateral and residual limb groups and the relationship between some of these factors and BMI/time since amputation/socket use

Research Question to be Answered	Measurement	Hypothesis: There is a significant...	Normal Distribution	Statistical Test Used
2	Interface Pressure	... relationship between the measurement and applied cuff pressure	Yes	Pearson's Correlation
2		... difference in the measurement between limb groups and measurement sites	Yes	T-Test
2	% change in T _c PO ₂ and T _c PCO ₂	... relationship between the measurement and cuff pressure for control/contralateral/residual limbs	Yes	Pearson's Correlation
2	% change in T _c PO ₂ and T _c PCO ₂ from baseline to 60 mmHg cuff pressure	... difference in the measurement between limb groups	Yes	T-Test
3		... relationship between the measurement and percentage of adipose tissue (Sections 3.4.2 and 4.3.2) for control/contralateral/residual limbs	No	Spearman's Correlation
2		... relationship between the measurement and time since amputation/socket use (Sections 3.4.3-3.4.4 and 4.3) for contralateral/residual limbs	Yes	Pearson's Correlation
2		... % change in biomarker ratio from baseline to post-loading for control/contralateral/residual limbs	No	Wilcoxon Signed Rank
2	% change in IL-1 α /Total Protein and IL-1RA/Total Protein from baseline to post-loading	... difference in the measurement between limb groups	No	Mann-Whitney U
3		... relationship between the measurement and percentage of adipose tissue (Section 3.4.2 and 4.3.2) for control/contralateral/residual limbs	No	Spearman's Correlation
2		... relationship between the measurement and percentage change in T _c PO ₂ and T _c PCO ₂ for control/contralateral/residual limbs	No	Spearman's Correlation
2		... relationship between the measurement and time since amputation/socket use (Sections 3.4.3-3.4.4 and 4.3) for contralateral/ residual limbs	No	Spearman's Correlation

Differences and associations were considered to be statistically significant at the 5 % level

($p < 0.05$) as this is a well-used benchmark of significance. Strength of association can be examined using the correlation coefficient (r) and guidelines specify that an $r > 0.5$ indicates strong correlation [251]. However, r doesn't take into account the number of participants and with an n of 10 in each limb group correlations are somewhat arbitrary and therefore, although r will be reported, the significance (p) of the correlation provides a more appropriate measure of the relationships.

Given the sample size and heterogeneity of participants, it was deemed appropriate to also analyse data on a case-by-case basis and focus on the clinical relevance as opposed to r and p values. The full correlation analysis for each measurement has been presented in tabulated form and significant or clinically interesting results have been graphically presented to provide context.

5.3 Results

Demographics of participants have been reported in Section 4.3.

5.3.1 Interface Pressure

As indicated in Figure 5.1, there was a significant monotonic increase in interface pressures with cuff inflation pressure at all three tests sites in all limbs ($r > 0.93$ and $p < 0.01$ in all cases). Before the cuff was inflated i.e. at 0 mmHg, finite interface pressures were recorded (mean < 20 mmHg in all cases). At a cuff pressure of 60 mmHg, the mean interface pressures had increased ranging from 66.2 to 73.7 mmHg (8.8 to 9.8 kPa), 69.9 to 75.1 mmHg (9.3 to 10.0 kPa) and 72.0 to 83.6 mmHg (9.6 to 11.1 kPa) in control, residual and contralateral limbs, respectively (Figure 5.1).

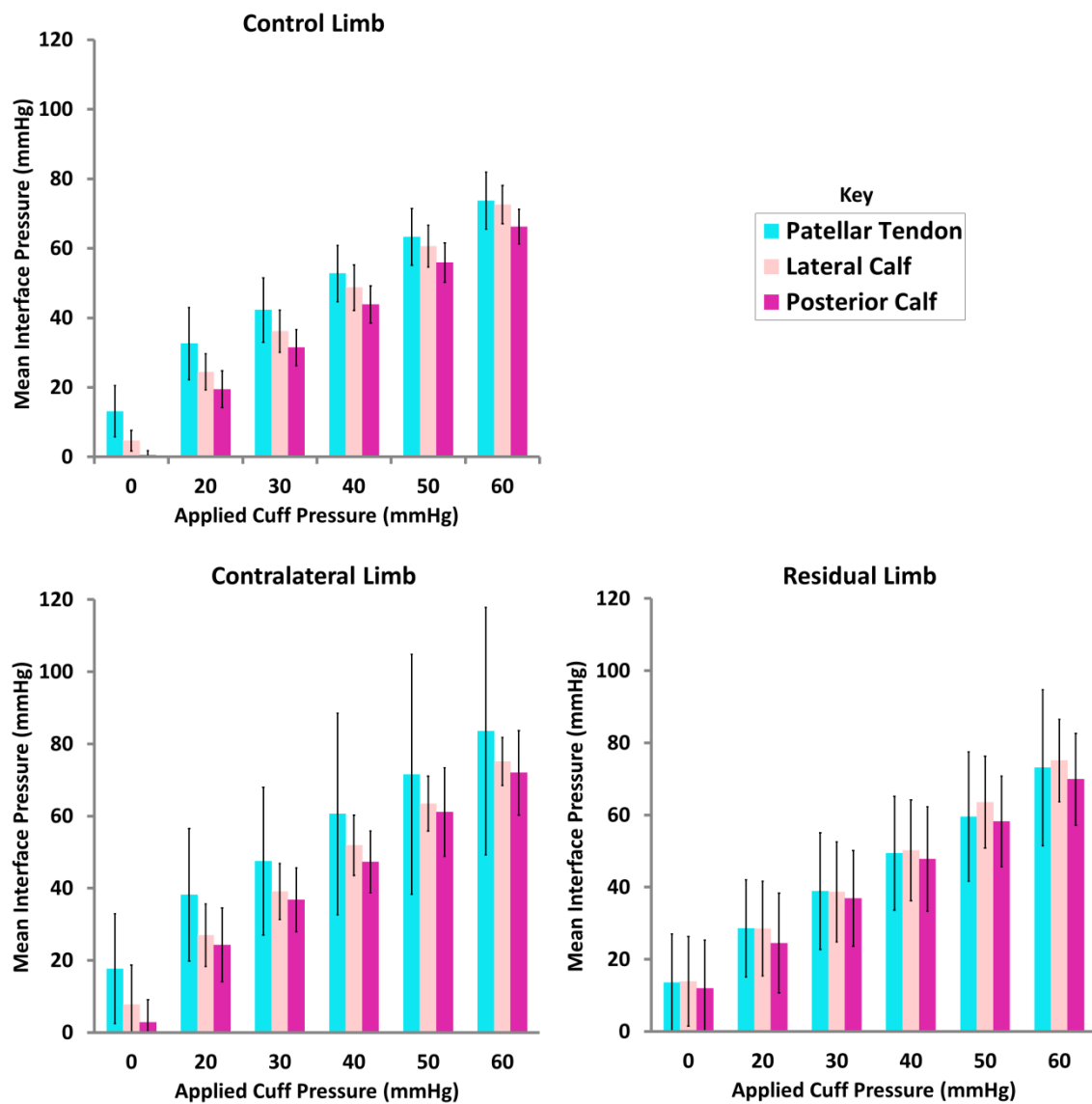


Figure 5.1 The effects of incrementally applied cuff pressures on mean (\pm SD) interface pressures at three measurement sites in intact and residual lower limbs

5.3.2 Tissue Ischaemia

Often the baseline T_{cPO_2} and T_{cPCO_2} was lower in residual limbs compared to the control and contralateral limbs, particularly at the patellar tendon site (Figure 5.2). Significant differences were evident for mean baseline T_{cPO_2} at the patellar tendon site between contralateral and residual limbs ($p = 0.01$), and mean baseline T_{cPCO_2} between control and residual limbs ($p < 0.01$).

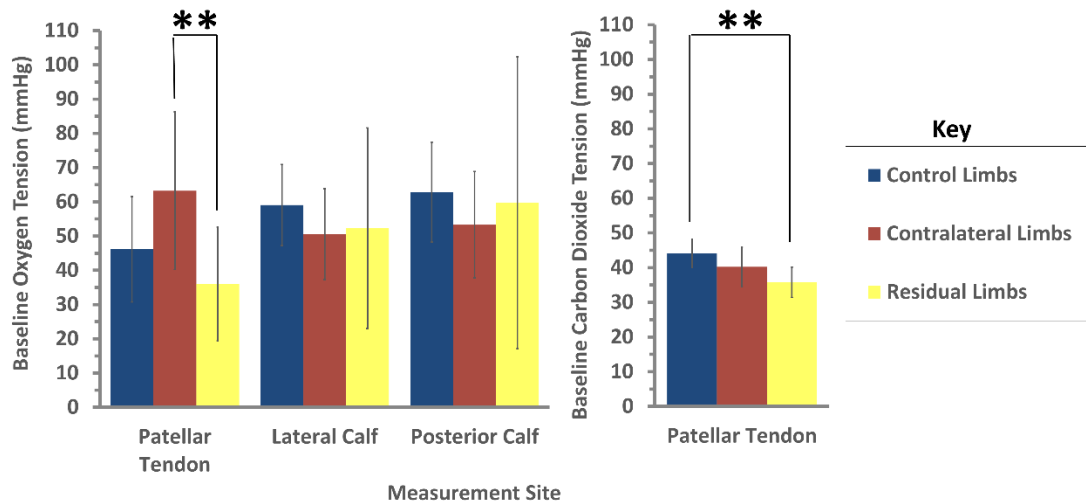


Figure 5.2 Mean baseline oxygen (left) and carbon dioxide (right) tensions at three measurement sites in the right control limb of ten participants without amputation and both contralateral and residual limbs of ten participants with unilateral transtibial amputation. Note: error bars represent \pm SD and, ** = $p \leq 0.01$

A decrease in T_cPO_2 was observed with increasing cuff inflation at all measurement sites, as illustrated for two participants in Figure 5.3. The cohort data (detailed in Appendix G) exhibited two common trends at the patellar tendon site:

Trend 1: A Category 3 response [215], with decreasing T_cPO_2 at elevated cuff pressure associated with >25 % increase in T_cPCO_2 above baseline levels (Figure 5.3, left).

Trend 2: A Category 2 response, with minimal changes in T_cPCO_2 (<25 %) despite a reduction in T_cPO_2 (Figure 5.3, right).

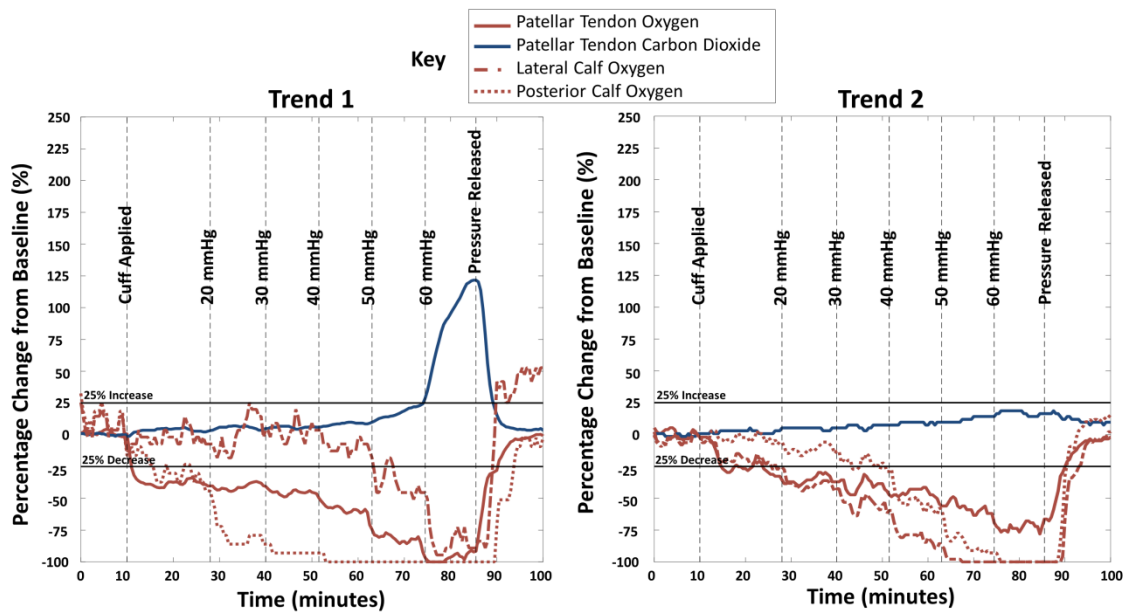


Figure 5.3 Exemplar data showing percentage change from baseline T_cPO_2 and T_cPCO_2 measurements under incremental cuff pressures from 20 to 60 mmHg from the residual (left) and contralateral (right) limbs of participant #3A, revealing two main trends observed at the patellar tendon site within the research cohort: Trend 1 a Category 3 response (left) and Trend 2 a Category 2 response (right)

The majority (8/10) of control limbs displayed a Category 3 response (Figure 5.4). Within the cohort of participants with transtibial amputation a Category 3 response was displayed in 3/10 residual limbs and 5/10 contralateral limbs (Figure 5.5).

Inter- and intra-participant variation in ischaemic response at the patellar tendon indicated

differences in tolerance to the applied cuff pressures. For example, with a cuff pressure of 20 mmHg (2.7 kPa) only one control limb (Figure 5.4) and one contralateral limb (Figure 5.5)

exhibited a Category 3 response at the patellar tendon. By contrast, at 60 mmHg (8.0 kPa) eight control limbs, four contralateral limbs and three residual limbs exhibited a Category 3 response

(Figure 5.4 and Figure 5.5). It should be noted that for one participant (#5A) as a safety precaution due to a lack of sensation and an increased risk of tissue damage arising from their underlying Type 1 diabetes, skin was checked for non-blanchable erythema after each cuff inflation pressure.

The test session was ended at a lower cuff pressure as a more slowly resolving mark on the skin

from the transcutaneous electrode was observed. A Category 2 or 3 ischaemic response had been observed in both limbs prior to session stoppage.

Control Limb

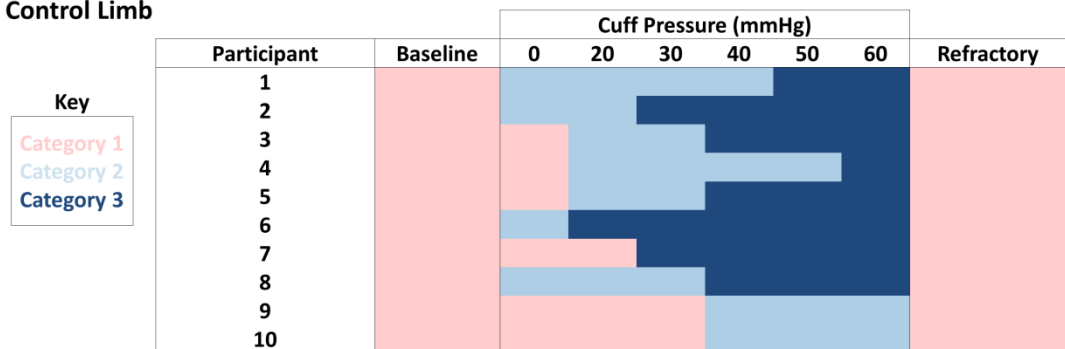


Figure 5.4 Ischaemic response at the patellar tendon to incremental cuff pressures using categorical analysis [215], to indicate tolerance in ten participants without amputation

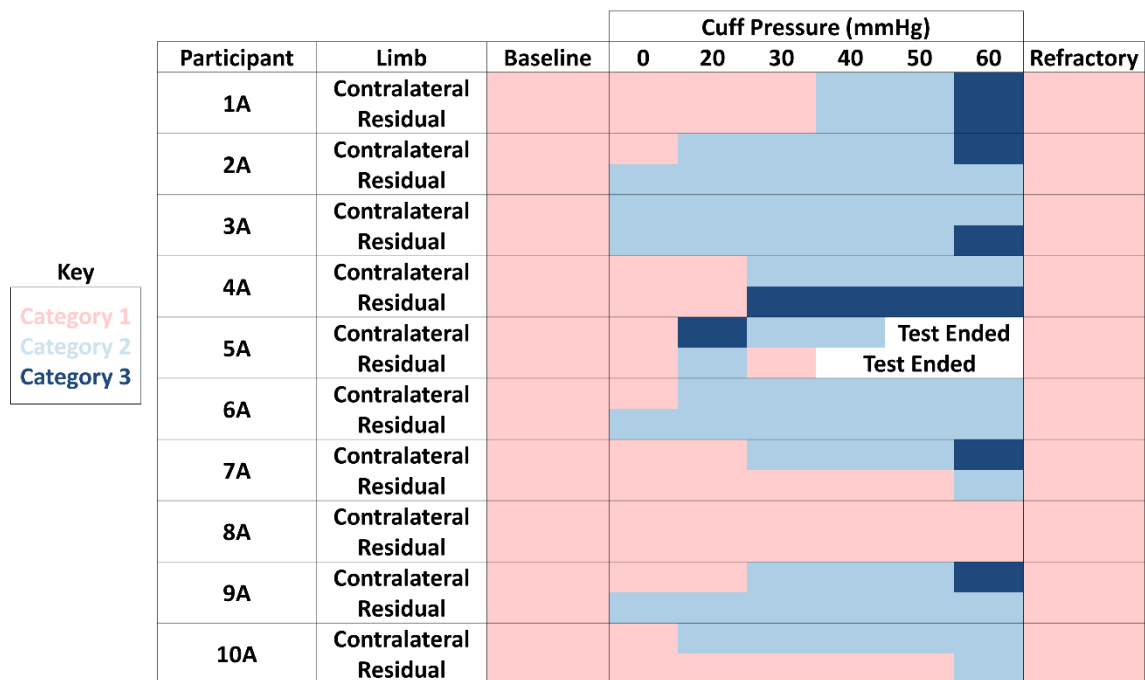


Figure 5.5 Ischaemic response at the patellar tendon to incremental cuff pressures using categorical analysis [215], to indicate tolerance in ten participants with transtibial amputation

There was a significant decrease in T_cPO_2 with incremental cuff pressures at all three measurement sites in each test limb (Figure 5.6) ($r > 0.84$ and $p < 0.04$ in all cases). Some saturation, T_cPO_2 values at ≈ 0 mmHg was observed when the pressures exceeded 50 mmHg (6.7 kPa). Immediately following load removal, all values were restored to at least baseline values. Some T_cPO_2 recovery values, particularly in residual limbs, increased with respect to baseline, represented by the negative values in Figure 5.6. Each skin site exhibited similar trends with respect to cuff loading. Higher decreases in T_cPO_2 values were generally observed at the patellar tendon and lateral calf sites, notably at cuff pressures below 40 mmHg. At the maximum cuff pressure of 60 mmHg (8.0 kPa), at the lateral calf site, the decrease in T_cPO_2 was significantly lower in the residual limb group ($63 \pm 39 \%$, $p = 0.04$) compared to the control limb group ($97 \pm 6 \%$). At the patellar tendon the T_cPO_2 decrease at a cuff inflation of 60 mmHg (8.0 kPa) was significantly lower in the contralateral limb group ($70 \pm 24 \%$, $p = 0.03$) compared to the control limb group ($91 \pm 13 \%$).

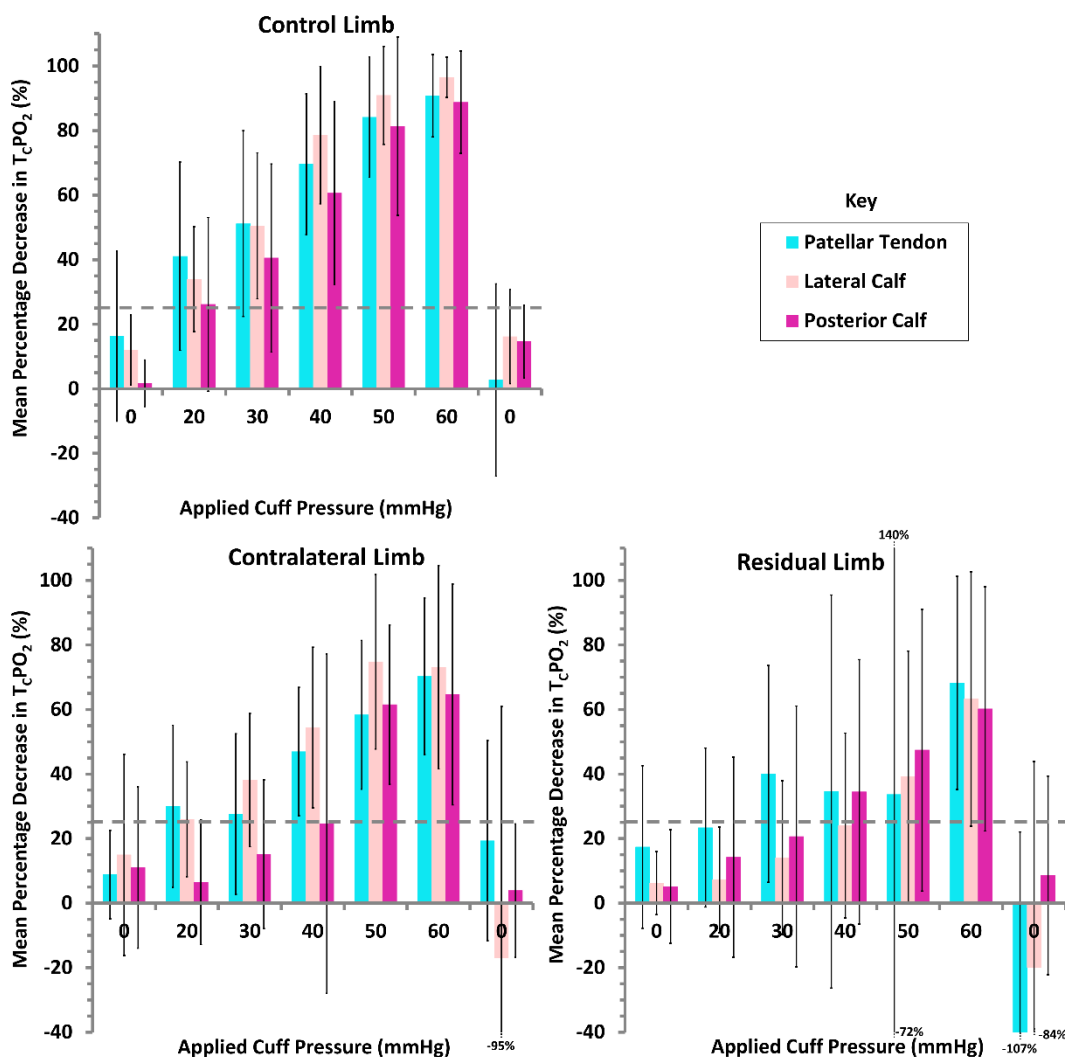


Figure 5.6 The effects of cuff pressures on mean (\pm SD) percentage decrease in T_cPO_2 at the three measurement sites in intact and residual lower limbs. Note: Dashed line at 25% decrease indicates Category 3 ischemia threshold

There was a significant correlation between cuff pressure and percentage increase in $T_c\text{PCO}_2$ at the patellar tendon in all three limb groups (Figure 5.7, $r > 0.87$ and $p < 0.02$ in all cases). At a cuff inflation of 60 mmHg, the percentage change in $T_c\text{PCO}_2$ values were significantly lower in the residual limb ($40 \pm 61\%$, $p=0.02$) and contralateral limb groups ($16 \pm 20\%$, $p<0.01$) compared to the control limb group ($130 \pm 84\%$).

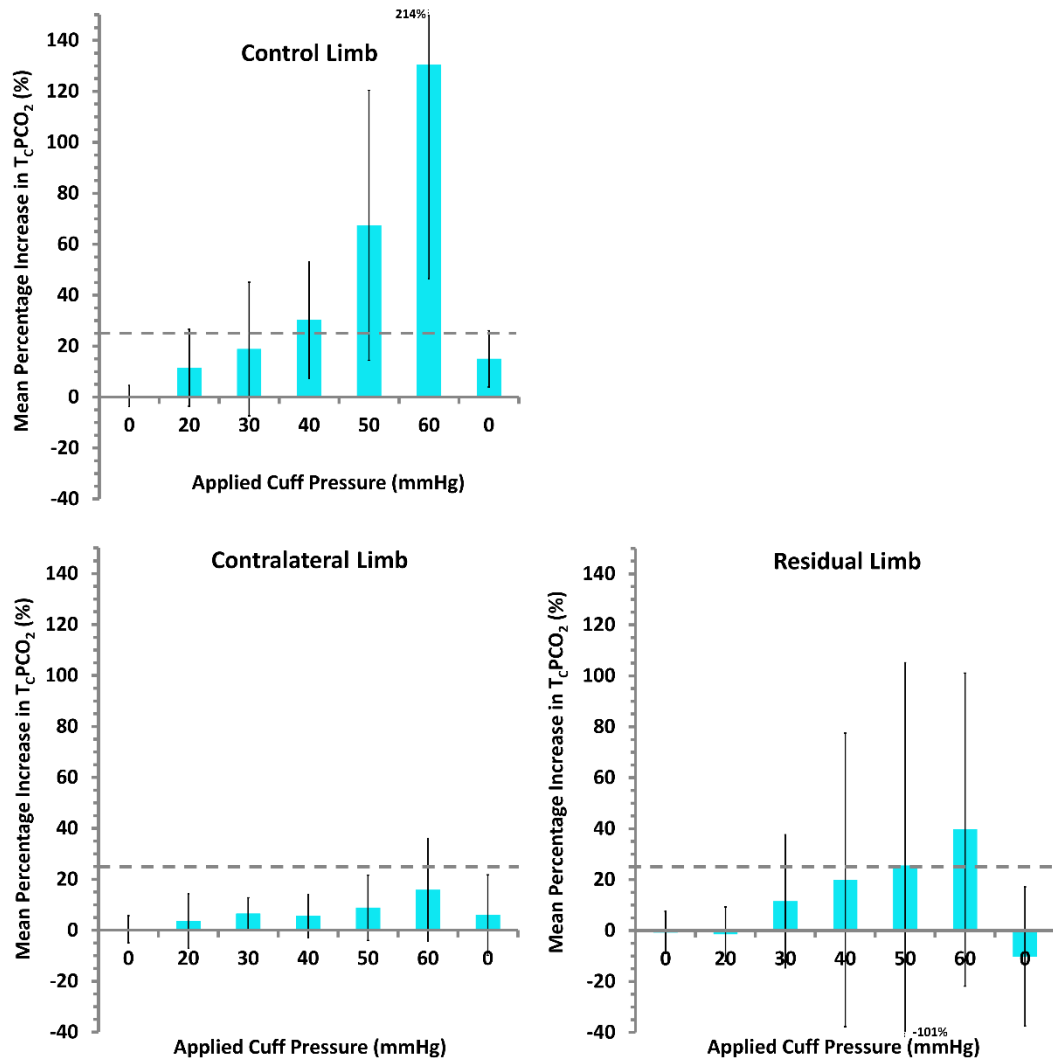


Figure 5.7 The effects of cuff pressure on mean (\pm SD) percentage increase in $T_c\text{PCO}_2$ at the three measurement sites in intact and residual lower limbs. Note: Dashed line at 25% increase indicates Category 3 Ischaemia threshold

Trends across the heterogeneous cohort were evaluated using scatter graphs, to assess correlations between both baseline and percentage changes in T_cPO_2 and T_cPCO_2 under cuff loading, and relevant demographic factors including;

- time since amputation,
- socket use and
- superficial adipose (Figure 5.8 to Figure 5.9).

Varied responses were observed between transcutaneous gas tensions and socket use and superficial adipose percentage (Table 5.2 to Table 5.3). No trends were statistically significant although a positive trend between baseline T_cPO_2 and superficial adipose reached borderline significance (Table 5.2).

Table 5.2 Correlation analysis for A. baseline and B. percentage change at 60 mmHg cuff inflation in oxygen tension (T_cPO_2) at three measurement sites in the right control limbs of ten participants without amputation and the contralateral and residual limbs of ten participants with unilateral transtibial amputation. Note: results displayed as r (p) and green represents a result indicating strong correlation ($r > 0.5$) and bold represents significance ($P < 0.05$)

A

Correlation between baseline T_cPO_2 and:	Limb	Measurement Site		
		Patellar Tendon	Lateral Calf	Posterior Calf
Time Since Amputation	Contralateral	-0.11 (0.77)	0.35 (0.33)	0.57 (0.09)
	Residual	0.84 (<0.01)	-0.15 (0.69)	-0.21 (0.57)
Socket Use	Contralateral	-0.36 (0.30)	0.62 (0.06)	0.12 (0.69)
	Residual	0.17 (0.64)	0.25 (0.48)	0.05 (0.90)
Superficial Adipose %	Control	0.39 (0.27)	0.51 (0.13)	0.03 (0.94)
	Contralateral Residual	-0.15 (0.68)	-0.2 (0.58)	0.19 (0.60)
		0.63 (0.05)	-0.29 (0.41)	-0.33 (0.35)

B

Correlation between percentage decrease in T_cPO_2 at 60 mmHg Cuff Inflation and:	Limb	Measurement Site		
		Patellar Tendon	Lateral Calf	Posterior Calf
Time Since Amputation	Contralateral	0.26 (0.49)	-0.12 (0.75)	0.10 (0.79)
	Residual	0.47 (0.20)	0.08 (0.83)	-0.33 (0.40)
Socket Use	Contralateral	-0.15 (0.69)	0.20 (0.62)	0.09 (0.82)
	Residual	0.10 (0.79)	-0.13 (0.74)	0.12 (0.76)
Superficial Adipose %	Control	-0.37 (0.29)	0.31 (0.38)	-0.02 (0.95)
	Contralateral Residual	-0.06 (0.87)	0.02 (0.97)	0.04 (0.90)
		-0.02 (0.97)	0.14 (0.71)	-0.07 (0.86)

Table 5.3 Correlation analysis for A. baseline and B. percentage change at 60 mmHg cuff inflation in carbon dioxide tension (T_cPCO_2) at the patellar tendon measurement site in the right control limbs of ten participants without amputation and the contralateral and residual limbs of ten participants with unilateral transtibial amputation. Note: results displayed as r (p) and green represents a result indicating strong correlation ($r > 0.5$) and bold represents significance ($P < 0.05$)

A

Correlation between baseline T_cPCO_2 and:	Limb	Measurement Site
		Patellar Tendon
Time Since Amputation	Contralateral	0.17 (0.65)
	Residual	0.07 (0.86)
Socket Use	Contralateral	0.34 (0.33)
	Residual	0.12 (0.75)
Superficial Adipose %	Control	-0.25 (0.50)
	Contralateral Residual	0.37 (0.30)
		0.42 (0.22)

B

Correlation between percentage increase in T_cPCO_2 at 60 mmHg Cuff inflation and:	Limb	Measurement Site
		Patellar Tendon
Time Since Amputation	Contralateral	-0.42 (0.27)
	Residual	0.67 (0.05)
Socket Use	Contralateral	0.49 (0.18)
	Residual	-0.13 (0.73)
Superficial Adipose %	Control	-0.31 (0.39)
	Contralateral Residual	0.15 (0.70)
		0.04 (0.92)

Baseline T_cPO_2 displayed a strong, significant trend with the time since amputation in the residual limb group at the patellar tendon (Figure 5.8, Table 5.2). Indeed, more established limbs (longer period post-amputation) had higher baseline T_cPO_2 values than those that were recently amputated. By contrast, the relationship between percentage loss in T_cPO_2 at 60 mmHg cuff inflation and time since amputation was more variable particularly at shorter times since amputation (Figure 5.8). Variability decreased with time since amputation at the patellar tendon for percentage change in T_cPO_2 (11 to 100 % and 58 to 99 %, for short and long periods post-amputation respectively). Interestingly participants #3A and #6A, who have been observed to be matched in a number of variables including age, amputation cause, time since amputation, socket use and infiltrating adipose percentage (Figure 4.10), also have very similar T_cPO_2 baselines (≈ 62 mmHg) and similar percentage decrease values at 60 mmHg (≈ 92 and 74 %, respectively) (Figure 5.8). However, #6A a female had a much lower T_cPCO_2 increase (-4 %) than #3A (121 %), a male, indicating a greater tolerance in the patellar tendon of #6A (Figure 5.9). Participants #1A and #2A had the lowest basal T_cPO_2 (25 and 17 mmHg respectively) and this corresponded with a near total reduction in T_cPO_2 under load ($\approx 99\%$ decrease) (Figure 5.8). Responses were more varied in contralateral limbs and other residual limb sites with no significant trends.

Percentage change in T_cPCO_2 at 60 mmHg cuff inflation also displayed a borderline significant positive correlation in residual limbs and in contrast to T_cPO_2 loss, variability increased with time since amputation with data appearing to form clear clusters of;

- little increase in T_cPCO_2 for participants who were short times since amputation,
- little increase in T_cPCO_2 for participants with established amputations (#6A, #9A), or
- elevated T_cPCO_2 for participants with established amputation (#3A, #4A) (Figure 5.9).

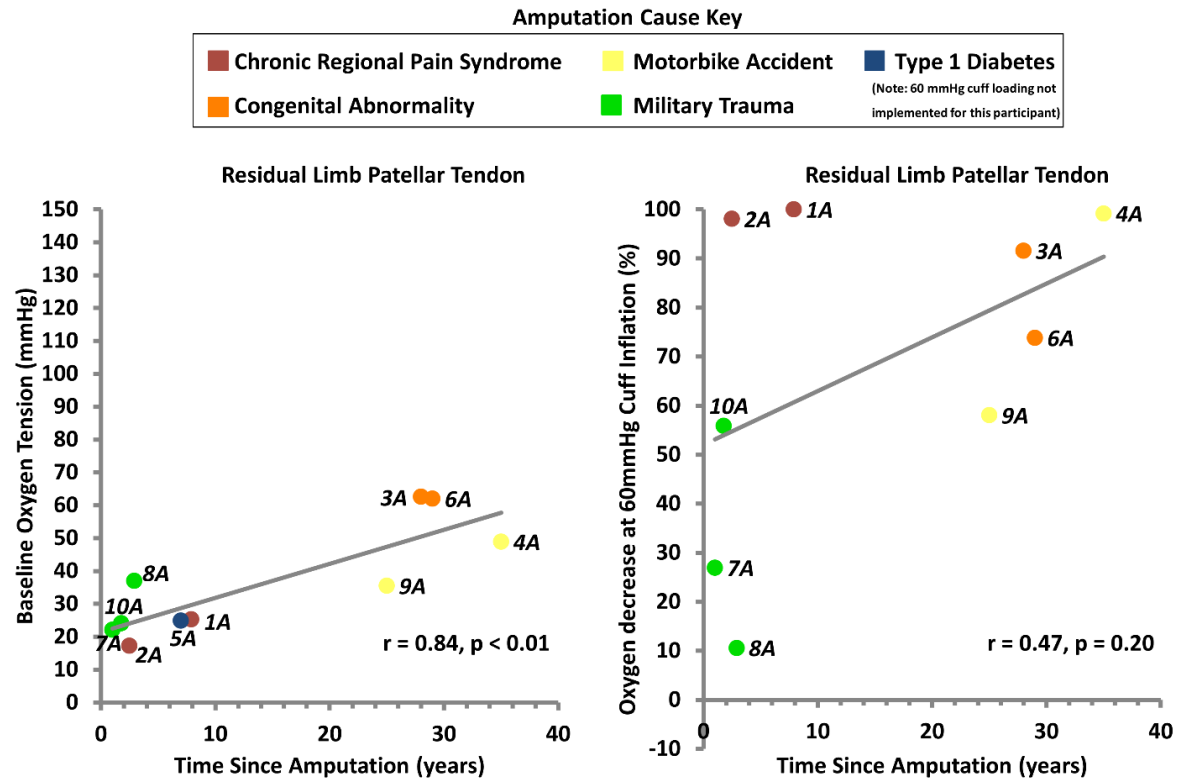


Figure 5.8 Baseline T_cPO_2 (left) and percentage decrease in T_cPO_2 at 60 mmHg cuff inflation (right), against time since amputation for residual limb patellar tendon site of ten participants with unilateral transtibial amputation. NOTE: number represents participant identification

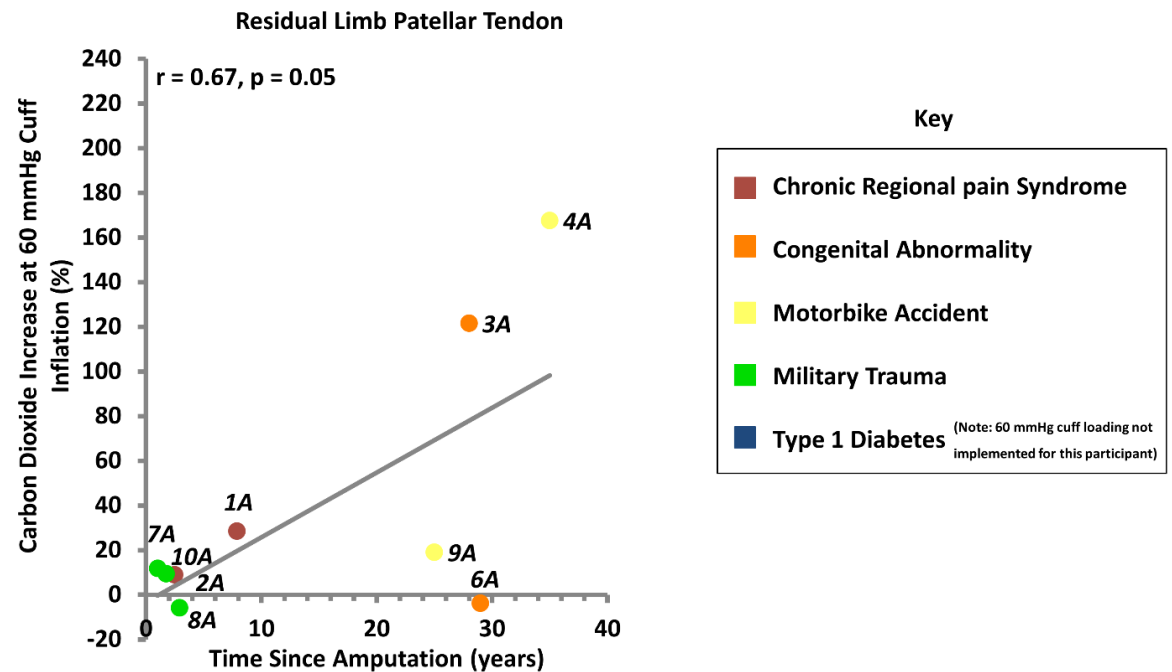


Figure 5.9 Percentage increase in T_cPCO_2 at 60 mmHg cuff inflation against time since amputation for the residual limb patellar tendon site of nine participants with unilateral transtibial. NOTE: number represents participant identification

5.3.3 Inflammatory Response

The cumulative effect from the incremental loading regime up to 60 mmHg resulted in variable increases in the ratios of IL-1 α /TP and IL-1RA/TP across each limb group (Figure 5.10). Similar median percentage increases in IL-1 α /TP ratios were observed in the intact limb groups, with the median at the three measurement sites ranging from 19 to 99 % and 33 to 91 % for control and contralateral limbs respectively. In contrast, it is evident that there were only minimal changes due to cuff loading in the median percentage increase in IL-1 α /TP ratios at the three measurement sites of the residual limb (-3 to 5 %). Similar trends were observed in the median IL-1RA/TP ratio values due to cuff loading. Statistically significant differences between IL-1 α /TP at baseline and post-incremental loading were evident at the patellar tendon for both biomarkers in control limbs ($p < 0.05$), the lateral calf for both biomarkers and posterior calf for IL-1 α /TP in control limbs ($p < 0.05$), and both lateral and posterior calf sites for both biomarkers in the contralateral limb ($p < 0.01$).

No significant differences between conditions were evident for the residual limb group.

Differences were significant at the patellar tendon between control and residual limb groups for both biomarkers ($p < 0.04$).

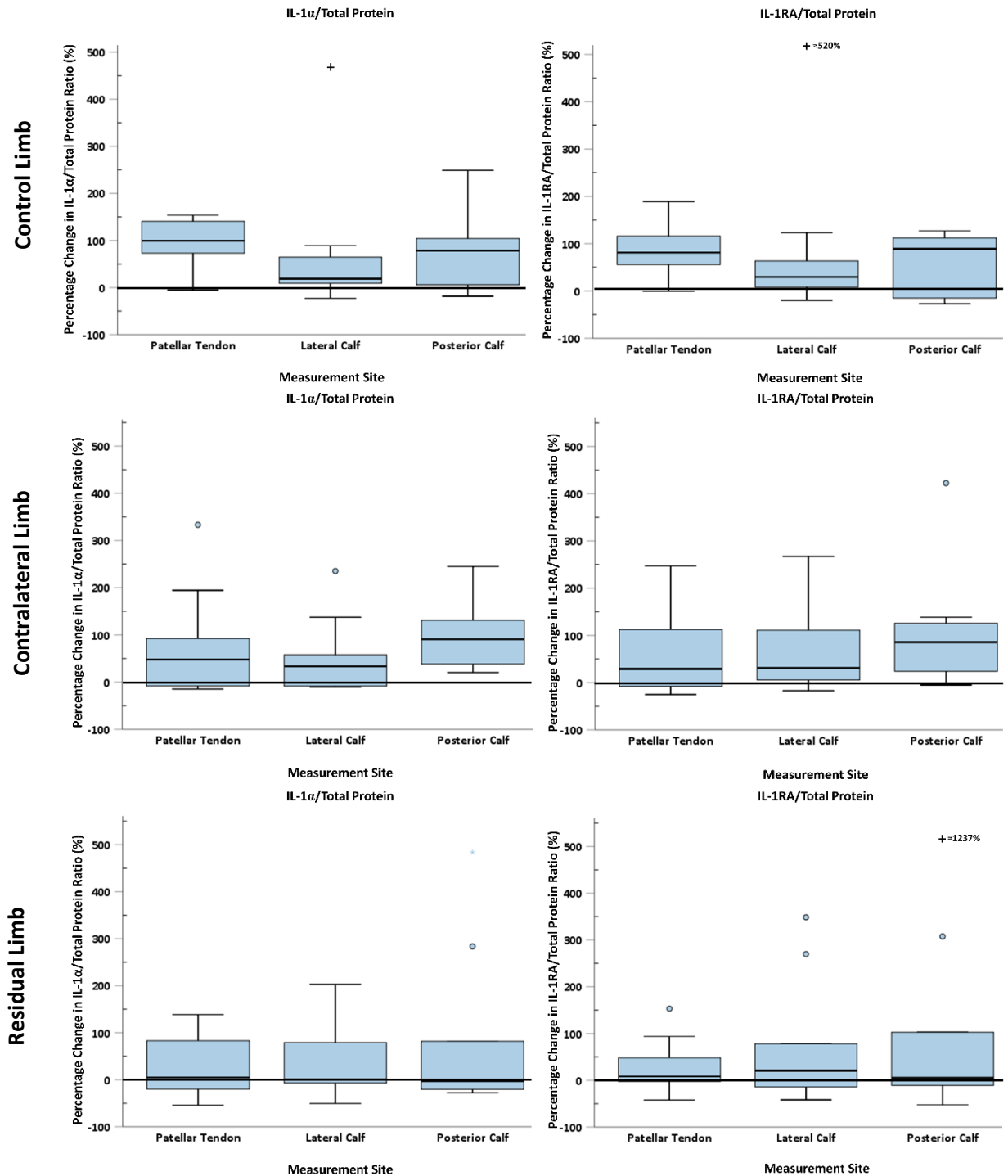


Figure 5.10 Box and whisker plot showing IL-1α/Total Protein (left) and IL-1RA/Total Protein (right) ratios, at three measurement sites on the control limbs of 10 participants without amputation (top) and the contralateral (middle) and residual (bottom) limbs of 10 participants with unilateral transtibial amputation, expressed as a percentage change from baseline resulting from cuff loading at 60 mmHg. Note: ○ and + indicate outliers that are 1.5 and 3 times the Interquartile Range (IQR) respectively

With respect to individual responses, there was an increase in IL-1 α /TP ratio following the cuff

pressure regimen in the majority of cases, namely:

- 9/10 for all sites in control limbs,
- 7/10 at the patellar tendon and lateral calf sites and 9/10 at the posterior calf site in contralateral limbs, and
- 5/10 at the patellar tendon and lateral calf sites and 4/10 at the posterior calf site in residual limbs.

There was considerable variation in magnitude of response between individuals and within measurement sites (Figure 5.11 to Figure 5.13). For example, in control participant #4 (female, aged 36), the post-loading IL-1 α /TP ratio was more than two times the baseline IL-1 α /TP ratio at the patellar tendon and posterior calf, whereas minimal change was observed at the lateral calf.

For the majority of participants without amputation (9/10), there was an increase in IL-1 α /TP ratio in excess of 50 % at the patellar tendon. This response was less consistent at the lateral and posterior calf sites. With respect to IL-1RA/TP ratios, there was a comparable upregulation, although there were again considerable inter- and intra-participant variations (Figure 5.11).

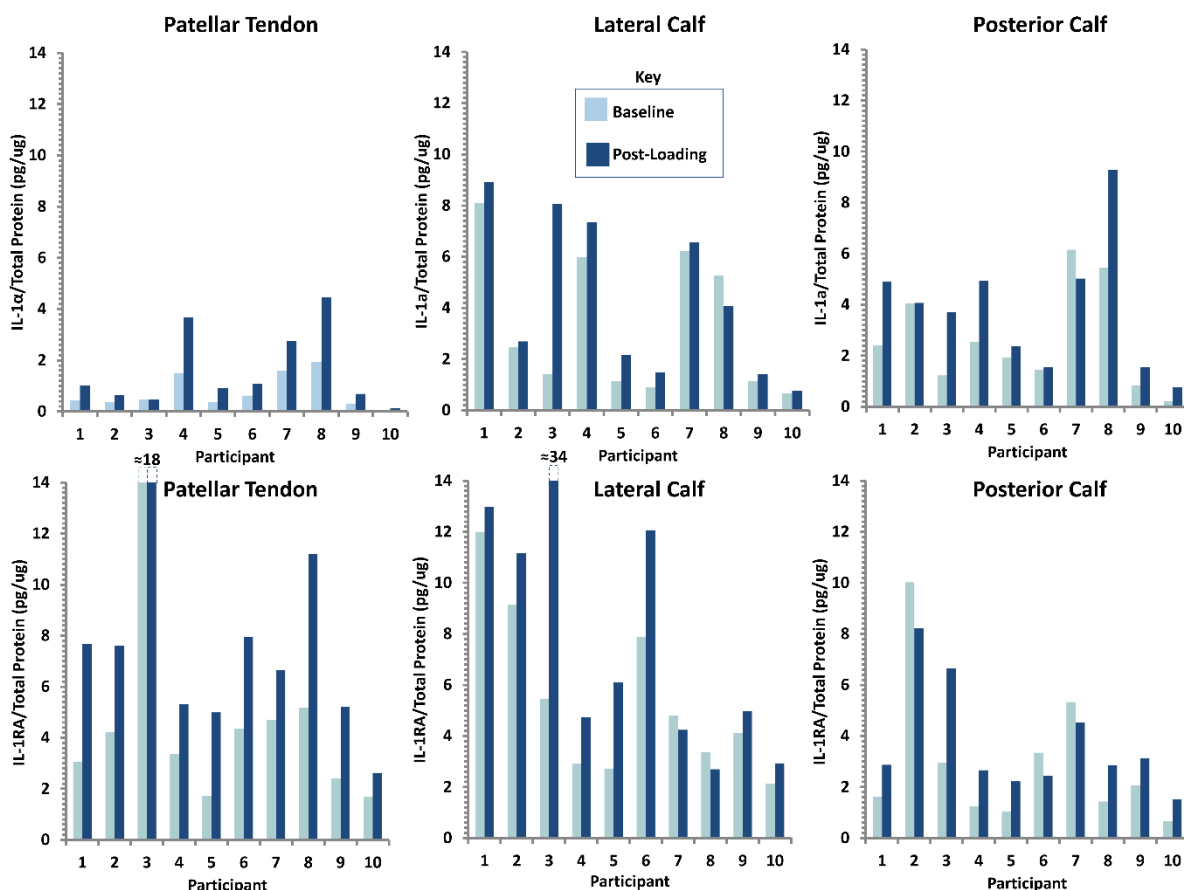


Figure 5.11 IL-1 α /Total Protein (top) and IL-1RA/Total Protein (bottom) ratios, at three measurement sites on the right limbs of 10 participants without amputation, at baseline and following cuff loading up to 60 mmHg

In participants with amputation, the increase in IL-1 α /TP ratio in the residual limb was generally lower than the response at their contralateral limb (Figure 5.12). Indeed, the observed increase in IL-1 α /TP ratio was lower in residual limbs compared to contralateral limbs, in:

- 8/10 cases at the patellar tendon
- 6/10 cases at the lateral calf, and
- 6/10 cases at the posterior calf.

In contrast to the control group (9/10), IL-1 α /TP ratio increases in excess of 50 % were only observed in 5/10 contralateral limbs and 3/10 residual limbs. Interestingly only one individual (#5A) appears in the high-response group for both limbs, potentially showing lower conditioning as an effect of their Type 1 diabetes.

In participants with amputation changes in IL-1RA/TP ratios were mostly comparable to changes in IL-1 α /TP ratios, although as in the control group there was considerable variation in inter- and intra-participant values (Figure 5.13).

December 2020

J.Bramley

Physiological Response

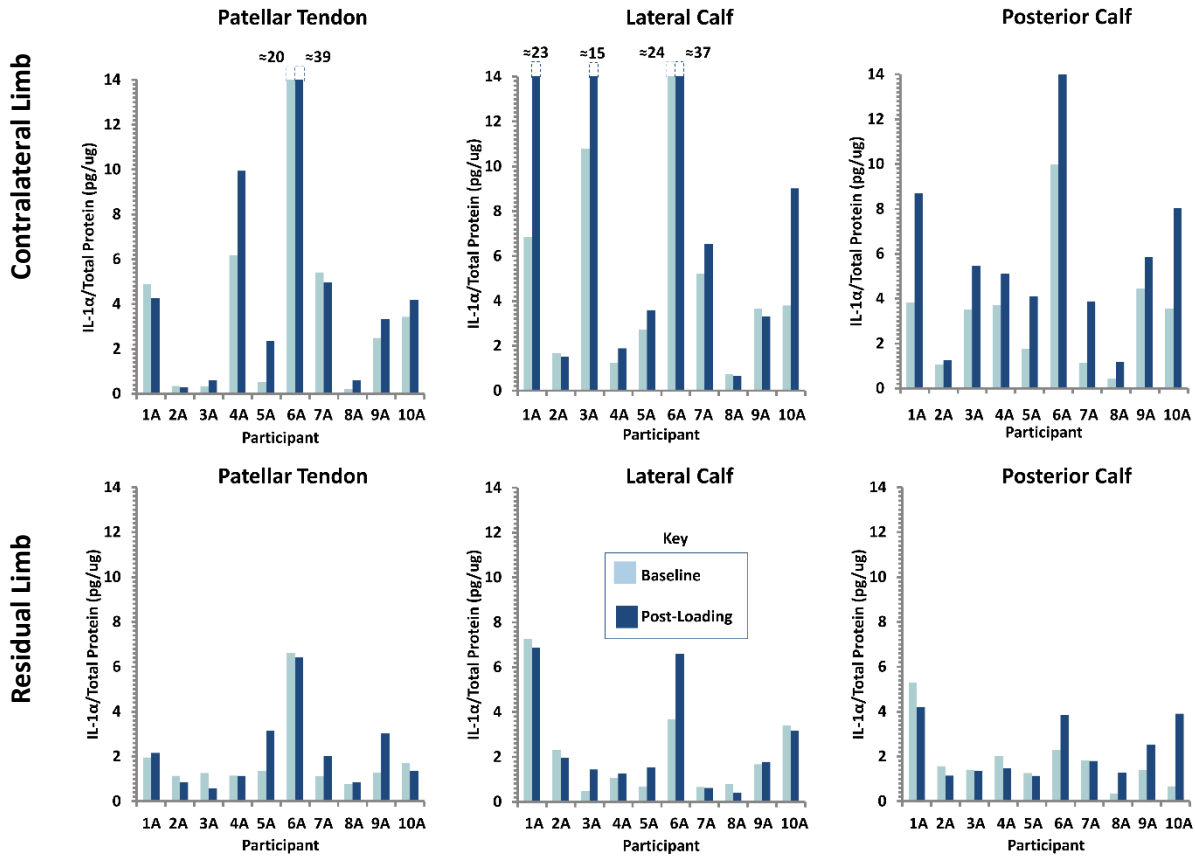


Figure 5.12 IL-1 α /Total Protein ratios, at three measurement sites on the contralateral (top) and residual (bottom) limbs of 10 participants with unilateral transtibial amputation, at baseline and following cuff loading up to 60 mmHg

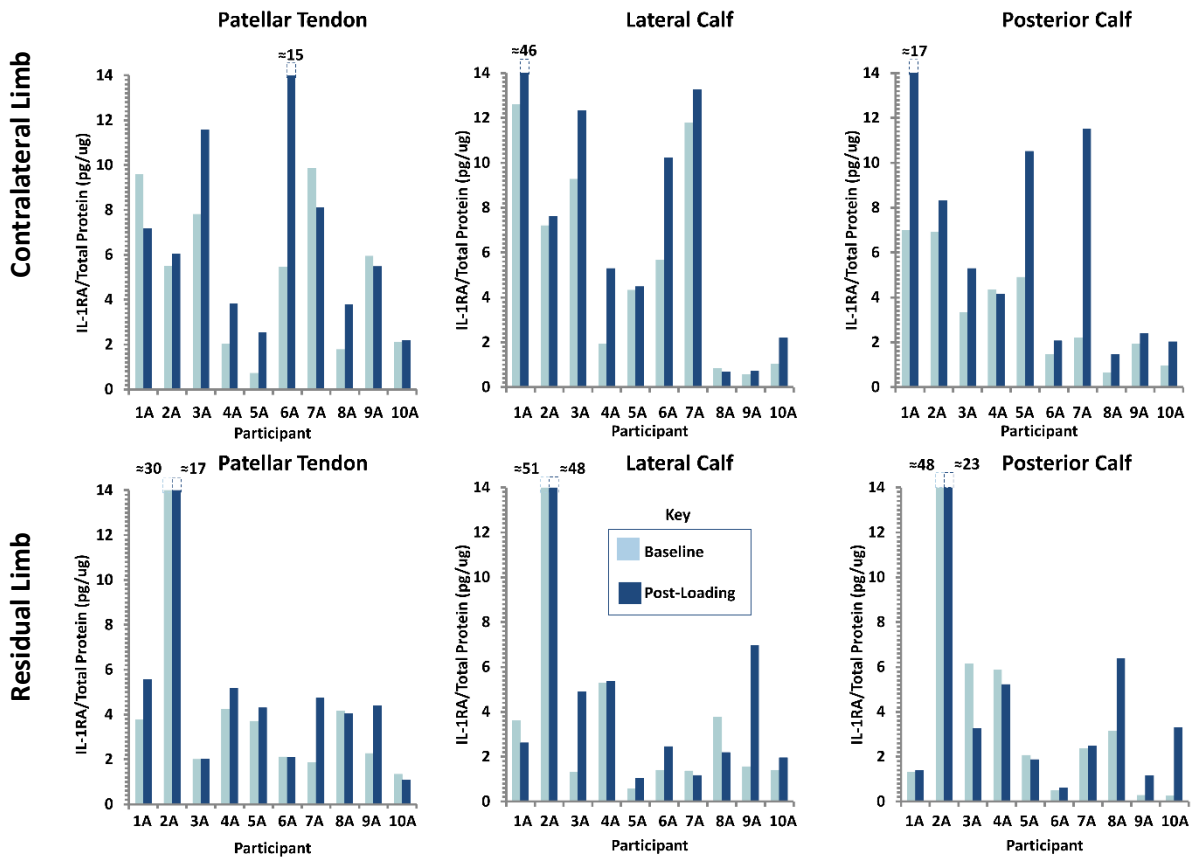


Figure 5.13 IL-1RA/Total Protein ratios, at three measurement sites on the contralateral (top) and residual (bottom) limbs of 10 participants with unilateral transtibial amputation, at baseline and following cuff loading up to 60 mmHg

Trends between the changes in biomarker ratios and demographic factors including; time since amputation, socket use, adipose percentage and percentage change in T_cPO_2 and T_cPCO_2 were evaluated using scatter graphs and correlation analysis. Varied and mostly weak correlations were observed (Table 5.4 to Table 5.5 and Figure 5.14 to Figure 5.17).

Table 5.4 Correlation analysis for percentage change IL-1 α /Total protein at three measurement sites in the right control limbs of ten participants without amputation and the contralateral and residual limbs of ten participants with unilateral trans-tibial amputation. Note: results displayed as r (p) and green represents a result indicating strong correlation (r >0.5) and bold represents significance (P<0.05)

Correlation between Percentage change in IL-1 α /Total Protein and:	Limb	Measurement Site		
		Patellar Tendon	Lateral Calf	Posterior Calf
Time Since Amputation	Contralateral	0.39 (0.26)	0.29 (0.43)	-0.48 (0.16)
	Residual	-0.12 (0.75)	0.69 (0.03)	-0.33 (0.35)
Socket Use	Contralateral	-0.30 (0.40)	-0.06 (0.87)	-0.31 (0.39)
	Residual	-0.38 (0.27)	0.26 (0.46)	-0.54 (0.11)
Superficial Adipose %	Control	0.18 (0.63)	0.46 (0.19)	0.08 (0.83)
	Contralateral	-0.22 (0.53)	0.82 (<0.01)	0.08 (0.83)
Infiltrating Adipose %	Residual	-0.30 (0.41)	0.29 (0.43)	0.47 (0.17)
	Control	-0.07 (0.84)	-0.27 (0.45)	0.44 (0.21)
T_cPO_2 % Change	Contralateral	0.43 (0.22)	0.28 (0.43)	0.10 (0.78)
	Residual	0.28 (0.43)	0.51 (0.14)	-0.20 (0.58)
T_cPCO_2 % Change	Control	0.14 (0.70)	0.23 (0.52)	0.41 (0.24)
	Contralateral	-0.38 (0.31)	0.11 (0.78)	-0.44 (0.24)
	Residual	-0.38 (0.31)	0.06 (0.88)	0.41 (0.27)
	Control	-0.01 (0.99)	T_cPCO_2 not measured at this site	T_cPCO_2 not measured at this site
	Contralateral	-0.94 (<0.01)		
	Residual	-0.06 (0.88)		

Table 5.5 Correlation analysis for percentage change IL-1RA/Total protein at three measurement sites in the right control limbs of ten participants without amputation and the contralateral and residual limbs of ten participants with unilateral transtibial amputation. Note: results displayed as r (p) and green represents a result indicating strong correlation (r >0.5) and bold represents significance (P<0.05)

Correlation between Percentage change in IL-1RA/Total Protein and:	Limb	Measurement Site		
		Patellar Tendon	Lateral Calf	Posterior Calf
Time Since Amputation	Contralateral	0.37 (0.29)	0.44 (0.20)	-0.56 (0.09)
	Residual	0.16 (0.65)	0.43 (0.21)	-0.18 (0.63)
Socket Use	Contralateral	-0.02 (0.95)	0.04 (0.91)	-0.13 (0.72)
	Residual	-0.06 (0.87)	0.02 (0.96)	-0.63 (0.05)
Superficial Adipose %	Control	-0.09 (0.82)	0.33 (0.35)	0.09 (0.80)
	Contralateral	-0.30 (0.41)	0.84 (<0.01)	0.13 (0.73)
Infiltrating Adipose %	Residual	0.10 (0.78)	0.24 (0.51)	0.42 (0.23)
	Control	-0.18 (0.62)	-0.33 (0.36)	0.23 (0.53)
T_cPO_2 % Change	Contralateral	0.22 (0.54)	0.14 (0.70)	-0.07 (0.84)
	Residual	0.28 (0.43)	0.31 (0.38)	0.15 (0.69)
T_cPCO_2 % Change	Control	0.21 (0.56)	0.54 (0.10)	0.86 (<0.01)
	Contralateral	-0.07 (0.87)	0.10 (0.79)	-0.25 (0.51)
	Residual	0.03 (0.93)	0.24 (0.54)	0.03 (0.95)
	Control	0.22 (0.54)	T_cPCO_2 not measured at this site	T_cPCO_2 not measured at this site
	Contralateral	-0.79 (0.01)		
	Residual	0.54 (0.13)		

At the residual limb lateral calf there was a significant trend of greater inflammatory response with increasing time since amputation, contrasting to the weak negative trends observed at the other residual limb sites (Figure 5.14). It was observed that some correlation values were influenced by a sub-set of participants. For example, #10A and #8A skewed the data in the posterior calf to create a negative correlation between IL-1 α /TP and time since amputation (Figure 5.14). Likewise, the lateral calf trend seems to be influenced by cases #3A, #6A and #5A.

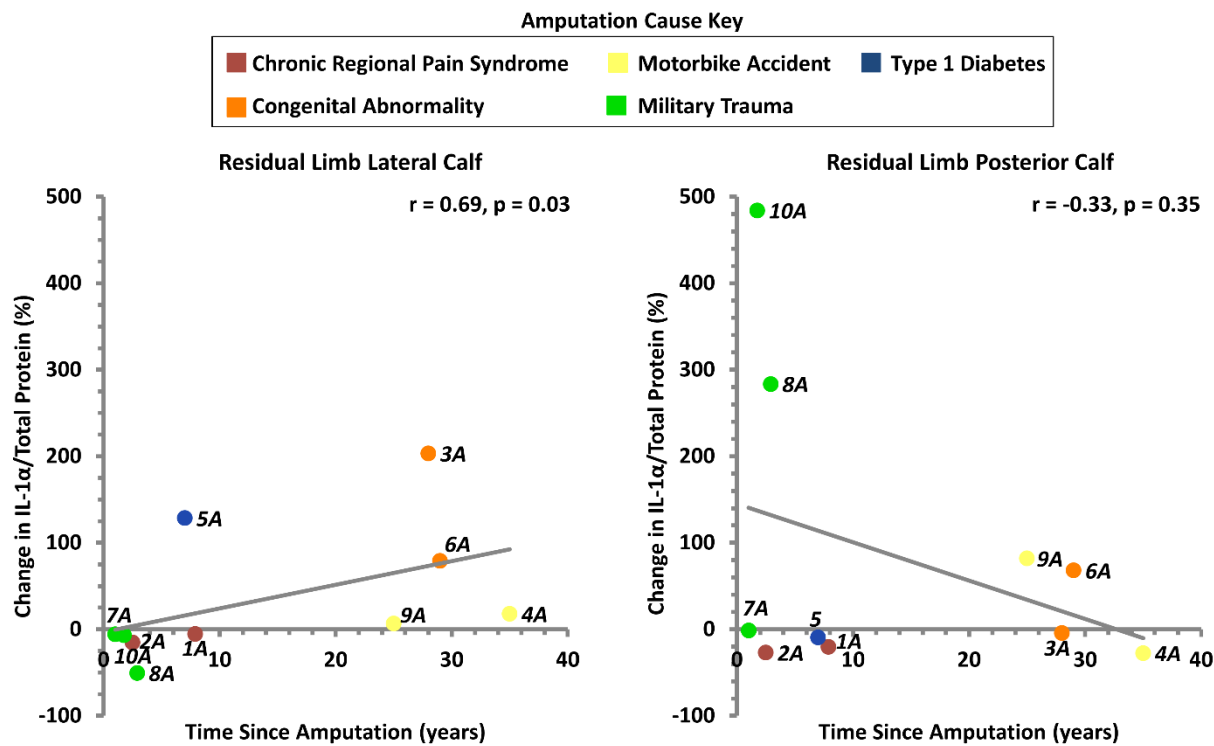


Figure 5.14 Percentage change in IL-1 α /Total Protein against time since amputation for the lateral (left) and posterior (right) calves of the residual limbs of ten participants with unilateral transtibial amputation

There was general trend of a lower percentage increase in IL-1 α /TP with higher socket use particularly at the posterior calf, but these trends were not significant (Table 5.4). This trend was also observed with percentage increase in IL-1RA/TP at the posterior calf of residual limbs, with borderline significance (Table 5.5, Figure 5.15). Again, it appears that the high percentage change observed in #10A is influencing the trend however the same overall tendency would remain without that participant (Figure 5.15).

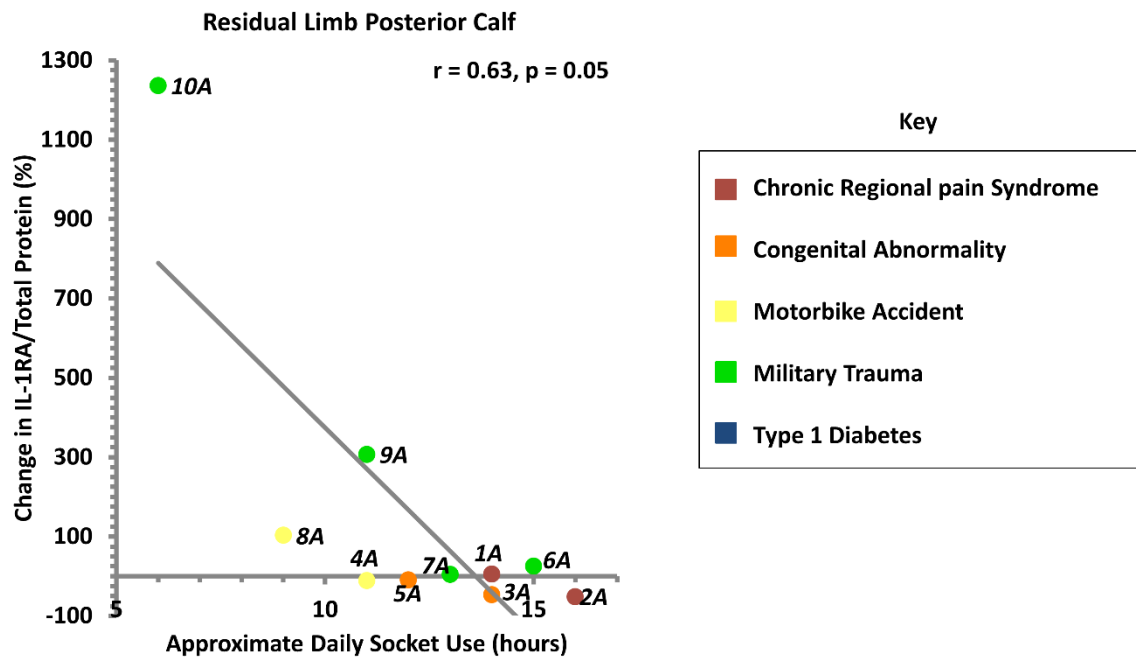


Figure 5.15 Percentage change in IL-1RA/Total Protein against approximate daily socket use for the residual limb posterior calf of ten participants with unilateral transtibial amputation

A tendency of increasing inflammatory response with increased percentage of superficial adipose tissue was observed in both calf sites for all groups, though very weak in the posterior calves of intact limbs (Table 5.4 to Table 5.5). This trend was significant in contralateral limbs at the lateral calf site (Figure 5.16). This trend was also observed, but was generally less apparent, with infiltrating adipose particularly at the residual limb lateral calf and the posterior calf site for both intact limb groups (Table 5.4 to Table 5.5).

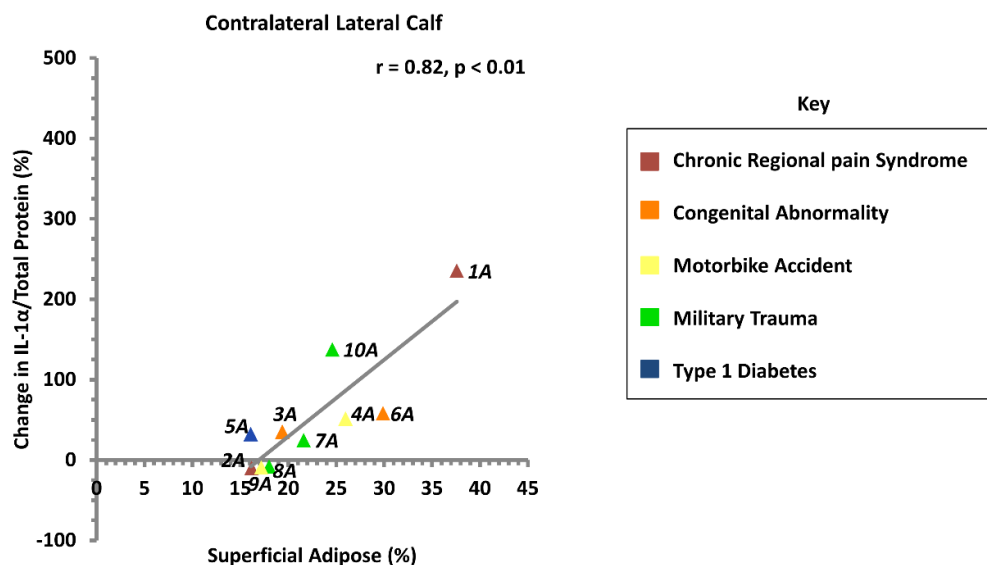


Figure 5.16 Percentage change in IL-1 α /Total Protein against superficial adipose for the contralateral limb lateral calf of ten participants with unilateral transtibial amputation

In contralateral and residual limbs there was a clear, significant trend of decreasing inflammatory response with higher percentage increase of T_cPCO₂ from basal values reaching significance in the contralateral limb group, indicating differences between ischaemic and inflammatory responses (Figure 5.17).

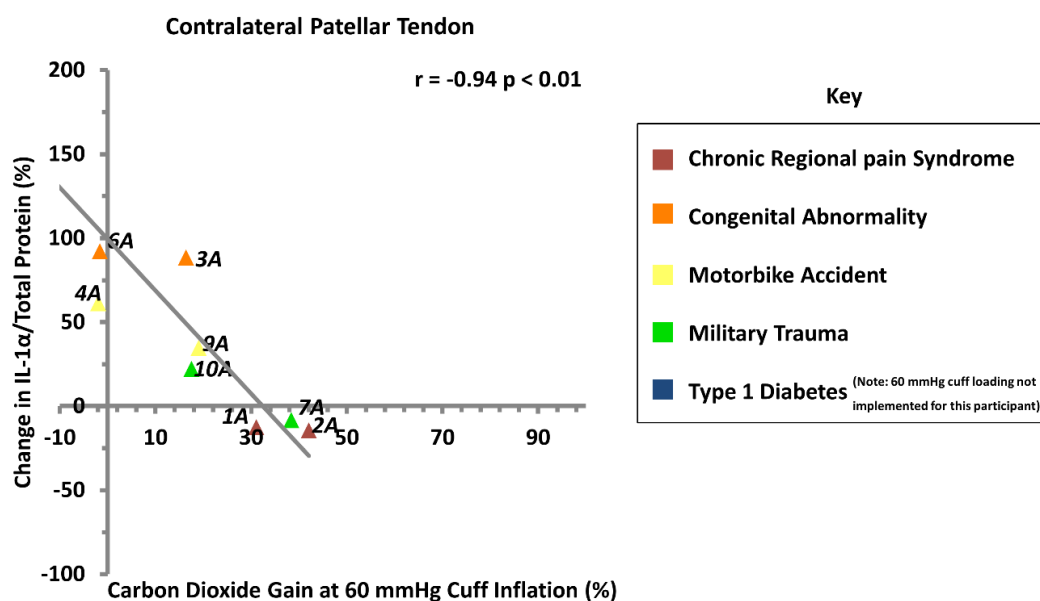


Figure 5.17 Percentage change in IL-1 α /Total Protein against carbon dioxide increase at 60 mmHg cuff inflation for the contralateral patellar tendon site of ten participants with unilateral transtibial amputation

5.4 Discussion

This protocol was designed to establish a measurement array and associated test protocol to assess tissue tolerance at the residual limb-socket interface to elicit further understanding of how soft tissues respond during prosthetic loading. This was achieved through the application of a pressure cuff up to 60mmHg (8.0 kPa) over a 60 minute period. Corresponding tissue physiology parameters were observed to produce a transient compromise in viability, as reflected in local ischaemia and an upregulation of inflammatory biomarkers. This demonstrated the potential of the protocol to distinguish between unloaded and loaded conditions and investigate tissue tolerance. The protocol was observed to detect similar tissue changes in both intact and residual limbs, and a generally lower percentage change in ischaemic and inflammatory biomarkers in residual limbs suggested a greater tolerance to loading (Figure 5.4 to Figure 5.7 and Figure 5.10).

5.4.1 Measurements and Analysis

Pressure cuff loading up to 60 mmHg (8 kPa) occluded microvascular vessels by applying an approximately hydrostatic pressure on the limb. Although not representative of a more focally-rectified socket, this loading is characteristic of a total surface bearing socket or rehabilitation device. In particular, the PPAM Aid has been estimated to apply interface pressures at the distal residuum ranging from 4 to 95 mmHg, with a median of 26 mmHg during standing (0.5 to 13.0 kPa, median 3.5 kPa) [53]. This is comparable to interface pressures measured in this study ranging from 66 to 84 mmHg (8.8 to 11.2 kPa). In the test setup, the presence of the transcutaneous gas electrodes caused local internal shear strain as would be predicted when rectified socket designs are used (Section 4.3.4).

Ischaemic trends were observed following incremental loading at the patellar tendon, where a Category 3 response was measured in 8/10 control limbs, 5/10 contralateral limbs and 3/10 residual limbs (Figure 5.3 to Figure 5.5). Close examination of the demographic data (Table 4.2) revealed no discernible demographic reason for two participants without amputation to demonstrate a Category 2 response at a cuff inflation of 60 mmHg (Figure 5.4). Participant #9 was a female aged 28 with a BMI of 23.5 kg/m² and maximum calf circumference of 360 mm, and #10 was a male aged 23 with a BMI of 25.0 kg/m² and maximum calf circumference of 410 mm. They may have both had the highest maximum calf circumference observed for females and males respectively. However, other participants who demonstrated a Category 3 response also had the same calf circumference. A smaller percentage of the cohort demonstrated a Category 3 response at the patellar tendon in the residual limbs, suggesting biomechanical adaptation over the period post-amputation, which ranged from 1 to 36 years in this heterogeneous cohort.

A strong significant correlation was observed between both decrease in T_cPO_2 and increase in T_cPCO_2 and applied cuff pressure (Figure 5.6 and Figure 5.7). This indicates that the selected incremental pressure range was suitable to elicit appropriate precursors to ischaemia as reflected in maximum reduction in T_cPO_2 at the highest cuff pressure of 60 mmHg (8 kPa). The body has a natural response, known as Pressure-Induced Vasodilation (PIV) where cutaneous blood flow is increased to maintain oxygenation under low pressure loading [264]. Indeed, at lower cuff pressures a number of participants in this study showed partial recovery in T_cPO_2 between loading increments, demonstrating some vascular adaptation to load [265] (Figure 5.3). Individuals with amputation in this study could have been demonstrating an adapted PIV response, whereby they can withstand mechanical loads of greater magnitude or duration. A T_cPO_2 reduction >75% was observed in all locations for 7/10 in the control group, but only in 3/9 and 2/9 for the contralateral and residual limb groups (Figure 5.6). Equivalent responses have been observed using indenters and liner application on calf tissues of participants with and without amputation [82, 210]. The former study reported mean surface pressure values at the calf that to reduce T_cPO_2 to 0 mmHg of 71 ± 16 mmHg and 42 ± 8 mmHg over muscle and skin over bone, respectively [210]. In the present study, generally lower pressures were required to reduce T_cPO_2 at the patellar tendon site, an area of reduced soft tissue coverage compared to the calf sites (Figure 5.6).

Baseline T_cPO_2 in healthy individuals is thought to range from approximately 48 to 95 mmHg [79-81, 215]. However, T_cPO_2 lower than 48 mmHg has been recorded in both the present study and in previous research examining transtibial limbs of participants without co-morbidities [82] (Figure 5.2). It is of note that in past clinical studies, tissue sites which yielded T_cPO_2 levels below approximately 35 mmHg were observed to be at risk of poor healing post-amputation and those below 15 to 20 mmHg were observed to be at risk of incomplete healing [76-78, 81, 217, 266]. In the present study, several participants from each group had baseline T_cPO_2 values <35 mmHg, mostly with no discernible demographic reasons, suggesting caution should be used when employing these simple thresholds for clinical decision making. Participants #5A and #10A were the only two individuals with amputation to have baseline values <35 mmHg recorded at their contralateral limb as well as residual limb. Close examination of their demographics revealed that this might be explained by #5A presenting with Type 1 diabetes which is known to lead to impaired vascularity and #10A having the highest BMI (37.5 kg/m^2) value [30].

Reduced residual baseline values could indicate tissue adaptation from socket loading. Indeed, plantar heel tissue is adapted for load bearing and its thicker, stratum corneum has been observed to result in lower and more inaccurate T_cPO_2 measurements [80, 267]. As the patellar tendon is a common site for prosthetic load bearing it could have adapted in a similar way to heel tissue producing the lower baseline T_cPO_2 values observed (Figure 5.2).

Rink et al also observed lower mean baseline T_cPO_2 measurements in participants with transtibial amputation ($57.8 \pm SE 9.2$ mmHg) compared to participants without amputation ($79.5 \pm SE 7.4$ mmHg) [82].

In the present study as well as baseline T_cPO_2 measurements <35 mmHg, baseline values >95 mmHg were observed in several participants with amputation (Figure 5.2). Values exceeding physiological limits were thought to be caused by measurement errors such as the electrode becoming detached, excess hairs at the test site effecting electrode fixation and a malfunctioning electrode.

High variability of both baseline and percentage changes in T_cPO_2 and T_cPCO_2 measurements was observed particularly when measured at the residual limb (Figure 5.2 to Figure 5.7), potentially due to factors such as time since amputation, socket use, cause of amputation and comorbidities. Indeed, variability of T_cPO_2 measurements was observed to decrease with time since amputation suggesting both recovery and adaptation under prosthetic loading (Figure 5.8). However, clusters of individuals with established amputations and both high and low T_cPCO_2 increase were observed, indicating that a diverse range of factors affect ischaemic response (Figure 5.9).

Adipocytes are highly vascularised so it may be expected that tissues with increased adipose may have higher baseline T_cPO_2 and a more sensitive ischaemic response to loading [257]. However, only insignificant trends of increased baseline measurements with superficial adipose were observed at the patellar tendon of residual limbs and lateral calf of control limbs (Table 5.2).

Regarding the inflammatory cytokine measurements, IL-1 α /TP increased significantly post-loading for control limbs at all sites and contralateral limbs at both calf sites (Figure 5.10). Similar changes have also been observed during the application of different medical devices, including respiratory masks [138], cervical collars [139] and spinal boards [140]. Conversely, smaller IL-1 α /TP changes (median -3 to 5 %, IQR 70 to 96 across all sites) were observed in residual limbs, indicating a suppressed inflammatory response to the same loading conditions. Large variability was observed between and within participant responses with percentage change in IL-1 α /TP ranging across all sites from -23 to +470 %, -15 to +333 % and -54 to +484 % in control, contralateral and residual limb groups respectively (Figure 5.10 to Figure 5.12). Measurement site and environment have been shown to influence biomarker upregulation [244], although in the present study sampling was performed at a consistent location in a laboratory environment. Furthermore, the variability in biomarker expression is more likely a result of the differences between individuals and their respective physiological response to the applied loads. Similar variability in response has been reported in other studies, with distinct sub-populations of healthy cohorts demonstrating both high and low inflammatory responses [139, 206, 224].

The susceptibility to inflammation is worthy of further investigation, in conjunction with an examination of the temporal trends of inflammatory biomarker expression, regarding both pro-inflammatory and antagonistic cytokines [140, 224, 268]. Similar trends were observed in percentage change in IL-1RA/TP ratio, which increased significantly at two sites in both control (patellar tendon and lateral calf sites) and contralateral (lateral and posterior calf sites) limbs (Figure 5.10, Figure 5.12 and Figure 5.14). The ratio of IL-1RA to IL-1 α is considered to reflect homeostatic regulation against inflammation [227, 228] and the comparable biomarker responses observed in this study indicate a balanced inflammatory response, expected from healthy tissues. Elevated levels of IL-1RA have been observed in diabetic participants in previous research [269]. However, this was not observed in the present study's participant #5A, who has Type 1 Diabetes (Figure 5.13). Close examination of individual responses showed elevated changes in IL1-RA/TP compared to IL-1 α /TP at patellar tendon and posterior calf residual limb measurement sites for #2A, indicating an imbalanced inflammatory response (Figure 5.12 to Figure 5.13). The release of both IL-1 α and IL-1RA is time-dependent and further knowledge of the temporal aspects will help understanding of the body's inflammatory response. Furthermore, although IL-1 α is sensitive to mechanical loading it can also be released in response to a number of other stimuli so has limited specificity. Previous research suggests that analysis of IL-1 α in conjunction with secondary inflammation mediators, such as IL-8 or IL-6, could provide more specific detection of inflammation due to loading [138].

Hair removal was implemented via shaving at least 48 hours in advance of testing sessions to avoid an upregulation of pro-inflammatory cytokine due to its associated mechanical irritation [245]. However, participant #8A did not want to risk ingrown hairs by hair removal and participants #2A and #3A required further hair removal for contralateral posterior and residual lateral calf sites, and all contralateral limb sites respectively, on arrival for the testing sessions. This may have affected inflammatory response results and caused an upregulation of the biomarkers. However, results at these shaved sites were comparable to other sites on the same and other participants that were not shaved immediately prior to testing (Figure 5.12 to Figure 5.13). Baseline levels of IL-1 α /Total Protein ratio are quite low for both limbs of #8A potentially due to hair impeding the uptake of sebum on the Sebutape (Figure 5.12).

Varied trends were observed between inflammatory response at residual limb sites and time since amputation (Table 5.4 to Table 5.5 and Figure 5.14). The observed residual limb trends were being influenced by a few cases with high inflammatory responses, namely #3A, #6A and #5A at the lateral calf. Individuals #3A and #6A have the same amputation cause and are both able to weight bear on their residuum end, potentially resulting in less socket loading at the lateral calf and therefore less tolerance. #5A is the only participant not grouped with the other short time since amputation cases, potentially due to this individual's co-morbidity of Type 1 diabetes.

At the posterior calf it appears that particularly case #10A influenced the trend and this participant could be less tolerant due to mainly wheelchair use for mobility. Inflammatory response was generally more variable between individuals with a shorter time since amputation, potentially due to factors such as cause of amputation affecting the amputation procedure itself and trauma to the soft tissues as well as personal factors such as co-morbidities and mobility. A pattern of lower percentage increase in both biomarkers was observed particularly in the posterior calf of residual limbs (Table 5.5, Figure 5.15). This trend is intuitive as increased socket use would be likely to lead to more tolerant tissue and it also corresponds with the observation of decreased infiltrating adipose with increased socket use (Figure 4.10).

There was a tendency of increased inflammatory response with higher percentage of adipose, particularly superficial adipose (Table 5.4 to Table 5.5 and Figure 5.16). Previous research suggests elevated markers of inflammation with increased adipose infiltrating muscle [196, 254]. However, markers studied include IL-6 and TNF- α , which have not been analysed in this research. Ratios of IL-6 and TNF- α have been analysed pre- and post-loading in previous research, but IL-6 revealed less consistent trends than IL-1 α [138], and a significant increase in TNF- α was only evident after the onset of structural tissue damage [223].

Monitoring cytokine response would enable assessment of applied loading. Such an approach would be both difficult to achieve and expensive in the clinical setting, using currently available devices but there is a potential for low cost devices to be developed offering point of care biomarker analyses. Indeed there are current developments with lab-on-a-chip technologies to produce cheaper and quicker solutions that could, even if not suitable for real-time analysis, be translated to the clinic and indicate tissue health post-prosthetic loading to help inform future use [142].

The inflammatory and ischaemic tissue tolerance marker responses at 60 mmHg (8.0 kPa) cuff inflation were compared (Table 5.4 to Table 5.5). In contralateral and residual limbs with lower inflammatory response, greater T_cPCO₂ gain was observed (Figure 5.17). It is important to note these are two different measurement techniques and the body's temporal response will differ for both. However, generally a lower percentage increase in T_cPCO₂ and lower inflammatory response were observed in residual and contralateral limbs compared to control limbs, indicating greater tolerance to loading for participants with amputation (Figure 5.4 to Figure 5.8 and Figure 5.10).

5.4.2 Limitations

The small sample size ($n = 10$ for each limb group) limited generalisations. However, the sample heterogeneity enabled increased insight into tissue composition and tolerance post-amputation with a range of amputation causes and time since amputation. Static pressure cuff loading was applied to the limbs of participants and cyclic loading may be more relevant to tissue damage during daily living activities with lower limb prosthetics. However, static loading provided a suitable starting point to further understand tissue tolerance using in-depth measurement tools in a controlled environment. Indeed, Soetens et al [224] observed a significant change in inflammatory response upon loading and load removal at the sacrum, for both continuous and intermittent loading regimens. Further research is required to establish whether cyclic loading will increase the damage risk compared to static pressures in amputees [145] or, in some cases, provide a pumping mechanism to enhance vascular flow to the tissues [224]. The applied pressures were not randomised, as this would have required additional refractory periods in order to avoid effects from prior loading cases. Furthermore, incremental loading enabled a risk mitigation strategy to stop the protocol in case of concerns around a participant's loading tolerance prior to 60 mmHg, which was used in the case of #5A who had sensory impairment.

In this study the participants' limbs were in a supine position supported by foam cushions so vascular flow would have been less affected by gravity. However, studies utilising both seated and supine participant positions have also observed varying ischaemic responses between and within participants, studying both support surfaces and prosthetic devices [82, 210, 212, 215]. The inflammatory response in this study is an accumulation of the pressures, time and materials interacting with the skin. Distinguishing between these factors was beyond the scope of this PhD.

5.4.3 Summary

For the first time an array of measurement techniques has been implemented to characterise both the ischaemic and inflammatory response of healthy calf and residual limb soft tissues under representative prosthetic loading. Results demonstrate the potential of transcutaneous gas and inflammatory biomarker measurement for early detection of precursors to tissue damage, with representative static prosthetic loading causing temporary local tissue ischaemia and an upregulation of inflammatory biomarkers released from the skin surface. Reduced response to loading generally observed in residual limbs provides insight into residuum tissue adaptation and the presented data would support a hypothesis that this group presented with an increased tolerance to loading.

This research indicates that establishing standard thresholds for tissue health may prove problematic due to the large variability in transcutaneous and biomarker responses, even in a control cohort without amputation (Figure 5.6). This diverse response has also been observed in previous studies in participants without amputation and with amputation in the case of transcutaneous measurements [80, 82, 139, 206, 212, 215, 224]. A larger cohort of participants with amputation, including a range of times since amputation and causes, would help to further explore general trends in parameters of tissue viability and potentially determine tissue tolerance leading to identification of individuals who may be at higher risk of tissue damage. A simple power analysis was carried out using data from this research to estimate the approximate cohort size required when further investigating tissue tolerance between residual and intact limbs using transcutaneous gas and inflammatory response measurements. The following equation was used:

$$\text{Sample size } (n) = \frac{2K}{\Delta^2}$$

Where:

K = 7.85, derived from a level of significance (α) of 0.05 and the intended power of the test (80%)

Δ = effect size/variability

The difference between the residual limb mean and intact limb mean was used for effect size and mean standard deviation was used to define variability. This resulted in a required sample size of 139 for each group, residual and intact limb (Table 5.6).

Table 5.6 Effect size and variability for power analysis to determine approximate sample size required for transcutaneous gas and inflammatory response measurements

Measurement	Effect Size	Variability	≈ Required Sample Size
% Change in T _c PO ₂ decrease	16 %	26 %	42
% Change in IL-1 α /TP	32 %	95 %	139

These future studies are also needed to establish the presented non-invasive methods appropriately for use in clinical and community settings to monitor both the mechanical boundary conditions between the residual limb and socket, as well as the status of tissues. Stratifying such cohorts will also help to determine factors that increase susceptibility to tissue damage at the residual limb-socket interface.

6 Overall Discussion

This research presents the development and implementation of an experimental protocol to characterise residual limb soft tissues after amputation, both in terms of their biomechanical adaptation and their physiological response to loading. Further quantitative knowledge to characterise the temporal profile of adaptation in residual limb soft tissues and the resulting tolerance to prosthetic loading is required to inform rehabilitation protocols and minimise the risk of tissue damage. The novelty of this research is in the critical appraisal of an array of measurement techniques to provide detailed insight into tissue tolerance at the loaded tissue-socket interface.

6.1 Achievement of Research Aim & Objectives

A schematic of this research summarising achievements is indicated in Figure 6.1. Objective 1 was achieved through the development of a protocol implementing loading via a pressure cuff representative of what might be experienced during early prosthetic rehabilitation using a device such as the PPAM aid [53].

To achieve objective 2 a literature review was carried out for the selection of measurement tools based on critical appraisal. The developed protocol combined MRI and an array of tools to characterise skin and underlying soft tissue parameters to assess the response to representative prosthetic loading. Use of a carefully selected MRI protocol to produce fat saturated images enabled visualisation and robust quantification of both superficial adipose and adipose infiltrating muscle allowing differences in tissue composition post-amputation and between residual and intact limbs to be explored. The MyotonPro™ device, used for the first time at transtibial residual limb sites, enabled comparison of structural stiffness. T_cPO_2 and T_cPCO_2 measurement and collection of inflammatory biomarkers, used in combination for the first time on contralateral and residual limbs in a cohort of participants with amputation under representative loading, enabled evaluation of ischaemic and inflammatory response to loading.

To complete objectives 2 and 3 the protocol was successfully implemented first with the right lower limbs of a control cohort of participants without amputation, and subsequently with both contralateral and residual limbs of a cohort of participants with unilateral transtibial amputation. The combination of these techniques enabled associations to be assessed between tissue morphology (composition, stiffness, deformation) and local physiology (ischaemic response and inflammatory response). In addition, these trends in these parameters were assessed against subject characteristics, such as time since amputation and daily socket use. Exploration of these associations met objective 4.

Further insight into both residuum tissue adaptation, tolerance to prosthetic loading and associations between them were achieved, successfully fulfilling the overarching research aim 'To evaluate soft tissue tolerance of residual and intact limbs under representative prosthetic loads'.

Investigating the mechanisms of soft tissue damage at the residual limb-socket interface

Research Objectives:

1. Develop testing protocol with representative loading
2. Select measurement techniques and assess tissue tolerance in cohort of participants without amputation
3. Investigate tissue adaptation and tolerance in a cohort of participants with transtibial amputation
4. Assess associations between adaptation and tolerance

Research Questions:

1. Are there any changes to tissue composition in residual limbs following amputation?
2. How do residual and intact limbs respond biomechanically & physiologically to representative prosthetic loading?
3. How does soft tissue composition affect response to loading/tissue tolerance?

Chapter 3- Protocol Development

Development of loading technique via cuff inflation and selection of measurement techniques

Preliminary testing and testing on control limbs of participants without amputation

Final development of testing protocol for participants with amputation

Implementation of MRI testing session on participants with amputation

Implementation of laboratory testing session on participants with amputation

Chapter 4- Soft Tissue Constituents & Biomechanics

Based on 30 limbs:

- Generally higher infiltrating adipose in residual vs. intact limbs indicative of atrophy post-amputation
- Higher Myoton stiffness at residual limb patellar tendon suggesting adaptation under prosthetic loading
- Lowest deformation at residual limb patellar tendon
- Higher composition variability could explain greater shape change observed in residual compared to intact limbs

Chapter 5- Physiological Response

Based on 30 limbs:

- Both residual and intact limbs showed ischaemic responses
- Generally lower T_cPO_2 % decrease in residual compared to intact limbs with fewer residual limbs reaching a Category 3 ischaemic response, indicating greater tolerance to loading
- Generally a lower inflammatory response was observed in residual compared to intact limbs indicating greater tolerance to loading
- General trend observed in calf sites of increasing inflammatory response with increasing superficial adipose

Chapter 6- Overall Discussion

- Results indicate varying tissue adaptation post-amputation
- Generally residual limbs demonstrated increased tolerance to representative prosthetic loading
- Variable responses observed particularly in residual limbs
- Measurements show potential to assess tissue damage risk under prosthetic loading

Figure 6.1 Schematic summarising objectives and achievements of this research, Note: colour represents which research question is in-part being answered

6.2 Advances in Scientific Understanding

On reviewing the existing literature it became clear that there is limited research into the adaptation of residual limb soft tissues after amputation, and the temporal changes with respect to tolerance of loading [85].

It is important to understand the morphology of the residual limb as its mechanical integrity is a key consideration for the design and control of the socket and will affect how the soft tissues respond to loading. Muscle atrophy post-amputation has been observed in previous studies [49, 50], although there is little distinction between the two types of subcutaneous adipose tissue, namely the superficial and muscle infiltrating. This research presents, for the first time, MRI of the lower limbs of participants with unilateral transtibial amputation using DIXON VIBE sequencing, to quantify adipose tissue infiltration in their muscles. This present research provides evidence of muscle atrophy post-amputation with an increase in infiltrating adipose observed in residual tissues compared to those in intact limbs (Figure 4.8). Trends in composition observed within this cohort suggest that the proportion of infiltrating adipose tissue increases with time following amputation in residual limbs, with a less marked increase in infiltrating adipose composition in individuals who have higher levels of socket use and activity (Figure 4.10).

The structural integrity of the residuum's tissues will inevitably affect its response to loading. This research addresses this issue by determining a parameter of muscle stiffness measured at three sites of both limbs in participants with amputation using a commercial system (MyotonPRO™, Myoton AS, Estonia). Findings revealed increased stiffness in residual limb patellar tendon tissues compared to the contralateral site, which could be attributed to biomechanical adaptive response to prosthetic load bearing (Figure 4.11). Indeed, a positive correlation between Myoton stiffness and time since amputation was observed at the residual limb patellar tendon site (Table 4.6). However, this was not significant and negative correlations were observed between Myoton stiffness and socket use at all residual limb sites (Figure 4.14). It is important to note that the daily socket use recorded does not fully represent accumulation of tissue loading as use could mean anything from sitting with the prosthesis donned to running.

Interface pressure during static prosthetic weight bearing has been reported previously [108, 109, 112]. However, values range over three orders of magnitude from 4 to 938 mmHg (0.5 to 125.1 kPa), thus providing little confidence in assessment of both the biomechanical events and physiological response of the soft tissues at the loaded socket interface. Various bioengineering tools have been available to assess tissue health [34], for example, T_cPO_2 measurements have been collected to determine amputation levels where tissue viability is sufficient for healing [76-78], and from participants with and without amputation at rest to examine the effects of donning a prosthetic liner at the tissue interface [82]. It has also been reported that elevated and sustained CO_2 levels may prove a strong indicator of cell damage [218]. However, bioengineering tools have not previously been adopted to assess tissue status under representative prosthetic socket loading. The current research presents, for the first time, measures reflecting both ischaemic and inflammatory responses under representative prosthetic loading. Generally lower ischaemic and inflammatory responses were observed in residual compared to intact limbs (Figure 5.4 to Figure 5.7 and Figure 5.10). Again these findings suggest these residual limb tissues have increased in tolerance to loading, most likely due to repetitive loading through the prosthesis.

This research also enabled investigation of the associations between soft tissue adaptation and tolerance. This analysis suggested an increase in the tolerance of the tissues at the patellar tendon of the residual limb, as reflected in lower mean T_cPO_2 percentage decrease under loading, despite lower baseline values, compared to intact limbs and increased values of baseline T_cPO_2 with time since amputation (Figure 5.2 and Figure 5.4 to Figure 5.6). The lowest baseline T_cPO_2 measurements observed at the residual limb patellar tendon site could be indicative of this site having the thickest stratum corneum following adaptation from socket use, in a similar way to plantar heel skin. Previous research has observed the stratum corneum to be 16 times thicker in plantar skin, which is known to thicken in response to load and for its enhanced tolerance to mechanical loading [270]. As well as improving understanding of tissue tolerance, this knowledge could help engineered skin substitutes improve the load bearing ability of vulnerable skin such as that of the residuum [270].

Increased inflammatory response was generally observed with increased percentage of adipose (particularly superficial) in calf sites for all limb groups which may indicate reduction in tissue tolerance is a function of adipose percentage (Table 5.4 to Table 5.5 and Figure 5.16). Previous inflammatory biomarker research has also observed negative clinical implications associated with increased adipose; however, different markers were evaluated [196, 254]. A larger cohort of participants with amputation is required to explore this association further.

6.3 Limitations of the Research

The sample size of this current study was limited to 10 participants without amputation and 10 participants with unilateral transtibial amputation. A preference for age-matched cohorts was desired in the recruitment phase; however, this was difficult to achieve in practice. Although half the participants with amputation were within the same age range as those without amputation (median 28 years; range 23 to 36 years), the former cohort presented a higher median (41 years) and wider age range (25 to 62 years).

Inevitably there was variability between participants with amputation due to age, sex, reason for amputation, time since amputation and comorbidities, which limited the ability to generalise the findings across the population of individuals with amputation. However, the cohort's diverse demographics did provide the opportunity to acquire information on the adaptation and tolerance of the residuum tissues. Recruitment of participants with transtibial amputation proved to be very difficult. The testing sessions demanded a large time commitment from potential participants. The researcher attempted to schedule the sessions around individual availability but also needed to comply with coordinating MRI facilities and laboratory and equipment availability. Many recruitment avenues were explored for this research and a comprehensive list can be observed in Appendix E. Interestingly, the most successful recruitment methods proved to be word of mouth and poster advertisement at a PPI workshop with prosthetic limb users in South Hampshire.

High variability was observed in both tissue composition and responses to representative prosthetic loading. Similar variability has been reported with respect to tissue composition [50], transcutaneous gas response [80, 82, 212, 215] and in inflammatory biomarker response [139, 206, 224]. Currently, it is not known what differences are clinically relevant and establishing standard thresholds for specific parameters reflective of tissue health may prove problematic. It must be accepted that tissue damage is also a multifactorial, time dependent process requiring consideration of individual variability with respect to tissue tolerance to loading. Nonetheless the measurements presented in this research do enable comparisons and indications of a tissue's susceptibility to damage.

The experimental protocols included only static loading at relatively low magnitudes of pressure.

It is well accepted that cyclic loading is more representative of daily prosthetic use. However, compromises were necessary with existing equipment so more in-depth measurements in controlled conditions were selected over the representativeness of the cyclically loaded, in-socket sensing alternative. Furthermore, in the early stages post-amputation static weight bearing activities will be carried out during rehabilitation, and at this time the tissues will be particularly vulnerable to damage.

During testing sessions it was often difficult to support limbs in a consistent manner and measure at exactly the centre of measurement sites resulting in lower precision in limb comparisons. This was discussed in Section 4.4.2 but briefly was due to differing limbs anatomies, lengths and sensitivities. Measurement specific limitations are discussed in Sections 4.4 and 5.4. To summarise, MRI required mostly manual processing (Section 3.4.2) which increases time consumption and subjectivity, though it was determined for the small size of the cohort developing an accurate automated process would have taken longer. Deformation analysis was 2D further simplifying the MRI processing and providing an insight into biomechanical response, though limited in its simplification (Section 4.4.2) and will be further discussed in Section 6.5.2. With regards to the Myoton stiffness, we cannot be sure whether an individual's tissue was relaxed or tensioned at the time of measurement (Section 4.4.2).

High T_cPO_2 measurements were observed at baseline in three participants, most probably due to insufficient stabilisation period or infiltration of air which may have been less likely with a simpler testing protocol (Section 5.4.1). IL-1 α although sensitive to mechanical loading could have been increased by other stimuli, such as irritation from hair removal, limiting the specificity (Section 5.4.1).

6.4 Clinical Implications

Currently in the clinical setting expert multidisciplinary teams work together to manage residual limb health post-amputation. Although important interface measurements of pressure and strain do not necessarily correspond to the physiological response of the loaded tissue, demonstrated by the variation in responses observed within this research. Therefore, a combined biomechanical and physiological evaluation is advised to provide a more complete picture of tissue tolerance. The array of measurements presented and implemented in the current research could help identify individual susceptibility to tissue damage which, in turn, could inform clinicians of the most appropriate rehabilitation programme based on the degree of individual risk. This would also be beneficial for self-management strategies in the home environment, which is more difficult particularly if an individual has impaired sensory perception or mobility.

Table 6.1 summarises the benefits and practical issues associated with the clinical implementation post-amputation of the measurement techniques presented in this research. These criteria have been rated (as a total score up to 6) to compare the merits of each technique, with reference to the following categories:

- Benefit to evaluate residual limb tissue adaptation: 1) little, 2) moderate and 3) major; and
- Practicality to implement clinically: 1) low, 2) moderate and 3) high

Suggestions have then been provided to aid clinicians and individuals with amputation to reduce the risk of tissue damage. It is important to recognise that clinicians already include a number of set procedures with prescribed measurements in a routine assessment of an individual and so further time-consuming and complex measures could prove impractical to implement.

Table 6.1 Summary of current clinical applications of measurement techniques post-amputation and recommendations for use

Measurement Parameter	Benefits of Use? (Score/3)	Practicalities? (Score/3)	Overall (Score /6)	Suggestions for Implementation
Transcutaneous Gas Tension (T_cPO₂ and T_cPO₂)	<ul style="list-style-type: none"> - Assessment of tissue viability, i.e. is T_cPO₂ (≈45 to 90 mmHg) or T_cPO₂ (≈36 to 50 mmHg) outside the normal range - Evaluation of ischaemic response to loading (3)	<ul style="list-style-type: none"> - Provides real-time measurement though requires a stabilisation period of ≈15 minutes - Requires constant skin attachment at elevated temperature (43.5°C) - Ongoing equipment expense (2)	5	<ul style="list-style-type: none"> - Use for a simple and real-time assessment of residuum tissue health - Apply electrodes to corresponding site(s) on contralateral limb or another body site if possible for comparison - Simple tissue health check- Apply electrodes and take reading after measurements have stabilised - More thorough check of tissue tolerance to loading- After taking baseline measurements apply pressure cuff and inflate incrementally until a Category 3 response or 60 mmHg is reached
% Change in IL-1α/Total Protein and IL-1RA/Total Protein	<ul style="list-style-type: none"> - Evaluation of inflammatory response at baseline and in response to loading (2)	<ul style="list-style-type: none"> - Easy biomarker collection - Time consuming and expensive analysis - More realistic converted to a lab-on-chip device (2)	4	<ul style="list-style-type: none"> - Use IL-1α analysis in combination with T_cPO₂ and T_cPO₂ measurement for slower but more thorough assessment of residuum tissue health and tolerance to loading collecting biomarkers at both baseline and directly after incremental cuff loading as above - Also collect from corresponding site(s) on contralateral limb if possible - Assessing both IL-1α and IL-1RA will increase time and cost but enable further analysis as comparable response indicates a balanced inflammatory response
Interface Pressure	<ul style="list-style-type: none"> - To measure exactly what load is being applied at the interface, particularly important if measurement electrodes are in use under a pressure cuff (2)	<ul style="list-style-type: none"> - Easy to collect - Provides real-time measurement - Adds extra testing time (2)	4	<ul style="list-style-type: none"> - Use after more thorough T_cPO₂ and T_cPO₂ measurement assessing tissue tolerance to loading, positioning interface pressure sensors underneath T_cPO₂ and T_cPO₂ electrodes
MRI	<ul style="list-style-type: none"> - Visualisation of soft tissue composition (3)	<ul style="list-style-type: none"> - Expensive with limited access and can cause claustrophobia (1)	4	<ul style="list-style-type: none"> - Use if a detailed exploration into tissue adaptation and tissue health is required
Myoton	<ul style="list-style-type: none"> - Assessment of structural stiffness of tissue, though does not directly equate to a mechanical property (1)	<ul style="list-style-type: none"> - Easy to use providing quick real-time results (3)	5	<ul style="list-style-type: none"> - Use of the Myoton probe regularly during clinics could provide a simple methodology for quantitative comparison of tissue adaptation to prosthetic loading

A simple real-time assessment of residuum tissue health could be carried out by recording T_cPO_2 and T_cPCO_2 values at baseline. Electrodes could be applied early on during a clinic visit, allowing time for stabilisation whilst carrying out other tasks such as taking patient history, to reduce time burden. For a more thorough assessment involving an extended protocol, the application of pressure over the residuum and subsequent measurement of transcutaneous gas tensions could provide an estimation of tolerance to loading. To assess biomechanical adaptation, this could be repeated at future clinics to record how tolerance changes over time. If an individual with amputation is at higher risk of tissue damage due to comorbidities, such as PVD, biomarker samples could be collected at baseline and post-incremental loading to assess inflammatory response. Although biomarker collection takes a couple of minutes, analysis is costly and time consuming with samples often requiring to be sent to central facilities for analysis.

As baseline values for T_cPO_2 and T_cPCO_2 have a large range and normal inflammatory response is highly variable, results at different time points and at corresponding contralateral limb sites are important for comparison with individuals acting as their own controls. However, this does add further time burden to clinicians. Longitudinal studies employing individuals as their own controls are important to further understanding of normal variation and clinically important differences that indicate an increased risk of tissue damage.

MRI would also add a significant burden in terms of both cost and time to both clinicians and individuals with amputation and is currently only used in the UK for diagnostic purposes. However, MRI could be used for a detailed exploration of tissue adaptation and health, particularly focussing on superficial and infiltrating adipose percentage. Although the Myoton 'stiffness' measure does not directly equate to mechanical properties, these measurements would not add much time burden to a clinic but could provide a much easier and cheaper descriptive alternative to track tissue adaptation.

6.5 Future Work

6.5.1 Applications at Other Soft Tissue-Medical Device Interfaces

Currently Medical device-related Pressure Ulcers (MDRPUs) represent an increasing burden across global healthcare, impacting patients' quality of life and costing the health services time and money [142]. The research protocols developed herein to establish indicators of soft tissue health and tolerance to loading post-amputation could be adapted for use in other situations in which medical devices or orthoses can lead to damage when attached to the skin surface, particularly at vulnerable sites which have not been conditioned to mechanical loading. This could include non-invasive ventilation masks, cervical collars and spinal boards.

6.5.2 3D Strain Analysis

Due to the incompressibility of soft tissues the participants limbs were changing shape in three dimensions under the applied pressure cuff loading. Therefore, the prediction of 3D deviatoric strains would represent a more realistic view of the limb tissue condition than compression, under this form of applied pressure. Baseline and loaded MR image stacks could be segmented and then used to calculate displacement and strain fields. As an example, a baseline MRI stack of the contralateral limb of one participant (#1A) segmented into the gel liner, skin, superficial adipose, muscle and bone is illustrated in Figure 6.2.

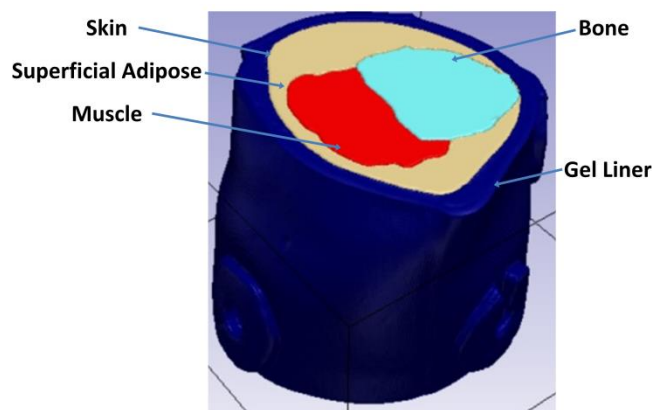


Figure 6.2 Segmented participant #1A baseline MRI stack

The resulting strain data could be used to calibrate 3D models of the residual limb soft tissues, helping to increase their accuracy and reliability and enable a wider range of socket loading and design questions to be investigated.

6.5.3 Temporal Inflammatory Response

Further investigation of the temporal inflammatory response to representative prosthetic loading by collecting samples at a greater number of time points would provide further insights into individual variability and tolerance to loading. Substantial variability in inflammatory response has been demonstrated in the present work, and therefore a carefully selected unloaded control site might offer both an internal reference and insights into the size of measurement produced by a true inflammatory response to loading.

6.5.4 Metabolite Response

Sweat metabolites lactate and urea are upregulated during anaerobic respiration and excreted as waste products. Increased levels from baseline to post-loading observed in past studies, indicate sensitivity to mechanical loading and the potential of metabolites as indicators of loaded tissue status is worthy of further exploration [211, 229, 271]. However, like inflammatory biomarkers, metabolite analysis requires an unloaded control site to distinguish between systemic and local changes and is costly and time consuming.

6.5.5 Real Time Translation for Clinical and Daily Life Application

It will be important to expand the work to include a larger cohort of participants with amputation across a wide range of ages, activity levels and co-morbidities to match the population. Such a dataset would enable some generalisations to be made with particular reference to the temporal profile of biomechanical adaptation and tissue tolerance at the residuum-socket interface.

Potential clinical recommendations might be derived from identification of patient strata within this population, who demonstrate high or low responses to loading and might be managed differently. Furthermore, implementation of these measurement protocols in cyclic loading, as in daily life, would evaluate their full potential to understand tissue status and produce recommendations to minimise the risk of tissue damage. As an example of clinical implementation both transcutaneous gas tension profiles and inflammatory responses could be adapted for real-time clinical and daily use. Indeed, development of wireless and portable sensors could provide critical additions to the currently available interface pressure and shear in-socket measurements to understand how the mechanical loading is affecting the biological status of the soft tissues [111]. A wearable device to measure transcutaneous oxygen is currently being developed by a US research team [272]. Although their prototype has been designed for babies, it is planned to be up-scaled for adults to provide a flexible wearable device controlled by a smartphone app. Currently inflammatory response analysis is an expensive and time consuming technique; however, there are many developments with lab-on-a-chip technologies to produce cheaper and quicker measurements that can be translated to the clinic [142]. More practical, wearable measurement sensors developed for in-socket use could be worn in everyday life to support the rehabilitation of an individual with amputation, improving independence and quality of life. This in combination with a smart phone app to inform users of real-time tissue health could be particularly helpful to those with limited mobility or sensation.

Measurements that are easily translatable could help clinicians to monitor and record tissue health, load tolerance and wound healing to determine the optimum rehabilitation interventions in the early days post-amputation to encourage adaptation, help minimise the risk of tissue damage and provide long-time comfort with prosthetic wear.

7 Appendices

Appendix A-Preliminary temperature and humidity testing results

Skin surface measurements of temperature and humidity were collected at the tibial tuberosity, medial calf and posterior calf, at baseline and after an applied cuff pressure (60 mmHg for 20 minutes).

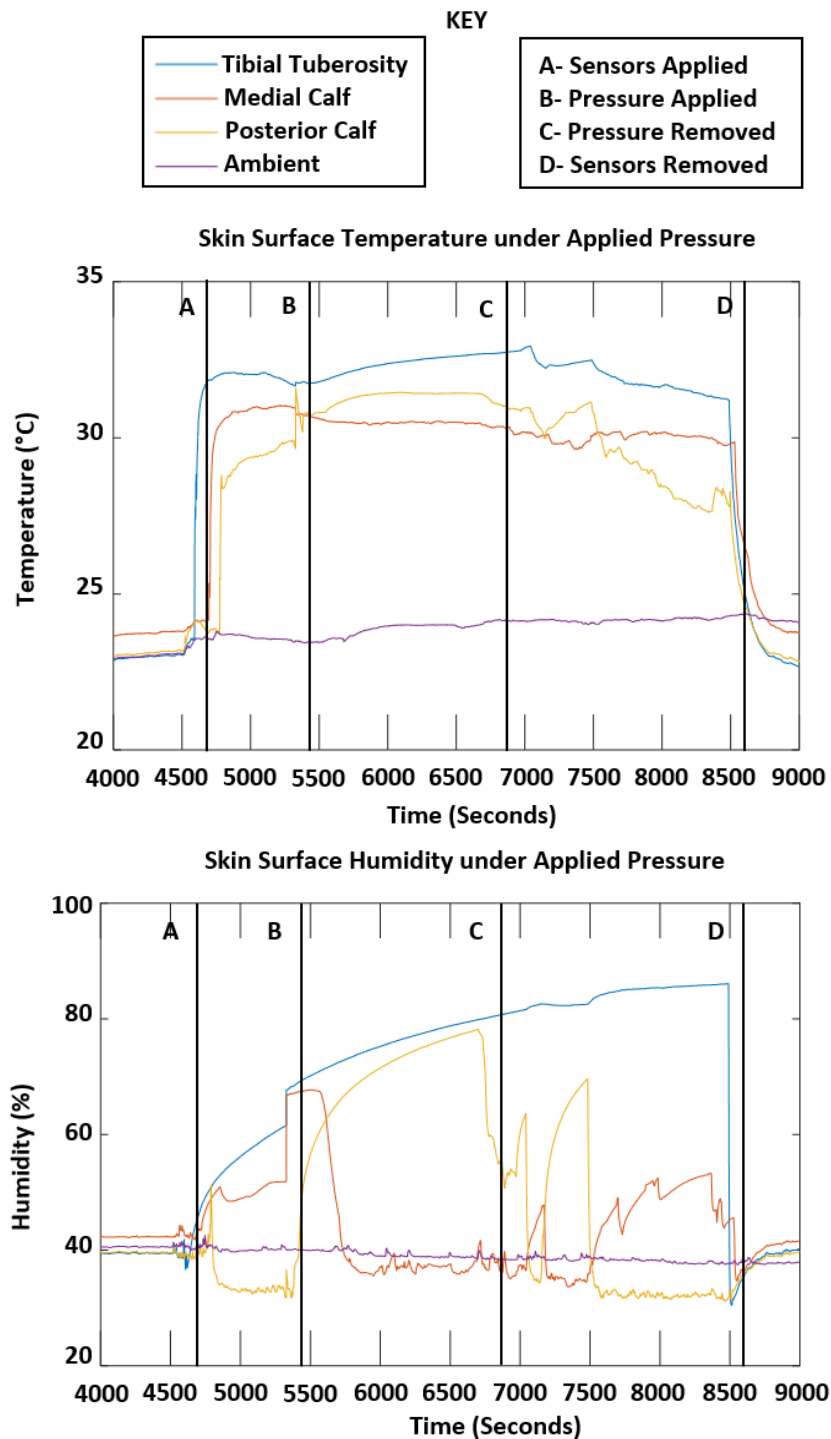


Figure 7.1 Skin surface temperature (top) and humidity (bottom) under 60 mmHg applied pressure during preliminary testing

Appendix B-Ethical Approvals (ERGO 29696 & ERGO 41864)

ERGO 29696



ERGO application form – Ethics form

All mandatory fields are marked (M*). Applications without mandatory fields completed are likely to be rejected by reviewers. Other fields are marked “if applicable”. Help text is provided, where appropriate, in italics after each question.

1. APPLICANT DETAILS

1.1 (M*) Applicant name:	Jennifer Bramley
1.2 Supervisor (if applicable):	Dr Alexander Dickinson, UoS, Research Fellow and Lecturer in Bioengineering, alex.dickinson@soton.ac.uk
1.3 Other researchers/collaborators (if applicable): <i>Name, address, email, telephone</i>	<p>Dr Peter Worsley, UoS, Lecturer, Faculty of Health Sciences, p.r.worsley@soton.ac.uk</p> <p>Professor Dan Bader, UoS, Professor, Faculty of Health Sciences, d.l.bader@southampton.ac.uk</p> <p>Dr Luciana Bostan, UoS, Senior Research Fellow, Faculty of Health Sciences, l.e.bostan@soton.ac.uk</p>

2. STUDY DETAILS

2.1 (M*) Title of study:	Measuring and predicting soft tissue strains following lower limb amputation: Preliminary control study
2.2 (M*) Type of study (e.g. Undergraduate, Doctorate, Masters, Staff):	Doctorate
2.3 i) (M*) Proposed start date:	21/08/2017
2.3 ii) (M*) Proposed end date:	01/04/2018

2.4 (M*) What are the aims and objectives of this study?

The overall aim of this research is to enhance knowledge related to soft tissue adaptation and behaviour following lower limb amputation and gain insight into the four mechanisms of soft tissue injury: direct mechanical damage, ischaemia, reperfusion and lymphatic impairment.

This will be accomplished by investigating the physiological effect of applying representative loads first to the healthy calf tissue of non-amputees (Preliminary control study- Phase 1), using a number of biophysical measures.

The key aims within this phase are to:

- Provide a base comparison for soft tissue physiological response to load
- Determine the most important measures to carry forward for Phase 2, with amputee participants

2.5 (M*) Background to study (a *brief* rationale for conducting the study):

Amputation is the surgical or traumatic loss of all or part of a limb or extremity. The care and rehabilitation of amputees is paramount to recover and maintain function, leading to an improved or restored quality of life. Amputation is a global healthcare concern, particularly with the growing and ageing population and an increase in risk factors for conditions that cause dysvascularity and neuropathy, such as diabetes. This research will focus on lower limb amputations (particularly trans-tibial/below knee) due to their high incidence and reliance on the lower limbs for mobility. Below Knee Amputation (BKA) is also the preferred surgical technique over Above Knee Amputation (AKA) due to superior function.

The residual limb, made up of soft tissues overlying an amputated bony stump, forms a critical interface with the socket, which is used to suspend most prosthetic limbs. It is of critical importance to understand the underlying physiology of the residual limb soft tissues, to understand how they tolerate loads. This knowledge can be used to enhance the design of prosthetic devices and enable clinicians to prevent compromise to the viability of skin, fat and muscle tissues, which can lead to the requirement of revision surgery to a higher level of amputation. Furthermore, the biomechanical adaptation of the limb post-amputation, is of interest. New knowledge in this area is required to assist in the development of effective practices to optimise residual limb care and gait rehabilitation and decrease the number of fitting iterations. An optimal socket will expedite biomechanical adaptation of the soft tissues to enable comfortable and stable load transfer.

Knowledge of residual limb tissue adaptation and behaviour will facilitate the creation of more realistic computational models of the residual limb to enable increased accuracy when predicting tissue strains and behaviour under applied loads. Utilisation of these predictions with sensor technologies could allow enhanced understanding of the mechanisms contributing to tissue injury at the stump-socket interface.

Results from this preliminary control study will provide a base comparison for amputees' soft tissue physiological response to load.

2.6 (M*) Key research question (Specify hypothesis if applicable):

- Key research question- To investigate the physiological effects of applying pressure and pressure in combination with shear to healthy calf tissue.
- Key hypothesis- Baseline and loaded biophysical measurements will be significantly different.

2.7 (M*) Study design (Give a *brief* outline of basic study design)

Outline what approach is being used, why certain methods have been chosen.

A multi-modal biophysical measurement study will be implemented, characterising the physiological behaviour of the soft tissues, with respect to mechanisms of tissue injury under static loading. A pressure cuff will be applied to the calf of participants, for 20 minutes, at pressure (60mmHg) and shear representative of loads that a recent amputee would experience during early post-amputation rehabilitation with early walking aids .

The following non-invasive measurements will be taken in three positions relevant to prosthesis load-bearing (tibial tuberosity, medial calf and posterior calf):

- Skin surface measurements of temperature and humidity (as microclimate is known to effect skin's tolerance to load).
- Oxygen and Carbon Dioxide transcutaneous gas tensions (TcPO₂/TcPCO₂) (as established predictive indicators for ischaemia).

- Biomarkers released at the skin will be collected using SebuTape (as the IL-1 α inflammatory cytokine is a known precursor to tissue injury).

- Lymphatic system activity will be observed using a sub-dermal injection of Indocyanine Green Contrast and Infra-Red imaging (as impaired lymphatic activity is a direct cause of tissue injury).

- Finally, Magnetic Resonance Imaging will be used for the first time in parallel with these measurements, to observe the volumetric soft tissue deformations which result from the applied surface loads and thus provide insight into the relative influences of the different soft tissue injury mechanisms.

Biophysical measurements and MRI will be implemented in two separate testing sessions each lasting approximately 2 hours, with each participant, as follows:
 Testing Session 1- MRI while calf is unloaded, and loaded with pressure, and pressure in combination with shear.
 Testing Session 2- Temperature and humidity and gas tension measurements, biomarker collection and Infra-Red lymphatic imaging while calf is unloaded, and loaded with pressure and pressure in combination with shear, and following unloading.

The methods and techniques utilised for this research are well-established and have previously been used in studies that have been granted ethical approval. Full informed consent must be given by each participant whom has the right to withdraw at any time without reason.

3. SAMPLE AND SETTING

3.1 (M*) How are participants to be approached? Give details of what you will do if recruitment is insufficient. If participants will be accessed through a third party (e.g. children accessed via a school) state if you have permission to contact them and **upload any letters of agreement to your submission in ERGO.**

Participants will be recruited by word of mouth and via poster advertisement from staff and postgraduate research students within the researchers' departments (Bioengineering Science Research Group, FEE, and the Skin Health Research Group, FoHS) and the University of Southampton.

3.2 (M*) Who are the proposed sample and where are they from (e.g. fellow students, club members)? List inclusion/exclusion criteria if applicable. NB The University does not condone the use of 'blanket emails' for contacting potential participants (i.e. fellow staff and/or students).

It is usually advised to ensure groups of students/staff have given prior permission to be contacted in this way, or to use of a third party to pass on these requests. This is because there is a potential to take advantage of the access to 'group emails' and the relationship with colleagues and subordinates; we therefore generally do not support this method of approach.

If this is the only way to access a chosen cohort, a reasonable compromise is to obtain explicit approval from the Faculty Ethics Committee (FEC) and also from a senior member of the Faculty in case of complaint.

Ten non-amputees (five male and five female, age-matched) will be recruited from staff and postgraduate research students within the researchers' departments (Bioengineering Science Research Group, FEE, and the Skin Health Research Group, FoHS) and the University of Southampton by poster advertisement and word of mouth.

The following inclusion criteria apply:

- Aged over 18 years old
- Healthy
- No allergy/sensitivity to any substance used in this study: Indocyanine Green, Micropore tape to secure sensors, Sebutape
- No contraindications to use of MRI
- Individual not at high risk of Deep Vein Thrombosis
- No active vascular, skin or lymphatic conditions
- No history of conditions affecting the skin, vascular system or lymphatics
- Individuals able to maintain still supine position for 20 minute periods during testing session 1
- Individuals able to maintain a still seated position for 20 minute periods during testing session 2 and hold their bladder for approximately 1.5-2 hours

The following exclusion criteria apply:

- Pacemaker, metallic or active implants
- Presence of metal fragments in the eyes
- Contraindications to use of Indocyanine Green (particularly sensitivity or allergy to iodide, kidney disease, liver disease, an overactive-thyroid or benign tumours of the thyroid) or allergies to Micropore tape
- Increased risk for Deep Vein Thrombosis (for example: genetic clotting disorders, use of recreational drugs, older than 60 years of age, presence of malignant tumour or cancer, obesity, smoking, recent surgery, congestive heart failure, irritable bowel disease)
- Inability to give informed written consent (e.g. due to cognitive impairment)
- Pre-existing skin condition
- Pre-existing medical conditions that are known to affect dermal vasculature such as diabetes mellitus or Peripheral Vascular Disease (PVD)
- Pregnancy
- Claustrophobia
- Unable to remain still for 20 minute periods

3.3 (M*) Describe the relationship between researcher and sample (*Describe any relationship e.g. teacher, friend, boss, clinician, etc.*)

Participants must be volunteers however they may be supervisors/colleagues/friends of the researcher.

3.4 (M*) Describe how you will ensure that fully informed consent is being given: (*include how long participants have to decide whether to take part*)

Potential participants will be given a Participant Information Sheet by email and will be given at least 24 hours to decide whether they would like to take part in the study. Participants will have the opportunity to ask the research team any questions and will be able to withdraw from the study, no questions asked, at any point. Participants will be asked to complete an informed consent form, a questionnaire and an MRI Safety Questionnaire prior to their participation. The MRI Safety Questionnaire will be countersigned by a trained radiographer or someone equivalent that is trained in taking informed consent for MRI. If a participant meets any of the exclusion criteria or does not adhere to the inclusion criteria they will not be able to participate in this research, for their own safety. One additional general study exclusion criterion is for people unable to provide informed consent due to cognitive impairment.

4.1 (M*) Give a brief account of the procedure as experienced by the participant
(Make clear who does what, how many times and in what order. Make clear the role of all assistants and collaborators. Make clear total demands made on participants, including time and travel). Upload any copies of questionnaires and interview schedules to your submission in ERGO.

A potential participant will be emailed a participant information sheet. If they decide that they would like to take part, they will first be asked to complete and return a questionnaire to assess whether they fit the criteria to participate.

If they fit the criteria, they will then be contacted by the researcher to meet at the University of Southampton Clinical Academic Facility at a pre-determined suitable time. The testing will be split up into two sessions each lasting approximately 2 hours. The researcher will ask the participant if they have read and understood the information in the participant information sheet and will answer any questions. If they would still like to participate they will then be asked to sign a consent form to confirm their informed participation.

Prior to Testing Session 1 the participant will be asked to complete a Magnetic Resonance Imaging (MRI) Safety Questionnaire to ensure their safety. If a participant answers yes to any of the safety questions, for their own safety, they will not be able to participate.

During Testing Session 1, after an acclimatisation period of 20 minutes, a participant's (right or left) leg will be imaged using Magnetic Resonance Imaging (MRI). For this testing session participants will be asked to wear a hospital gown and will be given time to change during the acclimatisation period. Prior to imaging the researcher will attach a number of small oil filled capsules to their leg, using double sided tape, which will be used to interpret scale in MR scans.

MR scans will be taken, by an MRI operator, at the end of three 20 minute periods with no loading applied and two different loading conditions applied. In all cases participants will lie on their back in the scanner with their leg slightly elevated. It will be important to remain as still as possible while the images are being taken. The loading conditions will consist of the researcher applying pressure and shear to a participant's calf using a pressure cuff. The order of the three imaging periods will be randomised. There will be an approximately 40 minute rest period in between the two loading conditions, in which participants will be able to use the toilet and walk around.

If at any point during the testing a participant does not feel comfortable in proceeding then the pressure cuff will be removed and they will be assisted out of the MRI suite.

During Testing Session 2 participants will be asked to lie on their back on a standard hospital bed with their leg (same as used in previous session) supported by a foam cushion. They will need to wear comfortable clothes for this and shorts or trousers that can be rolled up to above the knees. The following measurements will be set up by the researcher and taken during this session:

- Surface temperature and humidity will be measured in three places via combined sensors attached to the skin at the start of the session using tape.
- Oxygen and Carbon Dioxide gas tensions will be measured in three places via sensors stuck to the skin. Use of these sensors requires direct skin contact so participants will be asked to shave the three measurement areas 24 hours prior to the session. The sensors will feel warm as they are heated during use.

- Proteins secreted from the skin will be collected during the session using a special tape (SebuTape). The tape will be flattened on to the skin using a roller and removed after 2 minutes.

- Lymphatic activity will be imaged during the testing session using an Infra-Red camera. To enable this imaging a micro dose of Indocyanine Green contrast will be sub-dermally injected in between a participant's big toe and second toe, by a trained professional, at the start of this testing session. The lymphatic vessel being imaged will be marked on their leg using a black felt tip. The injection may cause a little discomfort for a short time.

The setup and full testing period will be approximately 2 hours during which the same loading conditions as in the MRI scan will be applied followed by 20 minute rest periods. It will be preferable if participants could stay attached to the measurement sensors throughout the whole testing session.

If at any point during the testing a participant does not feel comfortable in proceeding then the pressure cuff and measurement sensors will be removed. Pressure will be reduced at 2-3mmHg/second according to World Health Organisation guidelines, in order to avoid reperfusion injury.

Note- the order of the two testing sessions may be reversed dependent on a participant's availability and the availability of the MRI scanner. A participant will be notified which testing session they are attending.

5. STUDY MANAGEMENT

5.1 (M*) State any potential for psychological or physical discomfort and/or distress?

- The injection of the Indocyanine Green contrast for lymphatic activity imaging, in Testing Session 2, may cause temporary discomfort and there is a very rare chance (< 1/10,000) of a side effect occurring due to the use of the injected Indocyanine Green contrast (see below).
- The use of Magnetic Resonance Imaging could cause injury if a participant were to have a pacemaker or metallic implant, by heating or magnetic attraction. Some people can also find the MRI environment claustrophobic.

5.2 (M*) Explain how you intend to alleviate any psychological or physical discomfort and/or distress that may arise? (if applicable)

- The Indocyanine Green contrast used will be a microdose much lower (<1%) than the recommended dose when used for medical diagnosis, for example to investigate blood flow in the heart. Potential participants will not be able to participate in this study should they answer yes to any questions within the participant questionnaire that suggest they may be at a higher risk of being adversely affected by Indocyanine Green (kidney or liver problems or allergy to iodide). The testing sessions are also taking place at a University of Southampton site within University Hospital Southampton (UHS), so that emergency care will be available should any adverse reaction occur. As any injection might cause a little temporary discomfort, the trained professional administering this injection will do his/her best to make this as comfortable as possible and local anaesthetic can be used in the area.

- Potential participants will not be able to participate should they answer yes to any questions within the participant questionnaire or MRI questionnaire that suggest the MR scan would put them at any risk. During the MRI session participants will have contact with the researcher at all times so will be able to talk to them immediately

should they become uncomfortable in the MRI environment.
The MRI testing session is not a diagnostic scan, and the images will not routinely be seen by a doctor. However if any abnormality is observed by the MRI operator, the scans will be reviewed by a Radiologist and a participant will be contacted by a letter advising them to contact their GP, who will decide if further investigation is required.
- If a participant feels discomfort during either of the testing sessions the pressure cuff will be removed and the testing stopped.

5.3 Explain how you will care for any participants in 'special groups' (i.e. those in a dependent relationship, vulnerable or lacking in mental capacity) (if applicable)?

N/A

5.4 Please give details of any payments or incentives being used to recruit participants (if applicable)?

There are no payments or incentives being used to recruit participants. Travel expenses associated with the participation in this study will be reimbursed up to a total of £20 per session upon supply of a bus ticket or taxi receipt.

5.5 i) How will participant anonymity and/or data anonymity be maintained (if applicable)?

Two definitions of anonymity exist:

i) Unlinked anonymity - Complete anonymity can only be promised if questionnaires or other requests for information are not targeted to, or received from, individuals using their name or address or any other identifiable characteristics. For example if questionnaires are sent out with no possible identifiers when returned, or if they are picked up by respondents in a public place, then anonymity can be claimed. Research methods using interviews cannot usually claim anonymity – unless using telephone interviews when participants dial in.

ii) Linked anonymity - Using this method, complete anonymity cannot be promised because participants can be identified; their data may be coded so that participants are not identified by researchers, but the information provided to participants should indicate that they could be linked to their data.

Linked anonymity. Participant identifiable information will be anonymised with corresponding data being given an identification code assigned to the participant upon recruitment. Participant's data and the assigned identification code will be stored on a University password protected computer. The consent form and MRI Questionnaire will be the only places whereby a participant's identity and assigned identification code can be linked and these will be secured in the principal investigator's locked office. Only named researchers will have access to the password protected computer.

5.5 ii) How will participant confidentiality be maintained (if applicable)?

Confidentiality is defined as the non-disclosure of research information except to another authorised person. Confidential information can be shared with those who are already party to it, and may also be disclosed where the person providing the information provides explicit consent.

Only the consent form and MRI Safety Questionnaire will contain identifiable information and these will be kept confidential in a locked filing cabinet in the principal investigator's locked office. Other participant identifiable data will be anonymised and kept confidential with a random code being assigned to each participant's dataset. Participant data will be stored on a University password protected computer accessible to only the named researchers in this document.

5.6 (M*) How will personal data and study results be stored securely during and after the study? *Researchers should be aware of, and compliant with, the Data Protection policy of the University. You must be able to demonstrate this in respect of handling, storage and retention of data.*

Data and study results will be collected within the Clinical Academic Facility (Faculty of Health Sciences, at University Hospital Southampton) and stored on a password protected University computer for analysis. According to the University's Research Data Management Policy, the anonymised collected data will be stored for 10 years after collection.


5.7 (M*) Who will have access to these data?

The named researchers in this document will have access to the data for analysis. This research and results will be disseminated by publishing in appropriate research journals (such as the Journal of Tissue Viability, Medical Engineering & Physics, and Clinical Biomechanics) and presenting at appropriate conferences (for example International Society for Prosthetics and Orthotics (ISPO) Scientific Meetings and conferences).

Post-analysis anonymised collected data will also be used in as part of the PhD qualification. If participants would prefer their anonymised data to not be included in research publications any time during or after the study will be encouraged to inform the researcher.

N.B. - Before you upload this document to your ERGO submission remember to:

1. Complete ALL mandatory sections in this form
2. Upload any letters of agreement referred to in question 3.1 to your ERGO submission
3. Upload any interview schedules and copies of questionnaires referred to in question 4.1

 RECORD OF RISK ASSESSMENT	
Title of the risk assessment	Measuring and Predicting Soft Tissue Strains Following Lower Limb Amputation- Phase 1
Date risk assessment carried out	20/06/2017
Describe the work being assessed	Preliminary study- applying pressure (using a blood pressure cuff) to healthy calf tissue of non-amputees and measuring the temperature & humidity, Transcutaneous Gas Tensions, imaging lymphatic activity and collecting biomarkers at both baseline and post-load
Describe the location at which the work is being carried out	Clinical Academic Facility (Faculty of Health Sciences, SGH Campus)
Where appropriate list the individuals doing the work and the dates/times when the work will be carried out	Jennifer Bramley, Dr Alex Dickinson, Dr Peter Worsley, Dr Luciana Bostan (work will be carried out 2017/2018)
List any other generic or specific risk assessments or other documents that relate to this assessment-use hyperlinks if possible	Testing Protocol Participant Information Sheet Participant Consent Form COSHH Form for Indocyanine Green Contrast
Name and post of risk assessor	Jennifer Bramley, UoS, Postgraduate Resarcher, Faculty of Engineering and the Environment
List the names and posts of those assisting in compiling this risk assessment	Dr Alex Dickinson, Lecturer (FEE); Dr Peter Worsley, UoS, Lecturer, (FoHS); Professor Dan Bader, Professor (FoHS); Dr Luciana Bostan, Senior Research Fellow (FoHS)
Name, post and where required, signature of the responsible manager/supervisor approving the risk assessment	Dr Alex Dickinson, Lecturer, Bioengineering Science Research Group (FEE)
Reference number and version number of risk assessment	RA_17_1_V1

Assessment	
Title of risk assessment	Measuring and Predicting Soft Tissue Strains Following Lower Limb Amputation- Phase 1

Risk Acceptability		Risk Matrix						Overall Likelihood	Overall Severity	Residual Risk score	Any changes or extra controls?
1-3	Risk acceptable	Severity									
4-6	Risk to be reduced if readily possible	very low	low	medium	high	very high					
7-14	Risk to be reduced if reasonably practicable	1	2	3	4	5					
15-25	Risk unacceptable	1	2	3	4	5					
Likelihood	certainty	5	5	10	15	20	25				
	likely	4	4	8	12	16	20				
	possible	3	3	6	9	12	15				
	less likely	2	2	4	6	8	10				
	improbable	1	1	2	3	4	5				

ref	Task/Aspect of work	Hazard	Harm and how it could arise	Who could be affected?	Existing measures to control risk	Risk Factors		Residual Risk score	Any changes or extra controls?
1	Use of a number of electrical measurement sensors	Electrical	Injury due to electrical shock or tripping over wires	Participant or researchers	All electrical equipment to be used will have been PAT tested. Limited to three measurement sites and use of ties and tape to secure and position wires . Participants will be warned of the tripping hazard at the start of the testing session.	1	2	2	no
2	Application of pressure	Pressure	Discomfort or injury due to occlusion of blood supply and lymphatics if pressure is too high or duration of application too long	Participant	Pressure magnitude and duration have been previously used or exceeded in past research and watching participants lower limbs will be observed during testing. Participants will also be made aware (via the participant information sheet and verbally) they can stop the testing session at any point if they are feeling discomfort or do not wish to continue.	1	3	3	no
3	Injection of Indocyanine Green	Equipment	Injury due to poor use of needle	Participant, researcher or administrator of injection	Only a trained professional to administer injection and used needle to be disposed of immediately into a sharps bin	1	3	3	no

Risk Acceptability		Risk Matrix							Overall Likelihood	Overall Severity	Residual Risk score	Any changes or extra controls?
1-3	Risk acceptable	Severity										
4-6	Risk to be reduced if readily possible	very low	low	medium	high	very high						
7-14	Risk to be reduced if reasonably practicable	1	2	3	4	5						
15-25	Risk unacceptable	Likelihood	certainty	5	5	10	15	20	25			
			likely	4	4	8	12	16	20			
			possible	3	3	6	9	12	15			
			less likely	2	2	4	6	8	10			
			improbable	1	1	2	3	4	5			

ref	Task/Aspect of work	Hazard	Harm and how it could arise	Who could be affected?	Existing measures to control risk	Risk Factors				
4	Use of Indocyanine Green	Substances that are harmful	Misuse of Indocyanine Green or unknown allergic reaction could cause physical injury	Participant or researchers/laboratory users	A COSHH form will be completed for the control of Indocyanine Green to ensure its safe use. Exclusion criteria including contraindications to use of Indocyanine Green (particularly sensitivity or allergy to iodide) and pregnancy will form part of the Questionnaire that participants will complete prior to testing	1	3	3	no	
5	Magnetic Resonance Imaging	Non-Ionising radiation	Injury due to heating or magnetism of metallic implant or pace maker	Participant	Exclusion criteria including no participants with metallic implants or pacemakers; Participants completing a questionnaire and MRI Safety Questionnaire prior to the testing sessions.	1	3	3	no	
6	Magnetic Resonance Imaging	Psychological, confined spaces	Physiological harm occurring if participant is unaware of claustrophobia	Participant	Ensure participant can contact researcher and staff when inside MRI so they can be assisted to leave quickly if they need to	1	3	3	no	
7	Bioanalysis of Biomarkers	Environmental	Exposure to biohazards and/or chemical hazards causing injury due to not following precautionary and safety measures in laboratory	Researcher or colleagues using the laboratory	Induction training to use a biolab, assisted working at the start to learn techniques, use of Personal Protective Equipment (lab coat and gloves when in lab)	1	3	3	no	
8	Use of -80°C Freezer	Environmental	Cold burn injury due to misuse of freezer when storing/collecting Sebutape samples prior to analysis	Researcher or colleagues using the laboratory	Induction training to use freezer and use of appropriate personal protective equipment when using freezer (freezer gloves on top of normal lab gloves and glasses)	1	3	3	no	

Post Risk Assessment Actions

Title of risk assessment

Measuring and Predicting Soft Tissue Strains Following Lower Limb Amputation- Phase 1

Have any of the specialist control measures listed below been identified as required during this risk assessment? - indicate yes or no - if yes then include details on the post assessment action list below.	yes/no
is any exposure monitoring required?	no
Is any occupational health monitoring required?	no
Are there any hazards or other factors that could affect pregnant or nursing mothers?	no

Is any specific training required before people can carry out this work?	yes
Bio Laboratory Induction and training for ELISA bioanalysis techniques	

Are any additional procedures or risk assessments required as a result of this assessment?	no

Are any specialist disposal arrangements required?	no

Are any special emergency arrangements required?	no

Post Assessment actions			
ref	action	by whom	by when



Participant Information Sheet

Study Title: Physiological response of healthy calf tissue to application of pressure/pressure combined with shear

Researcher: Jennifer Bramley
ERGO ID: ERGO 29696

Please read this information carefully before deciding to take part in this research. It is up to you to decide whether or not to take part. If you are happy to participate you will be asked to sign a consent form.

What is the research about?

This study is part of a PhD project funded by the Institute for Life Sciences (IfLS) and Engineering and Physical Sciences Research Council (EPSRC).

The aim of this research is to further understand how skin and soft tissues react to pressure and shear forces applied over short periods of time. This initial phase of my PhD will focus on loading healthy individuals lower limbs. Subsequently, this information will be used to evaluate individuals who have undergone amputation and have to support their body weight through a prosthesis. Further understanding in this area will assist in the development of prosthetic devices and the rehabilitative process for amputees leading to improved function and comfort, increasing independent mobility and decreasing risk of soft tissue damage.

Why have I been asked to participate?

You have been chosen for this study as you are above 18 years of age, a non-amputee and in good health.

What will happen to me if I take part?

If you decide to take part, you will be asked to complete and return the attached questionnaire to assess whether you fit the criteria to participate. If you have any difficulties or questions about completing the questionnaire, please contact the researcher (see details below).

You will then be contacted by the researcher to meet her at the **University of Southampton Clinical Academic Facility**, University Hospital Southampton (UHS) at a time suitable for you. This testing will be split up into **two sessions each lasting approximately 2 hours**. The researcher will ask you if you have read and understood this information and will answer any questions. If you would still like to participate you will be asked to sign a consent form to confirm your participation.

Prior to **Testing Session 1** you will be asked to complete a Magnetic Resonance Imaging (MRI) Safety Questionnaire to ensure your safety. There are no documented risks of having an MRI scan as long as all of the pre-scan safety checks have been completed. If you answer yes to any of the safety questions there is a strong chance that, for your own safety, you will not be able to participate.

During **Testing Session 1**, after an acclimatisation period of 20 minutes, your (right or left) leg will be imaged using Magnetic Resonance Imaging (MRI). For this testing session you will be asked to wear a hospital gown, with shorts and t-shirt underneath, and will be given time to change during the acclimatisation period. Prior to imaging a number of small oil filled capsules will be attached to your leg, using double-sided tape, which we will use to interpret scale in MR scans (Figure 1). Your leg will then be scanned three times, first with no load, then with a small load applied by an inflatable cuff, then with the load and a pulling force against the cuff. The order of the three loading conditions will be randomised. Each scan will take approximately 20 minutes. In all cases you will lie on your back in the scanner with your leg slightly elevated (Figure 1).

[09/08/2017] [PIS_17_1_V1]

[ERGO ID: 29696]

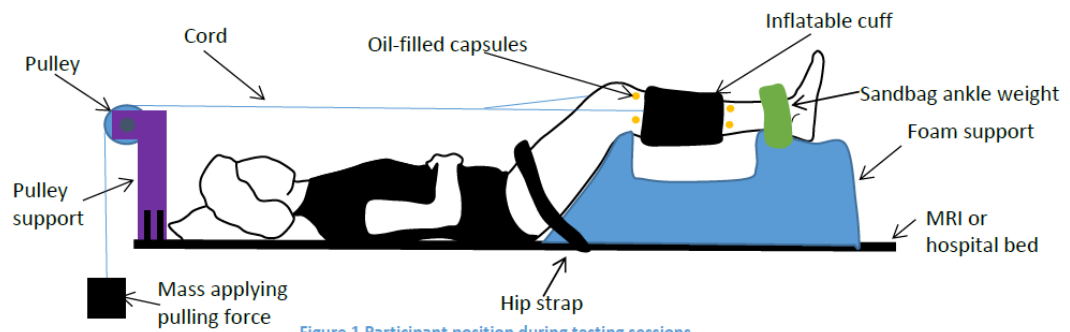


Figure 1 Participant position during testing sessions

It will be important to remain as still as possible while the images are being taken. There will be an approximately 40 minute rest period in between the loading conditions, in which you will be able to use the toilet and walk around.

If at any point during the testing you do not feel comfortable in proceeding then the pressure cuff will be removed and you will be assisted out of the MRI suite.

During **Testing Session 2** you will be asked to lie on your back on a standard hospital bed with your leg (same as used in previous session) supported by a foam cushion (Figure 1). You will need to wear comfortable clothes for this and shorts or trousers that can be rolled up to above the knees. The following measurements will be taken during this session:

- Surface temperature and humidity will be measured in three places via combined sensors attached to the skin using tape.
- Oxygen and Carbon Dioxide gas tensions will be measured in three places via sensors stuck to the skin. Use of these sensors requires direct skin contact so you will be asked to shave the three measurement areas 24 hours prior to the session. The sensors will feel warm as they are heated during use.
- Proteins secreted from the skin will be collected during the session using a special tape (SebuTape). The tape will be flattened on to the skin using a roller and removed after 2 minutes.
- Lymphatic activity will be imaged during the testing session using an Infra-Red camera. To enable this imaging a micro dose of Indocyanine Green contrast will be injected in between your big toe and second toe, by a trained professional, at the start of this testing session. The lymphatic vessel being imaged will be marked on your leg using a black felt tip. The injection may cause a little discomfort for a short time (less than 30 seconds).

The setup and full testing period will be approximately 2 hours during which you will have the same loading conditions applied as in the MRI scan followed by 20 minute rest periods. It will be preferable if you could stay attached to the measurement sensors throughout the whole testing session.

However, if at any point during the testing you do not feel comfortable in proceeding then the pressure cuff and measurement sensors will be removed.

Note- the order of the two testing sessions may be reversed dependent on your availability and the availability of the MRI scanner. You will be notified which testing session you are attending.

[09/08/2017] [PIS_17_1_V1]

[ERGO ID: 29696]

**Are there any benefits in my taking part?**

There are no direct benefits to you by taking part. However, you will be furthering knowledge of soft tissue tolerance to loading, providing a comparison to expand understanding of soft tissue adaptation post-amputation. This obtained knowledge can then be used in the development of more comfortable and functional prosthetic limbs and rehabilitation techniques for amputees.

Travel expenses associated with the participation in this study will be reimbursed up to a total of £20 per session. Please bring a bus ticket or taxi receipt with you for this.

Are there any risks involved?

Your safety will be ensured at all times and the researcher will stay with you throughout the testing sessions. There are small risks associated with two aspects of the testing, but we have taken measures to minimise the likelihood of any harm.

There is a very rare chance ($< 1/10,000$) of a side effect occurring due to the use of the injected Indocyanine Green contrast in Testing Session 2. The microdose we will use is much lower ($<1\%$) than the recommended dose when used for medical diagnosis, for example to investigate blood flow in the heart. You will not be able to participate in this study should you answer yes to any questions within the attached participant questionnaire that suggest you may be at a higher risk of being adversely affected by Indocyanine Green (kidney or liver problems or allergy to iodide). The testing sessions are also taking place at a University of Southampton site within University Hospital Southampton (UHS), so that emergency care will be available should any adverse reaction occur. As any injection might cause a little temporary discomfort, the trained professional administering this injection will do his/her best to make this as comfortable as possible and numbing cream can be used in the area.

The use of Magnetic Resonance Imaging can cause injury if you have a pacemaker or metallic implants, by heating or magnetic attraction so if you have these then you should not participate. During the MRI session you will have contact with the researcher at all times so will be able to talk to them immediately should you become uncomfortable in the MRI environment. You will not be able to participate in this study should you answer yes to any questions within the attached participant questionnaire that suggest the MR scan would put you at any risk.

The MRI testing session is not a diagnostic scan, and the images will not be seen by a doctor. However if any abnormality is observed by the MRI operator, the scans will be reviewed by a Radiologist and you will be contacted by a letter advising you to contact your GP, who will decide if further investigation is required.

Will my participation be confidential?

Yes your participation will be confidential. The researchers carrying out the testing sessions will keep a copy of your age, gender, height, weight and measurements taken during testing linked to a unique testing session code. Your consent form and MRI Safety Questionnaire will be stored securely. All data will be anonymised and stored on a password-protected computer or in a locked office for further analysis. According to the University's Research Data Management Policy, the anonymised collected data will be stored for 10 years after collection.

Post-analysis anonymised collected data will be used in publications and presentations to display work and as part of the PhD qualification. If you would prefer your data to not be included in research publications at any time during or after the study please inform the researcher.

What happens if I change my mind?

Your participation is voluntary and you may withdraw from the study at any time, without reason. Your withdrawal will not affect your legal and medical rights.

[09/08/2017] [PIS_17_1_V1]

[ERGO ID: 29696]

**What happens if something goes wrong?**

In the unlikely case of concern or complaint, you should contact the Head of Research Governance (02380 595058, rgoinfo@soton.ac.uk). Please note that the researchers, supervisors or any other persons involved in the study will not deal with any complaints.

Thank you very much for taking the time to read this information and considering participating.

If you would like to participate or would like more information please use the following contact details:

Jennifer Bramley- j.l.bramley@soton.ac.uk (Researcher)

Dr Alex Dickinson- alex.dickinson@soton.ac.uk (Head of Research Team)



CONSENT FORM

Study title: Physiological response of healthy calf tissue to application of pressure/pressure combined with shear

Researcher name: Jennifer Bramley *

ERGO ID: ERGO 29696

Please initial the box(es) if you agree with the statement(s):

I have read and understood the information sheet (09/08/2017/PIS_17_1_V1) and have had the opportunity to ask questions about the study.	
I have completed, to the best of my knowledge, and returned the Pre-Participation Questionnaire and the MRI Safety Questionnaire.	
I agree to take part in this research project and agree for my data to be used for the purpose of this study.	
I agree that my anonymised MRI images and data can be used for research (including future ethically approved research studies), teaching and training purposes only.	
I understand my participation is voluntary and I may withdraw (at any time) for any reason without my rights being affected.	

Name of participant (print name).....

Signature of participant.....

Date.....

Name of researcher (print name).....

Signature of researcher

Date.....

.....

09/08/2017 ICF_17_1_V1

ERGO ID: 29696

ERGO 41864



ERGO application form – Ethics form

All mandatory fields are marked (M*). Applications without mandatory fields completed are likely to be rejected by reviewers. Other fields are marked "if applicable". Help text is provided, where appropriate, in italics after each question.

1. APPLICANT DETAILS

1.1 (M*) Applicant name:	Jennifer Bramley
1.2 Supervisor (if applicable):	Dr Alexander Dickinson, UoS, Research Fellow and Lecturer in Bioengineering, alex.dickinson@soton.ac.uk
1.3 Other researchers/collaborators (if applicable): Name, address, email, telephone	<p>Dr Peter Worsley, UoS, Lecturer, Faculty of Environmental and Health Sciences, p.r.worsley@soton.ac.uk</p> <p>Professor Dan Bader, UoS, Professor, Faculty of Environmental and Health Sciences, d.l.bader@southampton.ac.uk</p> <p>Dr Luciana Bostan, UoS, Senior Research Fellow, Faculty of Environmental and Health Sciences, l.e.bostan@soton.ac.uk</p>

2. STUDY DETAILS

2.1 (M*) Title of study:	Measuring and predicting soft tissue strains following lower limb amputation: Phase 2 Plain English Title for participant facing documents: Measuring lower limbs response to pressure following amputation
2.2 (M*) Type of study (e.g. Undergraduate, Doctorate, Masters, Staff):	Doctorate
2.3 i) (M*) Proposed start date:	15/10/2018
2.3 ii) (M*) Proposed end date:	15/10/2019

2.4 (M*) What are the aims and objectives of this study?
<p>The overall aim of this research is to enhance knowledge related to soft tissue adaptation and behaviour following lower limb amputation and gain insight into the mechanisms of soft tissue damage: direct mechanical damage, ischaemia and reperfusion.</p> <p>This will be accomplished by investigating the physiological effect of applying representative loads first to the healthy calf tissue of people without amputation (Phase 1), and then the residual limb and contralateral limb of people with unilateral trans-tibial amputation (Phase 2), using a number of biophysical</p>

measures. Phase 1 was granted ethics approval (ERGO 29696) and has been implemented.

This proposal concerns Phase 2 of the research project: Residual limb and contralateral limb tissue's physiological response to representative prosthetic loading

The key objectives within this phase are to:

- Collect biophysical measurements for the residual and contralateral limb's, of people with trans-tibial amputation, under representative prosthetic loading
- Implement MRI to observe the biomechanical effect of representative prosthetic loading to the residual and contralateral limbs of people with trans-tibial amputation
- Implement MRI to observe the anatomical differences between residual and contralateral limbs of people with trans-tibial amputation.

2.5 (M*) Background to study (a brief rationale for conducting the study):

Amputation is the surgical or traumatic loss of all or part of a limb or extremity. The care and rehabilitation of people post-amputation is paramount to recover and maintain function, leading to an improved or restored quality of life. Amputation is a global healthcare concern, particularly with the growing and ageing population and an increase in risk factors for conditions that cause dysvascularity and neuropathy, such as diabetes. This research will focus on lower limb amputations (particularly trans-tibial/below knee) due to the high incidence and reliance on the lower limbs for mobility. Below Knee Amputation (BKA) is also the preferred surgical technique over Above Knee Amputation (AKA) due to superior function. The residual limb, made up of soft tissues overlying amputated bone, forms a critical interface with the socket, which is used to suspend most prosthetic limbs. It is of critical importance to understand the underlying physiology of the residual limb soft tissues, to understand how they tolerate loads. This knowledge can be used to enhance the design of prosthetic devices and enable clinicians to prevent compromise to the viability of skin, fat and muscle tissues, which can lead to the requirement of revision surgery to a higher level of amputation. Furthermore, the biomechanical adaptation of the limb post-amputation, is of interest. New knowledge in this area is required to assist in the development of effective practices to optimise residual limb care and gait rehabilitation and decrease the number of fitting iterations. An optimal socket will expedite biomechanical adaptation of the soft tissues to enable comfortable and stable load transfer. Knowledge of residual limb tissue adaptation and behaviour will facilitate the creation of more realistic computational models of the residual limb to enable increased accuracy when predicting tissue strains and behaviour under applied loads. Utilisation of these predictions with sensor technologies could allow enhanced understanding of the mechanisms contributing to tissue damage at the residual limb-socket interface.

2.6 (M*) Key research question (Specify hypothesis if applicable):

- Key research question- What are the physiological effects of applying representative prosthetic loading to the residual and contralateral limb soft tissues of people with unilateral trans-tibial amputation?
- Key hypothesis- Baseline and loaded biophysical measurements will be significantly different.

2.7 (M*) Study design (Give a brief outline of basic study design)

Outline what approach is being used, why certain methods have been chosen.

A multi-modal biophysical measurement study will be implemented, characterising the physiological behaviour of the soft tissues, with respect to mechanisms of tissue damage under static loading.

A pressure cuff will be applied, in turn, to the residual limb and contralateral limb calf of participants, and incrementally inflated from 20-60 mmHg in 10 mmHg increments every 10 minutes, representative of loads that a person with amputation would experience during early post-amputation rehabilitation with early walking aids.

The following non-invasive measurements will be taken in three positions relevant to prosthesis load-bearing (patellar tendon, lateral calf and posterior calf):

- Oxygen and Carbon Dioxide transcutaneous gas tensions (TcPO₂/TcPCO₂) as established predictive indicators for ischaemia.
- Biomarkers released at the skin will be collected using SebuTape, as the IL-1 α inflammatory cytokine is a known precursor to tissue injury.
- Mechanical properties of the tissues, namely tone, stiffness and elasticity, will be measured using the MyotonPRO device (Myoton AS, Tallinn, Estonia) to investigate adaptation.
- Finally, Magnetic Resonance Imaging will be used in parallel with these measurements, to observe the volumetric soft tissue deformations which result from the applied surface loads and thus provide insight into the relative influences of the different soft tissue injury mechanisms.

Biophysical measurements and MRI will be implemented in two separate testing sessions each lasting up to approximately 3 hours, with each participant, as follows:

Testing Session 1- Gas tension and MyotonPRO measurements and biomarker collection while contralateral and residual limbs are unloaded, loaded incrementally with representative pressure and following unloading.

Testing Session 2- MRI while residual and contralateral limbs are unloaded, and loaded using the pressure cuff.

The methods and techniques utilised for this research are well-established and have previously been used in studies that have been granted ethical approval. Full informed consent must be given by each participant whom has the right to withdraw at any time without reason.

3. SAMPLE AND SETTING

3.1 (M*) How are participants to be approached? Give details of what you will do if recruitment is insufficient. If participants will be accessed through a third party (e.g. children accessed via a school) state if you have permission to contact them and upload any letters of agreement to your submission in ERGO.

People with trans-tibial amputation will be recruited from the community via poster advertisement through organisations such as Finding Your Feet and LimbCare. Email responses of agreement have been uploaded with this application.

AMENDMENT 1: Colleagues Dr Alex Dickinson, Dr Maggie Donovan-Hall, Dr Cheryl Metcalf and Chantel Ostler will be conducting Patient & Public Involvement (PPI) workshops with prosthetic limb users local to Winchester. This activity is funded by the Institute for Life Sciences, and will be attended by several people who will potentially be eligible for the present study. I have the workshop organisers' permission to display the study poster at the events.

3.2 (M*) Who are the proposed sample and where are they from (e.g. fellow students, club members)? List inclusion/exclusion criteria if applicable. NB The University does not condone the use of 'blanket emails' for contacting potential participants (i.e. fellow staff and/or students).

It is usually advised to ensure groups of students/staff have given prior permission to be contacted in this way, or to use of a third party to pass on these requests. This is because there is a potential to take advantage of the access to 'group emails' and the relationship with colleagues and subordinates; we therefore generally do not support this method of approach.

If this is the only way to access a chosen cohort, a reasonable compromise is to obtain explicit approval from the Faculty Ethics Committee (FEC) and also from a senior member of the Faculty in case of complaint.

Thirty people with trans-tibial amputation will be recruited from the community via poster advertisement through organisations such as Finding Your Feet and LimbCare and at Institute for Life Sciences Patient and Public Engagement Workshops.

Inclusion Criteria:

- Aged over 18 years old
- Unilateral trans-tibial amputation
- No allergy/sensitivity to any substance used in this study: Micropore tape to secure sensors, Sebutape
- No contraindications to use of MRI
- Individual not at high risk of Deep Vein Thrombosis
- No active skin conditions in measurement areas
- Individuals able to lie on their back for 1 hour within an MRI scanner, remaining as still as possible for six 5 minute periods while images are being taken
- Individuals able to sit on a hospital bed, with an angle adjustable back rest, with their legs outstretched and if possible hold their bladder for approximately 1.5-2 hours while sensors are in place

Exclusion Criteria:

- Pacemaker, metallic or active implants
- Presence of metal fragments in the eyes
- Allergies of Micropore tape or Sebutape
- Increased risk for Deep Vein Thrombosis (for example: genetic clotting disorders, use of recreational drugs, presence of malignant tumour or cancer, recent surgery, congestive heart failure, irritable bowel disease)
- Inability to give informed written consent
- Current skin condition in measurement area
- Pregnancy
- Claustrophobia
- Unable to remain still for 20 minute periods

3.3 (M*) Describe the relationship between researcher and sample (Describe any relationship e.g. teacher, friend, boss, clinician, etc.)

Participants must be volunteers however they may be colleagues/friends of the researcher.

3.4 (M*) Describe how you will ensure that fully informed consent is being given: (include how long participants have to decide whether to take part)

Potential participants will be given a Participant Information Sheet by email and will be given at least 24 hours to decide whether they would like to take part in the study. Participants will have the opportunity to ask the research team any questions and will be able to withdraw from the study, no questions asked, at any point.

Participants will be asked to complete an informed consent form, prior to their participation and then a questionnaire and an MRI Safety Questionnaire prior to testing sessions. The MRI Safety Questionnaire will be countersigned by a trained radiographer or someone equivalent that is trained in taking informed consent for MRI. If a participant meets any of the exclusion criteria or does not adhere to the inclusion criteria they will not be able to participate in this research, for their own safety.

One additional general study exclusion criterion is for people unable to provide informed consent due to cognitive impairment.

4. RESEARCH PROCEDURES, INTERVENTIONS AND MEASUREMENTS

4.1 (M*) Give a brief account of the procedure as experienced by the participant

(Make clear who does what, how many times and in what order. Make clear the role of all assistants and collaborators. Make clear total demands made on participants, including time and travel). Upload any copies of questionnaires and interview schedules to your submission in ERGO.

A potential participant will be emailed a participant information sheet. If they decide that they would like to take part, they will first be asked to complete and sign a consent form to confirm their informed participation. They will then be asked to complete and return a questionnaire to obtain information about their amputation and further assess whether they fit the criteria to participate. The participant will also be asked to complete a Magnetic Resonance Imaging (MRI) Safety Questionnaire to ensure their safety. If a participant answers yes to any of the safety questions, for their own safety, they may not be able to participate.

If they fit the criteria, they will then be contacted by the researcher to meet at the University of Southampton Clinical Academic Facility at a pre-determined suitable time. The testing will be split up into two sessions each lasting up to approximately 3 hours. These sessions will be planned to fit best around a participant's schedule. They can be arranged for one long testing day, of ≈ 7 hours including ≈ 1 hour long break in between sessions, or split up over two dates. Sessions can also be scheduled for evenings or Saturdays. At the start of each session the researcher will ask the participant if they have read and understood the information in the participant information sheet and will answer any questions.

During Testing Session 1 participants will be asked to sit on a standard hospital bed with adjustable back rest with their legs supported by foam cushions. They will need to wear comfortable clothes for this and shorts or trousers that can be rolled up to above the knees. The following measurements will be set up by the researcher and taken during these sessions:

- Oxygen and Carbon Dioxide gas tensions will be measured in three places via sensors stuck to the skin. Use of these sensors requires direct skin contact so participants will be asked to shave the three measurement areas 48 hours prior to the sessions. The sensors will feel warm as they are heated during use.

- Proteins secreted from the skin will be collected during the sessions using a special tape (SebuTape). The tape will be flattened on to the skin using a roller and removed after 2 minutes.

- Mechanical properties of the tissues will be measured using the MyotonPRO. This is a hand held device that contacts the surface of the skin and measures oscillations from a mechanical impulse.

- Interface pressure measurements will be taken during loading conditions at the measurement areas using air filled bladders.

The setup and full testing period will be approximately 3 hours for each of the testing sessions during which the pressure cuff will be inflated incrementally from 20-60 mmHg. It will be preferable if participants could stay attached to the measurement sensors throughout the whole testing session.

If at any point during the testing a participant does not feel comfortable in proceeding then the pressure cuff and measurement sensors will be removed. Pressure will be reduced at 2-3mmHg/second according to World Health Organisation guidelines, in order to avoid reperfusion injury.

During Testing Session 2, after an acclimatisation period of 20 minutes, a participant's residual limb and contralateral leg will be imaged using Magnetic Resonance Imaging (MRI). For this testing session participants will be asked to wear a hospital gown and will be given time to change during the acclimatisation period. Prior to imaging the researcher will attach a number of small oil filled capsules to their leg, using double sided tape, which will be used to interpret scale in MR scans.

Five MR scans will be taken, by an MRI operator; three with no loading applied and the pressure cuff inflated to 20 and 60 mmHg. Each scan will take approximately 10 minutes. In all cases participants will lie on their back in the scanner with their legs slightly elevated.

It will be important to remain as still as possible while the images are being taken. There will be an approximately 20 minute rest period in between residual limb and contralateral limb imaging, in which participants will be able to use the toilet and walk around.

If at any point during the testing a participant does not feel comfortable in proceeding then the pressure cuff will be removed and they will be assisted out of the MRI suite.

Note- The order of testing session's may be different dependent on the participant's availability and the availability of the MRI scanner. Participant's will be notified which testing session they are attending.

5. STUDY MANAGEMENT

5.1 (M*) State any potential for psychological or physical discomfort and/or distress?

- The use of Magnetic Resonance Imaging could cause injury if a participant were to have a pacemaker or metallic implant, by heating or magnetic attraction. Some people can also find the MRI environment claustrophobic.

5.2 (M*) Explain how you intend to alleviate any psychological or physical discomfort and/or distress that may arise? (if applicable)

Potential participants will not be able to participate should they answer yes to any questions within the participant questionnaire or MRI questionnaire that suggest the MR scan would put them at any risk. During the MRI session participants will have contact with the researcher at all times so will be able to talk to them immediately should they become uncomfortable in the MRI environment. The MRI testing session is not a diagnostic scan. The images will be reviewed by a Radiologist Consultant and if any abnormality is observed a participant's GP will be contacted, who will decide if further investigation is required. - If a participant feels discomfort during any of the testing sessions the pressure cuff will be removed and the testing stopped.

5.3 Explain how you will care for any participants in 'special groups' (i.e. those in a dependent relationship, vulnerable or lacking in mental capacity) (if applicable)?

N/A

5.4 Please give details of any payments or incentives being used to recruit participants (if applicable)?

Participants will receive £75 at the start of each of the two testing sessions, to reimburse their travel and as a thank you for their time.

5.5 i) How will participant anonymity and/or data anonymity be maintained (if applicable)?

Two definitions of anonymity exist:

i) Unlinked anonymity - Complete anonymity can only be promised if questionnaires or other requests for information are not targeted to, or received from, individuals using their name or address or any other identifiable characteristics. For example if questionnaires are sent out with no possible identifiers when returned, or if they are picked up by respondents in a public place, then anonymity can be claimed. Research methods using interviews cannot usually claim anonymity – unless using telephone interviews when participants dial in.

ii) Linked anonymity - Using this method, complete anonymity cannot be promised because participants can be identified; their data may be coded so that participants are not identified by researchers, but the information provided to participants should indicate that they could be linked to their data.

Linked anonymity. Participant identifiable information will be anonymised with corresponding data being given an identification code assigned to the participant upon recruitment. Participant's data and the assigned identification code will be stored on a University password protected computer. The consent form and MRI Questionnaire will be the only places whereby a participant's identity and assigned identification code can be linked and these will be secured in the principal investigator's locked office. Only named researchers will have access to the password protected computer.

5.5 ii) How will participant confidentiality be maintained (if applicable)?

Confidentiality is defined as the non-disclosure of research information except to another authorised person. Confidential information can be shared with those who are already party to it, and may also be disclosed where the person providing the information provides explicit consent.

Only the consent form and MRI Safety Questionnaire will contain identifiable information and these will be kept confidential in a locked filing cabinet in the principal investigator's locked office. Other participant identifiable data will be anonymised and kept confidential with a random code being assigned to each participant's dataset. Participant data will be stored on a University password protected computer accessible to only the named researchers in this document.

5.6 (M*) How will personal data and study results be stored securely during and after the study? Researchers should be aware of, and compliant with, the Data Protection policy of the University. You must be able to demonstrate this in respect of handling, storage and retention of data.

Data and study results will be collected within the Clinical Academic Facility (Faculty of Health Sciences, at University Hospital Southampton) and stored on a password protected University computer for analysis. According to the University's Research Data Management Policy, the anonymised collected data will be stored for 10 years after collection.

5.7 (M*) Who will have access to these data?

The named researchers in this document will have access to the data for analysis. This research and results will be disseminated by publishing in appropriate research journals (such as the Journal of Applied Physiology, Medical Engineering & Physics, and Clinical Biomechanics) and presenting at appropriate conferences (for example International Society for Prosthetics and Orthotics (ISPO), Scientific Meetings and conferences). Post-analysis anonymised collected data will also be used in as part of the PhD qualification. If participants would prefer their anonymised data to not be included in research publications any time during or after the study will be encouraged to inform the researcher.

N.B. – Before you upload this document to your ERGO submission remember to:

1. Complete ALL mandatory sections in this form
2. Upload any letters of agreement referred to in question 3.1 to your ERGO submission
3. Upload any interview schedules and copies of questionnaires referred to in question 4.1

PART B – Action Plan**Risk Assessment Action Plan**

Part no.	Action to be taken, incl. Cost	By whom	Target date	Review date	Outcome at review date

Responsible manager's signature:		Responsible manager's signature:	
Print name:	Date:	Print name:	Date:

Assessment Guidance

1. Eliminate	Remove the hazard wherever possible which negates the need for further controls	If this is not possible then explain why	
2. Substitute	Replace the hazard with one less hazardous	If not possible then explain why	
3. Physical controls	Examples: enclosure, fume cupboard, glove box	Likely to still require admin controls as well	
4. Admin controls	Examples: training, supervision, signage		
5. Personal protection	Examples: respirators, safety specs, gloves	Last resort as it only protects the individual	

LIKELIHOOD	5	10	15	20	25
	4	8	12	16	20
	3	6	9	12	15
	2	4	6	8	10
	1	2	3	4	5
	1	2	3	4	5
	IMPACT				

Risk process

1. Identify the impact and likelihood using the tables above.
2. Identify the risk rating by multiplying the impact by the likelihood using the coloured matrix.
3. If the risk is amber or red – identify control measures to reduce the risk to as low as is reasonably practicable.
4. If the residual risk is green, additional controls are not necessary.
5. If the residual risk is amber the activity can continue but you must identify and implement further controls to reduce the risk to as low as reasonably practicable.
6. If the residual risk is red **do not continue with the activity** until additional controls have been implemented and the risk is reduced.
7. Control measures should follow the risk hierarchy, where appropriate as per the pyramid above.
8. The cost of implementing control measures can be taken into account but should be proportional to the risk i.e. a control to reduce low risk may not need to be carried out if the cost is high but a control to manage high risk means that even at high cost the control would be necessary.

Impact		Health & Safety
1	Trivial - insignificant	Very minor injuries e.g. slight bruising
2	Minor	Injuries or illness e.g. small cut or abrasion which require basic first aid treatment even in self-administered.
3	Moderate	Injuries or illness e.g. strain or sprain requiring first aid or medical support.
4	Major	Injuries or illness e.g. broken bone requiring medical support >24 hours and time off work >4 weeks.
5	Severe – extremely significant	Fatality or multiple serious injuries or illness requiring hospital admission or significant time off work.

Likelihood	
1	Rare e.g. 1 in 100,000 chance or higher
2	Unlikely e.g. 1 in 10,000 chance or higher
3	Possible e.g. 1 in 1,000 chance or higher
4	Likely e.g. 1 in 100 chance or higher
5	Very Likely e.g. 1 in 10 chance or higher

Participant Information Sheet



Participant Information Sheet

Study Title: Measuring lower limb response to pressure following lower limb amputation

Researcher: Jennifer Bramley
ERGO number: 41864

You are being invited to take part in the above research study. To help you decide whether you would like to take part or not, it is important that you understand why the research is being done and what it will involve. Please read the information below carefully and ask questions if anything is not clear or you would like more information before you decide to take part in this research. You may like to discuss it with others but it is up to you to decide whether or not to take part. If you are happy to participate you will be asked to sign a consent form.

What is the research about?

This study is part of a PhD project funded by the Institute of Life Sciences (ILS), part of the University of Southampton, and Engineering and Physical Sciences Research Council (EPSRC). Although this research will be conducted on NHS property, at Southampton General Hospital, the NHS is not sponsoring or involved in this study.

The project focusses around the care and rehabilitation of people with lower limb amputation to recover and maintain function, leading to an improved or restored quality of life. After amputation the remaining lower limb forms an important link with the prosthetic device. The use of a prosthetic during daily activities, such as walking, applies pressure to the amputated leg, which can result in damage, pain and discomfort. We are interested in studying how lower limb amputation and prosthetic use effects skin and muscle response to loading.

The aim of this research is to further understand how skin and muscles react to forces typically observed between the amputated limb and socket. Further understanding in this area will assist in the development of new prosthetic devices and aid the rehabilitation process after amputation.

Why have I been asked to participate?

You have been asked to volunteer for this study as you are above 18 years of age, have a below-knee amputation and are in good health.

Before proceeding please read the following inclusion and exclusion criteria for this study, carefully:

Inclusion Criteria:

- Have a below-knee amputation on one side, above the ankle
- No known allergies/sensitivity to medical tape which will be used to secure sensors
- No current skin conditions in the area below your knee and above your ankle
- Able to lie on your back for 1 hour within an MRI scanner, remaining as still as possible for six 5 minute periods while images are being taken
- Able to lie/sit on a hospital bed, with an angle adjustable back rest, with your legs outstretched and if possible not go to the toilet for approximately 1.5-2 hours while sensors are in place

Exclusion Criteria:

- Pacemaker, metallic or active implants
- Presence of metal fragments in the eyes
- Increased risk for Deep Vein Thrombosis (for example: genetic clotting disorders, use of recreational drugs, presence of malignant tumour or cancer, recent surgery, congestive heart failure, irritable bowel disease)

[24/08/2018] [PIS_18_1_V2]

[ERGO Number: 41864]

- Unable to give informed written consent- An informed consent form will be provided if you would like to participate.
- Current pregnancy
- Claustrophobia

What will happen to me if I take part?

If you would still like to participate you will be asked to sign a consent form to confirm your participation and that you have read and understood this information. You will be able to ask the researcher any questions at any point. If you decide to take part you will be asked to complete and return a questionnaire to assess whether you fit the criteria to participate and find out more about your amputation and prosthetic use. If you have any difficulties or questions about completing the questionnaire, please contact the researcher (see details below). You will also be asked to complete a Magnetic Resonance Imaging (MRI) Safety Questionnaire to ensure your safety. There are no documented risks of having an MRI scan as long as all of the pre-scan safety checks have been completed. If you answer yes to any of the safety questions there is a chance that, for your own safety, you will not be able to participate.

You will then be contacted by the researcher to meet her at the **University of Southampton Clinical Academic Facility**, University Hospital Southampton (UHS) at a time suitable for you. This research will be split up into **two separate sessions each lasting up to approximately 3 hours**. These sessions will be planned to fit best around your schedule. They can be arranged for one long testing day, of ≈ 7 hours including a ≈ 1 hour break in between sessions, or split up over two dates. Sessions can also be scheduled for evenings or Saturdays.

Approximately **two days prior to testing sessions** you will be asked to shave **5 x 5 cm** areas in three locations on both lower limbs (Figure 1). These areas will be used to measure blood flow and response at the skin surface.

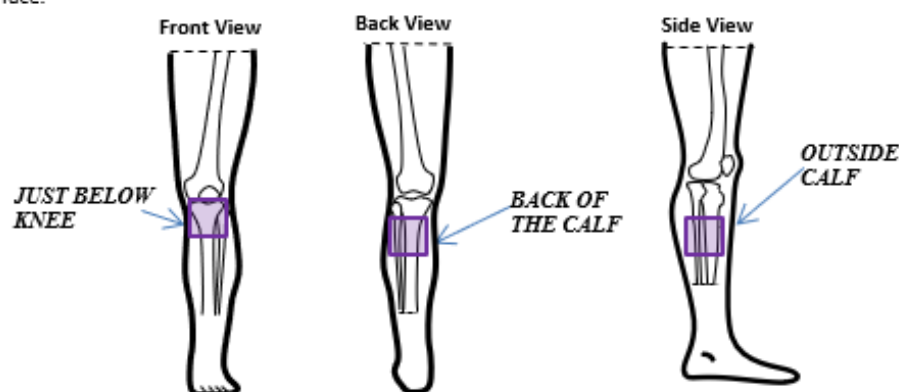


Figure 1 Labelled areas of measurement of the right leg (where measurements will be taken are in bold & highlighted purple)

At the start of each session the researcher will ask you if you are happy with what will happen during the session and if you have any questions.

During **Testing Session 1** you will be asked, by the researcher, for your age, gender, height and weight. Your limb circumferences will be measured and you will be asked about your activity levels and socket use. This should take no more than 15 minutes.

A silicone liner, with holes allowing for sensors will be wrapped around your limbs and a pressure cuff will be used to slowly apply pressure. Within this testing session you will be asked to sit on a hospital bed with your limbs supported by foam cushions.



You will be able to adjust the angle of the back rest to a comfortable position. You will need to wear comfortable clothes for this and shorts or trousers that can be rolled up to above the knees. The following measurements will be set up and taken during this session:

- Oxygen and Carbon Dioxide will be measured via sensors stuck to the skin. The sensors may feel warm as they are heated during use.
- Proteins released from the skin will be collected during the session using a special tape (SebuTape). The tape will be flattened on to the skin using a roller and removed after 2 minutes. The application and removal of the tape should not cause any discomfort.
- Muscle and fat properties will be measured by a hand-held device in contact with the skin that will apply brief gentle taps.
- Pressure will be measured using air filled sensors that will feel like a pulse.

Measurement set up will take approximately 20 minutes. Each pressure will be applied for 10 minute periods and up to five will be used. After which the pressure cuff will be removed and there will be a 30 minute rest period. During this 30 minutes sensors will continue to measure. While the pressure cuff is in place and during the rest period it would be preferable if you could stay attached to the measurement sensors.

During **Testing Session 2**, after an acclimatisation period of 20 minutes, your legs will be imaged using Magnetic Resonance Imaging (MRI). For this testing session you will be asked to wear a hospital gown, with your underwear underneath, and will be given time to change during the acclimatisation period. Prior to imaging a number of small oil filled capsules will be attached to your leg, using double-sided tape, as these appear bright on images.

Your legs will then be scanned five times, three times with no load, then with two different pressures applied by an inflatable cuff. Each scan will take approximately 10 minutes. In all cases you will lie on your back in the scanner with your legs slightly elevated on foam cushions.

If at any point during the testing you do not feel comfortable in proceeding then the pressure will be removed (if applicable) and measurement sensors will be removed.

Are there any benefits in my taking part?

A £75 Amazon voucher will be given at the start of each of the two testing sessions, after consent has been given, for travel expenses and as a thank you. You will also be helping to further knowledge regarding skin and muscle response to loading which could help the design of new prosthetic sockets and help to reduce amputated limb damage.

Are there any risks involved?

There are no anticipated physical or psychological risks involved in this testing, your safety will be ensured at all times and the researcher will remain with you throughout.

Electrical cables will be used in this study and could provide a tripping hazard. Cables will be kept as neat and tidy as possible but please do take care. Electrical equipment is being used so there is a theoretical chance of electrical shock. This would be very rare as all of the equipment in use is electrically insulated or battery charged and has been Portable Appliance Testing (PAT) tested for electrical safety.

**Will my participation be confidential?**

Your participation and the information we collect about you during the course of the research will be kept strictly confidential.

Only members of the research team and responsible members of the University of Southampton may be given access to data about you for monitoring purposes and/or to carry out an audit of the study to ensure that the research is complying with applicable regulations. Individuals from regulatory authorities (people who check that we are carrying out the study correctly) may require access to your data. All of these people have a duty to keep your information, as a research participant, strictly confidential.

The researcher's carrying out the testing sessions will keep a copy of your age, gender, height, weight and measurements taken during testing linked to a testing session code. All data will be securely stored in a password protected secure location and recorded data for further analysis will be anonymised. This study is part of funded research it is expected that the anonymised collected data will be stored in the University of Southampton's repository for at least 10 years after the study. This repository is highly secure to protect the stored data. All files will be kept in compliance with the University Data Protection Guidelines prior to being deposited in the repository.

Post-analysis anonymised collected data will be used in publications and presentations to display work and as part of the PhD qualification. If you would prefer your data to not be accessible to third parties at any time during or after the study please inform the researcher.

Do I have to take part?

No, it is entirely up to you to decide whether or not to take part. If you decide you want to take part, you will need to sign a consent form to show you have agreed to take part. If you would like to take part please contact the researchers using the details below and at the end of this information sheet.

What happens if I change my mind?

Your participation is voluntary and you may withdraw from the any of the sessions at any time, without reason. Your withdrawal will not affect your legal and medical rights. If you wish to withdraw please contact the researchers using the provided details.

What will happen to the results of the research?

Your personal details will remain strictly confidential. Research findings made available in any reports or publications will not include information that can directly identify you without your specific consent. Post-analysis anonymised collected data will be used in publications and presentations to display work and as part of the PhD qualification. If you would prefer your data to not be included in research publications at any time during or after the study please inform the researcher.

Where can I get more information?

If you would like more information, to participate or to contact the researchers please use the following details:

Jennifer Bramley- j.l.bramley@soton.ac.uk (Researcher)

Dr Alex Dickinson- alex.dickinson@soton.ac.uk (Head of Research Team)

What happens if there is a problem?

If you have a concern about any aspect of this study, you should speak to the researchers who will do their best to answer your questions.

If you remain unhappy or have a complaint about any aspect of this study, please contact the University of Southampton Research Integrity and Governance Manager (023 8059 5058, rgoinfo@soton.ac.uk).

**Data Protection Privacy Notice**

The University of Southampton conducts research to the highest standards of research integrity. As a publicly-funded organisation, the University has to ensure that it is in the public interest when we use personally-identifiable information about people who have agreed to take part in research. This means that when you agree to take part in a research study, we will use information about you in the ways needed, and for the purposes specified, to conduct and complete the research project. Under data protection law, 'Personal data' means any information that relates to and is capable of identifying a living individual. The University's data protection policy governing the use of personal data by the University can be found on its website (<https://www.southampton.ac.uk/legalservices/what-we-do/data-protection-and-foi.page>).

This Participant Information Sheet tells you what data will be collected for this project and whether this includes any personal data. Please ask the research team if you have any questions or are unclear what data is being collected about you.

Our privacy notice for research participants provides more information on how the University of Southampton collects and uses your personal data when you take part in one of our research projects and can be found at <http://www.southampton.ac.uk/assets/sharepoint/intranet/ls/Public/Research%20and%20Integrity%20Privacy%20Notice/Privacy%20Notice%20for%20Research%20Participants.pdf>

Any personal data we collect in this study will be used only for the purposes of carrying out our research and will be handled according to the University's policies in line with data protection law. If any personal data is used from which you can be identified directly, it will not be disclosed to anyone else without your consent unless the University of Southampton is required by law to disclose it.

Data protection law requires us to have a valid legal reason ('lawful basis') to process and use your Personal data. The lawful basis for processing personal information in this research study is for the performance of a task carried out in the public interest. Personal data collected for research will not be used for any other purpose.

For the purposes of data protection law, the University of Southampton is the 'Data Controller' for this study, which means that we are responsible for looking after your information and using it properly. The University of Southampton will keep identifiable information about you for 10 years after the study has finished after which time any link between you and your information will be removed.

To safeguard your rights, we will use the minimum personal data necessary to achieve our research study objectives. Your data protection rights – such as to access, change, or transfer such information – may be limited, however, in order for the research output to be reliable and accurate. The University will not do anything with your personal data that you would not reasonably expect.

If you have any questions about how your personal data is used, or wish to exercise any of your rights, please consult the University's data protection webpage (<https://www.southampton.ac.uk/legalservices/what-we-do/data-protection-and-foi.page>) where you can make a request using our online form. If you need further assistance, please contact the University's Data Protection Officer (data.protection@soton.ac.uk).

Thank you very much for taking the time to read this information and considering participating. If you would like to participate or would like more information please use the following contact details:

Jennifer Bramley- j.l.bramley@soton.ac.uk (Researcher)

[24/08/2018] [PIS_18_1_V2]

[ERGO Number: 41864]



CONSENT FORM

Study title: Measuring lower limb response to pressure following amputation

Researcher name: Jennifer Bramley

ERGO ID: ERGO 41864

Participant Identification Number:

Please initial the box(es) if you agree with the statement(s):

I have read and understood the information sheet (24/08/2018/PIS_18_1_V2) and have had the opportunity to ask questions about the study.	
I agree to take part in this research project and agree for my data to be used for the purpose of this study.	
I understand my participation is voluntary and I may withdraw (at any time) for any reason without my rights being affected.	

Name of participant (print name).....

Signature of participant.....

Date.....

I understand that the information collected about me will be used to support other research in the future, and may be shared anonymously with other researchers	
---	--

Name of participant (print name).....

Signature of participant.....

Date.....

Name of researcher (print name).....

Signature of researcher

Date.....

24/08/2018 ICF_18_1_V2



Pre-Participation Questionnaire

Study Title: Measuring lower limb response to pressure following amputation

Please answer all of the questions below. In case you answer yes, please provide further details.

Researcher: Jennifer Bramley

Ethics ID: ERGO 41864

(For researcher) Participant ID Number _____ **Date(s) of Sessions:** _____

Participant Details

Gender:

Age:

Weight (kg):

Height (cm):

On which side is your amputation?

Left/Right

Approximately when was your amputation?

To the best of your knowledge what was the cause of your amputation?

Approximately how many hours per day do you wear your socket?

To the best of your knowledge what type(s)/make(s) of prosthetic device do you use?

Do you use any non-prosthetic assistive devices such as a cane or walker? Please state if 'yes'

24/08/2018 PQ_18_1_V2

ERGO ID : 41864



Do you have any current
amputated limb skin problems?
(if 'yes' please give further details)

Yes/No

Have you ever had any amputated
limb skin problems?
(if 'yes' please give further details)

Yes/No

Do you have any other skin
conditions?

Yes/No

Do you have any pre-existing
medical conditions that are known
to effect skin blood flow (e.g.
Diabetes or Peripheral Vascular
Disease)? Please specify if 'yes'

Yes/No

Are you aware of any allergies?

Yes/No

Do you have any liver, heart,
kidney or bowel problems?

Yes/No

Do you have a pacemaker or any
metallic implants?

Yes/No



Are you aware of any increased risk for Deep Vein Thrombosis?

Yes/No

Do you have a genetic clotting disorder or take anticoagulant medication?

Yes/No

Do you smoke?

Yes/No

Have you had any surgical procedures in the last 6 weeks?

Yes/No

Do you suffer from claustrophobia?

Yes/No

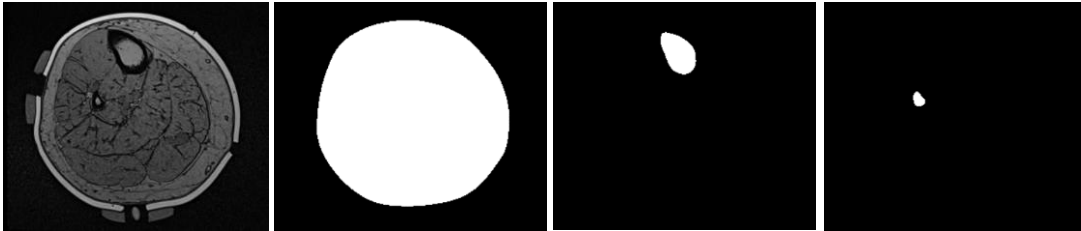
Are you able to remain lying on your back for 20 minute periods?

Yes/No

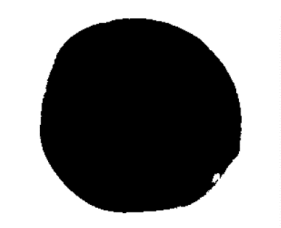
The Magnetic Resonance Imaging session is not for medical purposes. However, as part of the study images will be looked at by a radiologist consultant and if anything unexpected is observed your doctor will be contacted by letter to decide if further investigation is required. Please provide contact details for your doctor below:

Appendix C-Step-by-Step Tissue Composition Image Analysis

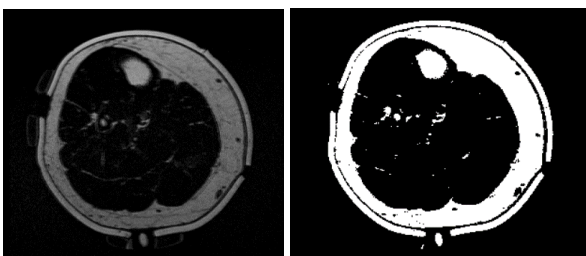
1. Use the out of phase image stack to determine slice to start and end processing and for interpolation.
2. Use interpolate macro and draw on liner edge and tibia and fibula edge to create masks of everything but the liner (mask1), the tibia and fibula. Use Polygon selection to draw every 5 slices and add each to ROI manager. Then interpolate, store segmentation, create mask and save mask as a tiff and an MHD/MHA file so that it can be used in ScanIP if required.



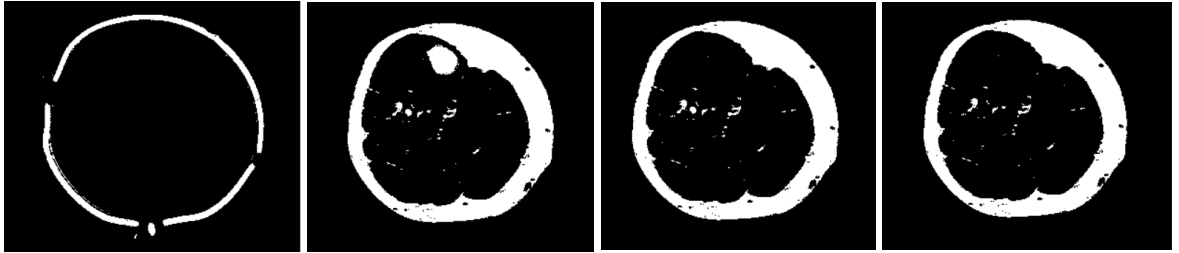
3. Calculate the whole soft tissue area by thresholding mask one to reverse the colours and then go to Analyse-Analyse Particles and specify 1000-20000, selecting to show masks and ensure that display results and add to manager are ticked. NOTE- Make sure mask has the correct scale (analyse-set scale 1.6 pixels = 1mm). Copy area results to Excel.



4. Use fat saturated baseline stacks for Fat Sat processing.
5. Subtract 10 from raw image to get rid of some of the background noise. Image-Adjust-Auto threshold stack. Use IsoData method.



6. Go to processing-image calculator and subtract Mask 1 from the auto threshold stack to get just the liner then subtract this from the auto threshold stack to get just the soft tissues and bone. Then subtract the tibia and fibula so that you are only left with adipose tissue.



7. Threshold to reverse the colours.



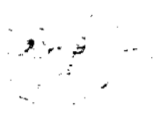
8. Use the first stack to measure the superficial adipose tissue area. Go to Analyse-Analyse Particles and specify 1000-20000, selecting to show masks and ensure that display results and add to manager are ticked. Copy area results to Excel.



9. Reverse the colours of the superficial adipose tissue mask by thresholding and subtract it from the fat only stack. Save superficial adipose and other masks as MHD/MHA files so that the masks can be used in ScanIP for segmentation if required.



10. To get the infiltrating adipose area reverse the colours of this mask by thresholding and go to Analyse-Analyse Particles and specify 1.44(size chosen as 2 pixels squared)-1000, Select to show masks and ensure that display results, add to manager and summarise are ticked. Copy area results to Excel.




Appendix D-Detailed Testing Session Activity Checklist- Participants without Amputation

Pre-Session Checklist

Phase	Overview	Detailed Activities	≈Start Time (hours:mins)	Complete
Pre-Session	Participant Discussion	Make sure participant has read information	At least 2 days before biophysical measures session 0:00	
		Pre-participation Questionnaire		
		MRI Questionnaire		
		Answer any questions		
		Complete consent form if participant happy to continue and after checking questionnaires		
		Complete participant demographics		
	Shaving Measurement Areas	Mark out 5 x 5 cm patellar tendon area- Bottom edge at top of, and central with, tibial tuberosity	0:20	
		Mark out 5 x 5 cm tibialis anterior area- Bottom of area 12 cm distal to top patella tendon area. Anterior of fibula with the head of the fibula outside of the top left corner		
		Mark out 5 x 5 cm posterior calf area- Bottom of area 12 cm distal to top patella tendon area and central		
		Shave areas		
		Measure calf circumference	0:35	
	Silicone Gel Liner	Cut length		
		Measure positions required for sensor holes		

Testing Session 1- Biophysical Measures Session Checklist

Phase	Overview	Detailed Activities	≈Start Time (hours:mins)	Complete
Pre-Session	Equipment set up	TCM (Technical Code 19100) and Pressure sensors ready for use	0:00 (carry out some activities day before if possible)	
		Sebutape application and retrieval equipment ready		
		Fluorbeam Infra-Red camera positioned (≈30 cm height)		
		USB/hard Drive ready for data storage		
		Participant bed, leg support and entertainment set up		
		Pressure cuff, liner and inserts ready for application		
	Remembraning 3 TGT transducers	Use filter paper to carefully remove moisture from sensor	0:15	
		Use prodder tool to remove 2 rubber bands and 2 membranes		
		Use filter paper to dab sensor		
		Holding sensor flat apply 2 drops of Electrolyte Solution (Dialysyte) on top (helps electron transfer of gas)		
		Push membrane on and discard green holder		
		Reattach sensor to monitor for calibration and press screen to calibrate		
	Making ICG 0.05% ICG solution for injection	Require ultra-pure water, ICG powder, needles, syringes, filter, vortex, scales, weighing basket, kitchen foil, gloves and lab coat - Wash equipment straight away after use. Get ultra-pure water from the test room (Siemens Ultra Clear) 2 squirts then wait until ≈0.06	0:30	
		Use weighing basket to measure out 0.01g ICG powder		
		Add 0.2ml ultra-pure water and mix until dissolved		
		Syringe 1.8ml (1800μl) ultra-pure water into a tube labelled 0.5% ICG stock		
		Add ICG mixture to 1.8ml to achieve 0.5% solution		
		Vortex for ≈1min to mix		
		Add 0.1ml of 0.5% solution to 1ml ultra-pure water to achieve desired 0.05% solution		
		Vortex for ≈1min to mix		
		Filter and place into short tube for better access, wrap with foil		
		Dispose of stock into orange bin		

Phase	Overview	Detailed Activities	≈Start Time (hours:mins)	Complete
Phase 1	Set up of Measurements and Acclimatisation	Collect Demographics and Consent if haven't already got. Record room temp & humidity	1:50	
		Intradermal injection (total 0.5 ml in two positions- toe webbing big toe and 2 nd toe) of ICG solution RECORD TIME - Participant to flex and extend toes for ≈30s	2:00	
		Apply O ₂ plus CO ₂ TGT sensor to Patellar Tendon - Peel backing off Fitment Ring and attach Fitment Ring in required position - Apply two drops of fitment fluid within Fitment Ring - Line up arrow on sensor with arrow on Fitment Ring and rotate clockwise approximately 90° until it feels tight/secure - Record time	2:03	
		Apply O ₂ TGT sensor to Tibialis Anterior as above - Record time	2:06	
		Apply O ₂ TGT sensor to posterior calf as above - Record time	2:09	
		Set TGT events- Record time and event	2:12	
		Apply sebutape 1 to patellar tendon (roller 5 times to secure in place) Start 2 minute stopwatch	2:15	
		Apply sebutape 2 to tibialis anterior (as above) Start 2 minute stop watch	2:16	
	 <p>Tweezers Position</p> <p>Sticky Side</p> <p>Take Baseline Measurements</p>	Remove sebutape 1 using tweezers and place into small tube (insert with non-sticky side facing outwards in tube)	2:17	
		Apply sebutape 3 to posterior calf (as above) Start 2 minute stop watch	2:17:30	
		Remove sebutape 2 as above	2:18	
		Remove sebutape 3 as above	2:19:30	
	*Mark Fluorbeam FOV on leg and measure	Ensure TGT measurements have stabilised (O ₂ 50-90mmHg, CO ₂ 36-50 mmHg)	2:20	PT-TA-PC-
		Use Fluorbeam (≈30 cm from leg, exposure ≈350 and make sure excitation box has been turned on) to locate a visible lymph vessel and mark on participants limb	2:25	
		5 minute imaging of lymph activity- RECORD TIME	2:30	

Category 1- O₂ (50-90), CO₂ (36-50)Ischaemia
CategoriesCategory 2- O₂ (decreases by >25%), CO₂ (minimal change)Category 3- O₂ (decreases by >25%), CO₂ (increases by >25%)

Phase	Overview	Detailed Activities	≈Start Time (hours:mins)	Complete
Phase 2	Set up liner and pressure cuff	Set TGT event. Apply silicone gel liner	2:35	
		Set event, apply pressure cuff, wait 10 mins		
	10 minute application of 20 mmHg	Record Time, set TGT event and inflate to 20 mmHg	2:50	PT-TA-PC-
		Start Lymph Imaging (after 5 mins application)	2:55	
	10 minute application of 30 mmHg	Record Time, set TGT event and inflate to 30 mmHg	3:00	PT-TA-PC-
		Start Lymph Imaging (after 5 mins application)	3:05	
	10 minute application of 40 mmHg	Record Time, set TGT event and inflate to 40 mmHg	3:10	PT-TA-PC-
		Start Lymph Imaging (after 5 mins application)	3:15	
	10 minute application of 50 mmHg	Record Time, set TGT event and inflate to 50 mmHg	3:20	PT-TA-PC-
		Start Lymph Imaging (after 5 mins application)	3:25	
	10 minute application of 60 mmHg	Record Time, set TGT event and inflate to 60 mmHg	3:30	PT-TA-PC-
		Start Lymph Imaging (after 5 mins application)	3:35	
Phase 3	Refractory Period same length as loading	Start another 5 minute lymph recording, record time, set TGT event and release pressure by 10 mmHg every 30 secs	3:40	
		Remove cuff and liner and set events	3:42	
		Stop lymph imaging (5 minutes into rest period)	3:45	
		Apply sebutape 1 to patellar tendon (roller 5 times to secure in place) Start 2 minute stopwatch	3:50	
		Apply sebutape 2 to tibialis anterior (as above) Start 2 minute stop watch	3:51:30	
		Remove sebutape 1 using tweezers and place into small tube (insert with non-sticky side facing outwards in tube)	3:52	
		Apply sebutape 3 to posterior calf (as above) Start 2 minute stop watch	3:53	
		Remove sebutape 2 as above	3:53:30	
		Remove sebutape 3 as above	3:55	
		Image lymph for final 5 minutes	4:25	
Phase 4	Interface Pressure Measurement	Apply pressure sensors underneath dummy TGT sensors	4:20	
		Apply liner and cuff- Record interface pressure	4:25	
		Inflate to 20 mmHg- Record pressure		
		Inflate to 30 mmHg- Record pressure		
		Inflate to 40 mmHg- Record pressure		
		Inflate to 50 mmHg- Record pressure		
		Inflate to 60 mmHg- Record pressure		
Release pressure, remove equipment and answer any participant questions			4:35	

Testing Session 2- MRI Session Checklist

Phase	Overview		Detailed Activities	≈Start Time (hours:mins)	Complete
Answer any participant questions				0:00	
Baseline	Set up and acclimatisation	Participant changes ready for MRI	0:05		
		Apply body coil in MRI participant supine	0:10		
	Global Baseline Image		0:20		
	Higher Resolution Baseline Images- FOV 6 cm over patellar tendon and 6 cm over other measurement areas		0:30		
Images During Loading	Apply fixation rings, dummy sensors, liner and set up pressure cuff		0:40		
	20 mmHg Cuff Pressure	Inflate pressure cuff to 20 mmHg	0:50		
		After 10 minutes take two high resolution images 6 cm over patellar tendon and 6 cm over other measurement areas	1:05		
	30 mmHg Cuff Pressure	Inflate pressure cuff to 30 mmHg	1:20		
		After 10 minutes take two high resolution images 6 cm over patellar tendon and 6 cm over other measurement areas	1:30		
	40 mmHg Cuff Pressure	Inflate pressure cuff to 40 mmHg	1:35		
		After 10 minutes take two high resolution images 6 cm over patellar tendon and 6 cm over other measurement areas	1:45		
	50 mmHg Cuff Pressure	Inflate pressure cuff to 50 mmHg	1:50		
		After 10 minutes take two high resolution images 6 cm over patellar tendon and 6 cm over other measurement areas	2:00		
	60 mmHg Cuff Pressure	Inflate pressure cuff to 60 mmHg	2:05		
		After 10 minutes take two high resolution images 6 cm over patellar tendon and 6 cm over other measurement areas	2:15		
Release pressure, remove equipment and answer any participant questions			2:25		

Appendix E-Comprehensive List of Recruitment Avenues

NOTE- green represents yes and red represents no.

Areas	Contacts	Contacted	Responded	Outcome
Charities	Limbless Association			Emailed and phoned a number of times and haven't heard back. May be able to put some study contact details in an article a colleague was contributing to in their StepForward Magazine.
	BLESMA			Study listed on research project webpage with deadline of 1st September 2019 for participant application: https://blesma.org/research-projects/current-research-projects/the-effect-of-pressure-on-skin-and-muscles-in-our-legs/
	Finding Your Feet			Posted study poster on their Facebook page.
	LimbCare			Posted study poster on their Facebook page.
	Help 4 Heroes			Study went through the Help 4 Heroes review board and was unsuccessful.
	Pilgrims Bandits			Although I didn't hear from them I think they distributed the poster as a potential participant contacted me and mentioned them.
	Limb Power			Salford University contact emailed Limb Power a study poster for me.
	British Army Motorsport Association			It was suggested to contact them.
Companies	Douglas Bader Foundation			I contacted them through an online form. Forwarded on to person who manages content.
	Blatchfords			I gave printed and PDF study posters to a contact when visiting and they distributed them to be displayed in non-NHS clinics. Also sent a PDF of the poster to another contact who kindly offered to distribute them as well.
	Dorset Orthopaedic			Contacted by a contact who is a private patient there and they said that it looks like an interesting study and would ask their clinic managers to print and display for potential patients.
	Lodon Prosthetics Centre			Colleague recommended to contact them.
	Dorset Prosthetics Centre			A contact suggested contacting but I think they are NHS based so we were not able to recruit participants there.
Motorsports	MSV			A couple of contacts suggested exploring this avenue for recruitment. Silverstone replied and forwarded my details onto the Chairman of the Motorsport UK Medical Committee. They asked their Disability representative, who is also the President of the FIA Disability Commission, if they could help, but they felt I may find more recruits via the armed forces and suggested contacting Headley Court where most injured servicemen undergo rehabilitation. The manager who looks after the British Touring Car Championship, Porsche, Renault, Ginetta and F4 said they don't really see many people with amputation. There are several licence holders in motorsport in various championships, but the vast majority are ex-servicemen who have suffered blast injuries. They said they would let everyone know what I am doing and pass on my contact details so they can be given to any competitors who may be interested in getting involved.
	Mission Motorsport			
	Thruxton Circuit			
	Silverstone Circuit			
Contacts	Friend who has transtibial Amputation			Participated and passed on study poster to people they think may be interested.
	Contact who I had met at ISPO conferences			Passed the study poster on to a friend who went on to participate and posted poster on the Amputee Friends UK FB group
	Lecturer in prosthetics at Salford University			I emailed after watching their presentation on prosthetics education at an ISPO socket workshop day and they distributed the study poster to potential participants in the area and Limbpower who may be able to help.
	Lecturer in Exercise Science and Bournemouth University			Another contact suggested contacting this individual as they were currently doing some work with the Armed Forces Para-Snowsport Team Charity.
	Occupational Therapist			Has potential participant contacts so took some printed study posters and a PDF to distribute.
	Senior Research Fellow at Bournemouth University			Carried out a study recruiting participants with amputation during his PhD and gave brilliant recruitment advice.
	Amputee Physiotherapist			A colleague suggested contacting after I presented at the Central Academic Facility monthly meeting.
Other	Physiotherapist			Paraolympic contacts with one participating.
	Local Gyms			One of two contacted local gyms replied and kindly offered to put study posters up on their notice boards.
	Past recruitment database			A colleague emailed all of the past participants with amputation to see if they would be interested in participating in this research study.
Other	PPI Workshop			Patient & Public Involvement (PPI) workshop with prosthetic limb users local to Winchester, on Monday 17th June. This activity is funded by the Institute for Life Sciences, and will be attended by several people who will potentially be eligible for the present study. I amended my ethics submission and got the workshop organisers' permission to display my poster at the event.

Appendix F-Detailed Testing Session Activity Checklist- Participants with Amputation


Pre-Testing Sessions Checklist

- Print testing session checklist
- Email participant approximately one week prior to testing to remind them to shave measurement areas at least 48 hours before and to provide them with parking information.
- Have razor ready just in case
- Arrange to collect Myoton
- Set up Myoton Patterns
- Generate anonymised participant ID
- Collect parking ticket from Travelwise office
- Print consent form and participant questionnaires to go into file
- Measure approximate size required for liner
- Print Amazon vouchers and receipt
- Photographic consent form
- Entertainment/kindle
- Set up lab
- Snacks

Phase	Overview	Detailed Activities	Complete
Pre-Session	Participant consent and information	Participant read PIS	
		Answer any questions	
		Complete consent form if participant happy to continue and after checking questionnaires	
		Pre-participation Questionnaire	
		MRI Questionnaire	
		Complete participant demographics	
	Measurement Areas (at least 2 days prior to testing send participant email reminder)	Mark out 5 x 5 cm patellar tendon area- Bottom edge at top of, and central with, tibial tuberosity	
		Mark out 5 x 5 cm tibialis anterior area- Bottom of area 12 cm distal to top patella tendon area. Anterior of fibula with the head of the fibula outside of the top left corner	
		Mark out 5 x 5 cm posterior calf area- Bottom of area 12 cm distal to top patella tendon area and central	
		Shave areas	

Testing Session 1- Biophysical Measures Session Checklist

Phase	Overview	Detailed Activities	Start Time (hours:mins)	Complete
Pre-Session	Equipment set up	TCM (Technical Code 19100 and new code TCM5PW1) check date/time	0:00 (carry out some activities day before if possible)	
		Sebutape application and retrieval equipment ready		
		Talley pressure sensors ready for use- Batteries Charged		
		MyotonPRO ready for use- Charged with participant and patterns set up and uploaded		
		Participant bed, leg support and entertainment set up		
		Pressure cuff, liner, gel rings and dummy sensors ready for application		
		Record room temp and humidity		
		USB/hard Drive ready for data storage		
	Transcutaneous Electrodes Preparation (4 O ₂ only and 1 combined electrodes will require Remembraning each time. Check new combined electrode as this requires Remembraning monthly)	Use filter paper to carefully remove moisture from sensor	0:30	
		Use prodger tool to remove 2 rubber bands and 2 membranes		
		Use filter paper to dab sensor		
		Holding sensor flat apply 2 drops of Electrolyte Solution (Dialysyte) on top (helps electron transfer of gas)		
		Push membrane on and discard green holder		
		Reattach sensor to monitor for calibration and press screen to calibrate		
	New TCM calibration (only requires re-membraning once per month on 27 th)	Membraning kits are same colour as electrodes		
		Clean electrode with any water (can be tap) for 10 seconds, to get rid of any contact gel, then dry with a paper towel until screen says at least 70%		
		Apply two drops of gel on new membrane and put electrode on top then close- return electrode to device to calibrate- it takes up to 4 hours to stabilise after remembraning		
		Make sure device is in neonate mode to record both O ₂ and CO ₂		

Phase	Overview	Detailed Activities	Start Time (hours:mins)	Complete
Phase 1	<p>ENSURE TCM'S ALL HAVE SAME SETTINGS OF 43.5°C WITHOUT SMART HEAT</p> <p>Set up of Measurements and Acclimatisation</p>	Collect Demographics if haven't already got, answer any questions	0:00	
		Give participant remuneration voucher and ask them to sign that they have received it	0:05	
		Allow participant to change/use the toilet if necessary before beginning sensor application	0:15	
		Apply O ₂ TGT electrodes to posterior calves while participant lies prone Thread electrodes through liner upon application. - Peel backing off Fitment Ring and attach Fitment Ring in required position - Apply two drops of fitment fluid within Fitment Ring - Line up arrow on sensor with arrow on Fitment Ring and rotate clockwise approximately 90° until it feels tight/secure - Record time	0:19	
		Apply O ₂ TGT electrode to lateral calves as above - Record time	0:22	
		Apply combined TGT electrodes to patellar tendons- old one as above - New sensor: Make sure press new patient, clean with alcohol wipe between participants, contact gel (grey label) apply two drops and press into fixation ring. - Record time	0:25	
		Set TGT events- Record time and event	0:25	
	 <p>Tweezers Position</p> <p>Sticky Side</p> <p>Take Baseline Measurements</p>	Apply sebutape to each patellar tendon area (roller 5 times to secure in place) Start 2 minute stopwatch	0:39	
		Apply sebutape to each lateral calf area (as above) Start 2 minute stop watch		
		Remove Patellar tendon sebutapes using tweezers and place into small tube (insert with non-sticky side facing outwards in tube)		
		Apply sebutape to each posterior calf area (as above) Start 2 minute stop watch		
		Remove sebutapes from lateral calves as above		
		Remove sebutapes from posterior calves as above		
		Ensure TGT measurements have stabilised (O ₂ 50-90mmHg, CO ₂ 36-50 mmHg)	0:40	

Ischaemia
Categories

Category 1- O₂ (50-90), CO₂ (36-50)
Category 2- O₂ (decreases by >25%), CO₂ (minimal change)
Category 3- O₂ (decreases by >25%), CO₂ (increases by >25%)

Phase	Overview	Detailed Activities	Start Time (hours:mins)	Complete
Phase 2	Set up liner and pressure cuff	Set TGT event. Apply silicone gel liner	0:40	
		Set event, apply pressure cuff, wait 10 mins		
	10 minute application of 20 mmHg	Record Time, set TGT event and inflate to 20 mmHg	1:00	PT- PT- LC- LC- PC- PC-
	10 minute application of 30 mmHg	Record Time, set TGT event and inflate to 30 mmHg	1:10	PT- PT- LC- LC- PC- PC-
	10 minute application of 40 mmHg	Record Time, set TGT event and inflate to 40 mmHg	1:20	PT- PT- LC- LC- PC- PC-
	10 minute application of 50 mmHg	Record Time, set TGT event and inflate to 50 mmHg	1:30	PT- PT- LC- LC- PC- PC-
	10 minute application of 60 mmHg	Record Time, set TGT event and inflate to 60 mmHg	1:40	PT- PT- LC- LC- PC- PC-
Phase 3	Refractory Period	Release pressure by 10 mmHg every 30 secs	1:50	
		Remove cuff and liner and set events		
		Apply sebutape to each patellar tendon area (roller 5 times to secure in place)		
		Start 2 minute stopwatch		
		Apply sebutape to each lateral calf area (as above)		
		Start 2 minute stop watch		
		Remove Patellar tendon sebutapes using tweezers and place into small tube (insert with non-sticky side facing outwards in tube)		
		Apply sebutape to each posterior calf area (as above)		
		Start 2 minute stop watch		
Phase 4	Interface Pressure Measurement	Apply pressure sensors underneath dummy TGT sensors	2:25	
		Apply liner and cuff- Record interface pressure	2:45	
		Inflate to 20 mmHg- Record pressure		
		Inflate to 30 mmHg- Record pressure		
		Inflate to 40 mmHg- Record pressure		
		Inflate to 50 mmHg- Record pressure		
		Inflate to 60 mmHg- Record pressure		
	Take MyotonPRO measurements	Measurements at each area in supine and prone positions		
Release pressure, remove equipment take answer any participant questions			3:00	

Testing Session 2- MRI Session Checklist

Phase	Overview	Detailed Activities	≈Start Time (hours:mins)	Complete
Answer any participant questions			0:00	
Set up and acclimatisation		Participant changes ready for MRI	0:05	
		Apply dummy sensors, liner, pressure cuff and body coil in MRI participant supine	0:10	
Residual Limb Baseline	Screening T2 Image		0:20	
	Baseline Image Global			
	Baseline Image Higher Resolution Over Measurement Areas: - Echo Time: 6.15 ms - Repetition Time: 17.10 ms - Field of View: 134 mm - In-slice resolution: 0.6 x 0.6 mm - Slice Thickness: 1.2 mm			
Residual Limb Pressurised	20 mmHg Cuff Pressure	Inflate pressure cuff to 20 mmHg	0:50	
		After 5 minutes take high resolution image over measurement areas		
	60 mmHg Cuff Pressure	Inflate pressure cuff to 60 mmHg		
		After 5 minutes take high resolution image over measurement areas		
Comfort break and set up			1:20	
Contralateral Limb Baseline	Screening T2 Image		1:40	
	Baseline Image Global			
	Baseline Image Higher Resolution Over Measurement Areas			
Contralateral Limb Pressurised	20 mmHg Cuff Pressure	Inflate pressure cuff to 20 mmHg	2:20	
		While waiting for 5 minutes take sagittal global image of residual limb FOV ≈40 cm		
		After 5 minutes take high resolution image over measurement areas		
	60 mmHg Cuff Pressure	Inflate pressure cuff to 60 mmHg		
		After 5 minutes take high resolution image over measurement areas		

Appendix G-Transcutaneous Gas Measurements for Cohort

Participants without Amputation

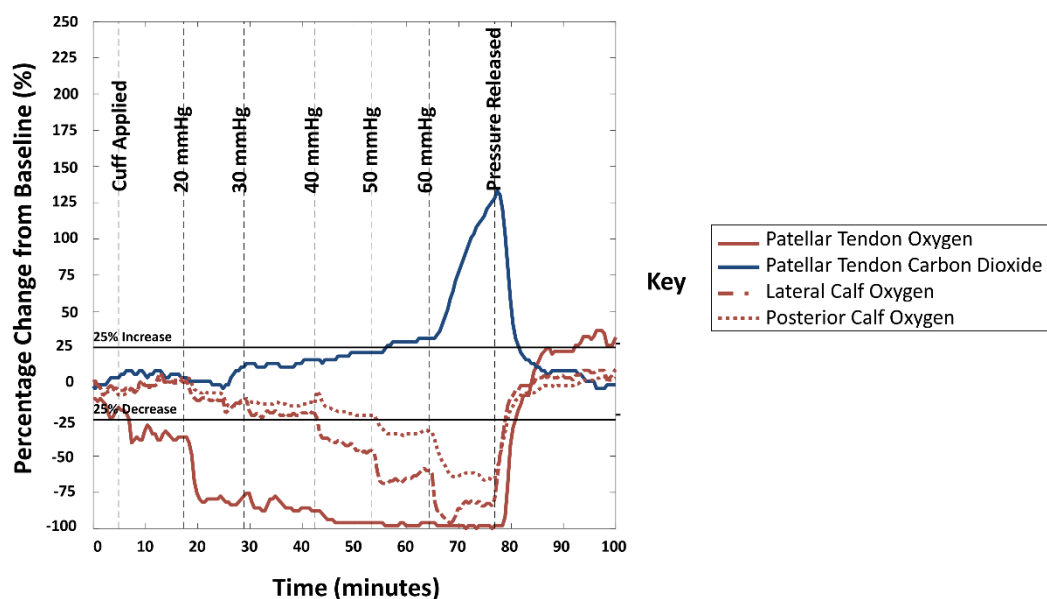


Figure 7.2 Data showing percentage change from baseline T_cPO_2 and T_cPCO_2 measurements under incremental cuff pressures from 20 to 60 mmHg from the right limb of participant #1

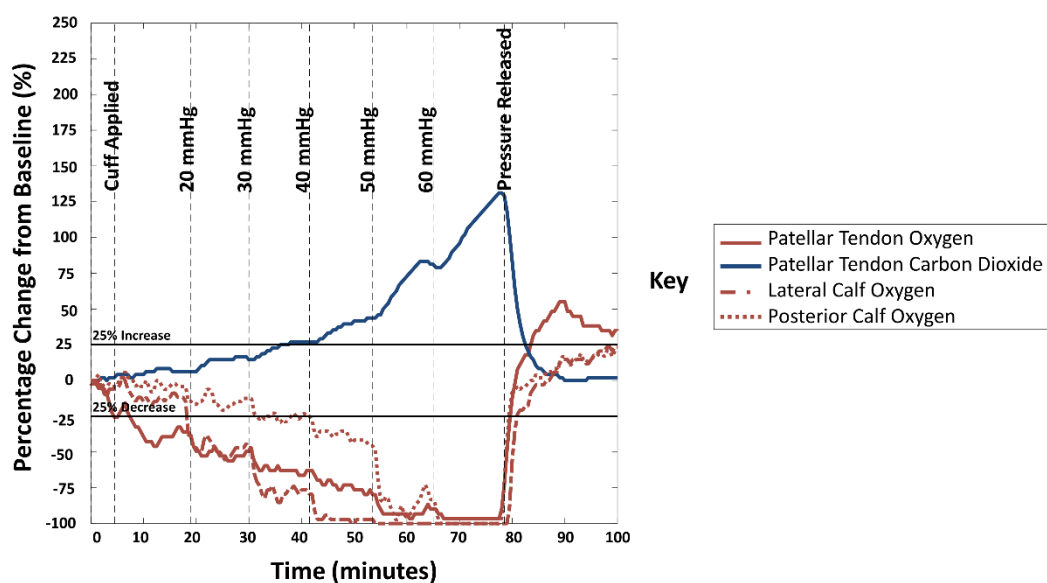


Figure 7.3 Data showing percentage change from baseline T_cPO_2 and T_cPCO_2 measurements under incremental cuff pressures from 20 to 60 mmHg from the right limb of participant #2

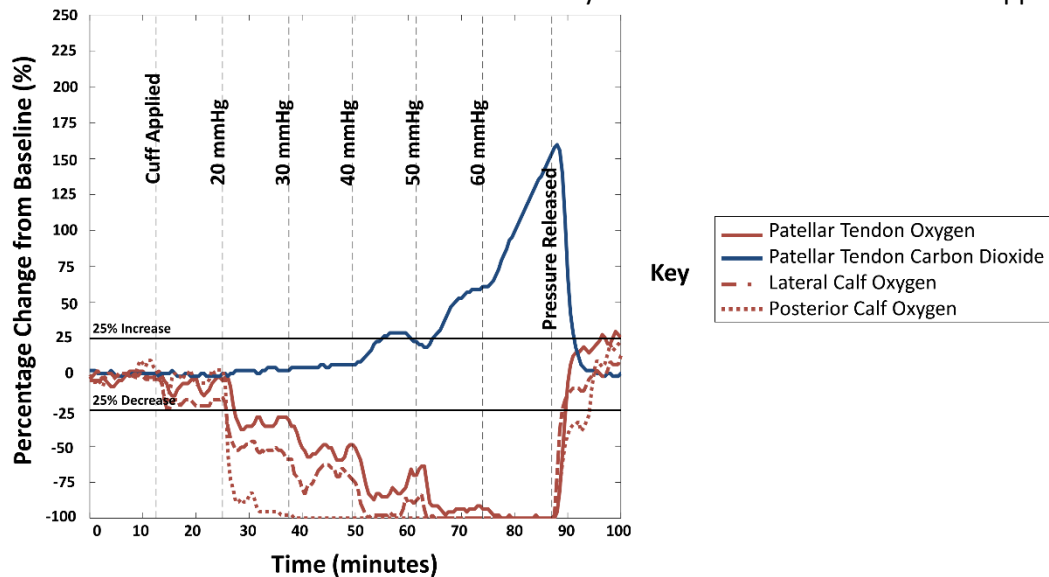


Figure 7.4 Data showing percentage change from baseline TcPO₂ and TcPCO₂ measurements under incremental cuff pressures from 20 to 60 mmHg from the residual (left) and contralateral (right) limbs of participant #3

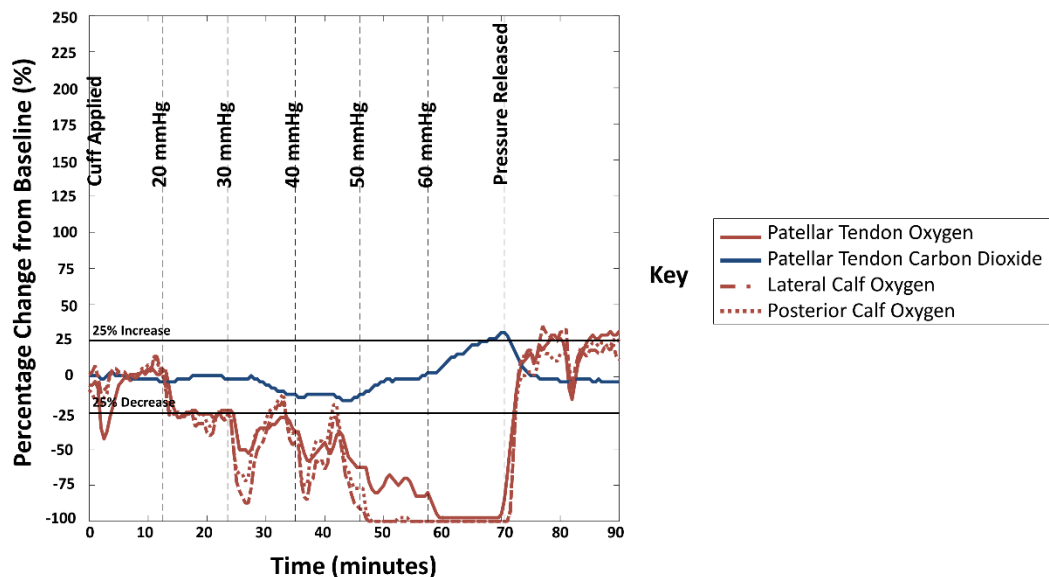


Figure 7.5 Data showing percentage change from baseline TcPO₂ and TcPCO₂ measurements under incremental cuff pressures from 20 to 60 mmHg from the residual (left) and contralateral (right) limbs of participant #4

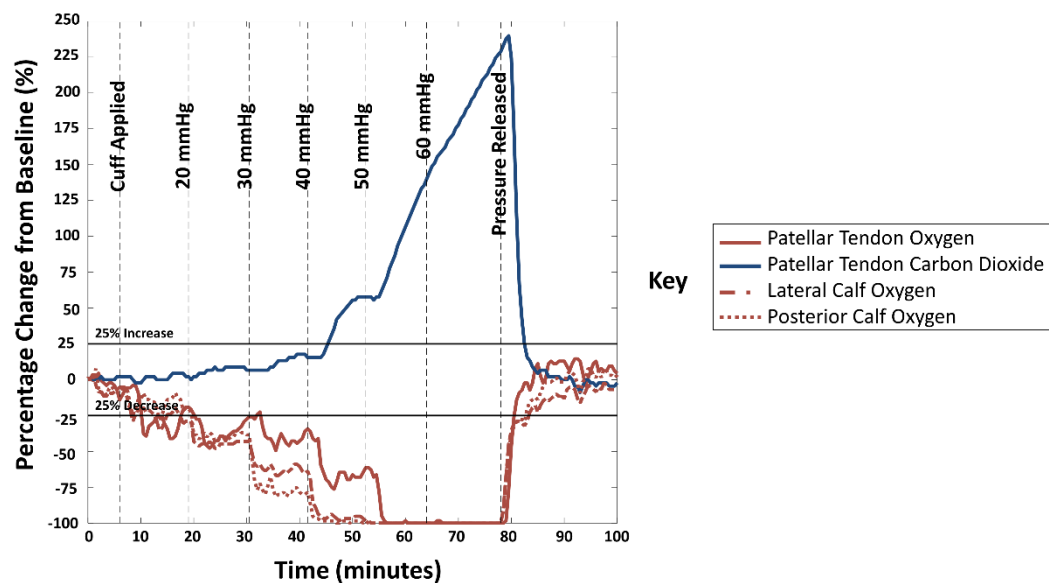


Figure 7.6 Data showing percentage change from baseline TcPO₂ and TcPCO₂ measurements under incremental cuff pressures from 20 to 60 mmHg from the residual (left) and contralateral (right) limbs of participant #5

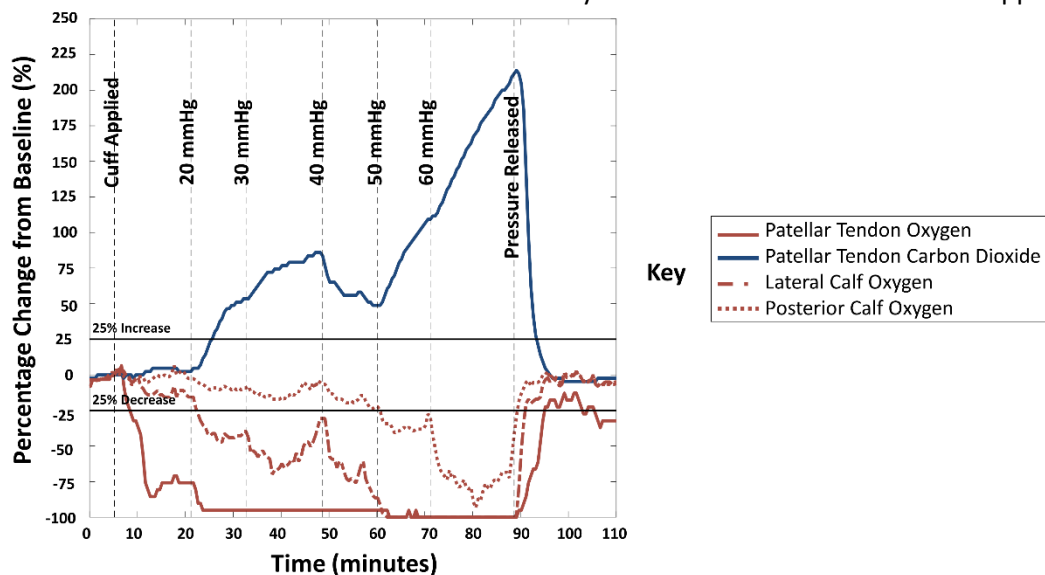


Figure 7.7 Data showing percentage change from baseline T_cPO_2 and T_cPCO_2 measurements under incremental cuff pressures from 20 to 60 mmHg from the residual (left) and contralateral (right) limbs of participant #6

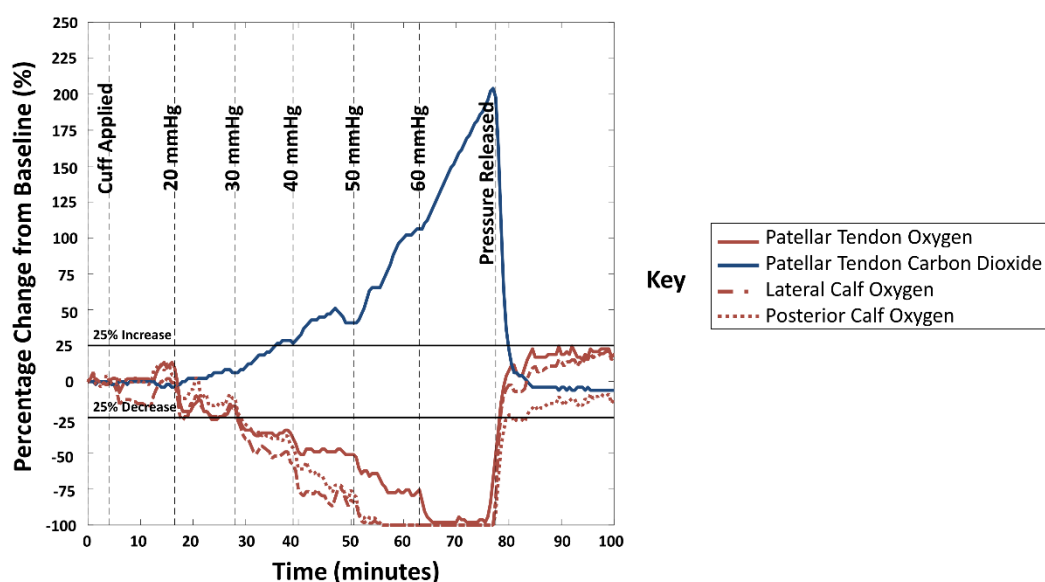


Figure 7.8 Data showing percentage change from baseline T_cPO_2 and T_cPCO_2 measurements under incremental cuff pressures from 20 to 60 mmHg from the residual (left) and contralateral (right) limbs of participant #7

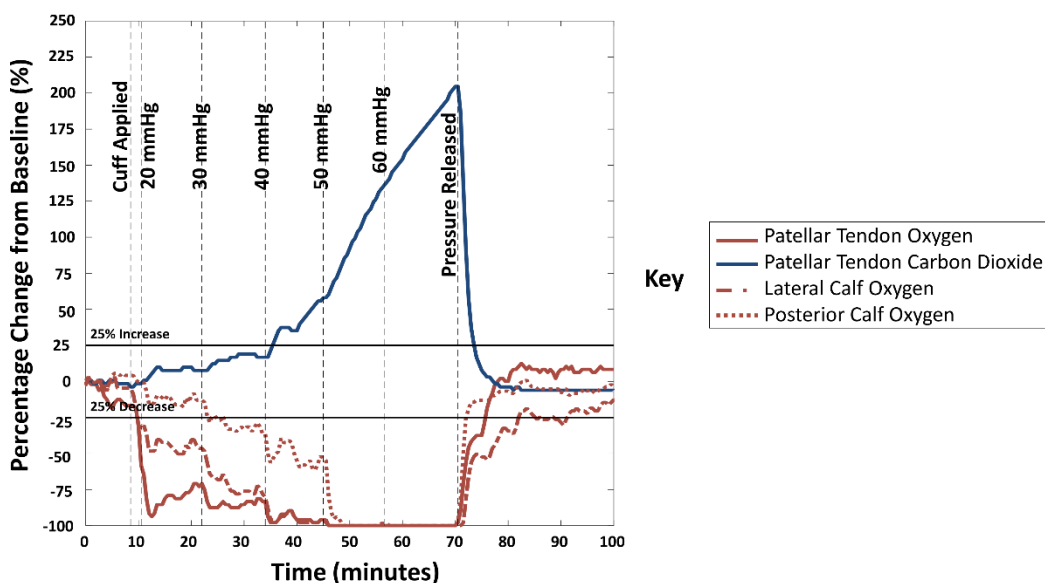


Figure 7.9 Data showing percentage change from baseline T_cPO_2 and T_cPCO_2 measurements under incremental cuff pressures from 20 to 60 mmHg from the residual (left) and contralateral (right) limbs of participant #8

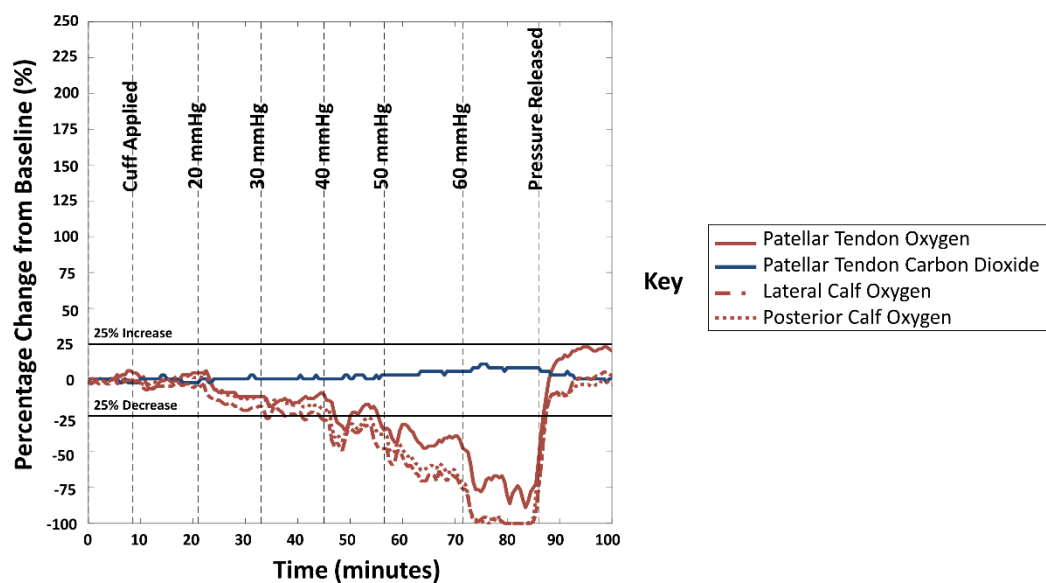


Figure 7.10 Data showing percentage change from baseline T_cPO_2 and T_cPCO_2 measurements under incremental cuff pressures from 20 to 60 mmHg from the residual (left) and contralateral (right) limbs of participant #9

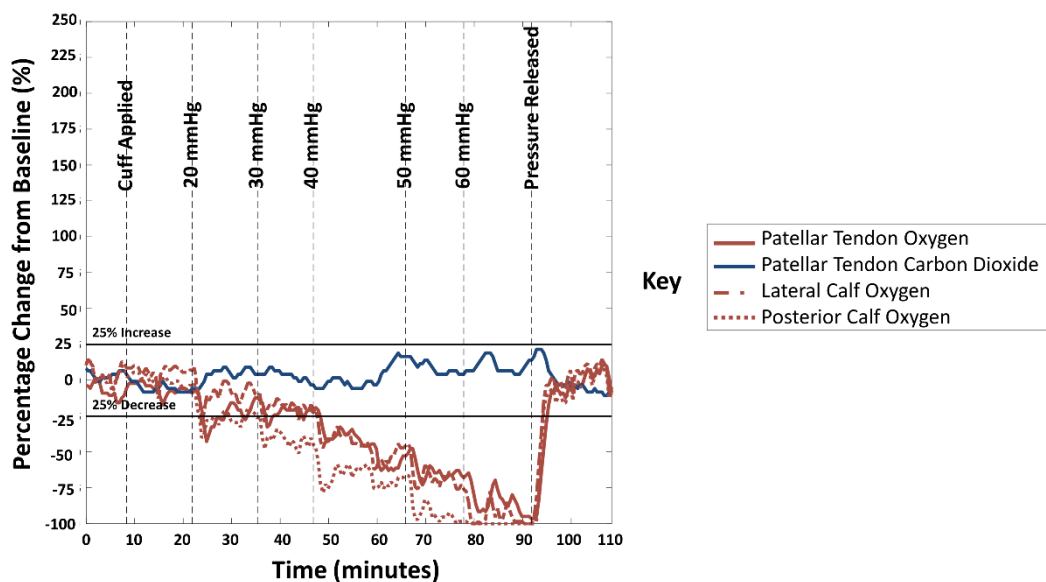


Figure 7.11 Data showing percentage change from baseline T_cPO_2 and T_cPCO_2 measurements under incremental cuff pressures from 20 to 60 mmHg from the residual (left) and contralateral (right) limbs of participant #10

Participants with Transtibial Amputation

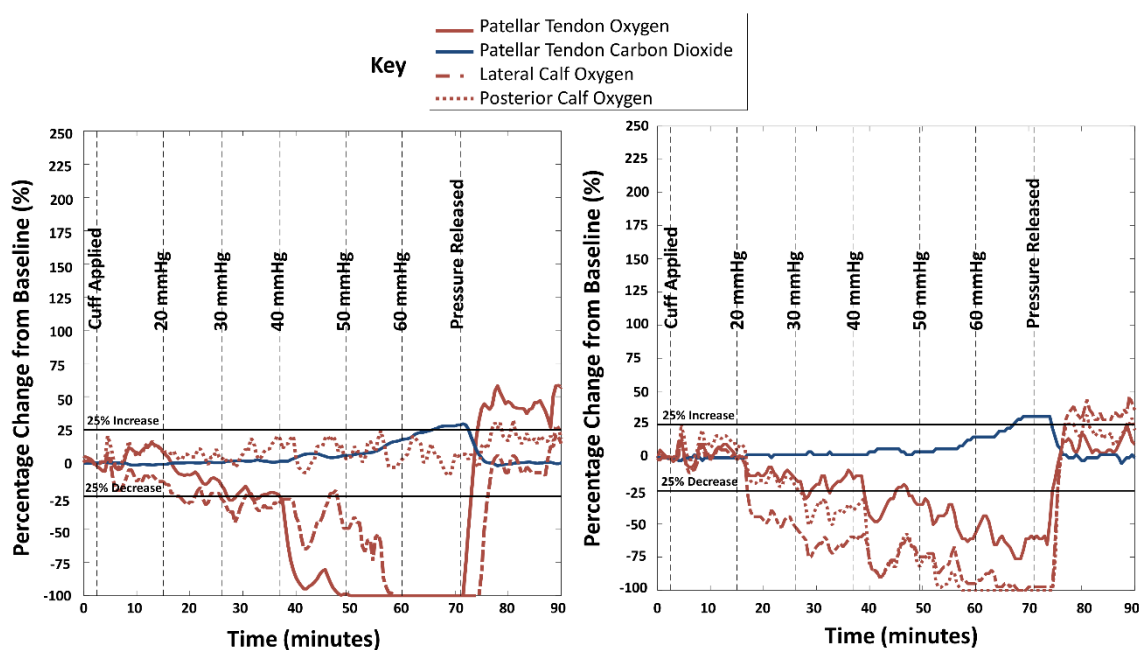


Figure 7.12 Data showing percentage change from baseline T_cPO_2 and T_cPCO_2 measurements under incremental cuff pressures from 20 to 60 mmHg from the residual (left) and contralateral (right) limbs of participant #1A

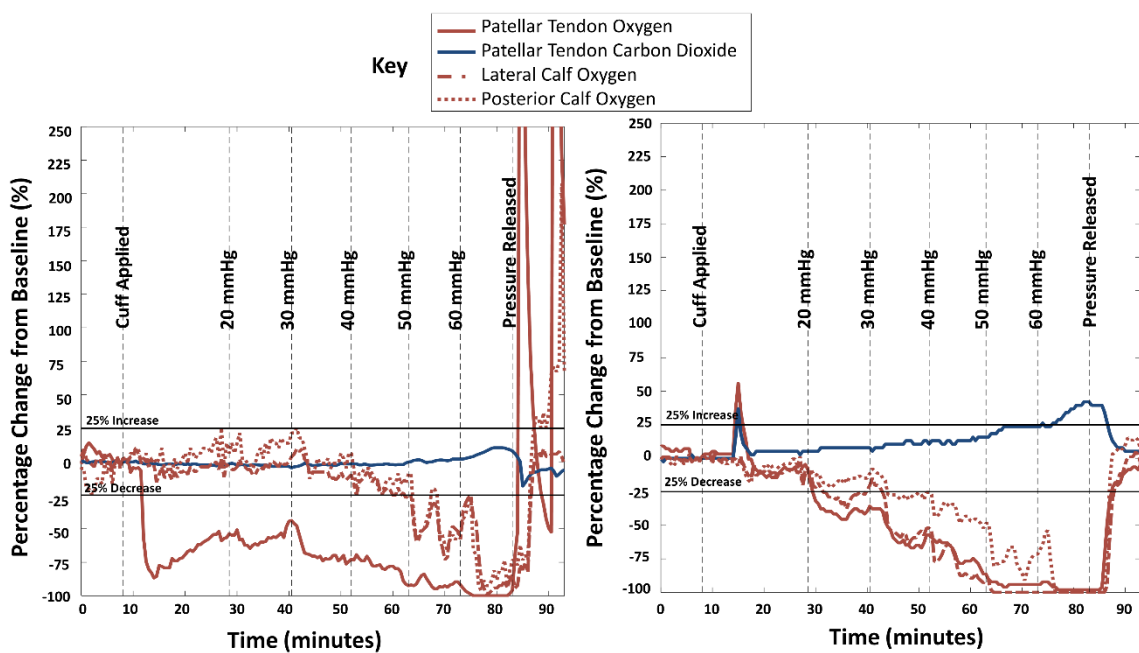


Figure 7.13 Data showing percentage change from baseline T_cPO_2 and T_cPCO_2 measurements under incremental cuff pressures from 20 to 60 mmHg from the residual (left) and contralateral (right) limbs of participant #2A

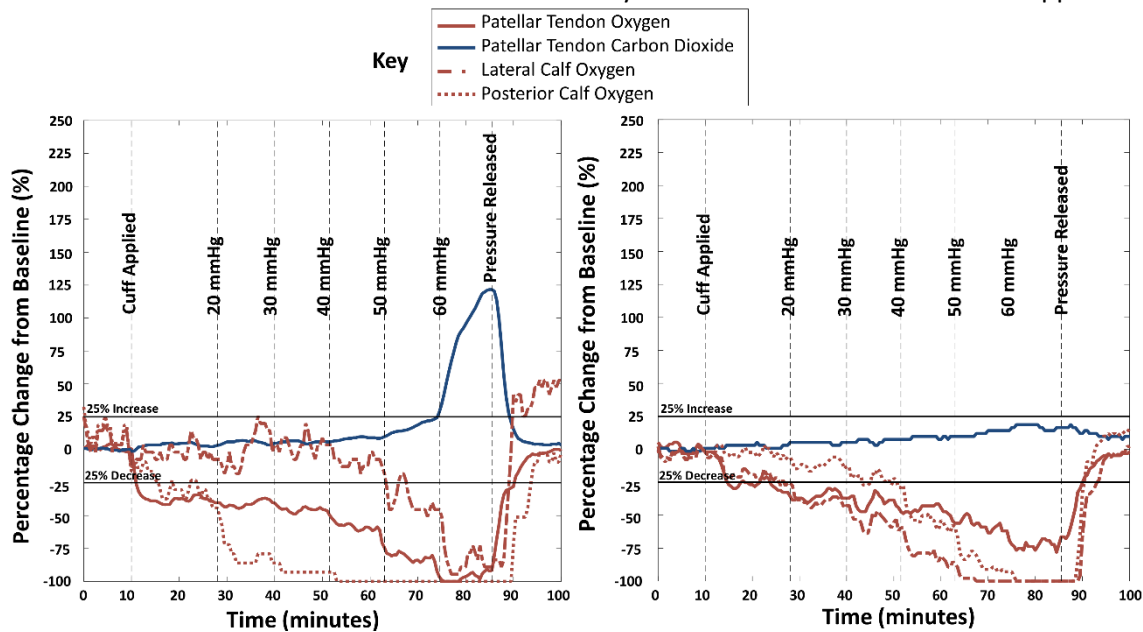


Figure 7.14 Data showing percentage change from baseline T_cPO_2 and T_cPCO_2 measurements under incremental cuff pressures from 20 to 60 mmHg from the residual (left) and contralateral (right) limbs of participant #3A

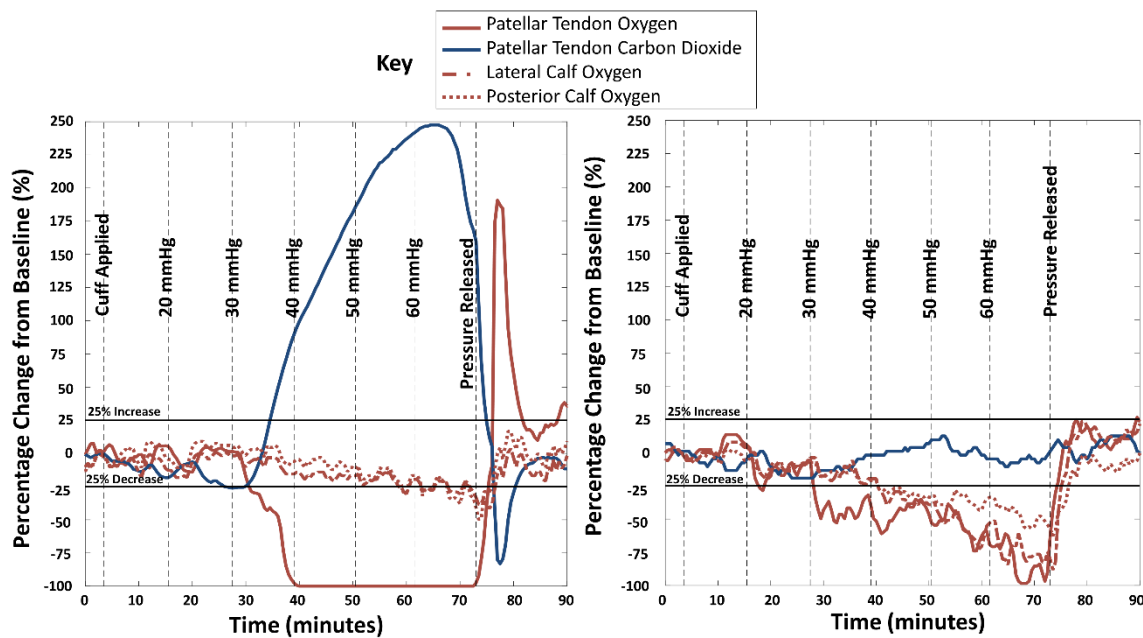


Figure 7.15 Data showing percentage change from baseline T_cPO_2 and T_cPCO_2 measurements under incremental cuff pressures from 20 to 60 mmHg from the residual (left) and contralateral (right) limbs of participant #4A

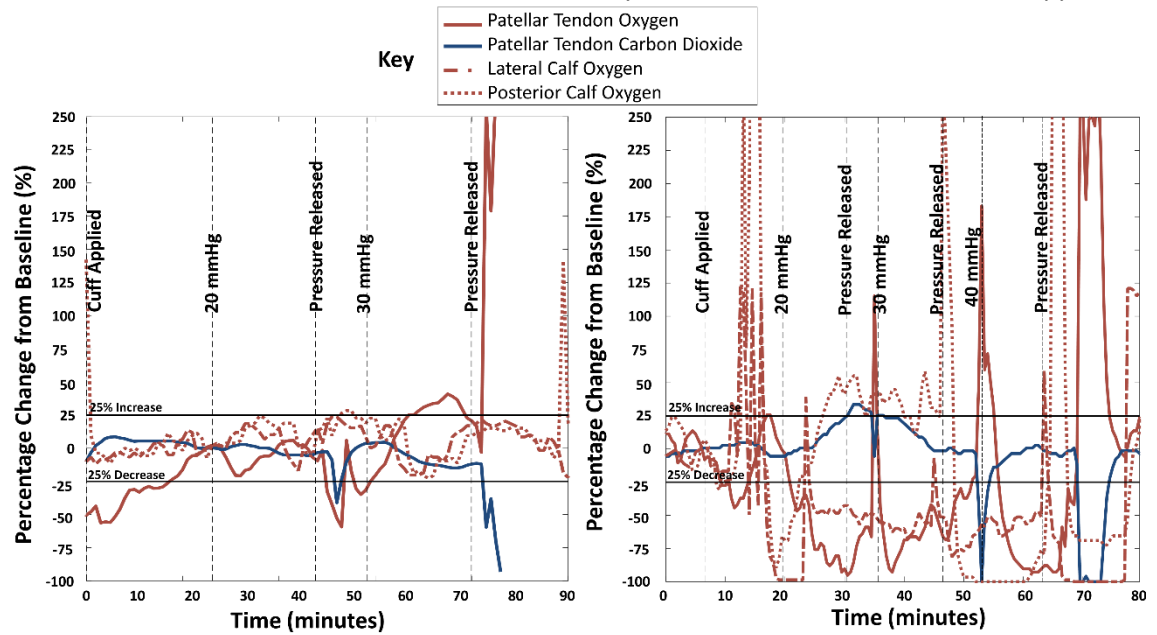


Figure 7.16 Data showing percentage change from baseline T_cPO_2 and T_cPCO_2 measurements under incremental cuff pressures from 20 to 60 mmHg from the residual (left) and contralateral (right) limbs of participant #5A

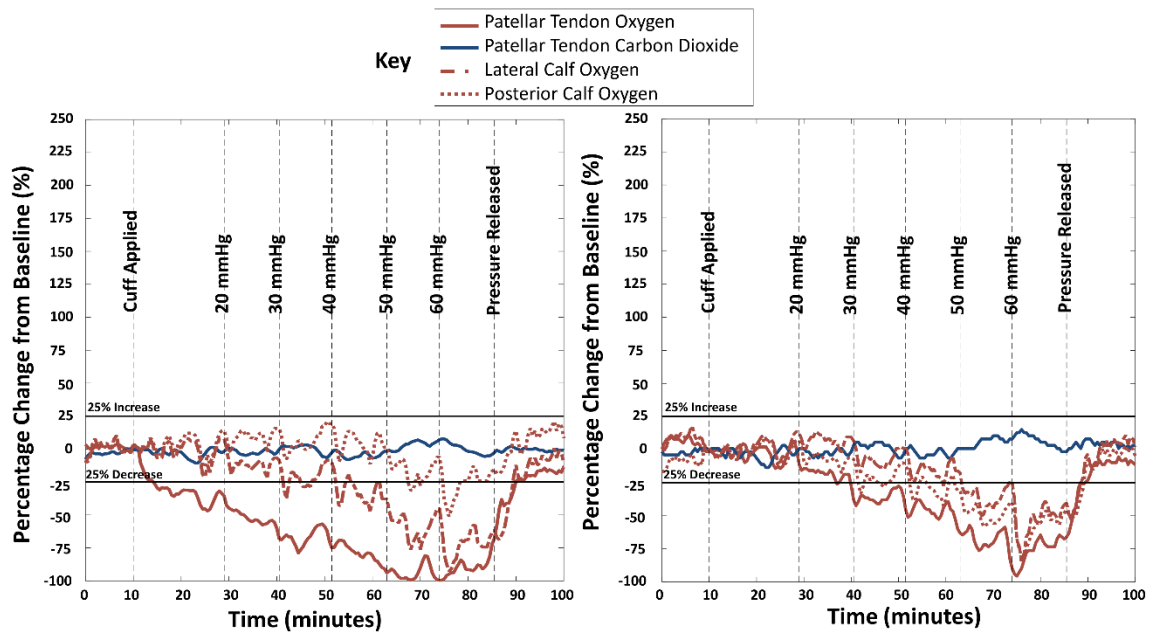
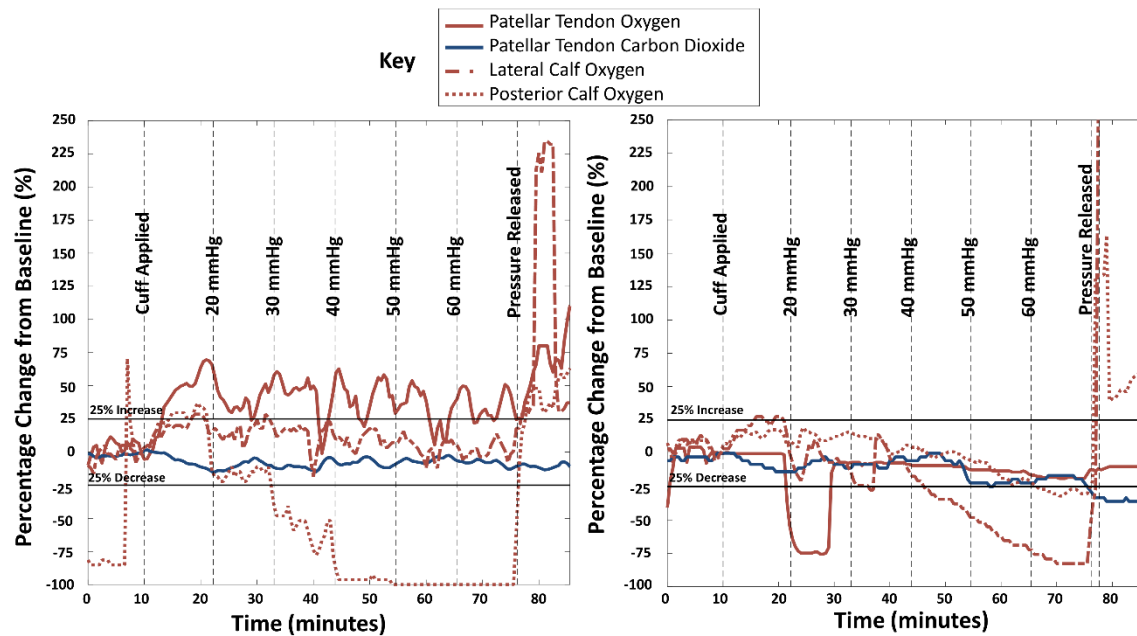
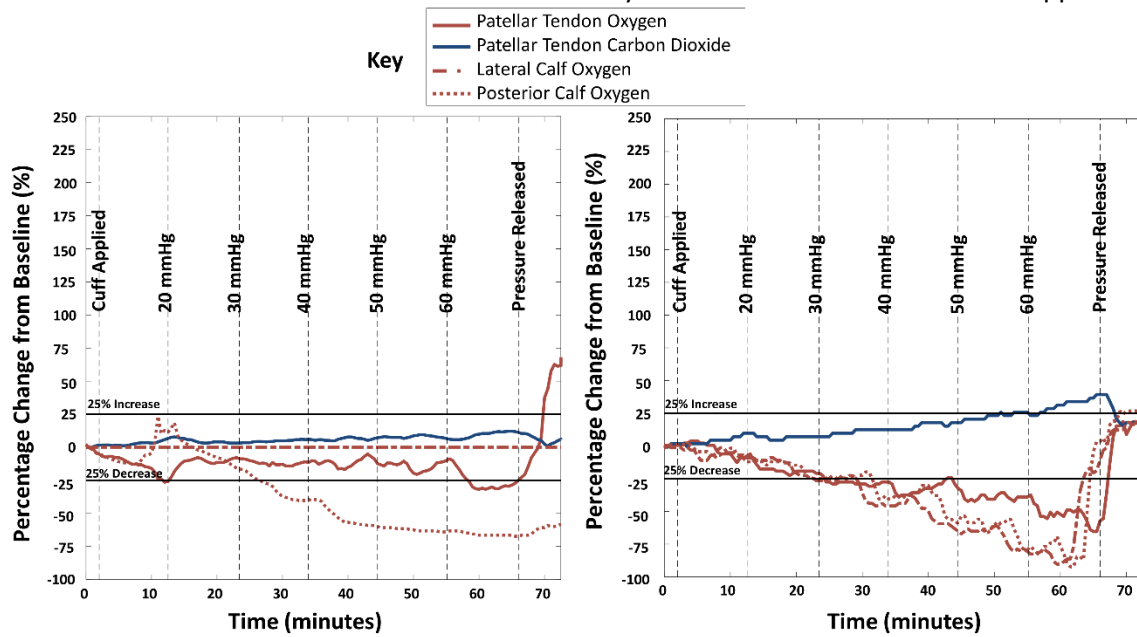


Figure 7.17 Data showing percentage change from baseline T_cPO_2 and T_cPCO_2 measurements under incremental cuff pressures from 20 to 60 mmHg from the residual (left) and contralateral (right) limbs of participant #6A



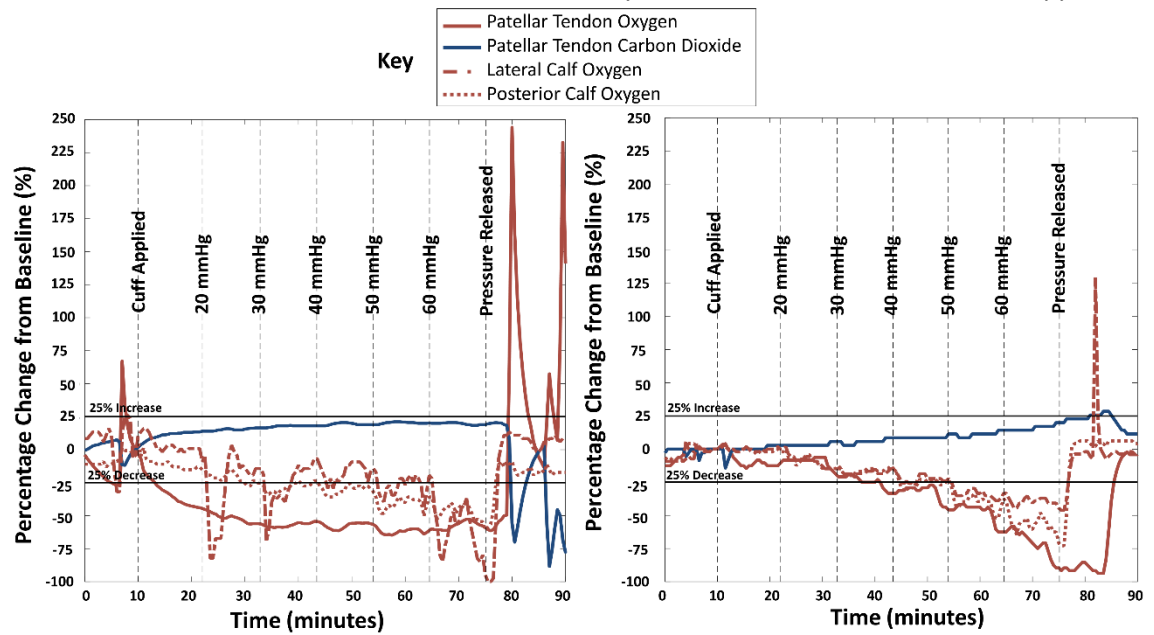


Figure 7.20 Data showing percentage change from baseline T_cPO_2 and T_cPCO_2 measurements under incremental cuff pressures from 20 to 60 mmHg from the residual (left) and contralateral (right) limbs of participant #9A

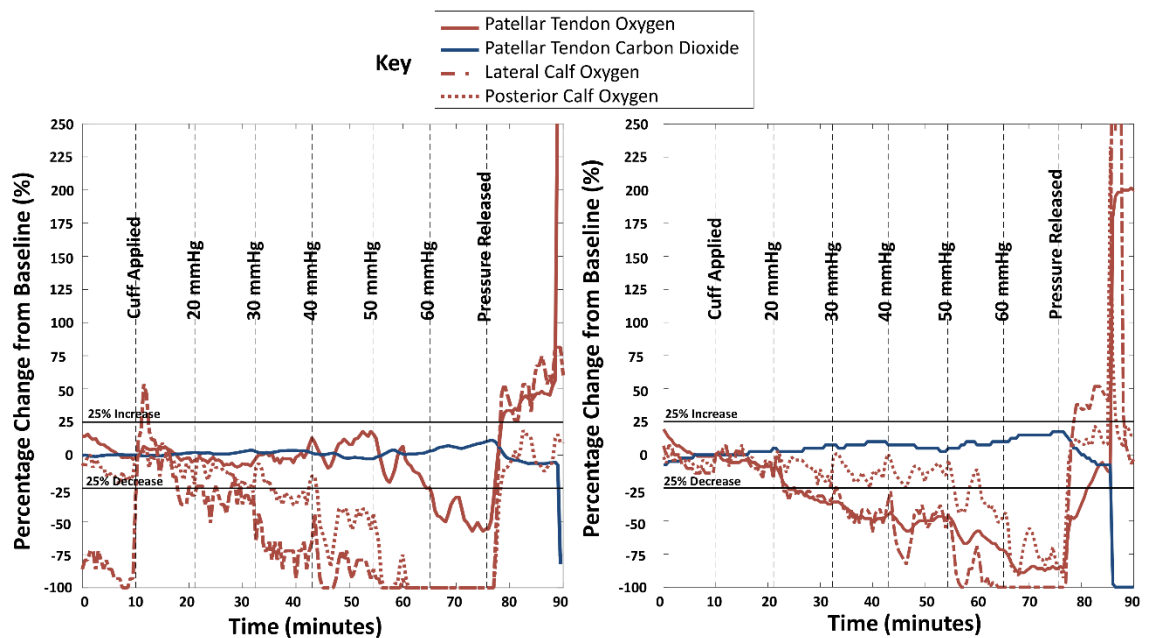


Figure 7.21 Data showing percentage change from baseline T_cPO_2 and T_cPCO_2 measurements under incremental cuff pressures from 20 to 60 mmHg from the residual (left) and contralateral (right) limbs of participant #10A

8 References

1. Bramley, J.L., et al., *Establishing a measurement array to assess tissue tolerance during loading representative of prosthetic use*. Med Eng Phys, 2020. **78**: p. 39-47.
2. Bramley, J., et al. *Investigating the Physiological Effects on Dermal Tissues Following Simulated Prosthetic Loading in Intact and Trans-Tibial Residual Limbs*. in *ISPO 17th World Congress Basics to Bionics*. 2019. Kobe Convention Center, Kobe, Hyogo, Japan.
3. Bramley, J., et al. *Investigating the Composition and Tissue Deformation During Simulated Prosthetic Loading of Intact and Trans-Tibial Residual Limbs*. in *ISPO 17th World Congress Basic to Bionics*. 2019. Kobe Convention Center, Kobe, Hyogo, Japan.
4. Robinson, K.P., *Historical aspects of amputation*. Annals of the Royal College of Surgeons of England, 1991. **73**: p. 134-136.
5. Wagels, M., et al., *History of lower limb reconstruction after trauma*. ANZ J Surg, 2013. **83**(5): p. 348-53.
6. National Institute for Health and Clinical Excellence, *National Costing Report: Lower limb peripheral arterial disease*. 2012, NHS.
7. Hoffmann, F., et al., *Impact of diabetes on costs before and after major lower extremity amputations in Germany*. J Diabetes Complications, 2013. **27**(5): p. 467-72.
8. Franklin, H., et al., *Cost of lower-limb amputation in U.S. veterans with diabetes using health services data in fiscal years 2004 and 2010*. J Rehabil Res Dev, 2014. **51**(8): p. 1325-30.
9. Bhatnagar, V., et al., *Lower-limb amputation and effect of posttraumatic stress disorder on Department of Veterans Affairs outpatient cost trends*. J Rehabil Res Dev, 2015. **52**(7): p. 827-38.
10. Kerr, M., G. Rayman, and W.J. Jeffcoate, *Cost of diabetic foot disease to the National Health Service in England*. Diabet Med, 2014. **31**(12): p. 1498-504.
11. England, N. *Prosthetics Service Review*. 2017; Available from: <https://www.england.nhs.uk/commissioning/spec-services/npc-crg/group-d/d01/prosthetics-review/>.
12. Moxey, P.W., et al., *Lower extremity amputations - a review of global variability in incidence*. Diabetic Medicine, 2011. **28**(10): p. 1144-1153.
13. The Global Lower Extremity Amputation Group, *Epidemiology of lower extremity amputation in centres in Europe, North America and East Asia*. The Global Lower Extremity Amputation Study Group. Br J Surg, 2000. **87**(3): p. 328-37.
14. Ahmad, N., et al., *The prevalence of major lower limb amputation in the diabetic and non-diabetic population of England 2003-2013*. Diab Vasc Dis Res, 2016. **13**(5): p. 348-53.
15. Peek, M.E., *Gender differences in diabetes-related lower extremity amputations*. Clin Orthop Relat Res, 2011. **469**(7): p. 1951-5.
16. Amin, L., et al., *Gender differences in the impact of poverty on health: disparities in risk of diabetes-related amputation*. Diabet Med, 2014. **31**(11): p. 1410-7.
17. Ahmad, N., et al., *Lower limb amputation in England: prevalence, regional variation and relationship with revascularisation, deprivation and risk factors. A retrospective review of hospital data*. J R Soc Med, 2014. **107**(12): p. 483-9.
18. WHO, *World Report on Disability*. 2011, Geneva.
19. Sexton, S., *Rehabilitation of people with physical disabilities in developing countries*. 2016, International Society for Prosthetics and Orthotics (ISPO): Brussels, Belgium.
20. Minc, S.D., et al., *Geographic variation in amputation rates among patients with diabetes and/or peripheral arterial disease in the rural state of West Virginia identifies areas for improved care*. J Vasc Surg, 2019.
21. Holman, N., R.J. Young, and W.J. Jeffcoate, *Variation in the recorded incidence of amputation of the lower limb in England*. Diabetologia, 2012. **55**(7): p. 1919-25.

22. Moxey, P.W., et al., *Epidemiological study of lower limb amputation in England between 2003 and 2008*. Br J Surg, 2010. **97**(9): p. 1348-53.
23. World Health Organization, *Global Report on Diabetes*. 2016, World Health Organization: France.
24. Diabetes UK, *The Future of Diabetes*. 2017.
25. Pasquina, P.F., et al., *Special Considerations for Multiple Limb Amputation*, in *Curr Phys Med Rehabil Rep*. 2014: United States. p. 273-289.
26. University of Salford, *Limbless Statistics A repository for quantitative information on the UK limbless population REFERRED for prosthetics treatment ANNUAL REPORT 2011-2012*, in *Limbless Statistics*, U.-U.N.I.f.P.O. Development, Editor. 2015: Manchester.
27. Aulivola, B., et al., *Major lower extremity amputation: Outcome of a modern series*. Archives of Surgery, 2004. **139**(4): p. 395-399.
28. de Cossart, L., et al., *The fate of the below knee amputee*. Ann R Coll Surg Engl, 1983. **65**(4): p. 230-2.
29. Lascar, N., et al., *Type 2 diabetes in adolescents and young adults*. The Lancet Diabetes & Endocrinology, 2018. **6**(1): p. 69-80.
30. Dillingham, T.R., L.E. Pezzin, and A.D. Shore, *Reamputation, mortality, and health care costs among persons with dysvascular lower-limb amputations*. Arch Phys Med Rehabil, 2005. **86**(3): p. 480-6.
31. Physiopedia. *Pathology Leading to Amputation- Diabetic Foot*. 2015; Available from: https://physio-pedia.com/File:Diabetic_foot.jpg.
32. Bruehl, S., *Complex regional pain syndrome*. Bmj, 2015. **351**: p. h2730.
33. Kanitakis, J., *Anatomy, histology and immunohistochemistry of normal human skin*. Eur J Dermatol, 2002. **12**(4): p. 390-9; quiz 400-1.
34. Bader, D.L. and P.R. Worsley, *Technologies to monitor the health of loaded skin tissues*. Biomed Eng Online, 2018. **17**(1): p. 40.
35. Kingsbury, T., et al., *Do patients with bone bridge amputations have improved gait compared with patients with traditional amputations?* Clin Orthop Relat Res, 2014. **472**(10): p. 3036-43.
36. Marshall, C. and G. Stansby, *Amputation and rehabilitation*. Surgery - Oxford International Edition, 2010. **28**(6): p. 284-287.
37. Krajchich, J.I., et al., *Atlas of Amputations and Limb Deficiencies Surgical Prosthetic and Rehabilitation Principles*. Fourth Edition ed, ed. A.A.o.O. Surgeons. Vol. Volume 2 Lower Limb Management Issues. 2016, Rosemont, IL 60018: American Academy of Orthopaedic Surgeons.
38. Humzah, M.D. and P.M. Gilbert, *Fasciocutaneous blood supply in below-knee amputation*. J Bone Joint Surg Br, 1997. **79**(3): p. 441-3.
39. Tisi, P.V. and M.M. Than, *Type of incision for below knee amputation*. Cochrane Database Syst Rev, 2014(4): p. Cd003749.
40. Allcock, P.A. and A.S. Jain, *Revisiting transtibial amputation with the long posterior flap*. Br J Surg, 2001. **88**(5): p. 683-6.
41. Burgess, E.M., et al., *Amputations of the leg for peripheral vascular insufficiency*. J Bone Joint Surg Am, 1971. **53**(5): p. 874-90.
42. Moran, S.L. and S.A. Sems, *Master Techniques in Orthopaedic Surgery: Soft Tissue Surgery*. Second ed. Master Techniques in Orthopaedic Surgery, ed. B.F. Morrey. 2017: Wolters Kluwer Health 2016.
43. Lilja, M. and T. Öberg, *Proper Time for Definitive Transtibial Prosthetic Fitting*. Journal of Prosthetics and Orthotics, 1997. **9**(Number 2): p. 90-95.
44. Johannesson, A., et al., *Comparison of vacuum-formed removable rigid dressing with conventional rigid dressing after transtibial amputation: similar outcome in a randomized controlled trial involving 27 patients*. Acta Orthop, 2008. **79**(3): p. 361-9.
45. Nawijn, S.E., et al., *Stump management after trans-tibial amputation: a systematic review*. Prosthet Orthot Int, 2005. **29**(1): p. 13-26.

46. Physiotherapy Inter Regional Prosthetic Audit Group, *Physiotherapy Exercises Following Transtibial (Below Knee) Amputation*. 2004, P.I.R.P.A.G.
47. Widmaier, E.P., H. Raff, and K.T. Strang, *Vander's Human Physiology The Mechanisms of Body Function*. Twelfth Edition ed. 2011, New York: McGraw-Hill Companies, Inc.
48. Shier, D., J. Butler, and R. Lewis, *Hole's Human Anatomy & Physiology*. Twelfth Edition ed. 2010, New York: McGraw-Hill Companies, Inc.
49. Lilja, M., P. Hoffmann, and T. Oberg, *Morphological changes during early trans-tibial prosthetic fitting*. *Prosthet Orthot Int*, 1998. **22**(2): p. 115-22.
50. Sherk, V.D., M.G. Bembien, and D.A. Bembien, *Interlimb muscle and fat comparisons in persons with lower-limb amputation*. *Arch Phys Med Rehabil*, 2010. **91**(7): p. 1077-81.
51. Redhead, R.G., et al., *Post-amputation pneumatic walking aid*. *Br J Surg*, 1978. **65**(9): p. 611-2.
52. Ortho Europe, *The Pneumatic Post-Amputation Mobility Aid Instructions for Use*. Abingdon, Oxford.
53. Scott, H., et al., *An evaluation of the Amputee Mobility Aid (AMA) early walking aid*. *Prosthet Orthot Int*, 2000. **24**(1): p. 39-46.
54. Vanross, E.R., S. Johnson, and C.A. Abbott, *Effects of early mobilization on unhealed dysvascular transtibial amputation stumps: a clinical trial*. *Arch Phys Med Rehabil*, 2009. **90**(4): p. 610-7.
55. Portsmouth Hospitals NHS Trust, *Clinical Policy & Associated Guidelines for Early Mobilisation of Unhealed Dysvascular Transtibial Amputees*. 2010, Portsmouth Hospitals NHS Trust.
56. Sanders, J.E., et al., *Preliminary investigation of residual-limb fluid volume changes within one day*. *J Rehabil Res Dev*, 2012. **49**(10): p. 1467-78.
57. Sanders, J.E., et al., *How do walking, standing, and resting influence transtibial amputee residual limb fluid volume?* *J Rehabil Res Dev*, 2014. **51**(2): p. 201-12.
58. Sanders, J.E., et al., *Residual limb fluid volume change and volume accommodation: Relationships to activity and self-report outcomes in people with trans-tibial amputation*. *Prosthet Orthot Int*, 2018: p. 309364617752983.
59. Sanders, J.E., et al., *How do sock ply changes affect residual-limb fluid volume in people with transtibial amputation?* *J Rehabil Res Dev*, 2012. **49**(2): p. 241-56.
60. Sanders, J.E., et al., *Changes in interface pressures and shear stresses over time on trans-tibial amputee subjects ambulating with prosthetic limbs: comparison of diurnal and six-month differences*. *J Biomech*, 2005. **38**(8): p. 1566-73.
61. Sanders, J.E. and S. Fatone, *Residual limb volume change: systematic review of measurement and management*. *J Rehabil Res Dev*, 2011. **48**(8): p. 949-86.
62. Zachariah, S.G., et al., *Shape and volume change in the transtibial residuum over the short term: preliminary investigation of six subjects*. *J Rehabil Res Dev*, 2004. **41**(5): p. 683-94.
63. Sanders, J.E., et al., *Effects of socket size on metrics of socket fit in trans-tibial prosthesis users*. *Med Eng Phys*, 2017. **44**: p. 32-43.
64. Sanders, J.E., M.R. Severance, and K.J. Allyn, *Computer-socket manufacturing error: how much before it is clinically apparent?* *J Rehabil Res Dev*, 2012. **49**(4): p. 567-82.
65. Sanders, J.E., et al., *Effects of elevated vacuum on in-socket residual limb fluid volume: case study results using bioimpedance analysis*. *J Rehabil Res Dev*, 2011. **48**(10): p. 1231-48.
66. Rink, C., et al., *Elevated vacuum suspension preserves residual-limb skin health in people with lower-limb amputation: Randomized clinical trial*. *J Rehabil Res Dev*, 2016. **53**(6): p. 1121-1132.
67. Sanders, J.E., et al., *Influence of prior activity on residual limb volume and shape measured using plaster casting: results from individuals with transtibial limb loss*. *J Rehabil Res Dev*, 2013. **50**(7): p. 1007-16.
68. Sanders, J.E., et al., *Preliminary evaluation of a novel bladder-liner for facilitating residual limb fluid volume recovery without doffing*. *J Rehabil Res Dev*, 2016. **53**(6): p. 1107-1120.

69. Dudek, N.L., et al., *Dermatologic conditions associated with use of a lower-extremity prosthesis*. Arch Phys Med Rehabil, 2005. **86**(4): p. 659-63.
70. Meulenbelt, H.E., et al., *Determinants of Skin Problems of the Stump in Lower-Limb Amputees*. Archives of Physical Medicine and Rehabilitation, 2009. **90**(1): p. 74-81.
71. Meulenbelt, H.E., et al., *Skin problems of the stump in lower limb amputees: 1. A clinical study*. Acta Derm Venereol, 2011. **91**(2): p. 173-7.
72. Coleman, S., et al., *Developing a pressure ulcer risk factor minimum data set and risk assessment framework*. J Adv Nurs, 2014. **70**(10): p. 2339-52.
73. Coleman, S., et al., *A new pressure ulcer conceptual framework*. J Adv Nurs, 2014. **70**(10): p. 2222-34.
74. Coleman, S., et al., *Patient risk factors for pressure ulcer development: systematic review*. Int J Nurs Stud, 2013. **50**(7): p. 974-1003.
75. Gerhardt, L.C., et al., *Skin-textile friction and skin elasticity in young and aged persons*. Skin Res Technol, 2009. **15**(3): p. 288-98.
76. Arsenault, K.A., et al., *The use of transcutaneous oximetry to predict healing complications of lower limb amputations: a systematic review and meta-analysis*. Eur J Vasc Endovasc Surg, 2012. **43**(3): p. 329-36.
77. Poredos, P., S. Rakovec, and B. Guzik-Salobir, *Determination of amputation level in ischaemic limbs using tcPO2 measurement*. Vasa, 2005. **34**(2): p. 108-12.
78. Columbo, J.A., et al., *Below-Knee Amputation Failure and Poor Functional Outcomes Are Higher Than Predicted in Contemporary Practice*. Vasc Endovascular Surg, 2016. **50**(8): p. 554-558.
79. Trinks, T.P., et al., *Transcutaneous oximetry measurements of the leg: comparing different measuring equipment and establishing values in healthy young adults*. Diving Hyperb Med, 2017. **47**(2): p. 82-87.
80. Blake, D.F., D.A. Young, and L.H. Brown, *Transcutaneous oximetry: variability in normal values for the upper and lower limb*. Diving Hyperb Med, 2018. **48**(1): p. 2-9.
81. Dowd, G.S., K. Linge, and G. Bentley, *Measurement of transcutaneous oxygen pressure in normal and ischaemic skin*. J Bone Joint Surg Br, 1983. **65**(1): p. 79-83.
82. Rink, C.L., et al., *Standardized Approach to Quantitatively Measure Residual Limb Skin Health in Individuals with Lower Limb Amputation*. Adv Wound Care (New Rochelle), 2017. **6**(7): p. 225-232.
83. Bader, D.L., P.R. Worsley, and A. Gefen, *Bioengineering considerations in the prevention of medical device-related pressure ulcers*. Clin Biomech (Bristol, Avon), 2019. **67**: p. 70-77.
84. Swanson, E.C., et al., *Optical coherence tomography for the investigation of skin adaptation to mechanical stress*. Skin Res Technol, 2020.
85. Graser, M., S. Day, and A. Buis, *Exploring the role of transtibial prosthetic use in deep tissue injury development: a scoping review*. BMC Biomedical Engineering, 2020. **2**(2).
86. Lilja, M., S. Johansson, and T. Oberg, *Relaxed versus activated stump muscles during casting for trans-tibial prostheses*. Prosthet Orthot Int, 1999. **23**(1): p. 13-20.
87. Pezzin, L.E., et al., *Use and satisfaction with prosthetic limb devices and related services*. Arch Phys Med Rehabil, 2004. **85**(5): p. 723-9.
88. Haggstrom, E.E., E. Hansson, and K. Hagberg, *Comparison of prosthetic costs and service between osseointegrated and conventional suspended transfemoral prostheses*. Prosthet Orthot Int, 2013. **37**(2): p. 152-60.
89. McDougall, A., *Prosthetics An Overview*. 2015, Endolite Institute.
90. Dr Webb, G., *Clinical Science in Amputee Rehabilitation*. 2015: Guy's and St Thomas' NHS Foundation Trust.
91. Pirouzi, G., et al., *Review of the socket design and interface pressure measurement for transtibial prosthesis*. ScientificWorldJournal, 2014. **2014**: p. 849073.
92. Safari, M.R. and M.R. Meier, *Systematic review of effects of current transtibial prosthetic socket designs-Part 1: Qualitative outcomes*. J Rehabil Res Dev, 2015. **52**(5): p. 491-508.
93. Hachisuka, K., et al., *Total surface bearing below-knee prosthesis: advantages, disadvantages, and clinical implications*. Arch Phys Med Rehabil, 1998. **79**(7): p. 783-9.

94. Yigiter, K., G. Sener, and K. Bayar, *Comparison of the effects of patellar tendon bearing and total surface bearing sockets on prosthetic fitting and rehabilitation*. Prosthet Orthot Int, 2002. **26**(3): p. 206-12.
95. Safari, M.R. and M.R. Meier, *Systematic review of effects of current transtibial prosthetic socket designs--Part 2: Quantitative outcomes*. J Rehabil Res Dev, 2015. **52**(5): p. 509-26.
96. Kahle, J.T., *Conventional and Hydrostatic Transtibial Interface Comparison* Journal of Prosthetics and Orthotics, 1999. **11**(4): p. 85-91.
97. Gholizadeh, H., et al., *A comparison of pressure distributions between two types of sockets in a bulbous stump*. Prosthet Orthot Int, 2016. **40**(4): p. 509-16.
98. Clark, M., et al., *International review. Pressure ulcer prevention: pressure, shear, friction and microclimate in context. A consensus document. Microclimate in context* London, Wounds International, 2010: p. 19-25.
99. Han, Y., et al., *A thermal management device for a lower-limb prosthesis*. Applied Thermal Engineering, 2015. **82**: p. 246-252.
100. Andrews, A.M., B. Wunderlich, and A. Linberg, *Core temperature changes in service members with and without amputations during the Army 10-Miler*. Mil Med, 2011. **176**(6): p. 664-8.
101. Nixon, J., et al., *Prognostic factors associated with pressure sore development in the immediate post-operative period*. Int J Nurs Stud, 2000. **37**(4): p. 279-89.
102. Gerhardt, L.C., et al., *Influence of epidermal hydration on the friction of human skin against textiles*. J R Soc Interface, 2008. **5**(28): p. 1317-28.
103. Hansen, C., et al., *Incidence, severity, and impact of hyperhidrosis in people with lower-limb amputation*. J Rehabil Res Dev, 2015. **52**(1): p. 31-40.
104. Kobayashi, T., et al., *Effect of prosthetic alignment changes on socket reaction moment impulse during walking in transtibial amputees*. J Biomech, 2014. **47**(6): p. 1315-23.
105. Reger, S., et al., *International review. Pressure ulcer prevention: pressure, shear, friction and microclimate in context. A consensus document. Shear and friction in context*. Wounds International, 2010.
106. Sanders, J.E., et al., *Material properties of commonly-used interface materials and their static coefficients of friction with skin and socks*. J Rehabil Res Dev, 1998. **35**(2): p. 161-76.
107. Zhang, M. and M. Mak, *In vivo properties of human skin*. Prosthet Orthot Int, 1999. **23**: p. 135-41.
108. Zhang, M., et al., *Clinical investigation of the pressure and shear stress on the trans-tibial stump with a prosthesis*. Medical Engineering & Physics, 1998. **20**(3): p. 188-198.
109. Zachariah, S.G. and J.E. Sanders, *Standing interface stresses as a predictor of walking interface stresses in the trans-tibial prosthesis*. Prosthet Orthot Int, 2001. **25**(1): p. 34-40.
110. Portnoy, S., et al., *Internal mechanical conditions in the soft tissues of a residual limb of a trans-tibial amputee*. Journal of Biomechanics, 2008. **41**(9): p. 1897-1909.
111. Laszczak, P., et al., *A pressure and shear sensor system for stress measurement at lower limb residuum/socket interface*. Medical Engineering & Physics, 2016. **38**(7): p. 695-700.
112. Swanson, E.C., et al., *Instrumented socket inserts for sensing interaction at the limb-socket interface*. Med Eng Phys, 2018. **51**: p. 111-118.
113. Zhang, M. and C. Roberts, *Comparison of computational analysis with clinical measurement of stresses on below-knee residual limb in a prosthetic socket*. Med Eng Phys, 2000. **22**(9): p. 607-12.
114. Portnoy, S., et al., *Surgical and morphological factors that affect internal mechanical loads in soft tissues of the transtibial residuum*. Ann Biomed Eng, 2009. **37**(12): p. 2583-605.
115. Sengeh, D.M., et al., *Multi-material 3-D viscoelastic model of a transtibial residuum from in-vivo indentation and MRI data*. Journal of the Mechanical Behavior of Biomedical Materials, 2016. **59**: p. 379-392.
116. Cagle, J.C., et al., *A finite element model to assess transtibial prosthetic sockets with elastomeric liners*. Med Biol Eng Comput, 2017.
117. Ramasamy, E., et al., *An Efficient Modelling-Simulation-Analysis Workflow to Investigate Stump-Socket Interaction Using Patient-Specific, Three-Dimensional, Continuum-*

- Mechanical, Finite Element Residual Limb Models*. Front Bioeng Biotechnol, 2018. **6**: p. 126.
118. Dickinson, A.S., J.W. Steer, and P.R. Worsley, *Finite element analysis of the amputated lower limb: A systematic review and recommendations*. Med Eng Phys, 2017. **43**: p. 1-18.
 119. Zhang, L., et al., *Finite element analysis of the contact interface between trans-femoral stump and prosthetic socket*. Conf Proc IEEE Eng Med Biol Soc, 2013. **2013**: p. 1270-3.
 120. Lacroix, D. and J.F. Patino, *Finite element analysis of donning procedure of a prosthetic transfemoral socket*. Ann Biomed Eng, 2011. **39**(12): p. 2972-83.
 121. Steer, J., *Developing parametric finite element models of the residual limb - prosthetic socket system towards clinical application*. 2019, University of Southampton.
 122. Steer, J.W., et al., *Key considerations for finite element modelling of the residuum-prosthetic socket interface*. Prosthet Orthot Int, 2020: p. 309364620967781.
 123. Portnoy, S., et al., *Effects of sitting postures on risks for deep tissue injury in the residuum of a transtibial prosthetic-user: a biomechanical case study*. Comput Methods Biomech Biomed Engin, 2011. **14**(11): p. 1009-19.
 124. Palevski, A., et al., *Stress relaxation of porcine gluteus muscle subjected to sudden transverse deformation as related to pressure sore modeling*. J Biomech Eng, 2006. **128**(5): p. 782-7.
 125. Gefen, A. and E. Haberman, *Viscoelastic properties of ovine adipose tissue covering the gluteus muscles*. J Biomech Eng, 2007. **129**(6): p. 924-30.
 126. Groves, R.B., et al., *An anisotropic, hyperelastic model for skin: experimental measurements, finite element modelling and identification of parameters for human and murine skin*. J Mech Behav Biomed Mater, 2013. **18**: p. 167-80.
 127. Hendriks, F.M., et al., *A numerical-experimental method to characterize the non-linear mechanical behaviour of human skin*. Skin Res Technol, 2003. **9**(3): p. 274-83.
 128. Stekelenburg A., Oomens C., and D. Bader, *Compression-Induced Tissue Damage: Animal Models*. In: Bader D.L., Bouten C.V., Colin D., Oomens C.W. (eds) *Pressure ulcer research current and future perspectives*. 1 ed. 2005: Springer, Berlin, Heidelberg.
 129. Tonuk, E. and M.B. Silver-Thorn, *Nonlinear elastic material property estimation of lower extremity residual limb tissues*. IEEE Trans Neural Syst Rehabil Eng, 2003. **11**(1): p. 43-53.
 130. Gavronski, G., et al., *Evaluation of viscoelastic parameters of the skeletal muscles in junior triathletes*. Physiol Meas, 2007. **28**(6): p. 625-37.
 131. Agyapong-Badu, S., et al., *Measurement of ageing effects on muscle tone and mechanical properties of rectus femoris and biceps brachii in healthy males and females using a novel hand-held myometric device*. Arch Gerontol Geriatr, 2016. **62**: p. 59-67.
 132. Chuang, L.L., et al., *Relative and absolute reliabilities of the myotonometric measurements of hemiparetic arms in patients with stroke*. Arch Phys Med Rehabil, 2013. **94**(3): p. 459-66.
 133. Kong, P.W., et al., *Effect of Post-Exercise Massage on Passive Muscle Stiffness Measured Using Myotonometry - A Double-Blind Study*. J Sports Sci Med, 2018. **17**(4): p. 599-606.
 134. National Pressure Ulcer Advisory Panel and European Pressure Ulcer Advisory Panel, *Prevention and Treatment of Pressure Ulcers: Clinical Practice Guideline*. 2014: Washington DC, USA.
 135. Kottner, J., T. Dassen, and N. Lahmann, *Prevalence of deep tissue injuries in hospitals and nursing homes: two cross-sectional studies*. Int J Nurs Stud, 2010. **47**(6): p. 665-70.
 136. VanGilder, C., et al., *The demographics of suspected deep tissue injury in the United States: an analysis of the International Pressure Ulcer Prevalence Survey 2006-2009*. Adv Skin Wound Care, 2010. **23**(6): p. 254-61.
 137. Bouten, C.V., et al., *The etiology of pressure ulcers: skin deep or muscle bound?* Arch Phys Med Rehabil, 2003. **84**(4): p. 616-9.
 138. Worsley, P.R., et al., *Investigating the effects of strap tension during non-invasive ventilation mask application: a combined biomechanical and biomarker approach*. Medical Devices-Evidence and Research, 2016. **9**: p. 409-417.

139. Worsley, P.R., et al., *Investigating the effects of cervical collar design and fit on the biomechanical and biomarker reaction at the skin*. Med Devices (Auckl), 2018. **11**: p. 87-94.
140. Hemmes, B., et al., *Cytokine IL1alpha and lactate as markers for tissue damage in spineboard immobilisation. A prospective, randomised open-label crossover trial*. J Mech Behav Biomed Mater, 2017. **75**: p. 82-88.
141. Panel, N.P.U.A., *Best Practices for Prevention of Medical Device-Related Pressure Injuries*. 2017, NPUAP.
142. Gefen, A., et al., *Device-related pressure ulcers: SECURE prevention*. J Wound Care, 2020. **29**(Sup2a): p. S1-s52.
143. National Pressure Ulcer Advisory Panel, European Pressure Ulcer Advisory Panel, and Pan Pacific Pressure Injury Alliance, *Prevention and Treatment of Pressure Ulcers: Clinical Practice Guideline*. 2014, Emily Haesler (Ed.). Cambridge Media: Osborne Park, Western Australia.
144. Oomens, C.W.J., et al., *Pressure Induced Deep Tissue Injury Explained*. Annals of Biomedical Engineering, 2015. **43**(2): p. 297-305.
145. Peirce, S.M., T.C. Skalak, and G.T. Rodeheaver, *Ischemia-reperfusion injury in chronic pressure ulcer formation: a skin model in the rat*. Wound Repair Regen, 2000. **8**(1): p. 68-76.
146. Jiang, L.P., et al., *Ischemia-reperfusion injury-induced histological changes affecting early stage pressure ulcer development in a rat model*. Ostomy Wound Manage, 2011. **57**(2): p. 55-60.
147. Gray, R.J., et al., *Monitoring contractile dermal lymphatic activity following uniaxial mechanical loading*. Medical Engineering & Physics, 2016. **38**(9): p. 895-903.
148. Gray, R.J., D. Voegeli, and D.L. Bader, *Features of lymphatic dysfunction in compressed skin tissues - Implications in pressure ulcer aetiology*. J Tissue Viability, 2016. **25**(1): p. 26-31.
149. Kasuya, A., J. Sakabe, and Y. Tokura, *Potential application of in vivo imaging of impaired lymphatic duct to evaluate the severity of pressure ulcer in mouse model*. Sci Rep, 2014. **4**: p. 4173.
150. Gefen, A. and J. Levine, *The false premise in measuring body-support interface pressures for preventing serious pressure ulcers*. Journal of Medical Engineering & Technology, 2007. **31**(5): p. 375-380.
151. Swain, I.D. and D.L. Bader, *The measurement of interface pressure and its role in soft tissue breakdown*. Journal of tissue viability, 2002. **12**(4): p. 132-4, 136-7, 140-6.
152. Kosiak, M., *Etiology and pathology of ischemic ulcers*. Archives of physical medicine and rehabilitation, 1959. **40**(2): p. 62-9.
153. Daniel, R.K., D.L. Priest, and D.C. Wheatley, *Etiologic factors in pressure sores: an experimental model*. Arch Phys Med Rehabil, 1981. **62**(10): p. 492-8.
154. Groth, K., *Klinische Beobachtungen und experimentelle Studien uber die Entstehung des Dekubitus*. Acta Chir Scand 87, 1942: p. 198-200.
155. Husain, T., *An experimental study of some pressure effects on tissues, with reference to the bed-sore problem*. J Pathol Bacteriol, 1953. **66**(2): p. 347-58.
156. Kosiak, M., *Etiology of decubitus ulcers*. Arch Phys Med Rehabil, 1961. **42**: p. 19-29.
157. Dinsdale, S.M., *Decubitus ulcers: role of pressure and friction in causation*. Arch Phys Med Rehabil, 1974. **55**(4): p. 147-52.
158. Gefen, A., *Reswick and Rogers pressure-time curve for pressure ulcer risk. Part 2*. Nurs Stand, 2009. **23**(46): p. 40-4.
159. Reswick, J. and J. Rogers, *Experience at Rancho Los Amigos Hospital with devices and techniques to prevent pressure sores*, in *Bed sore biomechanics: proceedings of a seminar on tissue viability and clinical applications organised in association with the Department of Biomedical*. 1976, Macmillan Press: London. p. 301-310.
160. Gefen, A., *Reswick and Rogers pressure-time curve for pressure ulcer risk. Part 1*. Nurs Stand, 2009. **23**(45): p. 64, 66, 68 passim.

161. de Wert, L.A., et al., *A new method to evaluate the effects of shear on the skin*. Wound Repair and Regeneration, 2015. **23**(6): p. 885-890.
162. Linder-Ganz, E., et al., *Pressure-time cell death threshold for albino rat skeletal muscles as related to pressure sore biomechanics*. J Biomech, 2006. **39**(14): p. 2725-32.
163. Gefen, A., et al., *Strain-time cell-death threshold for skeletal muscle in a tissue-engineered model system for deep tissue injury*. J Biomech, 2008. **41**(9): p. 2003-12.
164. Stekelenburg, A., et al., *Deep tissue injury: how deep is our understanding?* Arch Phys Med Rehabil, 2008. **89**(7): p. 1410-3.
165. Stekelenburg, A., et al., *Role of ischemia and deformation in the onset of compression-induced deep tissue injury: MRI-based studies in a rat model*. J Appl Physiol (1985), 2007. **102**(5): p. 2002-11.
166. Gawlitta, D., et al., *Temporal differences in the influence of ischemic factors and deformation on the metabolism of engineered skeletal muscle*. J Appl Physiol (1985), 2007. **103**(2): p. 464-73.
167. Ceelen, K.K., et al., *Compression-induced damage and internal tissue strains are related*. J Biomech, 2008. **41**(16): p. 3399-404.
168. Loerakker, S., et al., *Temporal effects of mechanical loading on deformation-induced damage in skeletal muscle tissue*. Ann Biomed Eng, 2010. **38**(8): p. 2577-87.
169. Loerakker, S., et al., *How does muscle stiffness affect the internal deformations within the soft tissue layers of the buttocks under constant loading?* Comput Methods Biomech Biomed Engin, 2013. **16**(5): p. 520-9.
170. Gefen, A., et al., *In vivo muscle stiffening under bone compression promotes deep pressure sores*. J Biomech Eng, 2005. **127**(3): p. 512-24.
171. Loerakker, S., et al., *The effects of deformation, ischemia, and reperfusion on the development of muscle damage during prolonged loading*. J Appl Physiol (1985), 2011. **111**(4): p. 1168-77.
172. Loerakker, S., et al., *Ischemia-reperfusion injury in rat skeletal muscle assessed with T2-weighted and dynamic contrast-enhanced MRI*. Magn Reson Med, 2011. **66**(2): p. 528-37.
173. Stekelenburg, A., et al., *Compression-induced deep tissue injury examined with magnetic resonance imaging and histology*. J Appl Physiol (1985), 2006. **100**(6): p. 1946-54.
174. Traa, W.A., et al., *There is an individual tolerance to mechanical loading in compression induced deep tissue injury*. Clin Biomech (Bristol, Avon), 2019. **63**: p. 153-160.
175. Nelissen, J.L., et al., *A MRI-Compatible Combined Mechanical Loading and MR Elastography Setup to Study Deformation-Induced Skeletal Muscle Damage in Rats*. PLoS One, 2017. **12**(1): p. e0169864.
176. Mueller, M.J. and K.S. Maluf, *Tissue adaptation to physical stress: a proposed "Physical Stress Theory" to guide physical therapist practice, education, and research*. Phys Ther, 2002. **82**(4): p. 383-403.
177. Sanders, J.E. and B.S. Goldstein, *Collagen fibril diameters increase and fibril densities decrease in skin subjected to repetitive compressive and shear stresses*. J Biomech, 2001. **34**(12): p. 1581-7.
178. Shoham, N., et al., *Contoured Foam Cushions Cannot Provide Long-term Protection Against Pressure-Ulcers for Individuals with a Spinal Cord Injury: Modeling Studies*. Adv Skin Wound Care, 2015. **28**(7): p. 303-16.
179. Kobayashi, T., et al., *Socket reaction moments in transtibial prostheses during walking at clinically perceived optimal alignment*. Prosthet Orthot Int, 2016. **40**(4): p. 503-8.
180. Ohura, T., M. Takahashi, and N. Ohura, *Influence of external forces (pressure and shear force) on superficial layer and subcutis of porcine skin and effects of dressing materials: Are dressing materials beneficial for reducing pressure and shear force in tissues?* Wound Repair and Regeneration, 2008. **16**(1): p. 102-107.
181. Mbithi, F.M., et al., *Predictive Control for an Active Prosthetic Socket informed by FEA-based Tissue Damage Risk Estimation*. Conf Proc IEEE Eng Med Biol Soc, 2019. **2019**: p. 2073-2076.

182. Lee, W.C. and M. Zhang, *Using computational simulation to aid in the prediction of socket fit: a preliminary study*. Med Eng Phys, 2007. **29**(8): p. 923-9.
183. Portnoy, S., et al., *Real-time subject-specific analyses of dynamic internal tissue loads in the residual limb of transtibial amputees*. Medical Engineering & Physics, 2010. **32**(4): p. 312-323.
184. Gunningberg, L. and C. Carli, *Reduced pressure for fewer pressure ulcers: can real-time feedback of interface pressure optimise repositioning in bed?* Int Wound J, 2016. **13**(5): p. 774-9.
185. Berthold, J., B.E. Dicianno, and R.A. Cooper, *Pressure mapping to assess seated pressure distributions and the potential risk for skin ulceration in a population of sledge hockey players and control subjects*. Disability and rehabilitation. Assistive technology, 2013. **8**(5): p. 387-91.
186. Reenalda, J., et al., *Clinical Use of Interface Pressure to Predict Pressure Ulcer Development: A Systematic Review*. Assistive Technology, 2009. **21**(2): p. 76-85.
187. Gefen, A., *Pressure-sensing devices for assessment of soft tissue loading under bony prominences: technological concepts and clinical utilization*. Wounds, 2007. **19**(12): p. 350-62.
188. Hornak, J.P. *The Basics of MRI*. 2017; Available from: <http://www.cis.rit.edu/htbooks/mri/inside.htm>.
189. Jung, B.A. and M. Weigel, *Spin echo magnetic resonance imaging*. J Magn Reson Imaging, 2013. **37**(4): p. 805-17.
190. Avril, S., et al., *Mixed experimental and numerical approach for characterizing the biomechanical response of the human leg under elastic compression*. J Biomech Eng, 2010. **132**(3): p. 031006.
191. Henrot, P., et al., *Imaging of the painful lower limb stump*. Radiographics, 2000. **20 Spec No**: p. S219-35.
192. Hong, C.W., et al., *Fat Quantification in the Abdomen*. Top Magn Reson Imaging, 2017. **26**(6): p. 221-227.
193. Hu, H.H. and H.E. Kan, *Quantitative proton MR techniques for measuring fat*. NMR Biomed, 2013. **26**(12): p. 1609-29.
194. Moore, C.D., et al., *Lower-extremity muscle atrophy and fat infiltration after chronic spinal cord injury*. J Musculoskelet Neuronal Interact, 2015. **15**(1): p. 32-41.
195. Wu, G.A. and K.M. Bogie, *Not just quantity: gluteus maximus muscle characteristics in able-bodied and SCI individuals--implications for tissue viability*. J Tissue Viability, 2013. **22**(3): p. 74-82.
196. Blew, R.M., et al., *Validation of Peripheral Quantitative Computed Tomography-Derived Thigh Adipose Tissue Subcompartments in Young Girls Using a 3 T MRI Scanner*. J Clin Densitom, 2018. **21**(4): p. 583-594.
197. Sherk, V.D., et al., *Effects of filtering methods on muscle and fat cross-sectional area measurement by pQCT: a technical note*. Physiol Meas, 2011. **32**(12): p. N65-72.
198. Quintavalle, P.R., et al., *Use of high-resolution, high-frequency diagnostic ultrasound to investigate the pathogenesis of pressure ulcer development*. Adv Skin Wound Care, 2006. **19**(9): p. 498-505.
199. Ahanchian, N., et al., *Estimating the material properties of heel pad sub-layers using inverse Finite Element Analysis*. Med Eng Phys, 2017. **40**: p. 11-19.
200. Telfer, S., J. Woodburn, and D.E. Turner, *Measurement of functional heel pad behaviour in-shoe during gait using orthotic embedded ultrasonography*. Gait Posture, 2014. **39**(1): p. 328-32.
201. Ranger, B.J., et al., *Motion compensation in a tomographic ultrasound imaging system: Toward volumetric scans of a limb for prosthetic socket design*. Conf Proc IEEE Eng Med Biol Soc, 2015. **2015**: p. 7204-7.
202. Courage + Khazaka, TM- *The Tewameter TM 300 Manual*. 2015.

203. Kelleher, M., et al., *Skin barrier dysfunction measured by transepidermal water loss at 2 days and 2 months predates and predicts atopic dermatitis at 1 year*. J Allergy Clin Immunol, 2015. **135**(4): p. 930-5.e1.
204. Kottner, J., et al., *Skin response to sustained loading: A clinical explorative study*. J Tissue Viability, 2015. **24**(3): p. 114-22.
205. Schario, M., et al., *Effects of two different fabrics on skin barrier function under real pressure conditions*. J Tissue Viability, 2017. **26**(2): p. 150-155.
206. Bostan, L.E., et al., *The influence of incontinence pads moisture at the loaded skin interface*. J Tissue Viability, 2019. **28**(3): p. 125-132.
207. Bates-Jensen, B.M., et al., *Subepidermal moisture differentiates erythema and stage I pressure ulcers in nursing home residents*. Wound Repair Regen, 2008. **16**(2): p. 189-97.
208. Heinrich, U., et al., *Multicentre comparison of skin hydration in terms of physical-, physiological- and product-dependent parameters by the capacitive method (Corneometer CM 825)*. Int J Cosmet Sci, 2003. **25**(1-2): p. 45-53.
209. Scheel-Sailer, A., et al., *Challenges to measure hydration, redness, elasticity and perfusion in the unloaded sacral region of healthy persons after supine position*. J Tissue Viability, 2015. **24**(2): p. 62-70.
210. Sangeorzan, B.J., et al., *Circulatory and mechanical response of skin to loading*. J Orthop Res, 1989. **7**(3): p. 425-31.
211. Knight, S.L., et al., *Establishing predictive indicators for the status of loaded soft tissues*. Journal of Applied Physiology, 2001. **90**(6): p. 2231-2237.
212. Worsley, P.R., et al., *Monitoring the biomechanical and physiological effects of postural changes during leisure chair sitting*. J Tissue Viability, 2018. **27**(1): p. 16-22.
213. Woodhouse, M., et al., *The physiological response of soft tissue to periodic repositioning as a strategy for pressure ulcer prevention*. Clinical Biomechanics, 2015. **30**(2): p. 166-174.
214. Worsley, P.R., B. Parsons, and D.L. Bader, *An evaluation of fluid immersion therapy for the prevention of pressure ulcers*. Clin Biomech (Bristol, Avon), 2016. **40**: p. 27-32.
215. Chai, C.Y. and D.L. Bader, *The physiological response of skin tissues to alternating support pressures in able-bodied subjects*. Journal of the Mechanical Behavior of Biomedical Materials, 2013. **28**: p. 427-435.
216. Bogie, K.M., I. Nuseibeh, and D.L. Bader, *Early progressive changes in tissue viability in the seated spinal cord injured subject*. Paraplegia, 1995. **33**(3): p. 141-7.
217. Wang, Z., et al., *A systematic review and meta-analysis of tests to predict wound healing in diabetic foot*. J Vasc Surg, 2016. **63**(2 Suppl): p. 29S-36S.e1-2.
218. Mirtaheri, P., et al., *A review of the role of the partial pressure of carbon dioxide in mechanically loaded tissues: the canary in the cage singing in tune with the pressure ulcer mantra*. Ann Biomed Eng, 2015. **43**(2): p. 336-47.
219. Manorama, A.A., et al., *Blood perfusion and transcutaneous oxygen level characterizations in human skin with changes in normal and shear loads--implications for pressure ulcer formation*. Clin Biomech (Bristol, Avon), 2010. **25**(8): p. 823-8.
220. Park, H.S., et al., *Role of Laser Doppler for the Evaluation of Pedal Microcirculatory Function in Diabetic Neuropathy Patients*. Microcirculation, 2016. **23**(1): p. 44-52.
221. Prochazka, V., et al., *Cell therapy, a new standard in management of chronic critical limb ischemia and foot ulcer*. Cell Transplant, 2010. **19**(11): p. 1413-24.
222. Bronneberg, D., et al., *Cytokine and chemokine release upon prolonged mechanical loading of the epidermis*. Experimental Dermatology, 2007. **16**(7): p. 567-573.
223. Cornelissen, L.H., et al., *The Transport Profile of Cytokines in Epidermal Equivalents Subjected to Mechanical Loading*. Annals of Biomedical Engineering, 2009. **37**(5): p. 1007-1018.
224. Soetens, J.F.J., et al., *Investigating the influence of intermittent and continuous mechanical loading on skin through non-invasive sampling of IL-1alpha*. J Tissue Viability, 2019.
225. Uchi, H., et al., *Cytokines and chemokines in the epidermis*. J Dermatol Sci, 2000. **24** Suppl 1: p. S29-38.

226. Rider, P., et al., *IL-1 α and IL-1 β recruit different myeloid cells and promote different stages of sterile inflammation*. J Immunol, 2011. **187**(9): p. 4835-43.
227. Terui, T., et al., *An increased ratio of interleukin-1 receptor antagonist to interleukin-1 α in inflammatory skin diseases*. Exp Dermatol, 1998. **7**(6): p. 327-34.
228. Mee, J.B., et al., *Counter-regulation of interleukin-1 α (IL-1 α) and IL-1 receptor antagonist in murine keratinocytes*. J Invest Dermatol, 2005. **124**(6): p. 1267-74.
229. Soetens, J.F.J., et al., *The expression of anaerobic metabolites in sweat and sebum from human skin subjected to intermittent and continuous mechanical loading*. J Tissue Viability, 2019.
230. Baran, U., et al., *OCT-based microangiography for reactive hyperaemia assessment within residual limb skin of people with lower limb loss*. Skin Res Technol, 2017.
231. Choi, W.J., H. Wang, and R.K. Wang, *Optical coherence tomography microangiography for monitoring the response of vascular perfusion to external pressure on human skin tissue*. J Biomed Opt, 2014. **19**(5): p. 056003.
232. Jung, S.Y., et al., *Comparison of sentinel lymph node biopsy guided by the multimodal method of indocyanine green fluorescence, radioisotope, and blue dye versus the radioisotope method in breast cancer: a randomized controlled trial*. Ann Surg Oncol, 2014. **21**(4): p. 1254-9.
233. Miller, G.E. and J. Seale, *Lymphatic clearance during compressive loading*. Lymphology, 1981. **14**(4): p. 161-6.
234. Miller, G.E. and J.L. Seale, *The recovery of terminal lymph flow following occlusion*. J Biomech Eng, 1987. **109**(1): p. 48-54.
235. Unno, N., et al., *A novel method of measuring human lymphatic pumping using indocyanine green fluorescence lymphography*. J Vasc Surg, 2010. **52**(4): p. 946-52.
236. Lopera, C., et al., *Investigating the Short-Term Effects of Manual Lymphatic Drainage and Compression Garment Therapies on Lymphatic Function Using Near-Infrared Imaging*. Lymphat Res Biol, 2017. **15**(3): p. 235-240.
237. Lohrmann, C., et al., *MR imaging of the lymphatic system: distribution and contrast enhancement of gadodiamide after intradermal injection*. Lymphology, 2006. **39**(4): p. 156-63.
238. Liu, N.F., et al., *Anatomic and functional evaluation of the lymphatics and lymph nodes in diagnosis of lymphatic circulation disorders with contrast magnetic resonance lymphangiography*. J Vasc Surg, 2009. **49**(4): p. 980-7.
239. Lu, Q., J. Xu, and N. Liu, *Chronic lower extremity lymphedema: a comparative study of high-resolution interstitial MR lymphangiography and heavily T2-weighted MRI*. Eur J Radiol, 2010. **73**(2): p. 365-73.
240. Lu, Q., et al., *MR lymphography of lymphatic vessels in lower extremity with gynecologic oncology-related lymphedema*. PLoS One, 2012. **7**(11): p. e50319.
241. Laing, S., et al., *Trans tibial Prosthetic Socket Shape in a Developing Country: A study to compare initial outcomes in Pressure Cast hydrostatic and Patella Tendon Bearing designs*. Gait Posture, 2017. **58**: p. 363-368.
242. boso, *User Instructions boso-profitest*. 2012, Bosch + Sohn GmbH u. Co. KG.
243. Allen, V., et al., *Accuracy of interface pressure measurement systems*. J Biomed Eng, 1993. **15**(4): p. 344-8.
244. Perkins, M.A., et al., *A noninvasive method to assess skin irritation and compromised skin conditions using simple tape adsorption of molecular markers of inflammation*. Skin Research and Technology, 2001. **7**(4): p. 227-237.
245. Cowley, K. and K. Vanoosthuyze, *The biomechanics of blade shaving*. Int J Cosmet Sci, 2016. **38 Suppl 1**: p. 17-23.
246. Logan, B.M., D.J. Bowden, and R.T. Hutchings, *Mcminn's colour atlas of lower limb anatomy*. Fifth ed. 2018: Elsevier.
247. Basu, A.S., *Droplet morphometry and velocimetry (DMV): a video processing software for time-resolved, label-free tracking of droplet parameters*. Lab Chip, 2013. **13**(10): p. 1892-901.

248. Kottner, J., et al., *Microclimate: A critical review in the context of pressure ulcer prevention*. Clin Biomech (Bristol, Avon), 2018. **59**: p. 62-70.
249. Rossides, C., S. Pender, and P. Schneider, *3D cyclorama: Digital unrolling of deformed tubes*. Submitted 2020.
250. Marusiak, J., et al., *Influence of number of records on reliability of myotonometric measurements of muscle stiffness at rest and contraction*. Acta Bioeng Biomech, 2018. **20**(4): p. 123-131.
251. Cohen, J., *Statistical Power Analysis for the Behavioral Sciences*. 1988, New York: Academic Press, Harcourt Brace Jovanovich.
252. Goodpaster, B.H., F.L. Thaete, and D.E. Kelley, *Thigh adipose tissue distribution is associated with insulin resistance in obesity and in type 2 diabetes mellitus*. Am J Clin Nutr, 2000. **71**(4): p. 885-92.
253. Chang, E., M. Varghese, and K. Singer, *Gender and Sex Differences in Adipose Tissue*. Curr Diab Rep, 2018. **18**(9): p. 69.
254. Addison, O., et al., *Intermuscular fat: a review of the consequences and causes*. Int J Endocrinol, 2014. **2014**: p. 309570.
255. Sopher, R., et al., *Effects of intramuscular fat infiltration, scarring, and spasticity on the risk for sitting-acquired deep tissue injury in spinal cord injury patients*. J Biomech Eng, 2011. **133**(2): p. 021011.
256. Tamai, N., et al., *The relationship between skin ultrasound images and muscle damage using skin blotting in wheelchair basketball athletes*. Spinal Cord, 2020.
257. Yuan, Y., J. Gao, and R. Ogawa, *Mechanobiology and Mechanotherapy of Adipose Tissue-Effect of Mechanical Force on Fat Tissue Engineering*. Plast Reconstr Surg Glob Open, 2015. **3**(12): p. e578.
258. Heid, H., et al., *On the formation of lipid droplets in human adipocytes: the organization of the perilipin-vimentin cortex*. PLoS One, 2014. **9**(2): p. e90386.
259. Hossain, M.G., et al., *Compressive force inhibits adipogenesis through COX-2-mediated down-regulation of PPARgamma2 and C/EBPalpha*. J Biosci Bioeng, 2010. **109**(3): p. 297-303.
260. Shoham, N., et al., *Adipocyte stiffness increases with accumulation of lipid droplets*. Biophys J, 2014. **106**(6): p. 1421-31.
261. Bhatt, H.B. and R.J. Smith, *Fatty liver disease in diabetes mellitus*. Hepatobiliary Surg Nutr, 2015. **4**(2): p. 101-8.
262. Wust, R.C., et al., *Sex differences in contractile properties and fatigue resistance of human skeletal muscle*. Exp Physiol, 2008. **93**(7): p. 843-50.
263. Lehnig, A.C. and K.I. Stanford, *Exercise-induced adaptations to white and brown adipose tissue*. J Exp Biol, 2018. **221**(Pt Suppl 1).
264. Fouchard, M., et al., *Alteration of Pressure-Induced Vasodilation in Aging and Diabetes, a Neuro-Vascular Damage*. Front Physiol, 2019. **10**: p. 862.
265. Bader, D.L., *Pressure Sores-Clinical Practice and Scientific Approach*. 15. Effects of compressive loading regimens on tissue viability. 1990, Basingstoke, Hampshire: MACMILLAN PRESS Scientific & Medical. 275.
266. Ruangsetakit, C., et al., *Transcutaneous oxygen tension: a useful predictor of ulcer healing in critical limb ischaemia*. J Wound Care, 2010. **19**(5): p. 202-6.
267. Rich, K., *Transcutaneous oxygen measurements: implications for nursing*. J Vasc Nurs, 2001. **19**(2): p. 55-9; quiz 60-1.
268. Cornelissen, L.H., et al., *Cytokine Release in Tissue-Engineered Epidermal Equivalents After Prolonged Mechanical Loading*. Epidermal Cells: Methods and Protocols, Second Edition, 2010. **585**: p. 335-344.
269. Herder, C., et al., *Elevated levels of the anti-inflammatory interleukin-1 receptor antagonist precede the onset of type 2 diabetes: the Whitehall II study*. Diabetes Care, 2009. **32**(3): p. 421-3.
270. Boyle, C.J., et al., *Morphology and composition play distinct and complementary roles in the tolerance of plantar skin to mechanical load*. Sci Adv, 2019. **5**(10): p. eaay0244.

271. Polgar, O., *Evaluating the level of sweat urea and lactate as a predictor of pressure ischemia and metabolic changes in lower-limb amputee patients*. 2019, University of Southampton.
272. Costanzo, I., D. Sen, and U. Guler, *A Prototype Towards a Transcutaneous Sensing Wearable*, in *Biomedical Circuits and Systems, BioCAS 2019*. 2019: Nara, Japan.